May 2007, Vol. 2, Issue 2

BioResources

A peer-reviewed Online Journal Devoted to the Science and Advanced Applications of Lignocellulosic Resources

In this Issue ...

146 – Editorial: Appropriate Technology

148 – Fiberboard water resistance

157 – Eucalyptus extractives

169 – Lignin analysis

296 – Flocculation of papermaking fibers

And much more ...

Cover image: Douglas Fir giant, *Pseudotsuga menziesii*, Scio, Oregon; Photo credit: Allen Hubbe.

BioResources is supported by NC State University, with database retrieval and online hosting at www.**bioresourcesjournal**.com, and backup files and author instructions at **ncsu.edu/bioresources**.

BioResources, a peer-reviewed journal devoted to the science of lignocellulosic materials, chemicals, and applications

NC STATE UNIVERSITY
College of Natural Resources
Department of Wood and Paper Science
Campus Box 8005
Raleigh, NC 27695-8005
919.515.7707/919.513.3022
919.515.6302 (fax)

BioResources

Contents: Vol. 2, Issue 2, May 2007

Hubbe, M. A. (2007). **"Appropriate technology in an age of renewables ,"** *BioRes.* 2(2), 146-147.

Hervillard, T., Cao, Q., and Laborie, M.-P. G. (2007). **"Improving water resistance of wheat straw-based medium density fiberboards bonded with aminoplastic and phenolic resins,"** *BioRes.* 2(2), 148-156.

Siverio, F. O., Barbosa, L. C. A., Maltha, C. R. A., Silvestre, A. J. D., Pilo-Veloso, D., and Gomide, J. L. (2007). **"Characterization of lipophilic wood extractives from clones of *Eucalyptus urograndis* cultivate in Brazil,"***BioRes.* 2(2), 157-168.

Parkås, J., Brunow, G., and Lundquist, K. (2007). **"Quantitative lignin analysis based on permanganate oxidation,"** *BioRes.* 2(2), 169-178.

Sridach, W., Hodgson, K. T., and Nazhad, M. (2007). **"Biodegradation and recycling potential of barrier coated paperboards,"** *BioRes.* 2(2), 179-192.

Khezami, L., Ould-Dris, A., and Capart, R. (2007). **"Activated carbon from thermo-compressed wood and other lignocellulosic precursors,"** *BioRes.* 2(2), 193-209.

Chakraborty, A., Sain, M. M., Kortschot, M. T., and Ghosh, S. B. (2007). **"Modeling energy consumption for the generation of microfibres from bleached kraft pulp fibres in a PFI mill,"** *BioRes.* 2(2), 210-222.

Colodette, J. L., Gomide, J. L., Júnior, D. L., and Pedrazzi, C. (2007). **"Effect of pulp delignification degree on fiber line performance and bleaching effluent load,"** *BioRes.* 2(2), 223-234.

Ruelle, J., Yamamoto, H., and Thibaut, B. (2007). **"Growth stresses and cellulose structural parameters in tension and normal wood from three tropical rainforest angiosperm species,"** *BioRes.* 2(2), 235-251.

Felissia, F. E., Area, M. C., Barboza, O. M., and Bengoechea, D. I. (2007). **"Anti-scaling agents in kraft pulping,"** *BioRes.* 2(2), 252-264.

Alma, M. H., Ertaş, M., Nitz, S., and Kollmannsberger, H. (2007). **"Chemical composition and content of essential oil from the bud of cultivated Turkish clove,"** *BioRes.* 2(2), 265-269.

Pérez, J. M., Rodríguez, F., Alonso, M. V., Oliet, M., and Echeverría, J. M. (2007). **"Characterization of a novolac resin substituting phenol by ammonium lignosulfonate as filler or extender,"** *BioRes.* 2(2), 270-283.

Altaner, C., Knox, J. P., and Jarvis, M. C. (2007). **"In situ detection of cell wall polysaccharides in sitka spruce (*Picea sitchensis* (Bong.) Carrière) wood tissue,"** *BioRes.* 2(2), 284-295.

Hubbe, M. A. (2007). **"Flocculation and redispersion of cellulosic fiber suspensions: A review of effects of hydrodynamic shear and polyelectrolytes,"** *BioRes.* 2(2), 296-331.

BioResources is a peer-reviewed journal devoted to the science of lignocellulosic materials, chemicals, and applications. The journal is a service of North Carolina State University, College of Natural Resources (http://cnr.ncsu.edu). Articles can be down-loaded without charge as PDF files at www.bioresourcesjournal.com. The *BioResources* website is hosted by Scholarly Exchange, and articles become indexed for scholars through the Open Journal System (http://pkp.sfu.ca/). **Author instructions**, journal policies, an editorial board list, and article files (secondary source) can be found at http://ncsu.edu/bioresources. Correspondence should be directed to co-editors Martin A. Hubbe (hubbe@ncsu.edu, 919-513-3022) and Lucian A. Lucia (lucian.lucia@ncsu.edu, 919-515-7707).

APPROPRIATE TECHNOLOGY IN AN AGE OF RENEWABLES

Martin A. Hubbe

In this editorial the author proposes that scientists and technologists can play essential roles in the selection of technological alternatives that are appropriate to people's long-term needs. Lessons learned in the 1970s and 80s, involving the design of simple and reliable mechanical systems for underdeveloped regions, can have relevance today in an increasingly interdependent, crowded, and polluted world. Specialists can help in two ways to promote technologies that make sense, providing for future well-being, and minimizing risks. First, we can exercise personal judgment in our work, as we pursue technological progress. We need to consider whether the likely products of our work are compatible with the world that we want to leave for our grandchildren. Second, we can provide guidance to our fellow citizens, as society grapples with the political and economic choices associated with progress.

Keywords: Appropriate technology, Renewable resources, Sustainability, Industrialization

Contact information: Department of Forest Biomaterial Science and Engineering, College of Natural Resources, North Carolina State University, Campus Box 8005, Raleigh, NC 27695-8005; hubbe@ncsu.edu

A CONCEPT BORROWED FROM THE DEVELOPING WORLD

The words "appropriate technology" have most often been used in the context of aid to third-world countries. Equipment and processes to be used in different parts of the world need to be suited to the local conditions, including the availability of electricity, running water, *etc*. It doesn't make sense to send a lot of plug-in refrigerators to a region that lacks a power grid. Likewise, expensive farming equipment will become useless in a land where there are no spare parts or people able to do the repairs.

In this editorial I would like to propose that the concepts of appropriate technology also are needed most urgently in the developed world. The idea is not new. For instance, the authors of the book *Appropriate Technology in Industrialized Countries* (Riedijk, W., ed., Delft Univ. Press, 1989) point out ways in which modern societies can benefit from technologies that are inherently simpler, cheaper, safer, or less centralized than the current state of the art.

Let's suppose that you are attempting to design a system to deliver water to nomadic people. Your clients, over many years, have developed patterns of living and knowledge of their environment that have allowed them to subsist and to avoid disaster (see Dunn, P. D., *Appropriate Technology: Technology with a Human Face*, Schocken Books, 1979). The priority, then, is to minimize risk. Your desert clients may face a disaster if they come to rely on a water system that depends on transmission lines or the delivery of fuel. A simpler system, relying on local resources and manual labor, might be less risky, even if less impressive.

The situation just described has some parallels with modern life. We all tend to become more vulnerable to political and economic changes when the resources upon which we depend come from far away. The fruit on your American table in winter may come from Chile. Gas in your car may come from Arabia, or maybe somewhere else equally far away. Most of us do not live in deserts, but our present lifestyles are becoming vulnerable due to the pressures of population growth, climatic change, and depletion of resources.

What are the patterns of living that will sustain members of spaceship Earth in years ahead? In his book *Small is Beautiful* (Harper and Row, 1973) E. F. Schumacher urged increased reliance on things that are local, cheap, simple, small, and requiring the input of manual labor. To that list one also could add environmentally favorable, healthy, relying on renewable resources, and tending to promote harmony among peoples. Words like "increased personal wealth," "personal freedom," and "a better life for our children" are usually left out of lists such as this, but we need to be realistic about rising expectations of future generations.

OUR ROLE AS SCIENTISTS AND TECHNOLOGISTS

How does one apply ideas, such as those just mentioned, in cases related to the utilization of cellulose-based materials? Many readers of this magazine are engaged in research and technology related to renewable resources. Proponents of appropriate technology would applaud us on that account, but what about the other issues? Here are some questions that each of us can ask ourselves about possible implementations of scientific findings:

1. Does the technology on which I am working require long shipping distances, increased vulnerability to disease, or risk of unintended consequences?
2. Does the technology on which I am working minimize, or at least not increase, the release of carbon dioxide or consumption of fossil fuels?
3. If implemented, is the technology on which I am working likely to pose risks to current or future generations? Is there a reliable way to minimize environmental hazards associated with it?

"But I'm just a scientist," someone may say. "I have no control over how and whether my results become implemented." As pointed out by Willoughby in his book *Technology Choice: A Critique of the Appropriate Technology Movement* (Westview Press, Boulder, 1990), people need to actively *select and implement* appropriate technological solutions. Individual initiative, on the part of those familiar with the underlying science, is critically needed. If scientists among us don't provide some guidance to our fellow citizens, relative to selection of what technologies to implement, then the inertia of scientific progress may take us in directions that we would not choose.

IMPROVING WATER RESISTANCE OF WHEAT STRAW-BASED MEDIUM DENSITY FIBERBOARDS BONDED WITH AMINOPLASTIC AND PHENOLIC RESINS

Thomas Hervillard[a], Qi Cao[b] and Marie-Pierre G. Laborie[b*]

A long standing problem in the manufacture of wheat-straw based composites with cost-effective formaldehyde-based resins is their poor water resistance as demonstrated by their large water thickness swell. In this study, wheat straw based medium density fiberboards were manufactured using 3 resin/wax systems: a melamine-urea-formaldehyde resin with either low or high wax content, and a phenol-formaldehyde resin with low wax content. The flexural properties, internal bond strength, and thickness swell of the resulting composites were evaluated and compared according to ASTM methods. The three MDF composites passed the requirements for MDF in interior application, except for the MDF manufactured with the aminoplastic resin and low wax content that failed to provide acceptable thickness swell. Using the phenolic resin in combination with low wax content resulted in a higher grade MDF composite, grade 120, than with the aminoplastic and high wax content. This study demonstrates that wheat straw based MDF manufactured with cost-effective aminoplastic and phenolic resins can have flexural properties, internal bond strength and thickness swell performance above the requirements from the American National Standards Institute.

Keywords: Wheat Straw, Medium Density Fiberboard, Aminoplastic Resin, Phenolic Resin, Thickness Swell, ANSI for MDF

*Contact information: a: Spie Batignolles TPCI , Service Expertises & Structures, Pôle Magellan - Parc St Christophe, 95862 Cergy Pontoise Cedex, France; b: Wood Materials and Engineering Laboratory, Washington State University, Pullman, WA 99164, PO Box 641806, USA; *Corresponding author: mlaborie@wsu.edu*

INTRODUCTION

The United States produces over 70 million tons (SI) of wheat straw residues (Kinsella 2004). Field burning is the most economic practice to dispose of these residues, but environmental pressure has resulted in increasingly stringent restrictions in the United-States. At the same time, the worldwide demand for fiberboards is predicted to double or triple from 1996 to 2010, creating a challenge to tumbling wood resources (Bowyer and Stockmann 2001). Increasing demands for fiberboards and depleted wood resources have therefore opened an opportunity for straw-based composites. As a result, intensive research and development have been conducted in the last decade to develop technology for manufacturing straw-based composites with thermosetting resins (Sauter 1996; Han et al. 2001b; Mantanis and Berns 2001; Wasylciw 2001; Mo et al. 2003) and more recently thermoplastic resins (Averous and Le Digabel 2006; Schirp et al. 2006).

Technological and economical challenges have limited the commercialization of the straw-based composites with thermosetting resins (Lengel 2001). Polymeric methylene bis(phenylisocyanate), pMDI, an effective but expensive adhesive, has generally been used for manufacturing straw-based thermosetting composites. pMDI, which is currently used in the few strawboard plants in operation, is four times more expensive than aminoplastic resins and two times more than phenolic resins (Zhang et al. 2003; Mo et al. 2005).

Also, commercialization has focused on particleboards rather than medium density fiberboards (MDF), which is at odds with the reported adequacy of wheat straw for fiber-based materials (Sauter 1996; Hague et al. 1998; Lengel 2001). The refiners used for MDF manufacture offer opportunities to manipulate and optimize the straw properties for bonding (Hague et al. 1998; Grigoriou 2000).

For straw-based composites to be competitive, a MDF manufacturing technology that could use the more economical formaldehyde-based resins, urea-formaldehyde and/or phenol-formaldehyde, is needed. However, there are well-known technical challenges associated with bonding wheat straw with formaldehyde-based resins. First, wheat straw is covered with a waxy cuticle that inhibits adhesion with water-based adhesives. Second, wheat straw has a high buffering capacity that interferes with the hardening of aminoplastic resins (Sauter 1996). Previous studies have demonstrated that pressure refining lowers the straw acid buffering capacity and disintegrates the waxy cuticle, thereby affording better adhesion with urea-formaldehyde resins (Sauter 1996; Hague et al. 1998), albeit not to the levels required by the standards for MDF of the American National Standards Institute (American National Standards Institute 2002). Other pretreatments, including a chemi-thermomechanical treatment (Markessini et al. 1997), a twin-screw/pressure refining treatment (Mantanis and Berns 2001) or simply high-pressure refining (Han et al. 2001b; Wasylciw 2001; Wasylciw 2002) have also been shown to improve the adhesion of wheat straw fibers with UF or MUF resins. Straw-based composites could therefore be manufactured with UF resins to pass the ANSI requirements for internal bond strength and flexural properties (Han et al. 2001b; Mantanis and Berns 2001; Wasylciw 2001). More recently, enzymatic treatments have been reported to improve the properties of straw-based particleboards (Zhang et al. 2003).

In spite of the improvements imparted by these treatments, the water resistance and dimensional stability of straw-based MDF composites is still an issue. According to ANSI standards, the thickness swell of panels, with thickness between 9.5 and 15 mm, should not exceed 1.5 mm, whereas that of panels with thickness higher than 15 mm should not exceed 10%. However, thickness swell values in the 20-30 % range have been repeatedly obtained (Markessini et al. 1997; Han et al. 2001b; Mantanis and Berns 2001), well above the allowance from the ANSI standard. To achieve acceptable water resistance, chemical modification of wheat straw has been performed prior to MDF manufacture with a phenolic resin and acetylated wheat straw (Gomez-Bueso et al. 2000). While efficient, the required chemical modification is expensive and impractical for industrial operations.

The objective of this research was to develop a simple technology to manufacture wheat-straw based MDF passing the minimum performance requirements for interior applications while using the low cost formaldehyde-based resins. In particular the

research aimed at addressing the low dimensional stability and poor thickness swell performance of wheat-straw based composites. To that objective, the more water-resistant resins, melamine-urea-formaldehyde (MUF) and phenol-formaldehyde (PF) resins were selected for this research.

EXPERIMENTAL

Materials

Wheat straw, of the MADSEN variety, one of the most common varieties in the state of Washington, was provided by local farmers. The wheat straw was hammer-milled into particles up to 5 cm long. The milled material was screened with a 0.5 cm screen to remove finer material. The straw was then soaked in cold water for 24 hours and processed in a disk refiner operating at atmospheric pressure and with spacing between the disks adjusted to 0.5 mm. After refining the straw was dried to a moisture content of approximately 1% in a rotating drum dryer before hot-pressing.

Two formaldehyde-based resins were selected and utilized to develop strong water resistance. These were a Melamine-Urea-Formaldehyde (MUF) resin formulated and synthesized by Dynea and a Phenol-Formaldehyde (PF) resin from Hexion Specialty Chemicals. The MUF resin was formulated to provide water-resistance and consisted of 10% wt melamine based on solids at an overall F/(M+U) molar ratio of 1.35. The resin also was incorporated with an inorganic internal catalyst. The MUF resin had a non-volatile solids content of 65.5%, a pH of 8.4, and a viscosity of 155 cps at 25°C. The base-catalyzed PF resin had a solids content of 51%, a pH in the 11.5-12.5 range and a viscosity in the 80-180 cps range at 25°C. In addition, a wax emulsion, Coscowax EW 58S was obtained from Hexion.

Methods

Manufacture of straw-based MDF composites

For each resin/wax combination, sufficient straw was refined to prepare three MDF panels of target density 850 kg/m^3 and dimensions 60×60×1 cm^3. Three resin/wax combinations were selected to manufacture the MDF panels (Table 1). Based on dry wheat straw mass, these were: 1) 12% MUF resin content with 0.5% wax content, 2) 12% MUF resin with 1.5% wax content, and 3) 12% PF resin with 0.5 % wax content.

Table 1. Parameters for MDF Manufacture Using 3 Resin/Wax Systems

Resin	Wax	Press cycle (sec)					Press temperature
(% solids on oven dry straw)		*Press Closing*	*Resin Cook*	*Degas*	*Press Open*	*Total*	(°C)
MUF (12%)	0.5%	45	345	30	60	480	160~166
MUF (12%)	1.5%	45	345	30	60	480	160~166
PF (12%)	0.5%	45	465	90	60	660	175

Pretreated wheat straw fibers, resin, and wax were loaded in a rotary blender. During blending, straw packets or balls formed, which could cause homogeneity problems in the furnish mat. The straw packets were therefore eliminated by passing through a Nelmor hammer mill.

The furnish mixture was then homogeneously placed in a forming mold with dimensions 61×61cm^2 by passing through a screen to even distribution. Panels were then hot-pressed in a 91x91cm^2 computed-controlled hydraulic press with oil-heated platens. Hot-pressing conditions are outlined in Table 1. After pressing, the panels were cooled to ambient temperature and panel thickness measured with a caliper. Specimens for materials properties were then machined.

Measurement of physical and mechanical properties

Internal bond strength (IB), modulus of elasticity (MOE), modulus of rupture (MOR), and thickness swell (TS) were determined according to ASTM D 1037-99 (American Society for Testing Materials 2006a). For each test, sample size was determined *a priori* according to ASTM E 122-00 (American Society for Testing Materials 2006b) using properties estimates based on the literature (Grigoriou 2000). As a result, 18 IB specimens, 9 MOE/MOR specimens and 9 TS specimens were prepared for each resin/wax combination from the three replicate boards. Dimensions for the test specimens were computed to be 50 x 50 x 10 mm^3 for IB, 290 x 76 x 10 mm^3 for flexural properties and 102 x 102 ×10 mm^3 for thickness swell. While ASTM calls for larger TS specimens, smaller samples are commonly utilized and were deemed acceptable for comparison. The specimen cut-up pattern for each panel was designed in order to randomize specimen location (Figure 1).

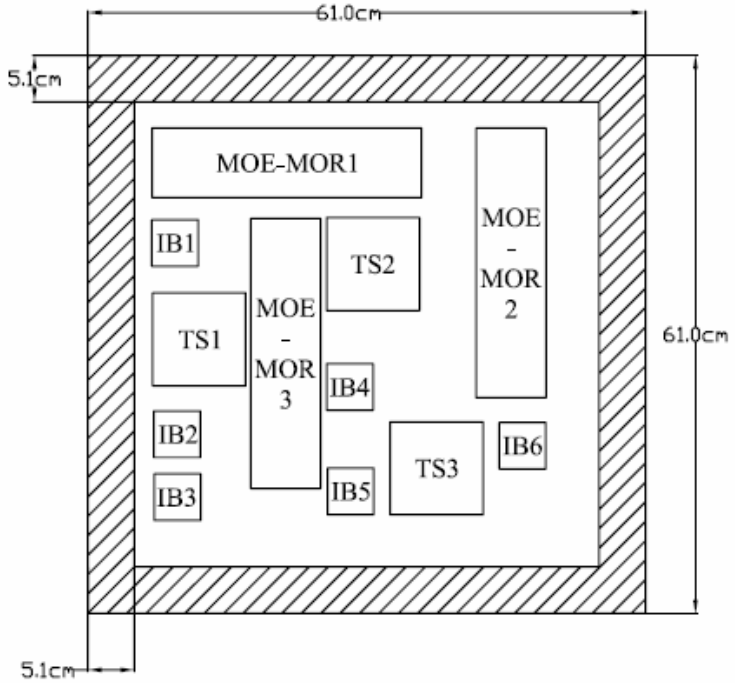

Fig. 1. Cut-up pattern for machining flexural (MOE-MOR), Internal bond (IB) and Thickness swelling (TS) specimens from each MDF panel.

Before IB and flexural property measurements, the specimens were equilibrated for 72 hours in a conditioning room having 65.4%± 0.1% relative humidity and at 20°C± 3°C. Weight and dimensions were measured on the IB specimens and the density was thus computed for each panel. In addition, the density profile was measured on the IB specimens using a QMS X-ray Density Profiler (Model QDP-01X. X-rays). Mechanical tests were performed on an INSTRON 4466. IB specimens were loaded at a crosshead speed of 0.78 mm/min. For flexural specimens, the loading rate was set at 0.47 mm/min and the test span was 234 mm. For thickness swelling test, the Method A, 2 Plus 22 hours submersion in water, of ASTM D 1037 was utilized. The measured properties for each of the three resin/wax combinations were compared to the requirements of the American national standard for MDF for interior applications. In addition, significant differences in the physical and mechanical properties measured for the three resin/wax combinations were detected by performing an ANOVA test at an α level of 0.1, followed by a Tukey test.

RESULTS AND DISCUSSION

Wheat straw based MDF panels with densities in the 870-920 kg/m^3 range were successfully manufactured using the three resin/wax combinations, MUF/0.5% wax, MUF/1.5% wax, and with the PF/0.5% wax. All the panels presented the typical density profile expected by mat densification. Namely, higher density was obtained near the panel face, while the core layer of the panel displayed a low density plateau (Figure 2).

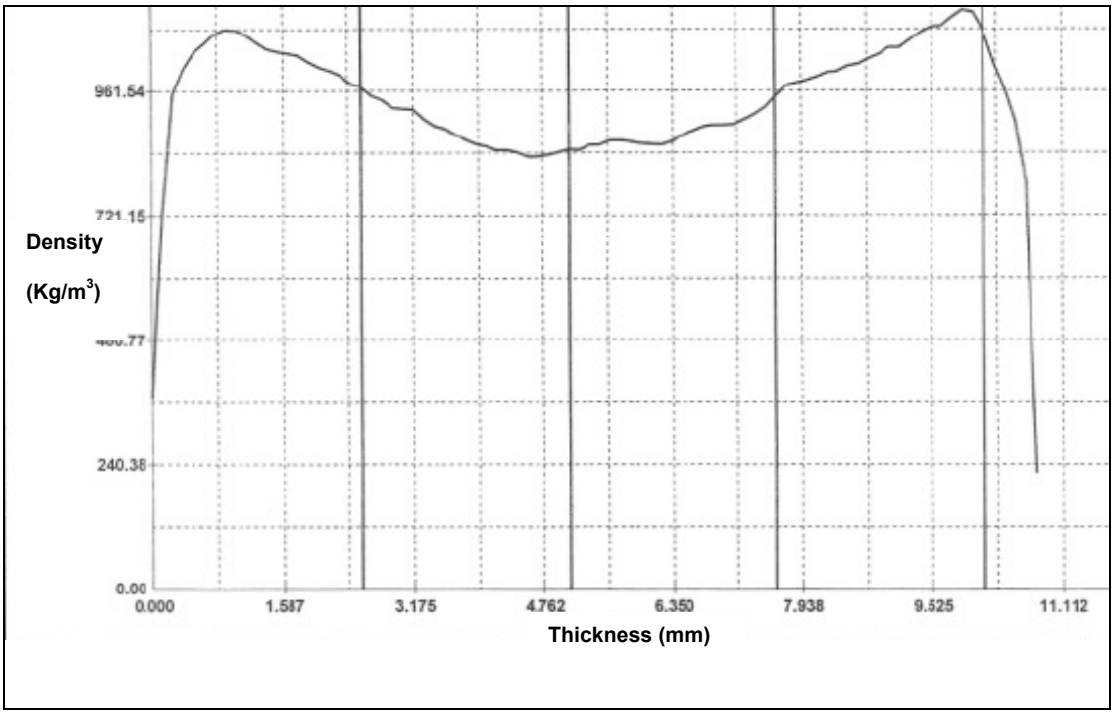

Fig. 2. Typical density profile of straw-based MDF boards

Table 2 summarizes the properties of the composites manufactured with the three resin/wax systems. In this table, significant differences in properties detected from the ANOVA/Tukey tests are indicated with the letter grouping. In addition, the data obtained in this study are compared to those obtained by Han et al. (2001b) on wheat straw MDF manufactured with UF resins. These composites had a density of 700 kg/m^3 and were obtained after pressure steaming and refining of the fibers (Han et al. 2001b). Finally the overall MDF grade obtained from the ANSI specifications for each property is indicated in Table 2. MDF is classified as 110, 120, 130, 140, 150, and 160 grades, with the 160 grade representing the best properties.

Table 2. Physical and Mechanical Properties of 10 mm Thick Wheat Straw-based MDF

	Density (kg/m^3)	MOE (N/mm^2)	MOR (N/mm^2)	IB (N/mm^2)	24h TS (mm)	MDF grade
MUF, 0.5 % wax	878±60	3895±651	33.1±2.7(A)	0.82±0.21 (A)	1.7±0.4(A)	**-**
MUF, 1.5 % wax	915 ±44	3773±440	26.3±3.3(B)	0.44±0.05 (C)	0.9±0.1(B)	**110**
PF, 0.5 % wax	916±60	3952±514	32.4±4.0(A)	0.57±0.09 (B)	1.0±0.3(B)	**120**
Han et al. 2001	~700	~2800	~32	~1	>25%	**-**

*(A), (B), (C) indicates Tukey grouping when significant differences were detected

For all the straw-based MDF manufactured, very high flexural properties were obtained and were minimally influenced by the choice of the resin/wax system. Similar MOE values were obtained with the three resin/ wax systems, above 3100 N/mm^2, which corresponds to the requirement for the best MDF grade, 160 grade (American National Standard Institute 2002). High MOR values were also measured, with the MUF/0.5% wax and the PF/0.5% wax systems ranking the best, again above the requirements for 160 grade MDF. When 1.5% wax was used in combination with the MUF resin, a lower MOR was obtained, but it still passed the grade 140 requirements for MDF. Altogether, the three resin/wax systems allowed for excellent flexural properties, which were likely related to the high density of the composites. These results are in line with previous work that measured high flexural properties in straw-based MDF (Grigoriou 2000; Han et al. 2001b; Mantanis and Berns 2001).

For internal bond strength, good values were also obtained with MDF manufactured with all 3 resin/wax systems, since all three passed the requirements for interior application. However, significant differences in IB were detected between the three resin/wax systems. The MUF resin in combination with 0.5% wax content performed best to a 140 grade MDF, above the PF/0.5% wax system, achieving a 120 grade, and well above the MUF/1.5% wax system, which reached a grade 110. Altogether, satisfactory internal bond strengths were obtained with both aminoplastic and phenolic resins. These results confirm that adequate adhesion can be obtained between wheat straw and aminoplastic or phenolic resins after simple fiber refining. As previously demonstrated, fiber refining improves the bondability of wheat straw by removing the waxy cuticle on the wheat straw surface and also by reducing its acid buffering capacity (Sauter 1996; Hague et al. 1998). The lowest IB measured in the

MUF/1.5% wax system is likely due to the wax interfering with the adhesion between the MUF and wheat straw.

The resin/wax combinations were selected with a view to improving the thickness swell properties, which have not been satisfactory to date with wheat-based straw MDF. When comparing the 24 hours thickness swell for the three resin/wax systems, it was evident that high wax content afforded the best TS properties. With the MUF/1.5% wax system, the composites had a low TS of 0.9 mm, well below the maximum allowance of 1.5 mm and corresponding to less than 10% TS. The PF resin with only 0.5% wax content performed similarly as the MUF/1.5% wax system within the ANSI requirements for MDF.

Phenol-formaldehyde resins are well known for their water-resistance and therefore are well suited to impart water resistance and low thickness swell properties to wheat-straw based composites even when used with low wax content. With the MUF resin on the other hand, high wax content must also be used to provide acceptable TS, since the MUF/0.5% wax content did not pass the MDF requirements for interior applications with a large TS of 1.7 mm. In the systems using MUF/1.5% wax and PF/0.5% wax, the average thickness swell was on the order of 10% maximum which was an improvement compared to previous reports of thickness swell of wheat straw-based MDF in the 20-30% range (Grigoriou 2000; Han et al. 2001b).

Overall, MDF composites prepared with MUF/1.5% wax and PF/0.5% wax both passed the minimum requirements for flexural properties, internal bond strength and also thickness swell, with the PF resin providing the best grade of MDF composite, 120 grade. With the MUF/1.5% wax system, the lowest MDF grade 110 was obtained overall. These results indicate that both MUF resins and PF resins could be used in combination with the appropriate wax content to manufacture wheat-straw based MDF composites that pass the ANSI requirements for interior applications, without resorting to expensive fiber modification (Gomez-Bueso et al. 2000; Han et al. 2001a). This is of significance because an impediment to the success of straw-based composites has been their low dimensional stability. Note that in this study the fiber preparation consisted of a simple refining step, suggesting that further improvement in physical and mechanical properties could be attained by optimizing the refining step using appropriate high-pressure conditions (Han et al. 2001b; Mantanis and Berns 2001).

CONCLUSIONS

1. Wheat straw-based MDF composites manufactured with aminoplastic and phenolic resins and appropriate wax contents passed the ANSI requirements for flexural properties, internal bond strength and also thickness swell for MDF used in interior applications.
2. The highest properties were achieved when a phenolic resin and a low wax content of 0.5% on wheat straw solids were used, resulting in a grade 120 straw-based MDF composite.
3. MDF composites bonded with a MUF resin and a wax content of 1.5% based on straw solids achieved a grade 110.

4. When wheat straw-based MDF composites were manufactured with a MUF resin in combination with low wax content of 0.5% on straw solids, the composites performed well above the standards for flexural and internal bond strength properties but failed to pass the ANSI requirement for thickness swell.

ACKNOWLEDGMENTS

This research was supported by the IMPACT (International Marketing Program for Agricultural Commodities and Trade) Center at Washington State University. The authors are thankful to Mark Anderson for specifically formulating a MUF resin for this project. The contribution of material from Hexion Specialty Chemicals is also acknowledged.

REFERENCES CITED

American National Standards Institute. (2002). *ANSI A208.2-2002: Medium Density Fiberboard (MDF) for Interior Applications*, Gaithersburg, MD, US.

American Society for Testing Materials. (2006a). *ASTM D 1037-99: Standard test methods for evaluating properties of wood-base fiber and particle panel materials* Philadelphia, PA.

American Society for Testing Materials. (2006b). *ASTM E 122-00: Standard practice for calculating sample size estimate, with a specified tolerable error, the average for a characteristic of a lot or process* Philadelphia, PA.

Averous, L., and Le Digabel, F. (2006). "Properties of biocomposites based on lignocellulosic fillers." *Carbohydrate Polymers* 66(4), 480-493.

Bowyer, J. L., and Stockmann, V. E. (2001). "Agricultural residues - An exciting bio-based raw material for the global panels industry." *Forest Products Journal* 51(1), 10-21.

Gomez-Bueso, J., Westin, M., Torgilsson, R., Olesen, P. O., and Simonson, R. (2000). "Composites made from acetylated lignocellulosic fibers of different origin - Part I. Properties of dry-formed fiberboards." *Holz Als Roh-Und Werkstoff* 58(1-2), 9-14.

Grigoriou, A. H. (2000). "Straw-wood composites bonded with various adhesive systems." *Wood Science and Technology* 34(4), 355-365.

Hague, J., McLauchlin, A., and Quinney, R. "Agri-materials for panel products: a technical assessment of their viability." *32nd international particleboard/ composite materials symposium*, Pullman, WA, 151-159.

Han, G. P., Umemura, K., Wong, E. D., Zhang, M., and Kawai, S. (2001a). "Effects of silane coupling agent level and extraction treatment on the properties of UF-bonded reed and wheat straw particleboards." *Journal of Wood Science* 47(1), 18-23.

Han, G. P., Umemura, K., Zhang, M., Honda, T., and Kawai, S. (2001b). "Development of high-performance UF-bonded reed and wheat straw medium-density fiberboard." *Journal of Wood Science* 47(5), 350-355.

Kinsella, S. (2004). "Environmental paper listening study Chapter four: tree free paper (http://www.conservatree.org/paperlisteningstudy/TreeFree/question51.html)."

Lengel, D. E. "Ag-Fiber "Dot gone"- A litany of failure." *35th international particleboard/ composite materials symposium*, Pullman, WA, 125-132.

Mantanis, G., and Berns, J. "Strawboards bonded with urea formaldehyde resins." *35th international particleboard/ composite materials symposium*, Pullman, WA, 137-144.

Markessini, E., Roffael, E., and Rigal, L. "Panels from annual plant fibers bonded with urea-formaldehyde resins." *31st international particleboard/ composite materials symposium*, Pullman, WA, 147-160.

Mo, X. Q., Cheng, E. Z., Wang, D. H., and Sun, X. S. (2003). "Physical properties of medium-density wheat straw particleboard using different adhesives." *Industrial Crops and Products* 18(1), 47-53.

Mo, X. Q., Wang, D., and Sun, X. S. (2005). "Straw-based biomass and biocomposites." Natural fibers, biopolymers, and biocomposites, A. K. Mohanty, M. Misra, and L. T. Drzal, eds., Taylor & Francis, Boca Raton, FL, 875 p.

Sauter, L. "Developing composites from wheat straw." *30th international particleboard/ composite materials symposium*, Pullman, WA, 197-214.

Schirp, A., Loge, F. J., Englund, K. R., Wolcott, M. P., Hess, J. R., Houghton, T. P., Lacey, J. A., and Thompson, D. N. (2006). "Pilot-scale production and material properties of extruded straw-plastic composites based on untreated and fungal-treated wheat straw." *Forest Products Journal* 56(10), 90-96.

Wasylciw, W. "Straw-based composite panels- attributes, issues, and UF bonding technology." *35th international particleboard/ composite materials symposium*, Pullman, WA, 145-153.

Wasylciw, W. (2002). "Methods of Straw fibre processing." C. Alberta Research Council, ed.

Zhang, Y., Lu, X., Pizzi, A., and Delmotte, L. (2003). "Wheat straw particleboard bonding improvements by enzyme pretreatment." *Holz Als Roh-Und Werkstoff* 61(1), 49-54.

Article submitted: Jan. 24, 2007; First-round reviews completed: February 13, 2007; Revised version accepted: Feb. 23, 2007; Published Feb. 25, 2007

CHARACTERIZATION OF LIPOPHILIC WOOD EXTRACTIVES FROM CLONES OF *Eucalyptus urograndis* CULTIVATE IN BRAZIL

Flaviano O. Silvério[a,b], Luiz C. A. Barbosa[a*], Célia R. A. Maltha[a], Armando J. D. Silvestre[c], Dorila Pilo-Veloso[b] and José L. Gomide[d],

The chemical compositions of the lipophilic extractives from four clones of *Eucalyptus urograndis* cultivated in Brazil were studied by gas chromatography-mass spectrometry (GC-MS) before and after alkaline hydrolysis. The four *E. urograndis* clones showed similar amounts of dichloromethane soluble (lipophilic) extractives (0.38-0.55% w/w). The major groups of compounds identified in the lipophilic fraction of extractives consisted mainly of fatty acids (mainly palmitic linoleic and oleic acids and small amounts of α- and ω-hydroxyacids), steroids (mainly β-sitosterol, β-sitostanol), followed by minor amounts long chain aliphatic alcohols, hydrocarbons and aromatic compounds. The relative abundances of these groups were similar for three of the clones with exception of the clone Ugc, which was shown to have much higher amounts of fatty acids and sterols. The high amounts of extractives found in these clones, and particularly of Ugc, when compared with other *Eucalyptus* species, suggests an increased risk of pitch formation during bleached pulp production.

Keywords: Lipophilic extractives, E. urograndis, Pitch, GC-MS analysis, Fatty acids, Steroid.

*Contact information: a: Department of Chemistry, Federal University of Viçosa, 36570-000, Viçosa, Brazil; b: Department of Chemistry, Federal University of Minas Gerais, 31270-901, Belo Horizonte, Brazil; c: CICECO and Department of Chemistry, University of Aveiro, 3810, Aveiro, Portugal; d: Department of Forest Engineering, Federal University of Viçosa, 36570-000, Viçosa, Brazil; *Corresponding author: lcab@ufv.br*

INTRODUCTION

Eucalyptus wood is at the present the most important short fiber source for pulp and paper production in Brazil due to its rapid growth and abundance throughout the country (Shatalov et al. 1999), as well as to its excellent pulp properties (Back and Allen 2000; Hillman 2002). Interest in the use of *Eucalyptus* species for pulp production has furthered research related to the chemical composition of this type of wood, aiming to improve the quality of clone plantations by means of genetic selection, considering especially the wood bulk chemical characteristics and the physico-mechanical properties of the ensuing bleached kraft fibres (Gonçalves et al. 2001; Caixeta et al. 2003a, 2003b).

In the last few years the study of the composition and behavior of *Eucalyptus* wood has been mainly focused on *E. globulus*, the dominant species cultivated in the Iberian Peninsula. Recently, the major features of *E. globulus* wood macromolecular

components (Neto et al. 2005) and extractives of this particular species (Silvestre et al. 2005) have been reviewed.

It is known that the amount and composition of wood extractives are important parameters in the wood processing for pulp and paper production (Back and Allen 2000; Hillman 2002). The *E. globulus* lipophilic extractives fraction, in particular, has been the subject of a significant number of papers (Swan and Akerblom 1967; Santos et al. 1997; Wallis et al. 1997; Gutiérrez et al. 1998, 1999; Gutiérrez and del Río 2001; Freire et al. 2002a, 2004) not only due to its impact on the formation of pitch deposits, giving rise to dark spots in bleached pulp and paper (Manji et al. 2005; Freire et al. 2002b; Gutiérrez et al. 1998), but also because these components might contribute to the consumption of bleaching chemicals (Freire et al. 2005, 2006a; Neto et al. 2004, 2005; Silvestre et al. 2005). These problems can be responsible for reducing levels of production, for increased operating costs and increased incidence of quality defects in the final product (del Río et al. 2000; Gutiérrez et al. 2001; Freire et al. 2002a).

Although the information gathered for *E. globulus* might be relevant to design strategies to prevent pitch episodes in bleached pulp mills operating with other *Eucalyptus* species, it is well known that for the *Eucalyptus* genus there are considerable variations in the chemical composition inter- and intra-species and with geographic location (Bland 1985; Gutíerrez et al. 1999; Freire et al. 2002a). Therefore, when intensive use of other species is to be implemented, it is strongly advisable to carry out detailed studies on its composition and behaviour during pulping and bleaching.

In Brazil, *E. urograndis* hybrids are one of the main species used for pulp production, representing nowadays the dominant *Eucalyptus* species planted in Brazil. This *Eucalyptus* hybrid shows very high forest productivity (in excess of 60 m^3/Ha/year), has a strong disease resistance, presents a high industrial pulping yield, and produces a high quality fiber for paper production (Gomide et al. 2005).

Due to the interest of this species in the Brazilian industrial context, several research programs have been implemented to improve *E. urograndis* wood quality and productivity (Rezende et al. 1994; Gonçalves et al. 2001; Gomide et al. 2005), involving genetic markers (Caixeta et al. 2003a) and other wood properties, including physical chemical and characteristics, and mechanical resistance (Caixeta et al. 2003b). In this context, the knowledge of the chemical composition of the newly selected plants woods is a fundamental step to understand and optimize their behavior during pulping and bleaching stages.

In this perspective, and within a wider project aiming to study the chemical composition of the selected plants in the pulping and bleaching process, in the present work we report a detailed characterization of lipophilic extractives of four clones of *E. urograndis*. These clones have been selected due to their high wood productivity and high industrial pulp yield (Gomide et al. 2005). Although a study on the chemical composition of lipophilic extractives of Brazilian *E. urograndis* (among other hardwood species) has been recently published (Freire et al. 2006), the wood samples used were of unspecified origin. This work aims to report the differences in lipophilic extractives composition of for specific clones of *E. urograndis,* from a of genetic selection program aiming to choose the best clones for pulp and paper production in Brazil.

EXPERIMENTAL

Samples

Wood samples of four selected *E. urograndis* clones (Uga, Ugb, Ugc and Ugd) were obtained from an eight-year old plantation from the state of Bahia in Brazil. The samples were obtained from the whole stem wood, as used in the pulp industry. The wood material was bark-free, chopped into small pieces (industrial size), and air-dried at ambient temperature for five days. It was then ground to pass a 1 mm sieve, screened in a vibratory sieving apparatus, and the 40-60 mesh fraction was used for chemical analysis.

Extraction

Air-dried powdered samples (2.00 g) were extracted with acetone for 6 hours using a Soxhlet apparatus. The solvent was removed under reduced pressure in a rotary evaporator, and the extracts were weighed. All extractions were carried out in triplicate, and the extraction yields were expressed in percentage in relation to the wood's dry weight.

To isolate the lipophilic fraction, the acetone extract was redissolved in dichloromethane (3 x 2 mL) and filtered off, as described by del Río et al. (1998). The derivatized dichloromethane soluble (lipophilic) residues were analyzed by GC-MS, before and after hydrolysis as described bellow.

Alkaline Hydrolysis

10 mg of the dichloromethane extract were added to a two-neck round-bottomed flask, followed by 1.8 mL aqueous solution of KOH (3 mol L^{-1}) and 0.2 mL of methanol. The mixture was refluxed under nitrogen atmosphere for 1h. It was then cooled down to room temperature, acidified with aqueous HCl (3 mol L^{-1}) to pH~2 and extracted with dichloromethane (3 x 2 mL). The combined organic extracts were dried over anhydrous $MgSO_4$, filtered off, and the solvent was completely removed under reduced pressure in a rotary evaporator.

Derivatization

Aliquots of hydrolyzed and non-hydrolyzed dichloromethane extracts (2.0 mg) were dissolved in pyridine (60 μL) in capped vials followed by the addition of 100 μL *bis*(trimethylsilyl)-trifluoroacetamide containing 1% chlorotrimethylsilane. The reaction mixture was heated at 70 ºC for 30 min. It was then cooled down to room temperature before GC-MS analysis (Cruz et al. 2006).

GC-MS Analysis

GC-MS analyses were performed on a Shimadzu PQ5050A GC-MS equipped with an AOC-5000 autoinjector and a DB-1 J&W capillary column (30 m x 0.25 mm i.d., 0.25 μm film thickness), using helium as carrier gas (35 cm/s). The chromatographic conditions were as follows: injector temperature 290 ºC; oven initial temperature 80 ºC held for 5 min; temperature rate 4 ºC/min; final temperature 285 ºC held for 40 min. The

transfer-line temperature was 290 ºC, and a split ratio of 1:10 was used. The mass detector was operated at electron impact mode (70 eV) with a scan range of 30 to 600 *m/z*.

For semi-quantitative analysis, the GC-MS equipment was calibrated with pure reference compounds, representative of the major extractives components (namely, hexadecanoic acid, hexadecan-1-ol, 16-hydroxyhexadecanoic acid, 2-hydroxyoctanoic acid, tetracosane, β-sitosterol and *trans*-ferulic acid), relative to hexanedioic acid and tetracosane used as internal standards, as described by Freire et al. (2002a). The corresponding response factors needed to obtain correct quantifications were calculated as an average of sixteen GC-MS runs.

Compounds were identified as TMS derivatives by comparing their mass spectra with the GC-MS spectral library (Willey 333.000), with data from the literature and when necessary, by injection of standard compounds.

RESULTS AND DISCUSSION

The present study has considered the analysis of the nonpolar extracts before and after alkaline hydrolysis to verify the amount of lipophilic compounds present in the woods in free and esterified forms, as has been reported by others (Swan and Akerblom 1967; Santos et al. 1997; Gutiérrez et al. 1999; Freire et al. 2002a, 2004; Silvestre et al. 2005). The lipophilic fraction can be selectively isolated from the more complex acetone extract by dissolution in small volumes of dichloromethane (del Río et al. 1998; Silvério et al. 2006).

The total amount of extractives (3.92%) from Ugc dry wood was much higher than the values found for the other three clones (1.32%; 1.92% and 2.17% for Uga, Ugb and Ugd, respectively). In terms of the lipophilic fraction, clones Ugd and Ugb presented slightly higher yields (0.53% and 0.55% w/w, respectively), than those found for Ugc and Uga (0.44% and 0.38% w/w, respectively).

The average percentage of lipophilic extractives (0.47%) found for the studied clones was superior to the typically reported values (~0.26%) for *E. globulus* (Gutiérrez et al. 1998, 1999; Freire et al. 2002a) and also to the values reported for *E. urograndis* (0.35%) and *E. grandis* (0.36%) (Freire et al. 2006b), suggesting that increased attention should be paid to avoid pitch problems while processing wood from these clones for bleached pulp production

Fig. 1 shows a typical GC-MS chromatogram obtained for *E. urograndis* (Uga) extract, after alkaline hydrolysis. The GC-MS analysis of the derivatized dichloromethane extracts before and after hydrolysis of the four *E. urograndis* clones (Uga, Ugb, Ugc and Ugd) revealed that they were quite similar in terms of qualitative composition, although from a quantitative point of view the extract of Ugc contained higher amounts of fatty acids and steroids (Table 1).

Fatty acids and sterols are the main groups of compounds found in the lipophilic extractives of the four studied *Eucalyptus* clones, along with smaller amounts of long chain aliphatic alcohols, hydrocarbons and aromatic compounds. The major classes of identified compounds and their abundances, before and after hydrolysis, are shown in Table 1 and Fig. 2.

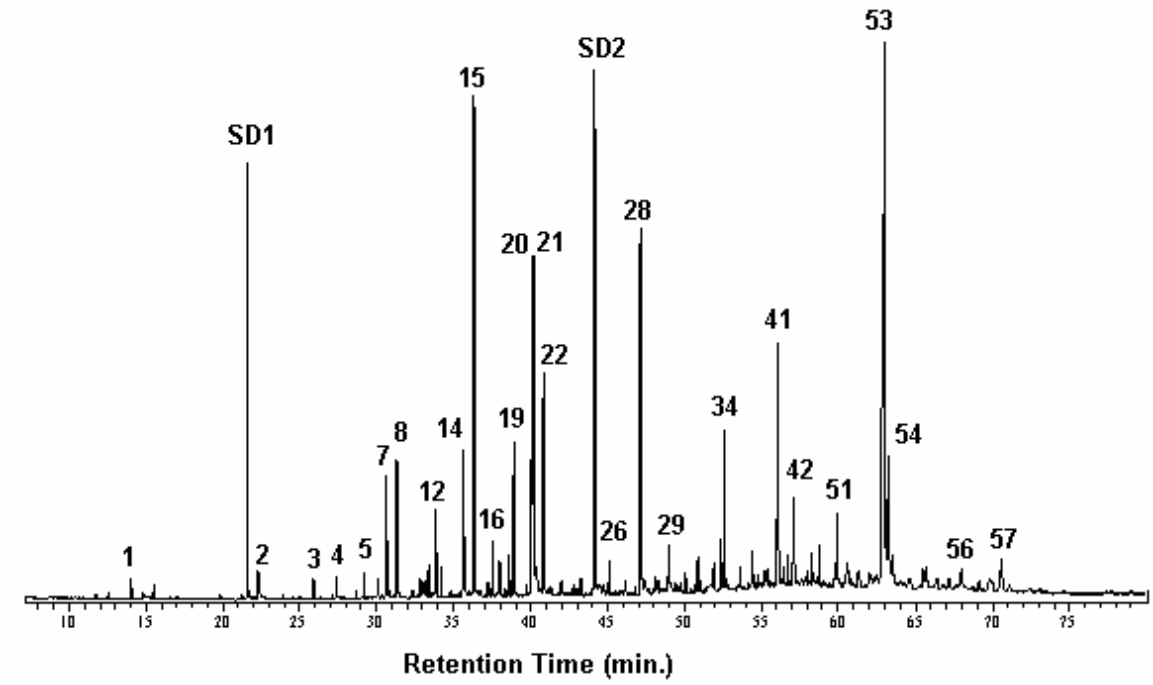

Fig. 1. Total ion chromatogram of the derivatized lipophilic extract of *E. urograndis* (Uga) wood: **IS1** and **IS2:** internal standards. **1**- Glycerol, **2**- 3-methoxy-4-hydroxy-benzaldehyde, **3** - Dodecanoic acid, **4**- 4-Hydroxy-3,5-dimethoxybenzoic acid, **5**- 4-Hydroxy-3-methoxybenzoic acid, **6**- Nonanodioic acid (azelaic acid), **7**- Tetradecen-9-enoic acid, **8-** Tetradecanoic acid, **9-** 4-Hydroxy-3,5-dimethoxybenzoic acid, **10-** pentadec-9-enoic acid, **11** *cis*-Ferulic acid, **12-** Pentadecanoic acid, **13-** Hexadecan-1-ol, **14 -** Hexadecan-9-enoic acid, **15 -** Hexadecanoic acid, **16 -** *trans*-Ferulic acid, **17-** Heptadec-9-enoic acid, **18-** Heptadecanoic acid, **19-** Octadecan-1-ol, **20**- Octadec-9,12-dienoic acid, **21**- Octadec-9-enoic acid, **22**- Octadecanoic acid, **23-** Hydrocarbon*, **24**- Nonadecanoic acid, **25**- Eicosan-1-ol, **26**- Eicosanoic acid, **27-** Hydrocarbon*, **28-** Hydrocarbon*, **29**- Docosanoic acid, **30**- 2-hydroxyhexadecanoic acid, **31**- Tricosanoic acid, **32-** Tetracosan-1-ol,,**33**- Hydrocarbon*, **34**- Tetracosanoic acid, **35-** Hydro- carbon*, **36**- Pentacosanoic acid, **37**- 2-Hydroxytetracosanoic acid, **38**- Hexacosan-1-ol, **39**- 22-Hydroxy-docosanoic acid, **40-** Hydrocarbon*, **41-** Hexacosanoic acid, **42**- Stigmast-5-en-3-ol, **43**- Hepta-cosanoic acid, **44**- Cholest-8-en-3-one, **45**- non-identified (n.i.) steroid, **46**- n.i. steroid, **47**- Cholestane-3,5-diol, **48**- n.i. steroid, 49- 24-Hydroxytetracosanoic acid, **50**- Octacosan-1-ol, **51**- Octacosanoic acid, **52**- n.i. steroid, **53**- β-Sitosterol, **54**- β-Sitostanol, **55**- 25-Hydroxy-pentacosanoic acid, **56**- 26-Hydroxyhexacosanoic acid, **57**- Stigmasta-5,22-dien-3-ol.*The compound was not completely identified as the molecular ion peak was not observed in the mass spectrum, but from the fragmentation pattern it was clearly a long chain hydrocarbon.

Although the percentage of lipophilic extractives from the wood of the four clones of *E. urograndis* varied within a narrow range (0.38 % to 0.55% w/w), a striking variation in the amounts of specific lipophilic compounds identified was verified by GC-MS. This significant variation is mainly due to fatty acids and sterols, as can be observed in Table 1. After alkaline hydrolysis, a substantial increase in the amount of both fatty acids and steroids was observed, as detected by GC-MS analysis (Table 1, Fig. 2). These results provide evidence of the presence of significant amounts of esterified structures,

such as sterols esters and other esters in the original extract, as reported in other studies (Wallis and Wearne 1997; Gutierrez et al. 1999; Freire et al. 2002a, 2002b).

The increase in the percentage of fatty acids after hydrolysis is due essentially to components containing 16 to 18 carbons atoms and others having 19 or more carbons atoms (Fig. 3), including saturated and unsaturated fatty acids and hydroxyacids. In accordance with our results, there have been reports of the association of these acids with sterols, alcohols, or glycerol (Gutierrez et al. 1999; Freire et al. 2002a).

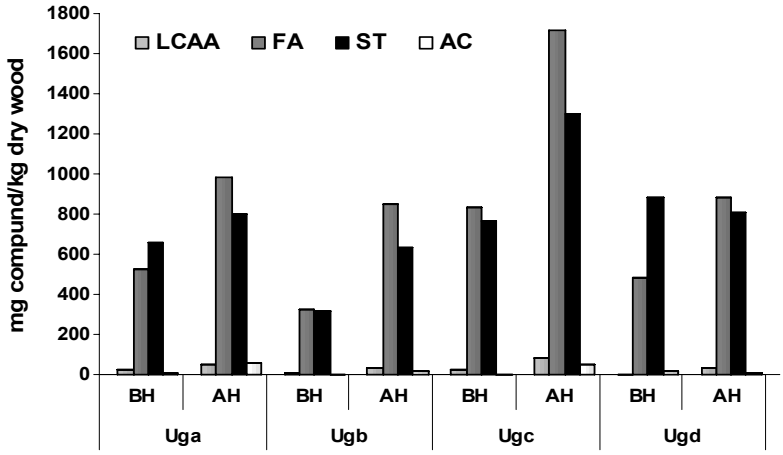

Fig. 2. Major families of compounds identified in the lipophilic extracts, before (**BH**) and after hydrolysis (**AH**), of *E. urograndis* clones (Uga, Ugb, Ugc and Ugd, respectively). LCAA: long chain aliphatic alcohols, FA: fatty acids, ST: sterols, AC: aromatic compounds.

The most abundant fatty acids found in the hydrolyzed and non-hydrolyzed dichloromethane extracts were palmitic, linoleic, and oleic acids. For the hydrolyzed extracts the amounts found were: palmitic (161.4, 162.7, 310.8 and 166.9 mg/kg for Uga, Ugb, Ugc and Ugd, respectively), linoleic (172.6, 78.6, 257.1 and 147 mg/kg for Uga, Ugb, Ugc and Ugd, respectively), and oleic (145.8, 127.2, 305.4 and 105.7 mg/kg for Uga, Ugb, Ugc and Ugd, respectively). Compared to previously published data, these figures are much higher than those reported in the hydrolyzed extracts of *E. globulus* (76.1 mg/kg of palmitic acid, 62.8 mg/kg of linoleic acid and 41.0 mg/kg of oleic acid) (Freire et al. 2002a).

Other identified fatty acids were dodecanoic, tetradecanoic, pentadecanoic, hexadecanoic, heptadecanoic, octadecanoic, eicosanoic, docosanoic, tricosanoic, tetracosanoic, pentacosanoic, hexacosanoic, heptacosanoic, and octacosanoic acids.

The total amount of fatty acids found in the hydrolyzed dichloromethane extracts for clones Uga, Ugb, Ugc, and Ugd were significantly higher (979.5, 841.5, 1930.3 and 886.0 mg/kg) when compared to the amount found in the dichloromethane extract of *E. globulus* (520.9 mg/kg) (Freire et al. 2002a). The same was observed for the non-hydrolyzed dichloromethane extract. These results suggest that all four *E. urograndis* clones studied are more prone to result in pitch deposition during pulp production, but

particularly the Ugc clone, when compared with *E. globulus*. Fatty acids were identified based on their characteristic fragmentation patterns (Budzikiowicz and Djerassi 1967; McLafferty and Turecek 1992; Freire et al. 2002a).

Table 1 – Main families of lipophilic components identified in the lipophilic extracts of woods of the *E. urograndis* clones and their contents (mg/kg dry wood) before (BH) and after (AH) alkaline hydrolysis.

Family	UGA		UGB		UGC		UGD	
	BH	AH	BH	AH	BH	AH	BH	AH
Fatty acids	**520.3**	**979.5**	**328.3**	**841.5**	**839.6**	**1930.3**	**485.9**	**886.0**
Saturated	305.1	516.5	176.9	569.2	416.3	1030.2	277.0	533.4
Unsaturated	209.5	405.9	144.6	240.2	420.5	832.9	195.6	329.1
Hydroxyacids	5.7	57.0	6.8	32.1	2.8	67.2	13.3	23.6
Aromatic compounds	**8.9**	**59.4**	**-**	**15.2**	**-**	**46.9**	**14.5**	**7.7**
Aromatic acids	8.9	49.7	-	15.2	-	46.9	6.8	11.9
Others	-	9.7	-	-	-	-	-	-
Long Chain Aliphatic Alcohols	**22.6**	**48.8**	**8.1**	**32.4**	**24.8**	**81.7**	**2.8**	**29.5**
<C20	18.3	45.6	8.1	22.1	21.8	42.8	2.8	29.5
>C20	4.3	3.2	-	10.3	3.0	38.9	-	-
Sterols	**604.1**	**781.4**	**314.7**	**621.3**	**768.4**	**1239.8**	**884**	**809.8**
Hydrocarbons	**67.8**	**27.7**	**119.2**	**18.4**	**18.6**	**8.3**	**15.0**	**14.2**
Others/unidentified	52.4	19.0	3.5	13.5	-	60.5	-	-
TOTAL	**1276.1**	**1915.8**	**773.8**	**1542.3**	**1641.4**	**3377.9**	**1388.7**	**1751.4**

GC-MS analysis also made it possible to identify four ω-hydroxy fatty acids, namely 22-hydroxydocosanoic, 24-hydroxytetracosanoic, 25-hydroxypentacosanoic, and 26-hydroxyhexacosanoic acids. These ω-hydroxy fatty acids were identified as TMS derivatives, based on their characteristic fragmentations (Draffan et al. 1968; Petersson 1972; Freire et al. 2002a), and the fragmentations confirmed by injection of a reference sample of 16-hydroxyhexadecanoic acid (as TMS derivative).

Two α-hydroxyfatty acids, namely 2-hydroxytetracosanoic and 2-hydroxy-hexadecanoic acid were found in *E. urograndis* wood extracts after alkaline hydrolysis, based on their characteristic fragmentation patterns (Budzikiewicz et al. 1967; Draffan et al. 1968; Petersson 1972; McLafferty and Turecedk 1992; Freire et al. 2002a), and the fragmentations confirmed by injection of compounds. The presence of *α*-hydroxyfatty acids has been previously reported in *E. globulus* (Freire et al. 2002a, 2002b).

It has been demonstrated that these α- and ω-hydroxyfatty acids are commonly found as abundant components of pitch deposits (Silvestre et al. 1999; Freire et al. 2002b). The significantly lower abundance of α- and ω-hydroxy fatty acids in the wood

of the *E. urograndis* clones studied seems to be clearly beneficial as far as pitch formation is concerned.

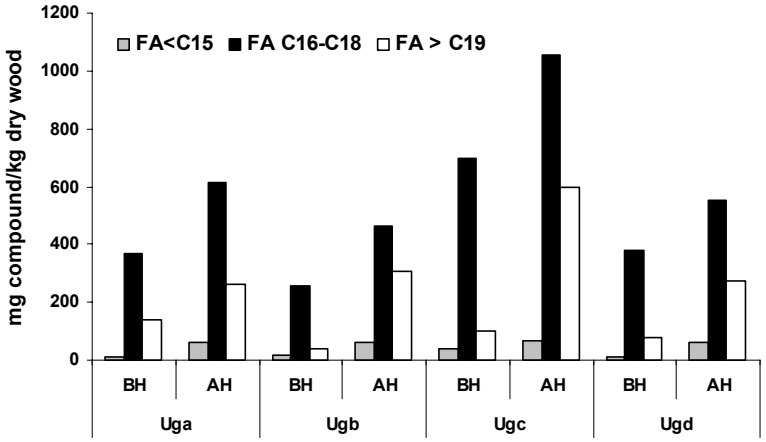

Fig. 3. Major fatty acids present in the lipophilic extracts of the clones of *E. urograndis* (**Uga**, **Ugb**, **Ugc** and **Ugd)** investigated before (**BH**), and after hydrolysis (**AH**), **FA <C15** fatty acids with less than 16 carbon atoms**, FA C16-C18** carbons atoms and **FA > 19** fatty acids with more than 19 carbons atoms**.**

In terms of total sterols content (Fig. 2; Table 1), it was observed that the hydrolysis caused an increase for all clones except Ugd, where it stayed roughly constant. These results indicate that the wood steroids are in both free and esterified forms. Among the steroids identified in all extracts, β-sitosterol and β-sitostanol were the main ones. In the hydrolyzed extracts, the amount of β-sitosterol for clone Ugb (429.9 mg/kg) was slightly higher than has been reported for *E. globulus* (346.7 mg/kg) (Freire et al. 2002a), while the quantities found in Uga (608.3 mg/kg), Ugc (907.0 mg/kg) and Ugd (708.4 mg/kg) were significantly higher. These compounds are quite common in *Eucalyptus* wood extracts, and their presence has been reported in pitch deposits (Freire et al. 2002b; Silvestre et al. 1999).

Other steroids, identified in smaller amounts, were stigmast-5-en-3-ol (Ugc and Ugd, after hydrolysis), cholest-8-en-3-one (Ugb, after hydrolysis), cholestane-3,5-diol (after hydrolysis), stigmaste-5,22-dien-3-ol (Uga, before and after hydrolysis), and stigmasta-4-en-3-one (Uga, before and after hydrolysis, Ugd, before hydrolysis). These compounds were identified based in their fragmentation characteristics (Budzikiewicz et al. 1967; Diekman and Djerassi 1967; Gustafsson et al. 1968; Brooks et al. 1979).

It is worth mentioning that the total amounts of the two most abundant families (after hydrolysis), i.e. fatty acids and sterols found in the four clones, is higher than the values previously reported for *E urograndis* (Freire et al. 2006), which clearly suggests that despite the higher quality of their woods for pulp production, there is an increased potential of pitch formation problems. This potential is particularly acute in the case of Ugc wood.

Fatty alcohols represented a small portion of the total extractives analyzed by GC-MS before and after hydrolysis (Table 1 and Fig. 2). Octadecan-1-ol and hexadecan-1-ol were the major components of this class, followed by eicosan-1-ol, tetracosan-1-ol, hexacosan-1-ol, and octacosan-1-ol. The compounds were identified based on their fragmentation characteristics (Budzikiewicz et al. 1967).

The aromatic fraction was mainly composed by 4-hydroxy-3-methoxy-benzaldehyde, 4-hydroxy-3,5-dimethoxybenzaldehyde, 4-hydroxy-3-methoxybenzoic, and 4-hydroxy-3,5-dimethoxybenzoic acids identified in the extracts in small amounts before (<15 mg/kg) and after (<60 mg/kg) hydrolysis. Ferulic acid (*cis* + *trans*) was found only in the hydrolyzed extracts; it represented the main aromatic compound identified in the extracts of clones Uga, Ugb, Ugc and Ugd (33.3, 8.9, 46.9 and 11.9 mg/kg, respectively).

The percentage of components identified in the hydrolyzed extracts of the clone Uga was approximately 50.5% of the total lipophilic extractives. These results are in good agreement with other reports in the literature for *E. globulus*, where only around 50% of the total mass of the extracts were identified (Freire et al. 2002a, 2002b, 2006b). However, for clones Ugb and Ugd the components identified represented only 28.2% and 33.1%, respectively, and for clone Ugc approximately 76.8% of the extractive compounds were identified in agreement with Gutierrez et al. (1999).

This considerable variability the total amounts of identified lipophilic extractives as well as the percentage of the lipophilic extract, is certainly due to the genetic variability between the four clones, together with the variation of growth location (Freire et al. 2006). These differences can be explained by the presence of steryl glycosides, not detected in this work. Steryl glycosides are compounds that do not hydrolyze easily under alkaline hydrolysis conditions, and consequently, may not be identified with the methodology used. These compounds have been reported in several *Eucalyptus* species (including *E. globulus*, *E. grandis*, and *E. urograndis*) as problematic for pitch deposition (Gutiérrez and del Río 2001; Freire et al. 2004, 2006b).

CONCLUSIONS

1. The present study reports the identification and quantification of fifty-five compounds present in the lipophilic extracts of four clones of *Eucalyptus urograndis*.
2. Fatty acids and sterols are responsible, respectively, for approximately 51% and 41.8% of the identified compounds in the extracts of the Uga, 54.5% and 41.2% of the Ugb, 57.1% and 38.5% of the Ugc, and 50.6% and 46.2% of the Ugd.
3. The main components of these two classes are palmitoleic, linoleic, and oleic acids, and β-sitosterol. In general the detected amounts of the components of both families increase considerably after alkaline hydrolysis, which suggest that they could in part be removed in the black liquor, during kraft pulping
4. Three of the studied clones (Uga, Ugb and Ugd) showed identifiable lipophilic extractives in amounts similar to those previously reported for *E. urograndis* (Freire et al. 2006b), whereas the other clone, Ugc, showed considerably higher amounts. In this perspective, and considering that these figures are in any case considerably

higher than those reported for Iberian *E. globulus*, the industrial processing of these clones of wood will require increased attention to the control of pitch formation.

5. Finally, future work will be required to explain the differences in the composition of the lipophilic fraction of the studied clones; and to study the steryl glucosides fraction, known to contribute to pitch deposition (Gutiérrez and del Río 2001; Freire et al. 2004, 2006b).

ACKNOWLEDGMENTS

The authors are grateful to Conselho Nacional de Desenvolvimento Científico e Tecnológico (CNPq) for financial support and research fellowships (LCAB, DPV) and a PhD studentship (FOS); Fundação de Amparo à Pesquisa do Estado de Minas Gerais (FAPEMIG) for financial support (Research grant nº CEX 81796-05).

REFERENCES CITED

Back, E. L. and Allen, L. H. (eds.) (2000). *Pitch Control, Wood Resin and Deresination*, Tappi Press, Atlanta.

Bland, D. E. (1985). "The composition and analysis of eucalypt wood," *Appita J*. 38(4), 291-294.

Brooks, C. J. W. (1979). "Some aspects of mass spectrometry in research on steroids," *Phil. Trans. R. Soc. London A,* 293, 53-67.

Budzikiewicz, H., Djerassi, C., and Williams, D. H. (1967). *Mass Spectrometry of Organic Compounds*, Holden-Day, London.

Caixeta, R. P., Carvalho, D., Rosado, S. C. S., and Trugilho, P. F. (2003a). "Variações genéticas em populações de *Eucalyptus* ssp. detectadas por meio de marcadores moleculares," *R. Árvore* 27(3), 357-363.

Caixeta, R. P., Trugilho, P. F., Rosado, S. C. S., and Lima, J. T. (2003b). "Propriedades e classificação da madeira aplicadas à seleção de genótipos de *Eucalyptus,*" *R. Árvore* 27(1), 43-51.

Cruz, M. P., Barbosa, L. C. A., Maltha, C. R. A., Gomide, J. L., and Milanês, A. F. (2006). "Chemical characterization of pitch in *Eucalyptus* pulp and paper industry." *Química Nova* 29(3), 459-466.

Del Río, J. C., A. Gutiérrez, F. C., González-Vila, F. J., Martin, F., and Romero, J. (1998). "Characterization of organic deposits produced in kraft pulping of *Eucalyptus globulus* wood," *J. Chromaotgr. A*. 823, 457-465.

Del Río, J. C., Romero, J., and Gutiérrez, A. (2000). "Analysis of pitch deposits produced in kraft pulp mills using a totally chlorine free bleaching sequence," *J. Chromaotgr. A*. 874(2), 235-245.

Diekman, J., and Djerassi, C. (1967). "Mass spectrometry in structural and stereochemical problems. CXXV. Mass spectrometry of some steroid trimethylsilyl ethers," *J. Org. Chem*. 32, 1005-1012.

Draffan, G. H., Stillwell, R. N., and McCloskey, J. A. (1968). "Electron impact-induced rearrangement of trimethylsilyl groups in long chain compounds," *Org. Mass. Spectr.* 1, 669-685.

Freire, C. S. R., Silvestre, A. J. D., and Neto, C. P. (2002a). "Identification of new hydroxy fatty acids and ferulic acid ester in the wood of *Eucalyptus globulus,*" *Holzforshung* 56(2), 143-149.

Freire, C. S. R., Silvestre, A. J. D., Pereira, C. C. L., Neto, C. P., and Cavaleiro, J. A. S. (2002b). "New lipophilic components of pitch deposits from an *Eucalyptus globulus* ECF bleached kraft pulp mill," *J. Wood Chem. Technol.* 22(1), 55-66.

Freire, C. S. R., Silvestre, A. J. D., Neto, C. P., Domingues, P., and Silva, A. M. S. (2004). "New glycosides in the wood and bark of *Eucalyptus* and Kraft pulps," *Holzforshung* 58(5), 501-503.

Freire, C. S. R., Silvestre, A. J. D., and Neto, C. P. (2005). "Lipophilic extractives in *Eucalyptus globulus* kraft pulps. Behaviour during ECF bleaching," *J. Wood Chem. Technol.* 25(1-2), 67-80.

Freire, C. S. R., Silvestre, A. J. D., Neto, C. P., and Evtuguin, D. V. (2006a). "Effect of oxygen, ozone and hydrogen peroxide bleaching stages on the contents and composition of extractives of *Eucalyptus globulus* kraft pulps," *Biores. Technol.* 97(3), 420-428.

Freire, C. S. R., Pinto, P. C. R., Santiago, A. S., Silvestre, A. J. D., Evtuguin, D. V., and Neto, C. P. (2006b). "Comparative study of lipophilic extractives of hardwoods and corresponding ECF bleached Kraft pulps," *BioResources* 1(1), 3-17.

Gonçalves, F. M. A., Rezende, G. D. S. P., Bertolucci, F. L. G., and Ramalho, M. A. P. (2001). "Progresso genético por meio da seleção de clones de eucalipto em plantios comerciais," *R. Árvore* 25(3), 295-301.

Gustafsson, J. A., Ryhage, R., and Sjövall. J. (1969). "Migration of the trimethylsilyl group upon electron impact in steroids," *J. Am. Chem. Soc.* 91(5), 1236-1234.

Gutiérrez, A., Del Río, J. C., Gonzáles-Vila, F. J., and Martin, E. F. (1998). "Analysis of lipophilic extractives from wood and pitch deposits by solid-phase extraction and gas chromatography," *J. Chromatogr. A* 823, 449-455.

Gutiérrez, A., Del Río, J. C., Gonzáles-Vila, F. J., Martin, E. F. (1999). "Chemical composition of lipophilic extractives from *Eucalyptus globulus* Labill wood," *Holzforschung* 53, 481-486.

Gutiérrez, A., Romero, J., and del Río, J. C. (2001). "Lipophilic extractives from *Eucalyptus globulus* pulp during kraft cooking followed by TCF and ECF bleaching," *Holzforschung* 55(3), 260-264.

Gutiérrez, A., and del Río, J. C. (2001). "Gas chromatography-mass spectrometry demonstration of steryl glycosides in eucalypt wood kraft pulp and process liquids,"*Rapid Commun. Mass Spectrom.* 15, 2515-2520.

Hillman, D. C. (2002). "Single-species pulping. The world's preferred market pulps," *Solutions*, Nov., 27-28.

Manji, A., Salgar. S., Constant, J., Silva, D. J. S., and Almeida, J. M. (2005). "Uma nova alternativa para eliminar o talco e reduzir pitch e extrativos na produção de celulose," *O Papel*, Maio, 82-87.

McLafferty, F. W., and Turecek, F. (1992). *Interpretation of Mass Spectra*, 4th Ed., University Science, Books, California.

Neto, C. P., Silvestre, A. J. D., Evtuguin, D. V., Freire, C. S. R., Pinto, P. C. R., and Santiago, A. S. (2004). "Bulk and surface composition of ECF bleached hardwood kraft pulp fibres," *Nord Pulp Paper Res. J.* 19(4), 513-520.

Neto, C. P., Evtuguin, D. V., and Pinto, P. C. (2005). "Componentes macromoleculares das madeiras de *Eucalyptus* e de outras folhosas: na aptidão ao cozimento e branqueamento," *O Papel/Aveiro* 1, 17-26.

Petersson, G. (1972). "Mass spectrometry of hydroxyl dicarboxylic acids as trimethylsilyl derivatives. Rearrangement fragmentations," *Org. Mass Spec*. 6, 565-576.

Rezende, G. D. S. P., Bertolucci, F. L. G., and Ramalho, M. A. P. (1994). "Eficiência da seleção precoce na recomendação de clones de eucalipto avaliados no norte do Espírito Santo e sul da Bahia," *Revista Cerne* 1(1), 45-50.

Santos, G. G., Alves, J. C. N., Rodilla, J. M. L., Duarte, A. P., Lithgow, A. M., and Urones, J. G. (1997). "Terpenoids and other constituints of *Eucalyptus globulus*," *Phytochem.* 44(7), 1309-1312.

Shatalov, A. A., Evtuguin, D. V., and Pascoal Neto, C. (1999). "2-O-α-D-Galactopyranosyl-4-O-methyl-α-D-glucurono)-D-Xylan from *Eucalyptus globulus* Labill," *Carbohydr. Res.* 320, 93-99.

Silvério, F. O., Barbosa, L. C. A., Gomide, J. L., Reis, F. P., and Pilo-Veloso, D. (2006). "Metodologia de Extração e Determinação do Teor de Extrativos em Madeiras de Eucalipto," *R. Árvore* 62(6), 1009-1016.

Silvestre, A. J. D., Pereira, C. C. L., Neto, C. P., Evtuguin, D. V., Duarte, A. C., Cavaleiro, J. A. S., and Furtado, F. P. (1999). "Chemical composition of *pitch* deposits from an ECF *Eucalyptus globulus* bleached kraft pulp mill: Its relationship with wood extractives and additives in process streams," *Appita J.* 52(5), 375-382.

Silvestre, A. J. D., Neto, C. P., and Freire, C. S. R. (2005). "Componentes lipofílicos da madeira de *Eucalyptus globulus*: Comportamento durante a produção de pasta de papel," *O Papel/Aveiro* 1, 5-16.

Swan, B., and Akerblom, I. S. (1967). "Wood extractives from *Eucalyptus globulus* Labill," *Svensk Papperstidn* 70(7), 239-244.

Wallis, A. F. A., Wearne, R. H., and Wright, J. P. (1997). "Analysis of resin in eucalypt woods and pulps," *Proc. 51st Annual General Conference. Appita*, Melbourne, Vol. I, pp. 45-50.

Wallis, A. F. A., Wearne, R. H., and Wright, J. P., (1999). "Analysis of resin in eucalypt woods and pulps," *Appita J.* 52(4), 295-299.

Article submitted: Jan. 18, 2007; First reviews completed: Feb. 13, 2007; Revised version accepted: Feb. 24, 2007; Published: Feb. 27, 2007.

QUANTITATIVE LIGNIN ANALYSIS BASED ON PERMANGANATE OXIDATION

Jim Parkås,[a†*] Gösta Brunow,[b] and Knut Lundquist [a]

Qualitative lignin analysis relies rather much on studies of lignin degradation products. As concerns precise quantification of lignin's composition such studies in general have obvious limitations. Aromatic acids obtained on permanganate oxidation of pretreated lignins (cleavage of ethers and alkylation of phenolic groups) offer a possibility to estimate the amounts of differently substituted aromatic units in lignins. An equation is derived for the calculation of the gross composition of lignins based on the yields of methoxy-substituted aromatic acids obtained on permanganate oxidation of lignins with methylated phenolic groups. The equation could also be used for the calculation of the phenolic content in a lignin sample based on permanganate oxidation data, provided that such data are available for a similar lignin sample with known phenolic content. Literature data for milled wood lignin from spruce are used to exemplify the calculations.

Keywords: Aromatic acids, Calculation, Lignin, Oxidation, Permanganate, Phenol

*Contact information: a: Forest Products and Chemical Engineering, Department of Chemical and Biological Engineering, Chalmers University of Technology, SE-41296 Göteborg, Sweden; b: Department of Chemistry, PO Box 55, FIN-00014, University of Helsinki, Finland; †: Present address: Södra Cell AB, R&D, SE-43024 Väröbacka, Sweden; *Corresponding author: jim.parkas@sodra.com*

INTRODUCTION

Degradation methods such as acidolysis (Lundquist 1992) and thioacidolysis (Rolando et al. 1992; Önnerud et al. 2003) provide lignin degradation products that in general can be traced to particular lignin structures with confidence. However, the analyses comprise primarily monomeric degradation products, and the examinations of dimeric degradation products are incomplete. Quantitative studies using these techniques are therefore essentially restricted to "uncondensed" units ("uncondensed" and "condensed" units are defined in Fig. 1). One group of lignin degradation methods [thioacetolysis (Nimz 1974), thioacidolysis/Raney Ni treatment (Lapierre et al. 1991), DFRC (Lu and Ralph 1998; Peng et al. 1998)] involves a degradation step and a subsequent reduction step. In these cases both monomeric and dimeric products are thoroughly investigated. Even so, the results represent "uncondensed" units to a greater extent than "condensed" units. The limitations of the degradation/reduction methods also pertain generally for hydrogenolysis (Sakakibara 1992). Degradation methods that permit the analysis of both "condensed" and "uncondensed" lignin units are permanganate oxidation (Erickson et al. 1973b; Gellerstedt 1992), nitrobenzene oxidation (Chen 1991), and the nucleus exchange method (Funaoka et al. 1992). Ozonation (Akiyama et al. 2005

and preceding work) offers a possibility to quantitatively analyze different types of side chains in lignins.

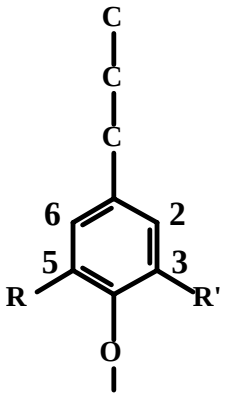

H R=R'= H
G R= H, R'= OCH_3
S R=R'= OCH_3

Fig.1. H, G and S represent different types of "uncondensed" lignin units. H, G and S units bound to another phenylpropane unit in additional ring positions (2, 3, 5 or 6) are designated "condensed" units.

Much attention has been paid to calculations of the composition of lignins based on results from permanganate oxidation studies (Erickson et al. 1973b; Morohoshi and Glasser 1979; Chen 1991; Gellerstedt 1992; Bose et al. 1998). A schematic description of the reaction sequence involved in these studies is shown in Fig. 2; the aromatic acids are usually analyzed as methyl esters.

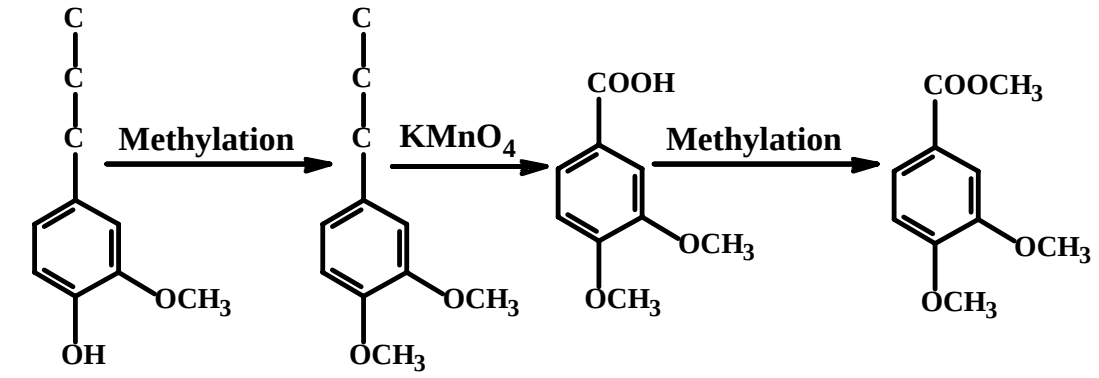

Fig.2. Schematic description of the reactions involved in methylation/permanganate oxidation/esterification of lignin leading to esters of methoxylated aromatic acids.

Analysis of lignins by permanganate oxidation is advantageous, since the degradation reaction has been thoroughly studied (Erickson 1973a), and convenient methods for the analysis of the degradation products have been worked out (Erickson 1973a). Furthermore, this degradation method specifically concerns phenolic lignin units (Fig. 2). In this paper we introduce an alternative method for the calculation of the compositions of lignins based on degradation products from permanganate oxidation studies. In conformity with all the earlier published calculation methods we have assumed that all the individual types of carbon atoms, attached to aromatic nuclei and susceptible to permanganate oxidation, are converted to carboxyl groups to the same extent. For the sake of simplicity we have restricted the presentation here to spruce lignin. We think that the principles for the calculations presented may be applicable to other degradation methods than permanganate oxidation.

MATERIALS AND METHODS

Conditions Used in the Cited Experimental Work

Results from permanganate oxidation studies of spruce lignin (milled wood lignin, MWL) published by Miksche and co-workers (Erickson et al. 1973b) are used as an example in the calculations presented in this paper. Erickson et al. (1973a,b) methylated the phenolic groups in MWL (dimethyl sulfate/KOH). The methylated lignin was degraded to aromatic acids by oxidation with $KMnO_4/NaIO_4$ complemented with a H_2O_2 treatment in a subsequent reaction step. The obtained aromatic acids were esterified with diazomethane and analysed by gas chromatography.

Deduction of Equations

The calculations are based on the yield (mg/100 mg lignin) of permanganate oxidation/esterification products **I-VII** (Fig. 3) and the amount of "trace constituents".

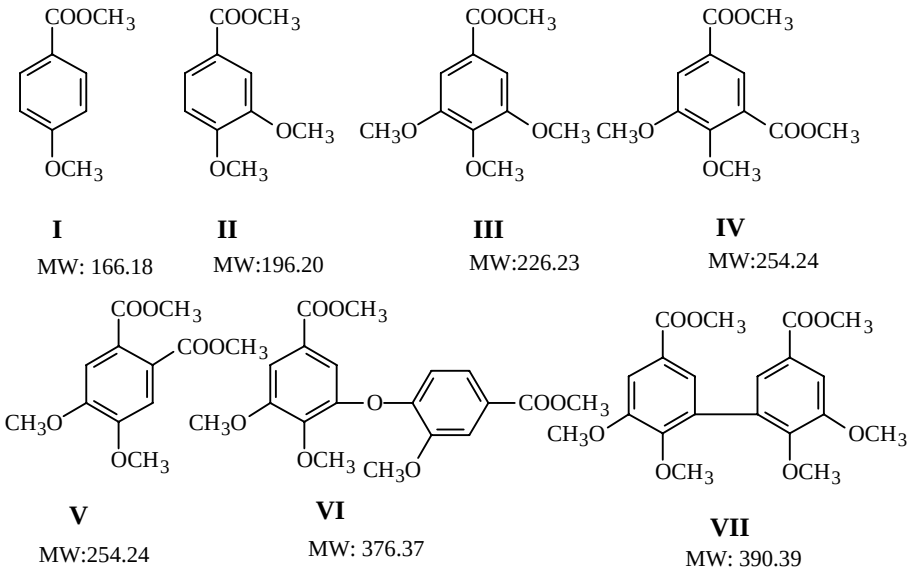

Fig.3. Esters obtained on methylation/permanganate oxidation/esterification of spruce lignin.

Esters of "trace constituents" constituted 3-5 % of the total of the esters (Erickson et al. 1973b). As an approximation we have assumed that 3-5 % of the spruce lignin sample consists of "trace constituents." Judged by the composition of the "trace constituents" (Larsson and Miksche 1969) we assume in the calculations that they consist of equal amounts of H and G units. The calculations are based on assumed or determined contents of phenolic groups (phenolic groups/phenylpropane unit). It is only aromatic acids from phenolic lignin units with protected phenolic group (alkylation, often methylation) that are analyzed in permanganate oxidation studies (Fig. 2). An equation (**Equation A**) has been derived for the calculations. It is assumed that all the individual types of carbon atoms, attached to aromatic nuclei and susceptible to permanganate oxidation, are converted to carboxyl groups to the same extent. The fraction of these carbon atoms that is converted to carboxylic groups is designated F. The conversion factor F can be calculated using **Equation A**. This equation is based on the condition that the amount (weight) of phenolic units in the lignin sample investigated must be equal to the amount of units (weight) derived from esters **I-VII** using the conversion factor F together with the phenolic fraction of the "trace constituents" (assumed to be phenolic to the same extent as the rest of the lignin). Note that the extent of conversion to dicarboxylic acids is determined by F^2. The determined factor F is used to calculate the distribution of different types of units in the lignin sample investigated. Furthermore it is possible to calculate the phenolic content in a lignin sample from **Equation A** provided the factor F is known. **Equation A**:

$$\frac{\mathrm{I\,(mg)}\times 157}{166.2\times \mathrm{F}}+\frac{\mathrm{II\,(mg)}\times 187}{196.2\times \mathrm{F}}+\frac{\mathrm{III\,(mg)}\times 217}{226.2\times \mathrm{F}}+\frac{\mathrm{IV\,(mg)}\times 187}{254.2\times \mathrm{F}^2}+\frac{\mathrm{V\,(mg)}\times 187}{254.2\times \mathrm{F}^2}+\frac{2\times \mathrm{VI\,(mg)}\times 187}{376.4\times 2\times \mathrm{F}^2}+$$

$$\frac{2\times \mathrm{VII\,(mg)}\times 187}{390.4\times \mathrm{F}^2}+\mathrm{Ph}\times \mathrm{Trace\ (total\ amount\ in\ the\ sample,\ mg)}=\mathrm{Ph}\times[100\ (\mathrm{lignin\ sample,\ mg})-\mathrm{Carbohydrates\ (mg)}]$$

[The degradation of a 100 mg sample of the lignin is considered, Ph is the fraction of the lignin units that is phenolic, designations and molecular weights of the degradation products (esters **I-VII**) appear in Fig. 3, the average lignin unit weights 157, 187 and 217 (corresponding to H, G and S units, Fig. 1) are taken from Larsson and Miksche (1971)].

When the factor F is known, it is possible to calculate the distribution of lignin units corresponding to esters **I-VII** and "trace constituents". For example, the fraction (%) of "uncondensed" G units (represented by ester **II**) is obtained by dividing the calculated amount (mmol) of such units:

$$\frac{\mathrm{II\,(mg)}\times 100}{196.2\times \mathrm{F}}$$

with the total amount (mmol) of calculated lignin units [trace constituents assumed to consist of equal amounts of H and G units (Larsson and Miksche 1969)]:

$$\frac{\mathrm{I\,(mg)}}{166.2\times \mathrm{F}}+\frac{\mathrm{II\,(mg)}}{196.2\times \mathrm{F}}+\frac{\mathrm{III\,(mg)}}{226.2\times \mathrm{F}}+\frac{\mathrm{IV\,(mg)}}{254.2\times \mathrm{F}^2}+\frac{\mathrm{V\,(mg)}}{254.2\times \mathrm{F}^2}+\frac{2\times \mathrm{VI\,(mg)}}{376.4\times \mathrm{F}^2}+\frac{2\times \mathrm{VII\,(mg)}}{390.4\times \mathrm{F}^2}+$$

$$\frac{\mathrm{Ph}\times \mathrm{Trace\ (total\ amount\ in\ the\ sample,\ mg)}}{(157+187)/2}$$

A second equation (**Equation B**) for the determination of the conversion factor F and the calculation of the distribution of units has been presented (Parkås et al. 2004). This equation is based on the same premises as **Equation A,** excepting that it is assumed that a pretreatment has resulted in a complete cleavage of phenolic ethers connecting lignin units (excepting the very stable diaryl ethers). **Equation B** (the designations are the same as those in **Equation A**):

$$\frac{\text{I (mg)} \times 157}{166.2 \times \text{F}} + \frac{\text{II (mg)} \times 187}{196.2 \times \text{F}} + \frac{\text{III (mg)} \times 217}{226.2 \times \text{F}} + \frac{\text{IV (mg)} \times 187}{254.2 \times \text{F}^2} + \frac{\text{V (mg)} \times 187}{254.2 \times \text{F}^2} + \frac{2 \times \text{VI (mg)} \times 187}{376.4 \times \text{F}^2} +$$

$$\frac{2 \times \text{VII (mg)} \times 187}{390.4 \times \text{F}^2} + \text{Trace (total amount in the sample, mg)} = 100 \text{ (lignin sample, mg)} - \text{Carbohydrates (mg)}$$

Excel Files for the Calculations

Excel files for the calculations are available on the website: http://www.sikt.chalmers.se/lignin/

Further details regarding the calculations are also given at this web-site. The Excel files can alternatively be obtained from the authors on request. The files are designed to solve a second order equation (**Equation A** or **Equation B**), which gives the conversion factor F. Based on this, the distribution of lignin units is calculated simultaneously. Calculations based on **Equation A** (Method Phenolic) and **Equation B** (Method Quadratic) are exemplified in the Excel-files. Calculations based on **Equation B** are also discussed by Parkås et al. (2004). The Excel-files can readily be adapted to calculations involving derivatives of the degradation acids other than **I-VII** (e.g. ethyl esters instead of methyl esters). Similarly unit weights can be adjusted to the type of lignin analyzed.

RESULTS AND DISCUSSION

General

Aromatic carboxylic acids obtained on permanganate oxidation of methylated lignins were subjected to detailed studies by Freudenberg and co-workers (Freudenberg 1968), and this approach to lignin analysis has later been extensively employed by several groups (Erickson et al. 1973b; Morohoshi and Glasser 1979; Chen 1991; Gellerstedt 1992; Bose et al. 1998; Tamminen and Hortling 1999). Figure 2 shows the reaction sequence involved in these studies; the aromatic acids are usually analyzed as methyl esters, but in some studies the initial methylation of phenolic groups has been replaced by an ethylation. A method for the analysis of the non-esterified acids has also been described (Javor et al. 2003). Important improvements of the lignin analysis based on permanganate oxidation were introduced by Miksche and co-workers (Erickson et al. 1973a). Experiments with lignin model compounds have shown that diarylmethane structures give only low yields of aromatic acids on permanganate oxidation (Erickson et al. 1973a; Meguro et al. 1998). However, such structures are not present in significant amounts in MWL of spruce (Erickson et al. 1973b). Another complication is that pretreatment with CuO/NaOH (to cleave ethers) results in formation of small amounts of

biphenyls (Bose et al. 1998). It is important to be aware of that it is only the phenolic portion of the lignin samples that is analyzed.

Determination of the Gross Composition of Lignins

Calculation of the structure of MWLs based on results from permanganate oxidation was introduced by Miksche and co-workers (Larsson and Miksche 1971; Erickson et al. 1973b). The calculations are based on the assumption that all the individual types of carbon atoms susceptible to permanganate oxidation and attached to aromatic nuclei are converted to carboxyl groups to the same extent. A further assumption is that a pretreatment with CuO/NaOH results in a complete cleavage of ethers connecting the lignin units (excepting the very stable diaryl ethers). An equation for this type of calculations was derived by Parkås et al. (2004) (**Equation B**, see Materials and Methods). A factor (F) for the conversion of carbon substituents to carboxyl groups can be calculated using this equation. Other groups (Gellerstedt 1992; Chen 1991) employ a value of conversion factor F based on permanganate oxidation experiments with lignin model compounds. A drawback, in this case, is that there is no connection between the magnitude of the factor and the actual yields of aromatic acids obtained from the particular lignin sample investigated. It has been recognized by two groups (Morohoshi and Glasser 1979; Bose et al. 1998) that a CuO/NaOH pretreatment to cleave ethers does not result in a complete cleavage of ether bonds and that some decomposition of lignin units may occur during this treatment. They have modified the conversion factor F in different ways to compensate for this. It is a fact (cf. Bose et al. 1998) that it is solely the phenolic portion of a lignin sample that give rise to esters **I-VII** (Figs. 2 and 3). We have derived an equation (**Equation A**, see Materials and Methods) in which this fact is taken into account, i.e. it is only the phenolic fraction of the samples that is considered in the calculations.

Erickson et al. (1973b) have published yields of **I-VII** (Fig. 3) obtained on permanganate oxidation of CuO/NaOH pretreated spruce MWL. Using their data we have applied **Equation A** to calculations of the distribution of units in spruce MWL. Table 1 shows the calculated distribution of units in spruce lignin assuming different phenolic contents. Undoubtedly the phenolic content of CuO/NaOH treated spruce MWL is high, but to our knowledge, it has not been determined experimentally. However, Bose et al. (1998) have determined the phenolic fraction of the lignin in CuO/NaOH treated spruce wood as 69%. One of the columns in the table shows a distribution of units practically identical with that obtained when the equation presented by Parkås et al. (2004) (**Equation B**) is applied. It is obvious from calculations based on **Equation A** (Table 1) that, provided the yields of esters are unchanged, a lower phenolic content (determined or assumed) requires a larger conversion factor (F), which in turn implies larger amounts of "uncondensed" units. The composition of the non-phenolic fraction is not known. It follows that the calculated distribution of lignin units is reliable only if the phenolic content is high and specified in the calculations. In that case the influence of the composition of the non-phenolic fraction on the gross composition of the lignin can be neglected.

The percentages of different types of units corresponding to esters **I-VII** given by Erickson et al. (1973b) are based on considerations similar to those expressed in

mathematical form in **Equation B** (cf. Parkås et al. 2004). However, their choice of conversion factor F is not based on precise calculations (cf. Larsson and Miksche 1971). Their results fairly closely correspond to those calculated based on **Equation A,** assuming a phenolic content of approx. 85 %. Since this is not very far from a probable phenolic content, the structural conclusions drawn by Erickson et al. (1973b) agrees fairly well with those derived from calculations based on **Equation A**. However, **Equation A** suggests a slightly lower proportion of "condensed" units.

Table 1. Distribution (%) of the lignin units in a spruce MWL sample (assumed carbohydrate content 1%) that gives rise to esters **I**-**VII** (Fig. 3). The distribution is calculated (**Equation A**) based on the yields of these esters (Erickson et al. 1973b) obtained on esterification of aromatic acids formed on permanganate oxidation of the CuO/NaOH treated and methylated sample assuming 70%, 80%, 90% or 96.5% phenolic units after the CuO/NaOH treatment. Regarding the interpretation of permanganate oxidation results in terms of structural elements in lignin, see Erickson et al. (1973 b).

	Amount (mg/100 mg lignin)	Distribution assuming 70% phenolic units (gives F=0.69)	Distribution assuming 80% phenolic units (gives F=0.63)	Distribution assuming 90% phenolic units (gives F=0.57)	Distribution assuming 96.5% phenolic units*** (gives F=0.55)
I	0.7	1.59	1.53	1.48	1.45
II	29.8	57.31	55.18	53.30	52.19
III	0.5	0.83	0.80	0.78	0.76
IV*	5	10.75	11.42	12.00	12.35
V	1.1	2.37	2.51	2.64	2.72
VI	2.1	6.10	6.48	6.81	7.01
VII	6	16.81	17.84	18.76	19.31
Trace**	4	4.24	4.23	4.22	4.22

* Assumed to originate from β-5 linked units (a contribution from 5-5 linked units is unlikely here since CuO/NaOH treatment results in extensive ether cleavage).
** Trace constituents, assumed to consist of equal amounts of **H** and **G** units (Larsson and Miksche 1969).
*** Comparable with calculations based on **Equation B**

Determination of Phenolic Groups in a Lignin Sample based on the Yields of I-VII on Permanganate Oxidation

It is possible to calculate the phenolic content in a lignin sample from the yields of **I**-**VII** using **Equation A**, provided that the conversion factor F is known. A probable factor F can be calculated using **Equation A** if data (phenolic content, yields of **I**-**VII**)

for a related lignin sample are known. Insertion of the yields of **I-VII** from spruce MWL reported by Erickson et al. (1973b) and the phenolic content (0.26) in spruce MWL adopted by these authors in **Equation A** gives the conversion factor (F) 0.70. Insertion of this factor and the yields of **I-VII** from CuO/NaOH treated MWL [reported by Erickson et al. (1973b) and shown in Table 1] in **Equation A** gives the phenolic content 0.69. Interestingly, this phenolic content in CuO/NaOH treated spruce MWL agrees with the value (also 0.69) reported by Bose et al. (1998) for the lignin in CuO/NaOH treated spruce wood. However, it should be kept in mind in this context that untreated spruce MWL is not an ideal reference lignin for CuO/NaOH treated lignin. Gellerstedt (1992) has estimated the phenolic content in lignins based on permanganate oxidation. In this case a conversion factor for formation of aromatic acids was selected based on model compound studies.

CONCLUSIONS

1. The calculation method developed (exemplified using the cited experimental work) improves the comparability of results obtained with different samples, since it is based on the fact that the phenolic content of the lignin sample examined defines the theoretical yield of the methoxylated acids obtained on methylation/permanganate oxidation.
2. The equations derived for the calculations make it possible to treat input data in a consistent way. "Trace constituents" and carbohydrate content are considered in the equations.
3. The solution of the equations using Excel-files is convenient. The Excel-files are readily adapted to different types of derivatives of the degradation acids. Similarly the parameters used in this paper can readily be replaced by others.

REFERENCES CITED

Akiyama, T., Goto H., Nawawi D.S., Syafii W., Matsumoto, Y., and Meshitsuka, G. (2005). "Erythro/threo ratio of beta-O-4-structures as an important structural characteristic of lignin. Part 4: Variation in the erythro/threo ratio in softwood and hardwood lignins and its relation to syringyl/guaiacyl ratio," *Holzforschung* 59(3), 276-281.

Bose, S. K., Wilson, K. L., Francis, R. C., and Aoyama, M. (1998). "Lignin analysis by permanganate oxidation. I. Native spruce lignin," *Holzforschung* 52(3), 297-303.

Chen, C.-L. (1991). "Lignins: Occurrence in woody tissues, isolation, reactions, and structure," In: *Wood Structure and Composition*, M. Lewin, and I. S. Goldstein (eds.), Marcel Dekker, New York, 184-261.

Erickson, M., Larsson, S., and Miksche, G. E. (1973a). "Gaschromatographische Analyse von Ligninoxydationsprodukten. VII. Ein verbessertes Verfahren zur Charakterisierung von Ligninen durch Methylierung und oxydativen Abbau," *Acta Chem. Scand*. 27(1), 127-140.

Erickson, M., Larsson, S., and Miksche, G.E. (1973b). "Gaschromatographische Analyse von Ligninoxydationsprodukten. VIII. Zur Struktur des Lignins der Fichte," *Acta Chem. Scand*. 27(3), 903-914.

Freudenberg, K. (1968). "The constitution and biosynthesis of lignin" In: *Constitution and Biosynthesis of Lignin*. K. Freudenberg, and A. C. Neish (eds.), Springer-Verlag, Berlin-Heidelberg, 47-122.

Funaoka, M., Abe, I., and Chiang, V. L. (1992). "Nucleus exchange reaction" In: *Methods in Lignin Chemistry*, S. Y. Lin, and C. W. Dence (eds.), Springer-Verlag, Berlin, 369-386.

Gellerstedt, G. (1992). "Permanganate oxidation" In: *Methods in Lignin Chemistry*, S. Y. Lin, and C. W. Dence (eds.), Springer-Verlag, Berlin, 322-333.

Javor, T., Buchberger, W., and Faix, O. (2003). "Capillary electrophoretic determination of lignin degradation products obtained by permanganate oxidation," *Anal. Chim. Acta* 484(2), 181-187.

Lapierre, C., Pollet, B., Monties, B., and Rolando, C. (1991). "Thioacidolysis of spruce lignin: GC-MS analysis of the main dimers recovered after Raney nickel desulphuration," *Holzforschung* 45(1), 61-68.

Larsson, S., and Miksche, G.E. (1969). "Gaschromatographische Analyse von Ligninoxydationsprodukten. III. Oxydativer Abbau von methyliertem Björkman-Lignin (Fichte)," *Acta Chem. Scand*. 23(10), 3327-3351.

Larsson, S., and Miksche, G.E. (1971). "Gaschromatographische Analyse von Ligninoxydationsprodukten. IV. Zur Struktur des Lignins der Birke," *Acta Chem. Scand*. 25(2), 647-662.

Lu, F., and Ralph, J. (1998). "The DFRC method for lignin analysis. 2. Monomers from isolated lignins," *J. Agric. Food Chem*. 46(2), 547-552.

Lundquist, K. (1992). "Acidolysis" In: *Methods in Lignin Chemistry*, S. Y. Lin, and C. W. Dence (eds.), Springer-Verlag, Berlin, 289-300.

Meguro, S., Xu, H., and Lai, Y.-Z. (1998). "Reactivity of lignin diphenylmethane model dimers. 2. Permanganate oxidation," *Holzforschung* 52(2), 175-179.

Morohoshi, N., and Glasser, W.G. (1979). "The structure of lignins in pulps. Part 5: Gas chromatography of permanganate oxidation products," *Wood Sci. Technol*. 13(4), 249-264.

Nimz, H. (1974). "Beech lignin - proposal of a constitutional scheme," *Angew. Chem. Internat. Edit*. 13(5), 313-321.

Parkås, J., Lundquist, K., and Brunow, G. (2004). "Quantitative lignin analysis," *Proc. 8th European Workshop on Lignocellulosics and Pulp*, Riga, Latvia, August 22-25. pp. 271-274.

Peng, J., Lu, F., and Ralph J. (1998). "The DRFC method for lignin analysis. 4. Lignin dimers isolated from DFRC-degraded loblolly pine wood," *J. Agric. Food Chem*. 46(2), 553-560.

Rolando, C., Monties, B., and Lapierre, C. (1992). "Thioacidolysis" In: *Methods in Lignin Chemistry*, S. Y. Lin and C. W. Dence (eds.), Springer-Verlag, Berlin, 334-349.

Sakakibara, A. (1992). "Hydrogenolysis," In: *Methods in Lignin Chemistry*, S. Y. Lin, and C. W. Dence (eds.), Springer-Verlag, Berlin. pp. 350-368.

Tamminen, T. L., and Hortling, B. R. (1999). "Isolation and characterization of residual lignin" In: *Advances in Lignocellulosics Characterization*, D. S. Argyropoulos (ed.), TAPPI Press, Atlanta, 1-41.

Önnerud, H., Palmblad, M., and Gellerstedt, G. (2003). "Investigation of lignin oligomers using electrospray ionisation mass spectrometry," *Holzforschung* 57(1), 37–43.

Article submitted: Jan. 29, 2007; First review cycle completed: Feb. 21, 2007; Revised version accepted: March 7, 2007; Published March 9, 2007.

BIODEGRADATION AND RECYCLING POTENTIAL OF BARRIER COATED PAPERBOARDS

Waranyou Sridach,[a] Kevin T. Hodgson,[b] and Mousa M. Nazhad* [c]

Four commercial barrier coated boards (i.e., internally-sized uncoated board, one-side polyethylene coated board, double-side polyethylene coated board, and multilayer laminated board) were examined for biodegradation using a soil burial approach on a laboratory scale. It was observed that the base-boards were fully biodegradable in a matter of weeks or months, and the degradation process could be accelerated either by sample size modification or enrichment of the soil microbial population. Freezing pretreatment of boards or the fiber directionality of boards had no influence on the rate of degradation. The boards were also found to be recyclable following a simple procedure of re-slushing and screening. The base-boards became almost fully separated from the polyethylene coated material without any special pretreatment.

Key words: Biodegradation, Base-board, Barrier coating, Recycling, Soil burial, Inoculum, Microorganism, Weight loss, Tensile strength.

*Contact information: a:Paper Science and Engineering Program, College of Forest Resources, University of Washington, 98195-2100, Lecturer, Prince of Songkhla University, Thailand; b: Paper Science and Engineering Program, University of Washington, Seattle, WA USA; c: Visiting Scientist, Paper Science and Engineering Program, University of Washington, Seattle, WA USA; *Corresponding author: mousanazhad@ait.ac.th, mousan@u.washington.edu, mousanazhad@yahoo.com*

INTRODUCTON

Paper and paperboard are by far the most prevalent sources of packaging materials the world over. Global production of paper for wrapping, packaging, corrugated boxes and other containers increased 75 percent over just the last 5 years (World Resources 2001). This rapid growth in paper packaging has also had the effect of exacerbating solid waste handling problems. In the United States alone, paper accounts for nearly 40 percent of municipal solid waste. Disposal of paper products in landfill sites can lead to emissions of the greenhouse gas methane, and incinerating chlorine-bleached paper at landfills may release dioxins into the atmosphere. As a result, the management of this waste has become one of the more pressing issues of the modern age.

Bringing solid waste issues under control has led to numerous government, private-sector, and voluntary initiatives to reduce the volume of waste going to landfills. This can be accomplished by: 1) increasing the recycling rate, 2) incineration as a source of energy, or 3) biodegradation by using microorganisms (Andrady et al. 1992; Sridach et al. 2006). The European Union has set strict guidelines, such as the Packaging Waste Directive (94/62EU) and Landfill Directive (99/31/EC) to help effectively manage these solid waste problems.

Due to a continual reduction of landfill sites in the US and Europe, biodegradability is considered a desirable alternative in the management of solid waste.

The paper and paperboard industry is also attempting to replace existing polymer coating formulations for paper and board with biodegradable coating formulations (Andrady et al. 1992; Sridach et al. 2006). Paperboard itself (without any coatings) is either almost pure holocellulose with a minimum amount of residual lignin (about 0.2%), or can contain up to 20% lignin depending on the end use of the board.

Biodegradability of polymers can be tested using screening tests which simulate in-situ conditions (Fig. 1). Screening tests by either enzymatic or aquatic means are inexpensive and fast, but real-life tests can be laborious and expensive. Neither of these two types of processes, however, actually simulate the conditions truly present in landfills.

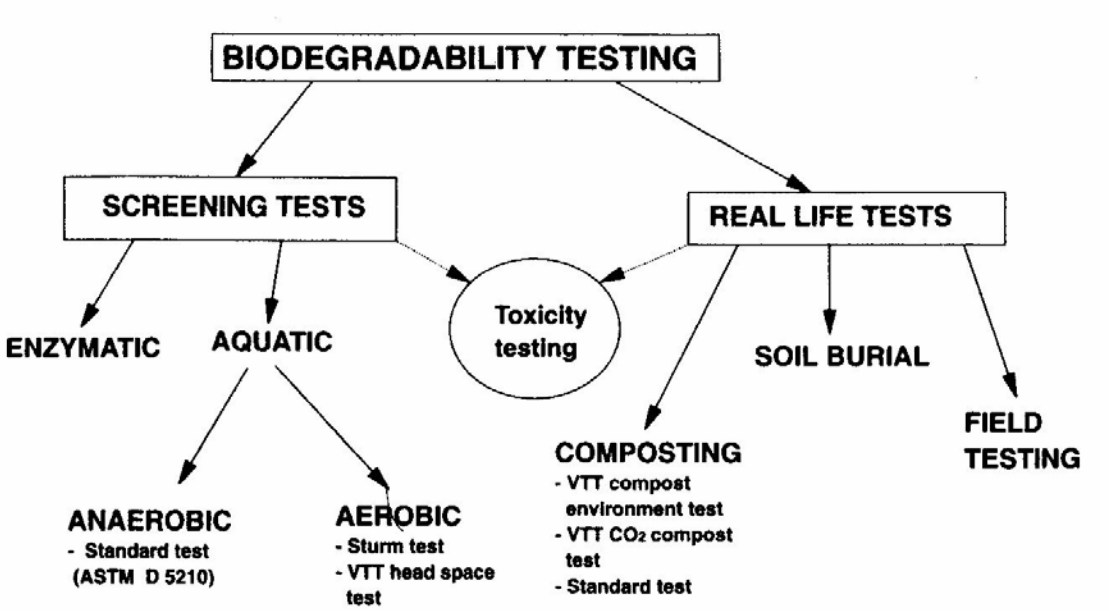

Fig. 1. Biodegradability testing of solid polymers (Itavaara and Vikman 1996).

Biodegradability and the rate of biodegradation depend in general on the substrate structure, the substrate composition as well as the microorganisms which are present (Ramos et al. 1993). Also, the rate of biodegradation decreases with the progress of the reaction. The cause of this decline in degradation rate is not yet totally clear. Although some substrate-related factors (such as crystallinity of cellulose) can perhaps partially explain why there is a gradual decrease in the hydrolysis rate of cellulose, several factors associated with the nature of the enzyme system used have also been suggested as being key to the decrease in rate of cellulose hydrolysis. These include shearing and thermal inactivation of enzymes, irreversible adsorption or nonspecific binding of cellulases, and end-product inhibition of the cellulose complex (Ramos et al. 1993). Ramos et al. (1993) observed that a short incubation time of 2 hours was all that was required to reduce the fiber length of bleached Kraft pulp (i.e. 48 fraction) from 920 to 170 microns. This observation suggests that the decrease in degradation rate most probably occurs at the stage of cellobiose conversion to sugar monomers. Also, the hydrolysis rate is usually accelerated by addition of beta-glucosidase to the mixture (Itavaara et al. 1999).

The degradation of lignin in a composting environment is almost comparable to soil degradation in its magnitude (Tuomela et al. 2000). In a composting environment, bleached Kraft pulp, stone groundwood (SGW) pulp, and sawdust were degraded 86%, 38%, and 10%, respectively, in 50 days at a temperature of 50° C. These results indicate the fact that lignin is a major barrier in degradation of lignocellulosic materials (Tuomela et al. 2001). Although the lignin content of both sawdust and SGW in the cell wall was similar, the degradation rate of SGW was almost fourfold that of sawdust. This has been attributed to more accessible surface of the SGW fibers as compared to sawdust (Tuomela et al. 2001). Nazhad et al. (1995) also proposed similar reasoning in interpreting the differences in degradation of different cellulosic substrates.

Soil bacteria (actinomycetes) and fungi are both capable of producing cellulolytic as well as lignolytic enzymes. Fungi including *Trichoderma*, *Penicillium*, and *Fusarium* spp. are all efficient producers of cellulolytic enzymes. *Trichoderma reesie* has an efficient and well-characterized cellulase system. The major cellulases of T. reesie are cellobiohydrolases I and II, endoglucanases I and II, and beta-glucosidase. Beta-glucosidase is essential for complete hydrolysis of cellulose (Itavaara et al. 1999). Artificial mixtures of cellulase systems may differ in composition or proportion from soil or compost microorganisms in nature. A cotton sample was not easily hydrolyzed using an enzyme system, but was rapidly decomposed by sludge microorganisms in the Sturm test (Itavaara and Vikman 1996).

In recent work, Nazhad et al. (2006) studied the possibilities of replacing polyethylene-coated boards with boards using a biodegradable coating. It was concluded that while this replacement might be possible, a reliable solution has not yet been found. However, the authors reported that a majority of the base-board samples tested biodegraded in a few weeks time, regardless of their coating composition.

The present work is developed from the premise that an accelerated biodegradation rate for commercial barrier coated boards could be achieved if pretreatment was done prior to the biodegradation stage, or, the living conditions of microorganisms was substantially improved. This work has also explored the recycling potential of barrier-coated boards as an alternative option to disposal in a landfill.

MATERIALS AND METHODS

Materials

Barrier-coated boards were obtained from commercial sources that supply such products to various Thailand food industries. The boards were folding boxboards, which were creased and formed into the desired shapes. The materials were: 1) bleached and internally-sized uncoated paperboard (alkenyl succinic anhydride (ASA) sizing), 2) one-side polyethylene (PE) coated paperboard with a pigment coating, 3) two-side polyethylene coated board without pigment coating, and 4) commercial liquid packaging board (LPK). The coating content (mass %) of one-side and two-side coated boards was 5% and 13%, respectively. Liquid packaging board (or multilayer laminated board) was a special product having 5 different layers of lamination. It was composed of polyethylene, aluminum, and cardboard in mass contents of 23.6%, 6.3% and 70.1%,

respectively in the structure *PE/Al/PE/cardboard/PE*. Inoculum was supplied by the Department of Land Development, Thailand. It was comprised of mixed microorganisms (bacteria, fungi and actinomycetes) and a dry medium for microorganisms. The soil used for this experiment was topsoil from the northern part of Bangkok, Thailand. It was an acid sulfate soil, common in South East Asia. After retrieval from the soil, samples are wet and virtually coated with soil debris. Washing the debris from the samples is a tedious job; however, this method is traditionally used for burial experimentation

Methods

The objective was to investigate the effects of: 1) freezing treatment, 2) microbial population, 3) surface area, and 4) the type of paperboard on the biodegradation of commercial coated boards. The biodegradation potential of the samples was estimated by burying the boards in soil and monitoring changes in weight and tensile strength as a function of burial time. For the freezing experiments, boards were conditioned at -20°C for one month. This was done to simulate the fact that many food packaging boards are subjected to freezing temperatures during their use. The sample sizes were 45 mm x 15 mm (rectangular), 26 mm x 26 mm (small square), and 150 mm x 150 mm (large square). Tests were done in both the machine-direction (MD) and cross-direction (CD) of the samples. To test the influence of either sample size or shape on biodegradation, the double-side PE coated board was used. For this sample, the edges of the board were the only accessible sites to the microorganism activity. Microorganisms could not penetrate through polyethylene coating in a time frame comparable to base-board (Nazhad et al. 2006), so the coating layer remains intact during the biodegradation process.

Given typical papermachine fiber orientation effects, the MD direction suggests more access to fiber *ends*, while the CD direction suggests more access to fiber *sides.* The magnitude of this difference depends on the type of the papermachine. The sample referred as small square (SQ) has the same area of the rectangular sample, but they are of course different in shape. The specific details of the soil condition and burying process are reported elsewhere (Nazhad et al. 2006).

The ash and moisture content of paperboard were measured according to TAPPI Standard T211 om-93 and TAPPI Standard T412 om-94, respectively. Polyethylene (PE) content of the boards was measured by subjecting them to hydrolysis in sulfuric acid (92% H_2SO_4) at 80° C. The PE film is then recovered, dried, and weighed (Andrady et al. 1992). The water vapor transmission rate (WVTR) was determined at 23° C and 85% RH by a Water Vapor Permeability Tester (WDDG). The testing area was 78.54 cm^2. Physical properties (basis weight, caliper, tensile strength, water absorption (Cobb test), opacity, and brightness) were measured according to TAPPI standards (See the reference list). After incinerating the liquid packaging boards in a muffle furnace at 575° C, the residue consists of ash and aluminum foil, where the aluminum foil is still in its solid form and separate from the ash. The quantity of aluminum foil was calculated using the following relation:

$$\text{Amount of aluminum foil (\%)} = \frac{\text{weight of aluminum foil after burning}}{\text{dry weight of coated board}} \times 100 \quad (1)$$

Moisture content and pH of the soil were measured according to British Standards 1377:1961 (UDC 624.131) and 1377:1961 (UDC 624.131), respectively. ASTM D422-63 was used for soil texture analysis (1985d). Soil microbial population (bacteria, fungi and actinomycetes) was determined by plate count technique according to cultural methods for soil microorganism (Wollum II 1982). Organic carbon present in the soil was determined according to the method suggested by Nelson and Sommers (1982). Total nitrogen in the soil was determined using the method of Bremner and Mulvaney (1982).

The boards were recycled to study the role of a coating layer in recycling. The samples were torn into pieces with typical size of 25 mm × 25 mm. Repulping was performed in 25° C soft-water at 1.5% consistency using a British laboratory disintegrator. The samples were soaked in 2 liters of water overnight before repulping for 30,000 revolutions in a British laboratory disintegrator using 25° C soft-water. Pulped samples were then diluted to a consistency of approximately 0.7 % (OD basis) and the debris from the coating layer was separated using a flat screen with a slot size of 0.2 mm. Flotation was done at 0.9% consistency with the addition of 0.25% (g/g od pulp) nonionic surfactant (Polyoxyethylene, Bando chemical, south Korea) using a Voith-Sulzer flotation cell to separate the residual stickies and other contaminants from the pulp fiber.

Table 1. Soil characteristics

Parameters	Units	Laboratory soil
Moisture	%	40
pH		7.49
Organic matter	%	5.5
Total nitrogen	%	0.53
Humidity *	%	62-91
Temperature*	C	25-33.5
*The ambient temperature was variable		

RESULTS

Physical characteristics of various samples (before degradation) are listed in **Table 2**.

Biodegradation of Paperboards

The influences of paperboard texture, sample size or shape, paper directionality, freezing pretreatment, and microbial population on biodegradation were all investigated. The changes in both weight and tensile strength were used to estimate the extent of the biodegradation progress. **Figure 2** shows the residual weight of large sample sizes vs. burial time, where it can be seen that the weight of the samples decreased with burial time. The weight loss for uncoated and one-side coated boards was approximately equal, and occurred at a much faster rate than the other two samples.

Table 2. Sample Physical Characteristics

Parameters	units	Samples			
		Uncoated	1S coating	2S coating	LPK
Moisture	%	8.3 ± 0.24	7 ± 0.10	7 ± 0.7	6.5 ± 0.7
Ash	%	7.7 ± 0.23	5.60 ± 0.12	3.32 ± 0.3	13.6 ± 0.2
PE coating wt	%	-	5 ± 0.35	13.23 ± 1	23.6 ± 0.4
Foil content	%	-	-	-	6.3 ± 0.03
Grammage	g/m2	313 ± 2	306 ± 3	319 ± 0.7	294 ± 2
Thickness	μ	398 ± 2	414 ± 3	442 ± 2.50	360 ± 3
Fiber length	mm	-	1.15 ± 0.01	1.21 ± 0.02	1.6 ± 0.04
Coarseness	mg/m	-	0.16 ± 0.01	0.17 ± 0.002	0.16 ± 0.01
Cobb test					
1st. Face	g/m2	30 ± 1	0	0	0
2nd. Face	g/m2	31 ± 1	31 ± 0.01	0	0

S: Side, LPK: Liquid packaging board

The uncoated board sample degraded fully after seven weeks, as the samples at this time could not be retrieved for further examination. The one-side coated boards were still retrievable after 7 weeks due to the polyethylene coating. The residual weight of the one-side PE coated boards after 20 weeks of burial was almost the entire weight of the coating material (5.7%), while the residual weight of the double-side PE coated board and liquid packaging board were 26.03% and 52.05 %, respectively. Degradation of double-side coated and LPK boards suggest that the enzymes diffused into the boards through the edges to degrade the unprotected cellulose.

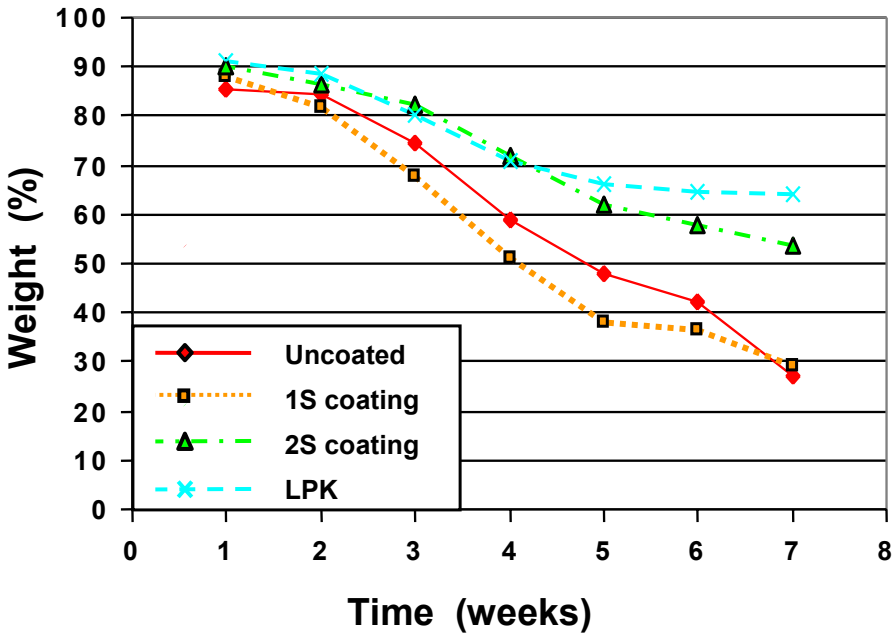

Fig. 2. Weight loss of paperboard samples

Biodegradation was also estimated by following changes in tensile strength of the boards during burial. As **Figure 3** indicates, the tensile strength of the boards deteriorated with an accelerated pace. Tensile strength of the samples (regardless of the board category) was reduced by about 90% in four weeks, while weight loss at the same 90% level needed about 12 weeks to occur. The failure of a specimen in the tensile test occurs at the weakest point. Therefore, tensile strength may potentially become severely decreased by having a very small decayed portion along the axis of the test specimen (Nazhad et al. 2006).

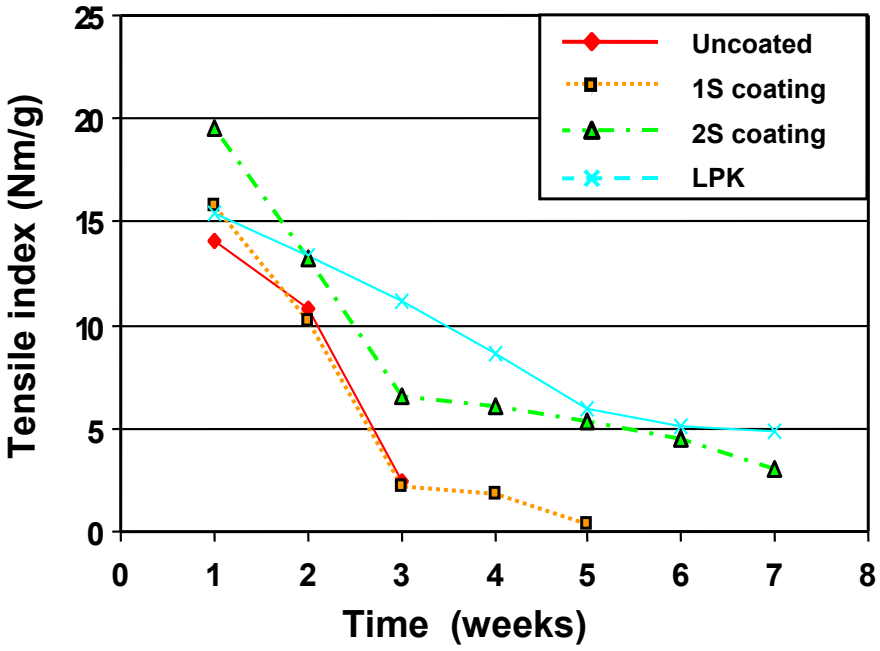

Fig. 3. Tensile strength of paperboards vs. burial time

The change in tensile strength is plotted versus weight loss for the samples in **Figure 4**. These data demonstrate that 50% to 80% of the tensile strength was lost during the first week of the burial process, whereby the corresponding loss in weight is about 10 – 20% for the samples. This result suggests that having a small number decayed sections along the test specimen has no real effect on weight loss.

Sample weight loss is due to migration of degraded material out of the substrate. This migration is possible of course as long as the degraded materials do not encounter any barriers along the pathway. Thus, a coating on the sample can represent a significant barrier to the migration process. This is speculated to be one of the reasons for the slow pace of weight loss of coated samples during the burial process (Nazhad, et al., 2006).

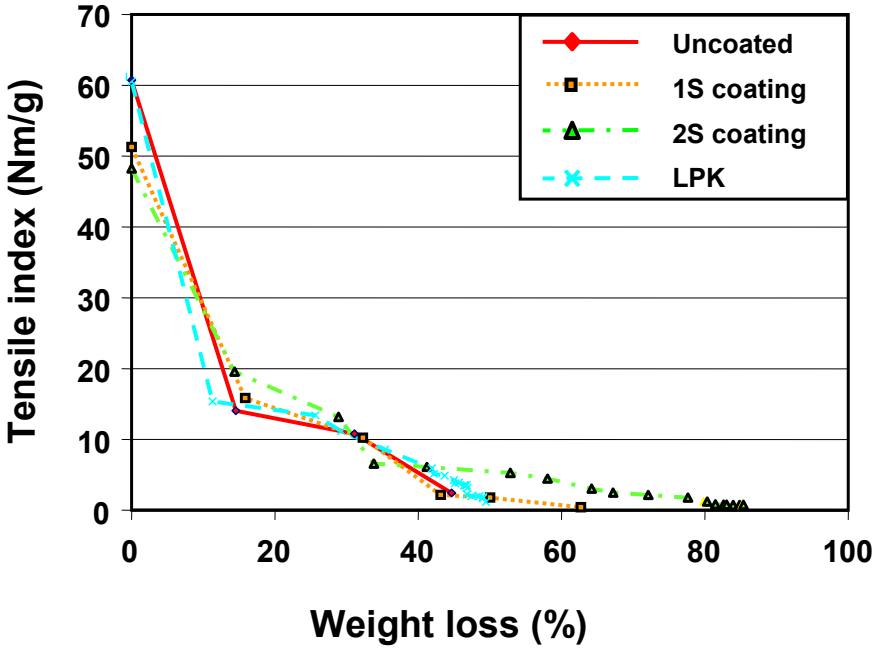

Fig. 4. Relation between tensile strength and weight loss

Effect of Sample Size or Shape

The influence of the sample size or shape on biodegradation is plotted in **Figure 5**.

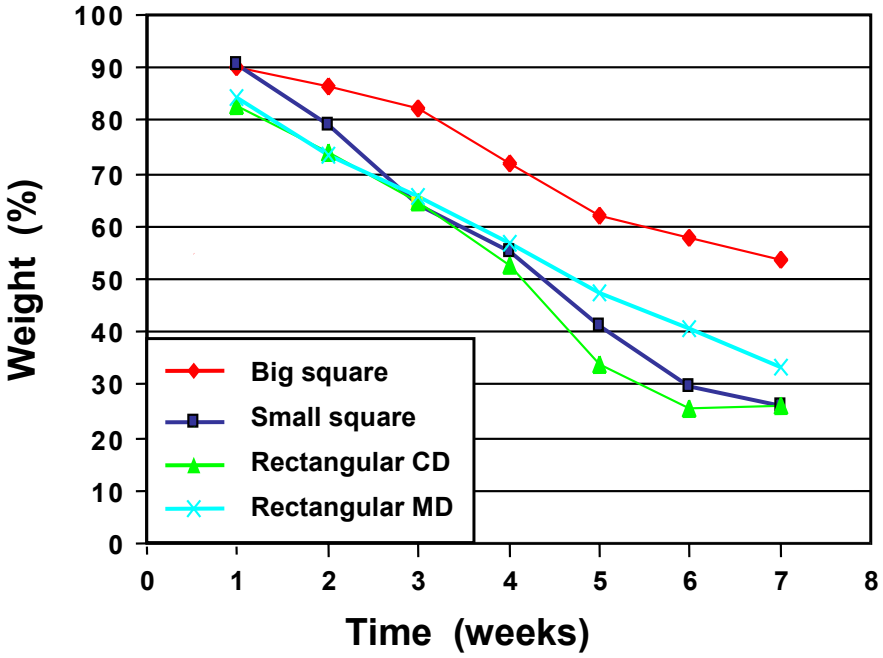

Fig. 5. Weight loss of double-side PE coated boards.

The data in **Figure 5** are for the double-side PE coated board, so only the edges were accessible sites for microorganism activity. Therefore, the smaller samples offered a greater fraction of accessible sites (based on the whole sample area) to microorganisms than the larger samples. As **Figure 5** shows, the curves of the two samples that were different in shape almost coincided, while the size effect seems to be significant. This observation suggests the importance of sample *size* in degradation of boards. It also shows that microorganisms were not sensitive to the directionality of paper. As noted earlier, fibers in the paperboard are more oriented in the machine direction (MD) than the cross direction (CD).

Effect of Freezing

Figure 6 shows the influence of a freezing pretreatment on biodegradation, along with the effect of using inoculum. The curves of frozen and non-frozen samples are very close, indicating that prior freezing does not change the biodegradation rate. Based on this observation, it has been speculated that the freezing does not alter the structure of the boards in such a fashion that eases the base-paper decomposition. However, it does appear to make the boards brittle based on the lower elongation values seen at tensile failure.

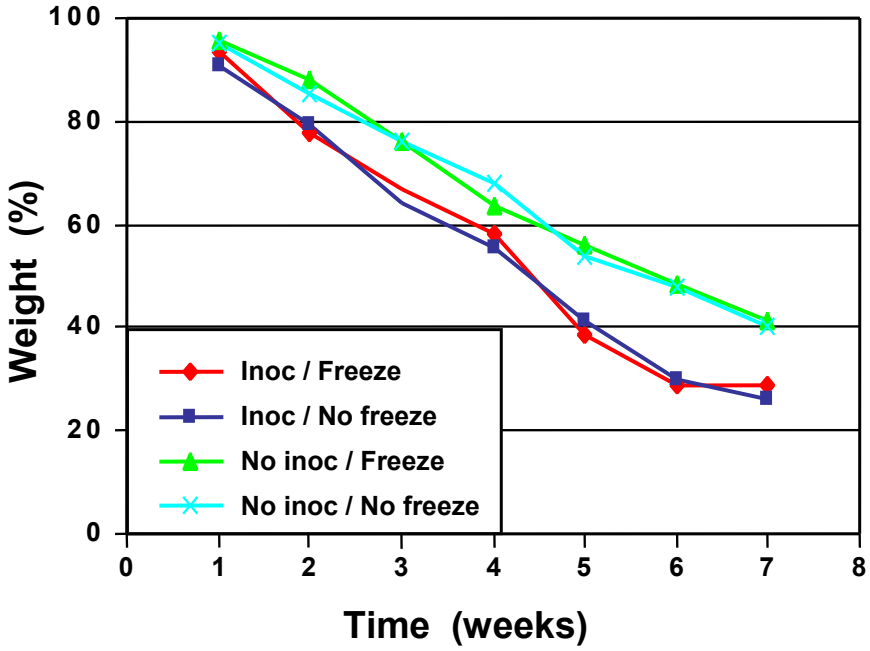

Fig. 6. Weight loss of two-side PE coated boards (frozen and non-frozen)

Freezing reduced elongation of the boards by a factor of 3 to 4, depending on the exact structure of the boards. Addition of inoculum altered the decomposition rate somewhat. The samples which were buried in the soil mixed with inoculum exhibited more extensive weight loss, regardless of the freezing treatment (Fig. 6).

Water Vapor Transmission Rate (WVTR) and Cobb Test Values

An attempt was made to trace biodegradation by using either the Cobb sizing test or the water vapor transmission rate (WVTR). Uncoated board could not be tested because of the development of one or more holes in the specimen during the first week. Two-side coated boards showed an increase in WVTR, but the increase was attributed to the presence of surface wrinkles, rather than changes due to mass loss by biodegradation. The data for two-side coated board only is reported in **Table 3**. Surface wrinkles potentially contribute in two opposing ways in determining the final outcomes. One, they *reduce* surface water absorption by increasing the contact angle (due to roughness effects); two, they can *increase* water absorption by initiating cracks in the coating layer or sized surface. One-side coated boards could only be tested for three weeks, but they also formed surface wrinkles. LPK boards did not show any change based on Cobb values.

Table 3. Cobb values of double-side coated boards at different stages of soil burial (g H_2O/m^2)

Parameters		Sample			
Time	Side	Microbial inoculum		No microbial inoculum	
(week)		F- treatment	No treatment	F- treatment	No treatment
2S coating					
1	A	0.25	0.05	0.1	0
	B	0.05	0.1	0	0
2	A	0	0	0.5	0
	B	0	0	0	0
3	A	0.2	0.1	0	0.3
	B	0.2	0.2	0	0
4	A	0.1	0.4	0.3	0.4
	B	0	0.1	0.3	0.3
5	A	0.3	0.6	0.6	0.8
	B	0.4	0.6	0.3	0.5

A: Top side; B: Bottom side; F: Freezing

Soil mixed with microorganisms for frozen and non-frozen samples *may* exhibit an increasing trend in the WVTR values with progress of biodegradation (Fig. 7). However, the data could also be interpreted as inconclusive, and therefore should be used with caution as a potential indicator of biodegradation.

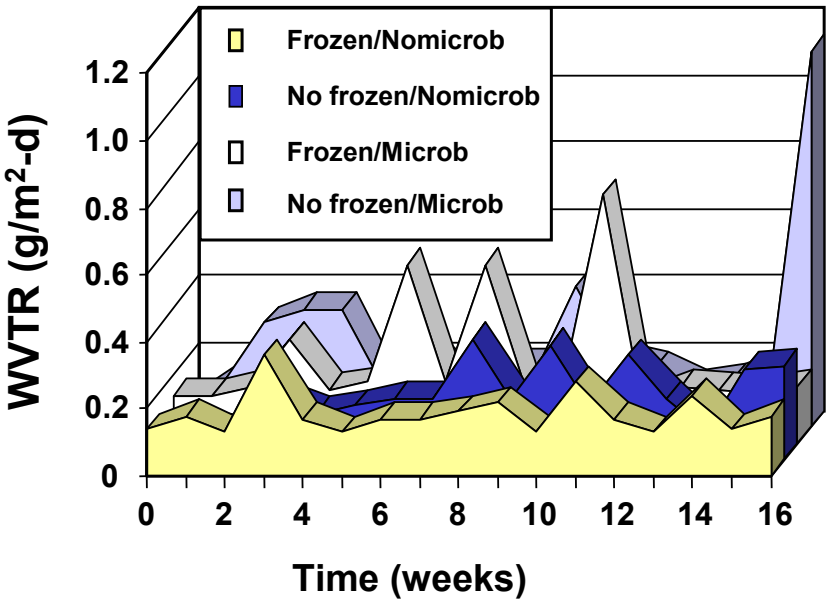

Fig. 7. WVTR for double-side coated board

Recycling

Table 4 shows the fiber yield and fiber properties after pulping and screening. As can be seen, it appears that the rejects from the board samples are correlated with the coating weight. Coating mass percentages of one-side coated, two-side coated, and liquid packaging board were 5%, 13%, and 30%, respectively. This observation suggests that the fibrous materials of the boards could be essentially fully recovered by screening. Flotation rejects were mostly fibers, fines or fillers, rather than pieces of polyethylene coating. Therefore, flotation is not recommended if the polyethylene particle size in the process of repulping is kept at macroscopic scale. As has been reported earlier, samples were collected from commercial sites, and thus specific information on the characteristics of the each baseboard was not available. However, the papermaking properties we found of the pulps are in the expected range of typical carton boards.

Table 4. Recycling of the coated boards

Sample ID	Unit	Screen reject	Screen accept	Flotn reject	Flotn accept
1S coating	%	6 ± 1	94 ± 1	9.5 ± 1.5	79 ± 4
2S coating	%	11.5 ± 0.3	88 ± 0.3	6 ± 0.5	76 ± 0.3
LPK	%	38 ± 0.4	62 ± 0.4	9 ± 3	49 ± 0.4

	Physical properties								
ID	1S coating			2S coating			LPK		
	Bright	Opac (%)	T-inx (Nm/g)	Bright	Opac (%)	T-inx (Nm/g)	Bright	Opac (%)	T-inx (Nm/g)
	78.6	89	14	78	86	16.5	65.4	76	16.5

Bright: Flotn = Flotation; Bright=Brightness; Opac=Opacity; T-inx = Tensile index.

DISCUSSION

This work shows that the cellulosic substrates of barrier-coated boards are biodegradable in a time frame of weeks or months, but not their coating layers. For example, biodegradation of polyethylene by microorganisms is a very slow process. It has been reported that polyethylene remained intact after 12 years of soil burial (Potts 1978). This has been attributed to its three dimensional structure, its high molecular weight, and its hydrophobic nature. It is assumed that to increase the rate of PE biodegradation, the structure should be altered, or perhaps the molecular weight should be reduced.

The present observations highlight the importance of sample size with respect to the rate of the degradation process. It was noted earlier that the sites accessible to microorganisms were the sample edges, due to the fact that the double-side polyethylene coated samples were used for this experiment. Therefore, edge-wise penetration was the only available route to the microorganisms. In contrast to the sample size, the sample shape did not have any significant effect. The directionality of paper also did not contribute in changing the degradation process. Therefore, it is inferred that one way to accelerate the biodegradation process might be to crumple the boards prior to their exposure in order to reduce the effective size.

The observations made here also suggest that microorganisms are not sensitive to fiber orientation. If microorganisms were attracted to fiber-ends more than the fiber-sides, as has been previously reported (Ramose et al.1993; Nazhad et al. 1995), then degradation in MD direction should be more extensive. The present experiments could not support this type of behavior in microorganisms, at least those used in this work.

This work also suggests that the barrier-coated boards are recyclable. The base-board could be easily separated from the coating layer by screening, and the fibers then recycled to produce a board comparable to the original product. The coating layer could be incinerated to produce energy. It has been reported that the heat value of polyethylene is higher than some of polyester-coated materials (Sridach et al. 2006).

CONCLUSIONS

1. The base-board of four different barrier-coated paperboards was found to be biodegradable in a soil environment, but the coating layer remained intact during the course of biodegradation.
2. Sample size and microbial population affected the rate of the biodegradation process, but the directionality of the samples or freezing treatment did not.
3. There was no preferential affinity of the microorganisms used to fiber-ends as compared to fiber-sides.
4. The coating layer of the sample boards was easily separated by disintegration followed by screening. The pulp yield was almost equivalent to the original weight of the base-board alone. .

REFERENCES CITED

Andrady, A. L., Parthasarathy, V. R., and Song, Y. (1992). "Biodgradation of paperboards: Loss in strength and weight of paperboard packaging materials under aerobic soil-exposure conditions," *Tappi J.* 75(4), 203-215.

Itavaara, M., Siika-aho, M. and Viikari, L. (1999). "Enzymatic degradation of cellulose-based materials," *J. Environ. Polym. Degrad.*, 7(2), 67-73.

Itavaara, M., and Vikman, M. (1999). "An overview of methods for biodegradability testing of biopolymers and packaging materials," *J. Environ. Polym. Degrad.*, 4(1), 29-36.

Nazhad, M. M., Ramos, L. P., Paszner, L., and Saddler, J. N. (1995). "Structural constraints affecting the initial enzymatic hydrolysis of recycled paper," *Enzyme Microb. Tech.* 17(1), 63-72.

Nazhad, M. M., Sridach, W., Retulainen, E., Kuusipalo, J. and Parpian, P. (2006). "Biodegradation of some barrier coated boards at different soil environment," *J. Appl. Poly. Sc.* 3193-3202.

Potts, J. E. (1978), "Aspects of degradation and stabilization of polymers," Jelinek, H. H. G. (eds.), *Elsevier:* New York.

Sridach, W., Retulainen, E., Nazhad, M.M., Kuusipalo J., and Parkpian, P. (2006), "Biodegradable barrier coating on paperboard; Effects on biodegradation, recycling and incineration,'' *Paperi Ja Puu – Paper and Timber* 88(1), 1-12.

Tuomela, M., Vikman, M., Hatakka, A., and Itavaara, M. (2000). "Biodegradation of lignin in a compost environment: a review," *Bioresource Technology* 72, 169-183.

Tuomela, M., Hatakka, A., Vikman, M., Raiskila, S., and Itavaara, M. (2001). "Biodegradation of radiolabelled synthetic lignin (14C-DHP) and mechanical pulp in a compost environment," *Appl Microbiol Biotechnol* 55, 492-499.

World Resources (Revised 2001), "No end to paperwork," Vendy Vanasselt (ed.), Staff of world resources program, http://earthtrends.wri.org/pdf_library/features/ene_fea_paper.pdf

STANDARDS CITED

Tappi Methods: Basis weight (T410 om-98); Caliper (T411 om-97); Tensile strength (T494 om-96); Cobb test (T441 om-90); Opacity (T425 om-91); Brightness (T452 om-92)

American Society for Testing Materials (1985d). "Standard Test Method for Particle-Size Analysis of Soil'', Vol. 04.08, Philadelphia. ASTM D422-63.

American Society of Agronomy (1982), Wollum II, A.G, "Cultural Methods for Soil Microorganism," in *Methods of Soil Analysis*, Part II, Chemical and Microbiological Properties, Second Ed., Wisconsin: pp. 781-801.

American Society of Agronomy (1982), Nelson, D.W. and Sommers, L. E., "Total Carbon, Organic Carbon and Organic Matter," in, *Methods of Soil Analysis*, Part II, Chemical and Microbiological Properties, Second Ed., Wisconsin. pp. 539-577.

American Society of Agronomy (1982), Bremner, J. M. and Mulvaney, C. S., "Nitrogen-Total'', in *Methods of Soil Analysis*, Part II, Chemical and Microbiological Properties, Second Ed., Wisconsin, pp. 595-622.

Article submitted: Jan. 2, 2007; Article resubmitted after formatting changes: Jan. 12, 2007; First round of reviewing completed: Feb. 5, 2007; Revised article received: April 12, 2007; Article accepted: April 13, 2007; Published April 15, 2007.

ACTIVATED CARBON FROM THERMO-COMPRESSED WOOD AND OTHER LIGNOCELLULOSIC PRECURSORS

Lotfi Khezami, Aissa Ould-Dris and Richard Capart*

The effects of thermo-compression on the physical properties such as bulk density, mass yield, surface area, and also adsorption capacity of activated carbon were studied. The activated carbon samples were prepared from thermo-compressed and virgin fir-wood by two methods, a physical activation with CO_2 and a chemical activation with KOH. A preliminary thermo-compression method seems an easy way to confer to a tender wood a bulk density almost three times larger than its initial density. Thermo-compression increased yield regardless of the mode of activation. The physical activation caused structural alteration, which enhanced the enlargement of micropores and even their degradation, leading to the formation of mesopores. Chemical activation conferred to activated carbon a heterogeneous and exclusively microporous nature. Moreover, when coupled to chemical activation, thermo-compression resulted in a satisfactory yield (23%), a high surface area (>1700 $m^2.g^{-1}$), and a good adsorption capacity for two model pollutants in aqueous solution: methylene blue and phenol. Activated carbon prepared from thermo-compressed wood exhibited a higher adsorption capacity for both the pollutants than did a commercial activated carbon.

Keywords: *Wood, Activated carbon, Thermo-compression, Microporosity, Adsorption properties*

Contact information: Université de Technologie de Compiègne, Département de Génie Chimique. Laboratoire de Génie des Procédés Industriels, UMR 6067 du CNRS-BP 20529 – 60205 Compiègne, France.
**Corresponding author: richard.capart@utc.fr, Tel: 33 3 44 23 44 45; Fax: 33 3 44 23 19 80*

INTRODUCTION

Activated carbon is used in a host of applications due to its adsorption capacity in gaseous or liquid phase. These applications can be found in many fields such as food industry, environment, water treatment, and catalysts manufacturing. Producing activated carbon consists of heating the precursor up to a temperature approximately between 600 and 1000 °C (Guo and Lua 1998). Two successive phases occur during heating:

- a first phase of pyrolysis associated with a strong devolatilisation of the precursor, leading to a carbon-enriched product.
- a subsequent phase of activation in which micro and mesopores develop within the carbonaceous matrix.

Many authors (Marsh 1987; Pastor-Villegas et al. 1998) reported works where the pyrolysis of the lignocellulosic precursor, without any subsequent activation, resulted in the formation of activated carbon (A.C.). The microporous structure is developed due to the removal of the volatile matter and to the progressive shrinkage that is, according to Pastor-Villegas et al. (1998), responsible for pore narrowing.

Activated carbon obtained from pyrolysis is considerably improved by activation treatment. There are two distinct ways of activation, which are commonly termed as physical and chemical activation. In physical activation, the activating agents are oxidising gases: CO_2 (Rodriguez-Reinoso and Molina-Sabio 1994) or H_2O (Warhurst et al. 1997), which react with carbon. According to Walker (1996), activation with CO_2 makes it possible to achieve a

greater uniformity of pores compared with activation using H_2O. The reaction mechanism is actually complex, involving the fixation and then the dissociation of CO_2 on active sites to form unstable intermediates, and the reaction is catalysed by inorganic compounds constituted by ashes.

In chemical activation, the development of the porous structure is important, and the required temperatures are generally lower than those prevailing in physical activation with CO_2 or H_2O. The activating agents are mainly inorganic compounds, introduced before heating by impregnation within the precursor (raw biomass or char). These activating agents can be acids H_3PO_4 (Toles et al. 1996), H_2SO_4 (Guo and Lua 1999), alkaline products KOH (Ubago-Pérez et al. 2006, Hu and Srinivasan 1999; Ahmadpour and Do 1996), or salts $ZnCl_2$ (Ahmadpour and Do 1996; Lopez-Gonzalez et al. 1980). Generally, chemical activation does not require as high temperatures as physical activation. In the industrial practice, activated carbon is often produced from a combination of these two modes of activation. Chemical activation using KOH was developed more recently than the other modes of activation. Thus, the KOH activated carbon has been commercially available only since the 1980s (O'Grady and Wennerberg 1986). Since then, extensive research has been devoted to this process. It was thus demonstrated that activation with KOH yields activated carbon with a highly microporous structure and a narrow pore-size distribution, while activation with an acidic agent (H_3PO_4) leads to a broader pore-size distribution and a larger production of macropores (Issa and Teresa 2000).

A link could be established between the development of pores and the catalytic activity of inorganic compounds containing some alkaline metal. In these alkaline catalysts, the atoms of oxygen also play a major role in the process of carbon oxidation, leading to the formation of pores. The actual mechanism of activation has not yet been definitely established. In the literature, various descriptions were proposed for this mechanism. For instance, Franck and Meraikib (1970) have postulated that the alkali metal intercalates in the lattices of carbon and acts as an electron donor, which promotes the reaction during gasification. In studying the effect of KOH on various cokes, Marsh et al. (1984) stated that the presence of oxygen in alkali resulted in the removal of cross-linking of carbon atoms in crystallites. The potassium metal liberated at high temperature may intercalate and force apart the separate lamellae of the crystallite. Hüttinger and Minges (1986) and Ehrburger et al. (1986) have given slightly different explanations of the mechanism.

In order to reduce the production costs, several manufacturers use precursors' wastes and by-products from agriculture and forestry (Gergova et al. 1994). Among the various other precursors, there are wood-sawdust (Tsai et al. 2001), stones of olives (Lopez-Gonzalez et al. 1980) and various fruits, sugar cane bagasse, trunks of palm trees, walnut shells, etc. For instance, coconut shell (Hu and Srinivasan 1999; Laine and Yunes 1992; Laine et al. 1989; Sodya et al. 1997) is a widely accepted material owing to its abundance and the quality of the derived activated carbon. Moreover, the good mechanical properties of the granules of carbon obtained from coconut shells partly results from the high density of this precursor.

In the present work, an attempt was made to confer to lumps of fir-wood, a density similar to that of a material like coconut shell, by thermo-compression. Two modes of activation were applied: a physical activation with CO_2 and a chemical activation with KOH. Classical investigations methods such as the pore surface area by BET method were performed on activated carbons. Activated carbon from thermo-compressed wood has been previously tested for the removal of chromium VI in aqueous solutions (Khezami and Capart 2005). In the present study, the adsorption capacity of A.C. from thermo-compressed wood was evaluated for two organic pollutants in aqueous phase: methylene blue and phenol. These two molecules are very often used to characterize the adsorption capacity of activated carbon.

Methylene blue is a typical product of the dye industry and can be regarded as a model compound for the removal of high molecular weight organic contaminants. The produced activated carbon from different raw materials according to different modes of activation have been compared with a commercial activated carbon (acticarbone CXV) supplied by CECA (France).

EXPERIMENTAL

Raw Material and Thermo-Compression

The raw material consisted of lumps of fir wood, the dimension of which being 12x16x20 mm (20 mm in the direction of fibres). The initial density of wood lump lay in the range 0.47-0.55 $g.cm^{-3}$. A part of them were compressed by using a hydraulic press Carver, equipped with 2 heating plates (15x15 cm by side). The maximal load of the press was 12 metric tons. Compression of fir-wood lumps was always made in the direction perpendicular to that of fibres. From previous trials of thermo-compression, it was shown that the ideal temperature of plates lies between 180 and 220 °C. Above approximately 220 °C, thermal decomposition of wood starts and the lumps tend to burst. The pre-moistening of wood by steam or hot water favours the thermo-compression but is not essential.

Preparation of activated carbon

The carbonisation-activation of fir-wood and other precursors was made in a stainless steel cylindrical reactor, 6 cm in diameter, vertically set up. The reactor was connected to cylinders of compressed gas (N_2 and CO_2) and the flow-rate of gas was controlled by a flow-meter. The activated carbon was produced from 3 kinds of treatment:

(i) A simple pyrolysis i.e. a heating under N_2 atmosphere
(ii) A "physical activation" or a heating under CO_2 atmosphere
(iii) A "chemical activation" i.e. a heating of the precursor material impregnated with KOH

For the simple treatment of pyrolysis, the operating variables were the heating rate (3 and 5 °C/min), the temperature of plateau, and the duration at temperature of plateau.

For the physical activation under CO_2, the operating parameters specifically studied were the maximal temperature of activation (or the temperature of plateau), between 700 °C and 900 °C, and the time of plateau, between 3 and 9 hours.

The used method for chemical activation was typically that proposed by Hu and Srinivasan (1999). In this method two successive steps are required: at first, the precursor was slowly carbonised under N_2 at 300 °C for one hour. The charcoal so produced was then impregnated, after cooling, with a boiling concentrated solution of KOH, in order to get KOH contents varying from 0.125 to 1. The KOH content being defined as the mass ratio: KOH/ anhydrous precursor.

At the end of each chemical activation treatment, the activated carbon was abundantly washed, firstly with a solution of HCl 0.1 M, then with distilled water up to a neutral pH. The produced A.C. is designated as following in the tables and figures: M.A./R.M./T/tp.

For example: $CK_{0.5}$/Wc/800/2 designates a KOH activated carbon prepared from thermo-compressed wood at 800°C for a time of plateau of 2 hours with KOH/char ratio equal to 0.5. By default the mass ratio is equal to 1.

M.A. is the mode of activation with
NP: carbonisation under N_2
CP: physically activated carbons under CO_2
CK: chemically activated carbons with KOH.
R.M. is the raw material with
W : virgin wood
Wc: thermo-compressed wood
CN: coconut shell
OS: olive stone.
T is the Temperature of plateau: 600, 750, 800, 850 °C.
tp is the time in plateau : 1, 2, 3, 6, 9 hours.

Caracterization of Samples

After each experiment, a part of the produced A.C. was milled into powder in order to characterise its porosity and the adsorption parameters for both of the model pollutants. The characteristics of pores were evaluated from the adsorption-desorption isotherms of N_2 at 77 K, through an apparatus ASAP 2010 (Micromeritics). Before each determination of isotherm, the A.C. sample was outgased for 12 hours at 300 °C under vacuum. The surface area of pores was calculated from the BET equation (Brunauer, Emmett and Teller). The volume of micropores and the surface area attributed to mesopores were calculated from the t-plot method of Lippens and de Boer (Lippens and de Boer 1965). For both of the model pollutants, phenol and methylene blue, the parameters of the models of Langmuir and Freundlich were evaluated after determination of experimental data of sorption at 25 °C, thus detailed. Several Erlenmeyer flasks were filled up with a suspension of A.C. (30 ± 0.1 mg) in 100 ml of a diluted solution of pollutant at various concentrations. The initial concentration of phenol was stepped from 10 to 150 mg l^{-1}, while that of methylene blue from 30 to 200 mg l^{-1}. After 24 hours of stirring, liquid samples from each flask were taken out and filtered. Their concentrations in non adsorbed free pollutant were measured by absorption spectrometry, UV at 269 nm of wavelength in the case of phenol, visible at 660 nm in the case of methylene blue. According to the theory of adsorption, the model of Langmuir is based on the fixation of a monolayer of adsorbate molecules on the surface of pores. Its mathematical formulation is the following (Langmuir 1918):

$$q_e = \frac{Q_0 . b . C_e}{1 + b . C_e} \quad (1)$$

where q_e (mg.g^{-1}) is the amount of solute adsorbed by 1g of activated carbon at the equilibrium concentration C_e (mg.l^{-1}). Q_0 (mg.g^{-1}) and b (l.mg^{-1}) are the Langmuir constants characterising the ultimate adsorption capacity and the surface binding energy respectively.

The amount of adsorbed solute q_e was determined as follows:

$$q_e = \frac{(C_0 - C_e) . V}{m_{ac}} \quad (2)$$

In the equation (2) C_0 is the initial concentration (mg.l^{-1}), V the volume of the pollutant solution (l) and m_{ac} the mass of activated carbon in the volume V.

The constants Q_0 and b were determined from the linear form of Langmuir equation i.e.:

$$\frac{C_e}{q_e} = \frac{1}{Q_0} C_e + \frac{1}{b \cdot Q_0} \quad (3)$$

If the adsorption isotherms are of type L, as it is the case for both the pollutants in the present work (fig. 4, 5, 7, and 8), then the empirical equation of Freundlich (Benefield et al. 1982) is well suited. It is defined by the following relationship in which k [$mg.g^{-1}(l.mg^{-1})^{1/n}$] and n are empirical constants.

$$q_e = kC_e^{\frac{1}{n}} \quad (4)$$

The values of k and $1/n$ are respectively obtained from the intercept and the slope of the linear plot of ln (q_e) versus ln (C_e). The constant k can be defined as the sorption or the distribution coefficient, and represents the quantity of adsorbed pollutant for a unit equilibrium concentration (i.e., C_e =1). The slope $1/n$ is a measure of the sorption intensity. For n = 1, the partition between the two phases is independent of the concentration. A value of $1/n$ below one indicates a normal Langmuir isotherm (of type L) while $1/n$ above one is indicative of a cooperative sorption i.e. with strong interactions between the molecules of adsorbate themselves.

For predicting the favourability of an adsorption system, the Langmuir equation, like the Freundlich equation, can also be expressed in terms of a dimensionless separation factor R_L, defined as (Mckay et al.1982):

$$R_L = \frac{1}{1 + b.C_{0max}} \quad (5)$$

C_{0max} being the initial concentration of the pollutant in solution. The R_L value implies the adsorption to be either unfavourable (R_L >1), linear (R_L = 1), favourable (0 < R_L < 1) or irreversible (R_L = 0).

RESULTS AND DISCUSSION

Thermo-compression of Fir Wood

Thermo-compression at 180 °C resulted in a slight weight loss of wood, about 0.8 % on a dry basis and about 7 to 8 % on a wet basis. The weight loss corresponds to the moisture content of wood, in equilibrium with the ambient air.

The rheological properties of wood suddenly changed when temperature reached 180 °C. Some softening and plasticisation of wood occurs at these temperatures. Thermo-compression involves a strong flattening of the fir lumps. Typically, the thickness of lumps was reduced from 12 to about 2 mm, whereas their breadth increased from 17 to 41 mm. Their length (i.e. in the fibres direction) did not change significantly. Figure 1 illustrates the simultaneous changes of thickness and breadth as a function of the load (in tons) applied by the press on a single lump of fir. It can be noted that the breadth linearly varied with load, while this was not the case for thickness. As a consequence of thermo-compression, the density of a wood lump increased by its flattening (Fig. 2).

The compression, up to a load of 5 tons, made it possible to multiply by 2.6 the initial density of a single lump of fir-wood, providing a slab with a density similar to that of coconut shell and larger than the average density of oak wood. A maximal load of 5 tons corresponds to a final pressure of 600 kgf/cm^2 applied on the wood lump. The pressure required to reach this density ratio was significantly lower than those experienced by Abe et al. (2001), between 1000 and 3000 kgf/cm^2, at ambient temperature. These authors found densities of compressed wood only twofold that of virgin wood.

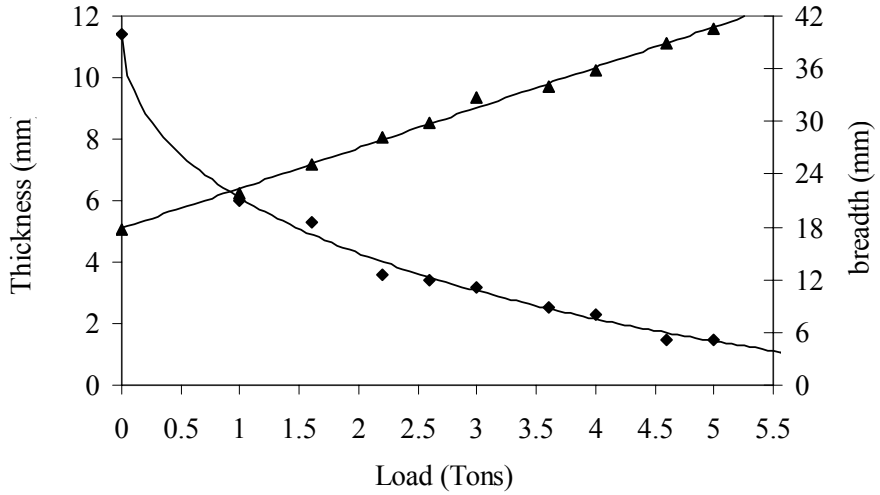

Fig. 1: Effect of thermo-compression at 180 °C on the dimensions of a fir lump. (▲) breadth, (♦) thickness

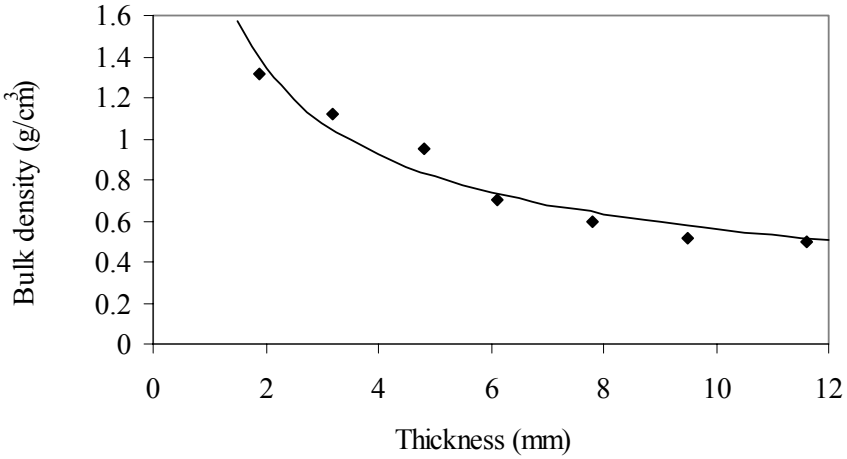

Fig. 2: Effect of thermo-compression at 180 °C on the bulk density of a fir lump.

Pyrolysis

In the case of a simple pyrolysis, without activation, the yield in charcoal increased with the extent of compression. This yield rose from 23.35 % to 24.52 % at a plateau temperature of 600 °C. Abe et al. (2001) also found a slight increase of pyrolysis yield of about 1.5 % by compression. During pyrolysis, the volatile tar products do not readily escape from a solid matrix, since they are densified by thermo-compression. As a possible consequence of the increased retention of volatile tars, the so called secondary reactions of pyrolysis are promoted, yielding thereby more solid carbon generated after graphitisation reactions. The yields found in this work are comparable to those found by Byrne and Nagle (1997a) that have pyrolysed seven wood species and found yields ranging from 24.8 to 32.5 percent.

A simple pyrolysis does not result in good properties for the produced char. The BET surface area of pyrolysed chars never exceeded 300 m^2g^{-1}. It even decreased with temperature and dropped to 27 m^2g^{-1} at 800 °C. These results are similar to those obtained by Hu and Srinivasan (1999), who reported a BET surface area as low as 16 m^2g^{-1} for the pyrolysis of

coconut shells. A decrease in the mass yield was observable when increasing the maximal temperature of pyrolysis from 600 °C to 800 °C. With only pyrolysed chars, the adsorption capacity of methylene blue appeared very low in comparison to that of phenol, which is relatively more significant. The influence of main components of wood, cellulose, hemicelluloses and lignin on the development of pores during pyrolysis was discussed by Khezami et al. (2005). It was found that cellulose plays a major role. Cellulose chains, partially crystalline, are associated in microfibrils. As stated by Byrne and Nagel (1997b), cellulose microfibrils dominate the mechanism of dimensional change during pyrolysis. This shrinkage is attributed to the formation of graphitic layers resulting from the aromatisation process after thermal decomposition of glycosidic chains. Authors including Pastor-Vilegas et al. (1998) and Babel (2003) have emphasised that micropores are essentially constituted by spaces created between the graphitic layers.

Physical Activation

The activation results from the oxidation of carbon according to the heterogeneous gas-solid reaction: $C+CO_2 \rightarrow 2CO$. This reaction tends to create pores within the matrix of carbon, leading to a mass loss of A.C. The characterisation of the porous structure usually has been made by physical adsorption of an inert gas, such as nitrogen or argon under reduced pressure. The shape of isotherms provides information about the sizes of pores, which are usually divided into micro, meso, and macropores. Figure 3 illustrates the shape of the N_2 adsorption-desorption isotherm at 77 K for the CO_2-activated carbon. The isotherms shown in Fig. 3 are clearly of type II, with a hysteresis of H4 type (Rouquerol et al. 1999). Occurring at elevated relative pressure P/P_0, the hysteresis of H4 type is due to the filling up of mesopores by capillary condensation. When the physical activation is increased, the walls of some micropores can be destroyed, yielding mesopores. This phenomenon of pore coalescence was reported by Rodriguez-Reinoso and Molina-Sabio (1994) for the activation of various cellulosic wastes (olive stones and almond shells). They found that in all cases, activation with CO_2 opens and widens micropores into meso and macropores. According to these investigators, the ablation of the outside of the particle is significant at high burn-off, indicating a complete destruction of the wall of pores. The various characteristics of physically activated carbons, particularly the parameters Q_0 and b for both the model pollutants, are presented in Table 1.

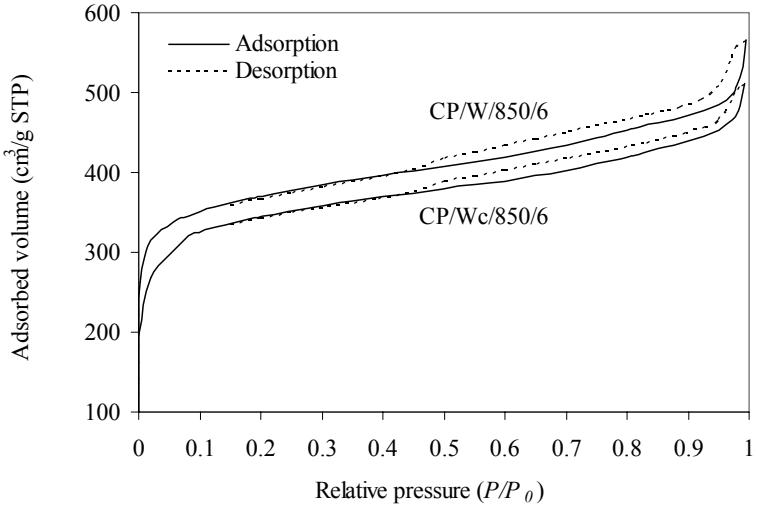

Fig. 3: CO_2 activated carbon. Adsorption-desorption isotherms of N_2 at 77 K

Table 1: Main characteristics of CO_2 activated carbons and pyrolytic char

Active Carbon	Mass yield	S.BET	Methylene Blue					Phenol				
			Q_0	b	R_L	$1/n$	k	Q_0	b	R_L	$1/n$	k
CP/W/750/3	15.90	587	190.89	0.02	0.2000	0.227	107.65	103.95	0.35	0.0187	0.336	24.73
CP/W/750/6	11.66	938	238.09	2.93	0.0017	0.122	172.55	123.45	0.75	0.0088	0.243	32.37
CP/W/750/9	9.64	963	454.54	5.50	0.0009	0.099	317.77	217.4	0.92	0.0072	0.158	100.26
CP/W/850/3	11.82	734	312.04	3.44	0.0014	0.130	213.07	136.89	0.68	0.0097	0.322	33.21
CP/W/850/6	5.60	1257	666.67	7.48	0.0007	0.102	472.67	188.68	0.29	0.0224	0.283	54.02
NP/Wc/600/1	24.52	291	72.48	0.02	0.2000	0.808	1.49	77.87	0.35	0.0187	0.297	26.13
CP/Wc/750/3	18.32	508	129.15	0.29	0.0169	0.319	40.00	138.07	0.18	0.0357	0.209	34.37
CP/Wc/750/6	15.32	647	165.04	1.42	0.0035	0.173	94.86	153.11	0.62	0.0106	0.194	71.35
CP/Wc/750/9	11.23	908	412.44	2.00	0.0025	0.136	272.08	231.57	0.99	0.0067	0.165	92.60
CP/Wc/850/3	13.98	611	258.23	2.24	0.0023	0.127	181.44	164.30	0.57	0.0115	0.196	50.70
CP/Wc/850/6	7.00	1162	563.14	3.63	0.0014	0.085	436.36	204.31	0.47	0.0140	0.152	108.53

The parameters Q_0 and b were found to be much larger after physical activation than after a simple pyrolysis. They were calculated from the sorption isotherms of both the pollutant models which are of type L i.e. similar to the type I for gaseous species. According to the values of the separation factor R_L, the adsorption processes were revealed to be favourable with CO_2-activated carbon. The values found for the parameter $1/n$, significantly lower than 1, are coherent with isotherms of type L (Figs. 4 and 5). Nevertheless for the adsorptions of methylene blue by simply pyrolysed char (see figure 5), the values of the parameters $1/n$ and R_L are relatively high when compared to the others in Table 2, indicating behaviour far from a normal Langmuir process. Raising either time or temperature allows extending the degree of activation, the BET surface area, in addition to the factors Q_0 and k. In the same time, the factor $1/n$ decreases, thus testifying to a more marked Langmuir behaviour of the adsorbent-adsorbate system, well depicted by the concave-shape of sorption isotherms (Figs. 4 and 5).

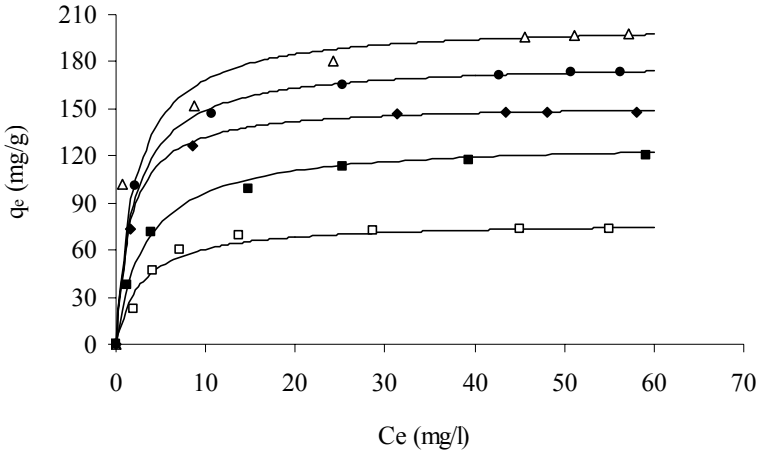

Fig. 4: Langmuir isotherms for phenol adsorption. Pyrolysed char (□) NP/Wc/600/1, CO_2-activated carbon (■) CP/Wc/750/3, (♦) CP/Wc/750/6, (●) CP/Wc/750/9 and (Δ) CP/Wc/850/6 at ambient temperature.

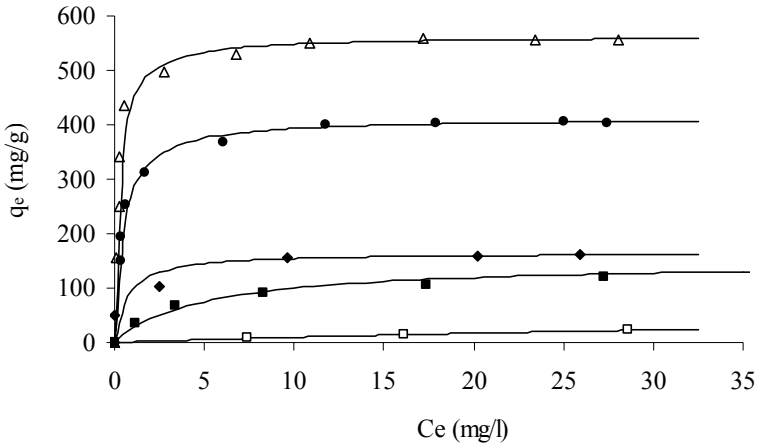

Fig. 5: Langmuir isotherms for adsorption of methylene blue Pyrolysed carbon (□) NP/ Wc /600/1, activated carbon: (■) CP/Wc /750/3, (♦) CP/ Wc /750/6, (●) CP/ Wc /750/9 and (∆) CP/ Wc /850/6 at ambient temperature

BET surfaces areas and adsorption capacities for model pollutants rise with both the temperature and time of activation. Thus, when the activation time in plateau passed from 6 to 9 hours, the increase in surface area was 300 m^2g^{-1} for A.C. from thermo-compressed wood, whereas it was only 25 m^2g^{-1} for A.C. from virgin wood. Unfortunately, a drastic decrease in the mass yield in A.C. occurs with increasing time and temperature of activation. The mass yield even drops to only 7-8 % for A.C. with usual BET surface areas larger than 1000 m^2g^{-1}. From Table 2 it is clear that the adsorption capacity of methylene blue varied as the BET surface area. In the case of phenol, this trend was not observed. It can be assumed that phenol adsorption does not only depend on the BET surface area, but also on the microporous nature of adsorbent, which is not the case with a larger molecule such as methylene blue. With other investigators, Lopez-Gonzalez et al. (1980) have observed, as in the present work, that slightly activated carbon or simply carbonised chars exhibit a quasi null adsorption capacity of methylene blue. Indeed, this kind of adsorbent shows a very low BET surface area, although its structure is exclusively micro-porous.

It is obvious from Table 1 that the pre-treatment of thermo-compression has an enhancing effect upon the mass yield in A.C. Concerning the adsorption capacity, a slight enhancing effect is observed only in the case of phenol adsorption.

Chemical Activation

As shown by Fig. 6, the adsorption isotherms of N_2 at 77 K for KOH-activated carbon are clearly of type I. Not exhibiting any hysteresis, such isotherms are typical of a structure mainly microporous with a narrow distribution of pore sizes. By contrast, H_3PO_4-activated carbon as Acticarbone CXV showed a sorption isotherm of N_2 very different, practically of type IV, which is indicative of a solid material rich in mesopores. The hysteresis of H4 type indicates a shape of pores more flat than cylindrical. Issa and Teresa (2000) have reported some similar influences of the activating agent, alkaline and acidic, on the aspect of sorption isotherms. Table 2 also regroups the main properties of KOH-activated char from various precursors: virgin and compressed wood, coconut shell and olive stones. By comparing the data in Tables 1 and 2, it can be concluded that the mass yields are significantly higher for the KOH-activated carbon than for the CO_2-activated samples, with the same BET surface area.

Furthermore, the KOH activation generates microporosity higher than any other mode of activation. It can be noted that the average pores diameter for KOH-activated carbons was found to be below 2 nm, indicating a rather microporous structure. The commercial activated carbon Acticarbone CXV, with an average pores diameter of 3.3 nm and a high mesopores surface area, can therefore be classified as mesoporous material. Issa and Teresa (2000) have shown that the KOH activated carbons have a homogeneous microporosity and a high surface area, while those activated by phosphoric acid exhibit a rather high mesoporous volume and a significantly lower surface area.

After activation, the washing of A.C. up to a neutral pH was crucial to remove the incrustations of mineral matter within the pores. Hence, in the present study, the measure of the BET surface area of a KOH activated carbon was 634 m^2g^{-1} before washing, and 1792 m^2g^{-1} after washing.

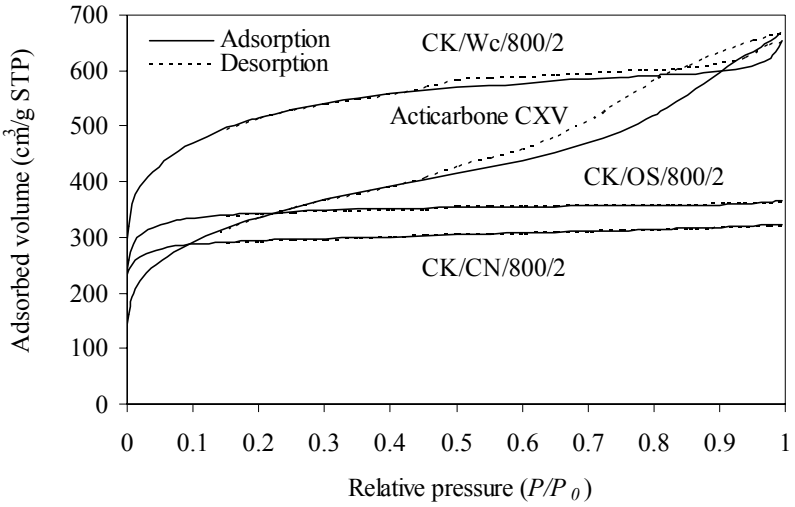

Fig. 6: KOH activated carbon. Adsorption-desorption isotherms of N_2 at 77 K

All tests of chemical activation were carried out with a plateau duration fixed to 2 hours. The variable parameters were the initial KOH content, the temperature of plateau, and the precursor material. First of all, it should be noted that an increase in the KOH content improved all the properties of activated carbon, except the mass yield as shown in Table 3. However, a KOH content of 0.125 appears too low, since the corresponding BET surface area was only 428 m^2g^{-1}. In the same experimental conditions, the BET surface area amounted to 1589 m^2g^{-1}, with a KOH content equal to 1. To achieve a satisfactory value of the BET surface area, the KOH content must not be lower than 0.4. For comparison, at 780 °C and one hour activation time, Wu et al (2005) reported surface area of 891 and 1371 $m^2 g^{-1}$ with KOH content of 0.5 and 1 respectively. These surface areas are close to those found in the present work (see Table 3). As other investigators, Wu et al. (2005) tested a larger KOH content up to 6 leading to activated carbon with a very high surface area up to 2794 $m^2 g^{-1}$. However, large KOH content results in too expensive activated carbons as far as a very high surface area is not really needed for usual applications.

All the properties of A.C. increase with the temperature of the plateau. A temperature of 600 °C is however too low to confer to the produced A.C. a high specific surface area of pores i.e. over 1000 $m^2.g^{-1}$. Concerning the precursor material, the A.C. from wood exhibits a better BET surface area than the A.C. from the other precursors. An acid-activated carbon as

Acticarbon CXV has a rather poor adsorption capacity in phenol and methylene blue despite of a good BET surface area (1210 $m^2.g^{-1}$), therefore, it should be less suited to water purification than a KOH activated carbon.

For the tested solutions of phenol, the initial pH was in the range 7-7.8. As reported by Rengaraj et al. (2002), the phenol removal is the highest and is constant in the pH range 4 – 9, while out of this range, the removal efficiency decreases. In the case of methylene blue adsorption, the pH was not fixed by addition of buffer solution, thus the pH was ranging from 7 (concentration 30 mg/l) to 8.4 (concentration 200 mg/l). It was demonstrated by various investigators such as El Qada et al. (2006) that the pH does not affect the uptake efficiency of methylene blue within a pH ranging from 4 to 9, while at alkaline pH (≥11) the uptake is higher.

The experimental isotherms for phenol and methylene blue were well fitted by the Langmuir model, as illustrated by Figs. 7 and 8. The parameter Q_0 related to both the model pollutants varied as the BET surface area when using KOH as activating agent, while the dependence of the parameter *b* with the BET surface was not so clear. From Table 3 it can also be noted that the very low values of the separation factor, R_L, attest to the favourable sorption power of all the KOH-activated carbons from the various precursors, moreover, as for the CO_2 activated chars, there is a good concordance between the parameters Q_0 and *k*. In all cases, the values of the parameter *1/n* <<1, are indicative of a Langmuir process and of very weak interactions between molecules of solute. However, the influence of the experimental conditions upon the parameter *1/n* is not obvious. There was a visible effect of the KOH content; indeed, *1/n* was clearly higher when the KOH content was below 50 %. Besides, the parameter *1/n* decreased with increasing temperatures, which could be justified by an evolution of the sorption system towards a normal Langmuir process.

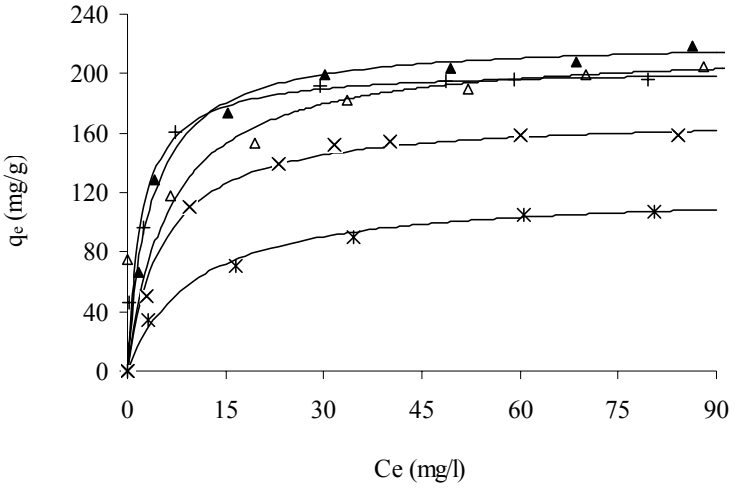

Fig. 7: Langmuir isotherms at 25 °C for the phenol adsorption: (▲) CK/Wc/800/2, (∆) CK/W/800/2, (x) CK/OS/800/2, (+) CK/CN/800/2, (*) Acticarbone CXV

Table 2: Main Characteristics of KOH Activated Carbons.

Activating Agent	Activated Carbon	Mass Yield (%)	Surface area ($m^2.g^{-1}$)	Methylene blue					Phenol				
				Langmuir			Freundlich		Langmuir			Freundlich	
				Q_0 ($mg.g^{-1}$)	b ($l.mg^{-1}$)	R_L	$1/n$	k	Q_0 ($mg.g^{-1}$)	b ($l.mg^{-1}$)	R_L	$1/n$	k
KOH	CK/W/600/2	21.56	766	140.5	0.88	0.0056	0.083	96.68	131.4	0.12	0.0526	0.334	30.17
	CK/Wc/600/2	24.09	906	169.4	0.64	0.0077	0.086	116.42	147.9	0.14	0.0454	0.293	40.84
	CK/W/700/2	18.12	1358	621.6	4.66	0.0011	0.124	421.42	164.3	0.22	0.0294	0.260	56.46
	CK/Wc/700/2	20.61	1589	646.1	5.10	0.0010	0.167	401.99	320.4	0.30	0.0217	0.242	116.41
	CK/W/800/2	15.98	1773	673.4	2.86	0.0017	0.082	495.80	216.4	0.28	0.0233	0.215	80.63
	CK/Wc/800/2	18.32	1792	631.2	3.58	0.0014	0.060	498.22	227.6	0.20	0.0323	0.212	87.77
	CK/CN/800/2	25.37	986	235.6	4.86	0.0010	0.062	118.52	203.6	0.23	0.0282	0.251	75.37
	CK/OS/800/2	24.12	1155	301.2	9.09	0.0005	0.025	284.44	171.4	0.42	0.0156	0.323	46.80
H_3PO_4	Acticarbone CXV	-	1210	235.6	8.31	0.0006	0.126	168.14	120.6	0.18	0.0357	0.361	23.86

Table 3: The effect of KOH content on the different characteristics of the activated carbons.

Activated Carbon	Mass Yield (%)	Surface area ($m^2.g^{-1}$)	Methylene blue					Phenol				
			Langmuir			Freundlich		Langmuir			Freundlich	
			Q_0 ($mg.g^{-1}$)	b ($l.mg^{-1}$)	R_L	$1/n$	k	Q_0 ($mg.g^{-1}$)	b ($l.mg^{-1}$)	R_L	$1/n$	k
CK_1/Wc/700/2	20.61	1589	646.1	5.10	0.0010	0.167	401.99	320.4	0.30	0.0217	0.242	116.41
$CK_{0.5}$/Wc/700/2	22.04	1108	442.2	4.06	0.0012	0.345	240.38	198.9	0.15	0.0425	0.319	49.29
$CK_{0.125}$/Wc/700/2	24.82	428	63.7	0.11	0.0435	0.286	16.91	111.8	0.12	0.0526	0.304	33.23

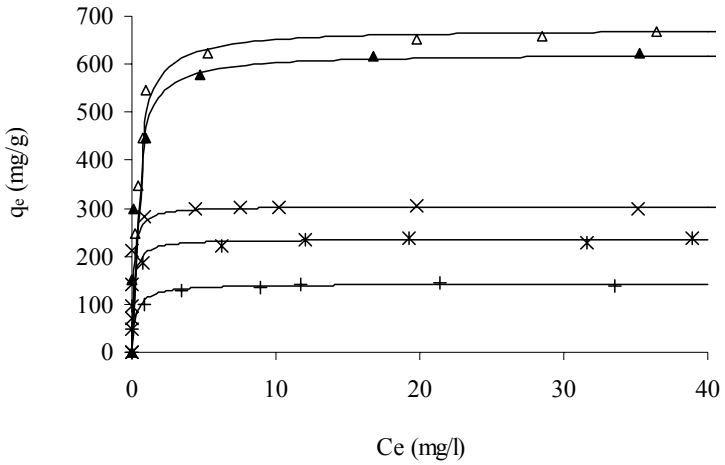

Fig. 8: Langmuir isotherms at 25 °C for the adsorption of methylene blue: (▲) CK/Wc/800/2, (∆) CK/W/800/2, (x) CK/OS/800/2, (+) CK/CN/800/2, (*) Acticarbone CXV

When considering the literature, there is a large scatter of the parameters of the Langmuir and Freundlich models due to a great diversity in the preparation mode of activated carbon and experimental conditions of adsorption (temperature, pH, amount of A.C.). Nevertheless, the parameters obtained in the present work are in the same magnitude as those reported in literature (Kumar et al. 2007).

For instance, the extreme values of Q_0 found from literature data, for phenol adsorption on A.C. were 3.22 and 572 mg/g, while Q_0 values of the present work were in the range 77-231 mg/g (see Table 2). As for Q_0, all the other identified parameters of both the models (b, 1/n, k) were within the limit values given in literature for adsorption of phenol and methylene blue.

As indicated in Table 3, thermo-compression allows increasing the mass yield in A.C. from wood, by 2 to 3 % that obviously appears economically interesting. Furthermore, thermo-compression results in some improvements, rather slight for the BET surface area and more important for the adsorption capacity of phenol. For the adsorption of methylene blue, thermo-compression does not show a marked enhancement as it has been observed by Abe et al. (2001) in adsorption tests with iodine solutions. These general trends are valid whatever the mode of activation.

The main characteristics of the different activated carbons determined by the t-plot method of Lippens and De Boer (1965) are presented in Table 4. The data of acticarbone CXV are in accordance with the trends revealed by the adsorption isotherms and confirms that it is mostly mesoporous in comparison to KOH activated carbon. The surface area of KOH activated carbon is strongly dependent on the ratio KOH/char. As testified by the average pore diameter (> 2.4 nm), the CO_2 activated carbon is also slightly mesoporous. Lastly, a thermo-compression seems improving the KOH activated carbon in terms of the BET surface area.

Table 4: Adsorption of N_2 at 77 K

Active carbon	Micropore surface area ($m^2.g^{-1}$)	Mesopore surface area ($m^2.g^{-1}$)	Micropore volume ($cm^{-3}.g$)	Average pore diameter (nm)
CP/W/850/6	836	421	0.390	2.48
CP/Wc/850/6	754	408	0.349	2.45
CK/W/600/2	545	221	0.250	1.88
CK/Wc/600/2	715	191	0.331	1.99
CK/W/700/2	978	380	0.449	1.96
CK/Wc/700/2	1219	370	0.564	1.95
$CK_{0.5}$/Wc/700/2	849	192	0.425	1.91
$CK_{0.125}$/Wc/700/2	428	53	0.199	1.9
CK/W/800/2	1492	282	0.468	2.14
CK/Wc/800/2	1606	186	0.510	2.04
CK/CN/800/2	836	150	0.388	2.02
CK/OS/800/2	949	206	0.442	1.94
ActicarboneCXV	230	980	0.091	3.33

CONCLUSIONS

1. In this work it has been shown that preliminary thermo-compression is an easy way of conferring to a tender wood a bulk density about 2.5 times larger than its initial density.
2. A simple pyrolysis under neutral atmosphere reveals that mass yield in charcoal increases with the extent of thermo-compression. Thermo-compression also slightly increases the mass yield in activated carbon, regardless of the mode of activation.
3. Potassium hydroxide is an efficient activating agent, since it confers to an active carbon prepared from various biomasses a high microporosity but it presents the disadvantage of using high ratios KOH/A.C. resulting in an expensive activated carbon.
4. In addition to the mass yield in active carbon, mentioned above, the main benefit of thermocompression seems to lie in a better performance of phenol removal from aqueous solutions. In fact, the micro-porous structure partly generated by thermo-compression seems to enhance the adsorption of a small size molecule as phenol.

References Cited

Abe I. , Fukuhara T., Iwasaki S., Yasuda K., Nagakawa K., Iwata Y., Kominami H., and Kera Y. (2001). "Development of a high density carbonaceous adsorbent from compressed wood," Carbon 39, 1485-1490.

Ahmadpour, A., and Do, D. D. (1996). "The preparation of active carbons from coal by chemical and physical activation," *Carbon* 34, 471-479.

Babel K. (2003)."Porous structure evolution of cellulose carbon fibres during heating in the initial activation stage," Fuel Processing Technology 85, 75-89.

Benefield L. D., Judkins J. F., and We, B. L.(1982). *Process Chemistry for Water and Wastewater Treatment*, Prentice-hall, Englewood Cliffs, NJ.

Brunauer S., Emett P.H. and Teller E. (1938). "Absorption of gases in multimolecular layers," J. A. Chem. SOC. 60, 309

Byrne C. E. and Nagle D. C. (1997a)."Carbonization of wood for advanced materials applications," Carbon 35, 259-266.

Byrne C.E., Nagle D.C. (1997b). "Carbonized wood monoliths-characterization," Carbon 35, 267-273.

Ehrburger, P., Addoun, A., Abdoun, F., and Donnet, J. B.(1986). "Carbonisation of coals in the presence of alkaline hydroxide and carbonates: formation of activated carbons," *Fuel* 65, 1447-1449.

El Qada, E. N., Allen, S. J., and Walker, G. M. (2006). "Adsorption of methylene blue onto activated carbon produced from steam activated bituminous coal: A study of equilibrium adsorption isotherm," *Chemical Engineering J.* 124, 103-110.

Franke F. H., and Meraikib, M. (1970). "Catalytic influence of alkalis on carbon gasification reaction," *Carbon* 8, 423-433.

Gergova, K., Petrov, N., and Eser, S. (1994). "Adsorption properties and microstructure of activated carbon produced from agricultural by-products by steam pyrolysis," *Carbon* 32; 693-702.

Guo, J., and Lua, A. C. (1998). "Characterisation of chars pyrolysed from oil palm stones for the preparation of activated carbons," *J. Analytical and Applied Pyrolysis*," 46, 113-125.

Guo J., and Lua, A. C. (1999). "Textural and chemical characteristics of activated carbon prepared from oil-palm stone with H_2SO_4 and KOH impregnation," *Microporous and Mesoporous Materials* 32, 111-117.

Hu, Z., and Srinivasan, M. P. (1999). "Preparation of high surface area activated carbons from coconut shell," *Microporous and Mesoporous Materials* 27, 11-18.

Hüttinger, K., J and Minges, R. (1986). "Influence of the catalyst precursor anion in catalysis of water vapour gasification of carbon by potassium," *Fuel* 65, 1112-1121.

Issa, I., and Teresa, J. (2000). "Comparison of the surface feature of two wood-based activated carbons," *Ind. Eng. Chem. Res*. 29, 301-306.

Khezami, L., and Capart, K. (2005). "Removal of chromium (VI) from aqueous solution by activated carbons: Kinetic and equilibrium studies," *J. Hazardous Materials* B123, 223-231.

Khezami L., Chetouani A., Taouk B. and Capart R. (2005)."Production and characterisation of activated carbon from wood components in powder: cellulose, lignin, xylan," Powder Technology 157, 48-56

Kumar A., Kumar S., Kumar S., and Gupta, D. V. (2007). "Adsorption of phenol and 4-nitrophenol on granular activated carbon in basal salt medium: Equilibrium and kinetics," *J. Hazardous Material*, in press.

Laine, J., and Yunes, S. (1992). "Effect of the preparation method on the pore size distribution of activated carbon from coconut shell," *Carbon* 30, 601-604.

Laine, J., Calafat, A., and Labady, M. (1989). "Preparation and characterisation of activated carbons from coconut shell impregnated with phosphoric acid," *Carbon* 27, 191-195.

Langmuir I. (1918). "The adsorption of gases on plane surfaces of glass, mica, platinum," J. *Am. Chem. Soc.* 40, 1361-1403.

Lippens, B. C., and De Boer, J. H. (1965). "Pore systems in catalysts. V. The t-method," *J. Catalysis* 4, 319-323.

Lopez-Gonzalez, J. D., Martinez-Vilchez, F., and Rodriguez-Reinoso, F. (1980). "Preparation and characterisation of active carbons from olive stones," *Carbon* 18, 413-418.

Marsh H. (1987). "Adsorption methods to study microporosity in coal and carbons – a critique," *Carbon* 25, 49-58.

Marsh, H., Yan, D. S., O'Grady, T. M., and Wennerberg, A. (1984). "Formation of active carbons from cokes using potassium hydroxide," *Carbon* 22, 603-611.

Mckay, G., Blair, H. S., and Gardner, J. R. (1982). "Adsorption of dye on chitin I. Equilibrium studies," *J. Appl. Polym. Sci.* 27, 3043.

O'Grady, T. M., and Wennerberg, A. N.(1986). "High surface area active carbon: Petroleum-derived carbons," ACS Symp. Ser., Washington DC, 303-302.

Pastor-Villegas J., Durán-Valle J., Valenzuela-Calahorro C. and Gómez-Serrano V. (1998)."Organic chemical structure and structural shrinkage of chars prepared from Rockrose," *Carbon* 36, 1251-1256.

Rengaray, Y., Seung-Hyeon, M. , Sivabalan, R., Arabindoo, B., and Murugesan, V. (2002). "Agricultural solid waste for the removal of organics: Adsorption of phenol from water and wastewater by palm seed coat activated carbon," *Waste Management* 22, 543- 548.

Rodriguez-Reinoso F. and Molina-Sabio M.(1994). "Activated carbons from lignocellulosic materials by chemical and/or physical activation," Carbon 30, 1111-1118.

Rouquerol, F., Rouquerol, J., and Sing, K. (1999). *Adsorption by Powder and Porous Solids: Principles, Methodology and Applications*, Academic Press, London.

Sodya Sai, P. M., Ahmed, J., and Kirshnaiak, K. (1997). "Production of activated carbon from coconut shell char in a fluidised bed reactor," *Ind. Eng. Chem. Res*. 36, 3625-3630.

Toles, B. C., Rimmer, S., and Hower, J. C. (1996). "Production of activated carbons from Washington lignite using phosphoric acid activation," *Carbon* 34, 1419-1426.

Tsai, W. T., Chang, C. Y., Lin, M. C., Chien, S. F., Sun, H. F., and Hsieh, M. F. (2001). "Adsorption of acid dye onto activated carbons prepared from agricultural waste bagasse by $ZnCl_2$ activation," *Chemosphere* 45, 51-58.

Ubago-Pérez R., Carrasco-Marín F., Fairén-Jiménez D. and Moreno-Castilla C. (2006) **"** Granular and monolithic activated carbons from KOH-activation of olive stones, **"** Microporous and Mesoporous Materials 92, 64-70.

Walker JR P.L. (1996). "Production of activated carbons: use of CO_2 versus H20 as activating agent," *Carbon* 34, 1297-1299.

Warhurst A. M., Fowler, G. D., McConnachie, G. L., and Pollard, S. J. (1997). "Pore structure and adsorption characteristics of steam pyrolysis carbons from Moringa Oleifera," *Carbon* 35, 1039-1045.

Wu, F. C., Tseng, R. L., and Juang, R. S. (2005)."Preparation of highly micoporous carbons from wood by KOH activation for adsorption of dyes and phenols from water," Separation and Purification Technology 47, 10-19.

Article submitted: March 2, 2007; Article resubmitted with formatting changes: March 5, 2007; First round of reviewing completed: April 1, 2007; Revised article received: April 13, 2007; Revised article accepted: April 13, 2007; Published: April 15, 2007

MODELING ENERGY CONSUMPTION FOR THE GENERATION OF MICROFIBRES FROM BLEACHED KRAFT PULP FIBRES IN A PFI MILL

Ayan Chakraborty,[a] Mohini M. Sain,[a,b*], Mark T. Kortschot[a] and Subrata B.Ghosh[b]

The objective of this paper is to model the energy consumed in generating cellulose microfibres, 1 µm in diameter, as reinforcing agents, by refining bleached softwood kraft pulp in a PFI mill. An average initial fibre diameter of 13 µm was assumed. 125,000 revolutions in a PFI mill was found to produce a high yield of fibres 1.3 µm in diameter, and the minimum refining energy needed to reduce the fibre diameter to 1.3 µm was estimated as 1875 kJ for each 24 g charge in the PFI mill. Since elastic deformation of the fibres was found to be negligible, the size reduction was assumed to follow Rittinger's Law. This gave a Rittinger's constant of 28 J.m/kg for the given system. Using this value of Rittinger's constant, the energy required to generate microfibres 1 µm in diameter was predicted as 2480 kJ for each 24 g charge in the PFI mill. It was deduced that microfibres generated in this way would cost a minimum of $2.37 per kilogram. Hence even this relatively inefficient method of grinding would not be prohibitively expensive, provided the resulting microfibres can be used as high quality reinforcements.

Keywords: cellulose microfibres, reinforcing agents, refining, PFI mill, Rittinger's Law

*Contact information: a: Department of Chemical Engineering and Applied Chemistry, University of Toronto, 200 College Street, Toronto, Ontario, Canada M5S 3B3; b: Faculty of Forestry and Centre of Biocomposites and Biomaterials Processing, University of Toronto, 33 Willcocks Street, Toronto Ontario, Canada M5S 3E5; *Corresponding author: m.sain@utoronto.ca*

INTRODUCTION

There is widespread interest in the production and use of micro- and nano-scale fibres for use as reinforcing agents. This trend originated with the production of nano-scale clay particles by researchers at Toyota, and has been accelerated because of the more recent introduction of carbon nano-tubes. There is also a great deal of interest in producing nano-scale cellulosic fibres from wood pulp and agricultural by-products; however, reliable and economical processes for doing this have yet to be developed.

In the present study, we examine the possibility of using refining as a method to generate microfibres 1 µm in diameter from wood pulp fibres of approximately 13 µm diameter. Such microfibres with high aspect ratio (length/diameter) would have the potential to act as excellent reinforcing agents in polymers. Refining is a specialized method of grinding fibres used in the pulp and paper industry; it is used in mechanical pulping, and also in developing fibre properties of pulp in papermaking. In a refiner, a dilute pulp suspension is forced through a gap between two surfaces moving rapidly relative to each other. Of these two surfaces, at least one has bars with sharp edges.

Although this attempt to generate microfibres through refining is novel, production of fines during mechanical pulping has been studied and reviewed extensively by various researchers (Brecht, Klemm 1953; Mohlin 1977; Corson 1980; Luukko and Paulapuro 1997; Luukko 1998; Courchene et al. 2002). Fines are defined by the Technical Association of the Pulp and Paper Industry (TAPPI) as "particles that will pass a round hole 76 μm in diameter or a nominally 200 mesh screen". Therefore, fines include both fibrillar materials of submicron diameter and hundreds of microns long, as well as chopped fragments of fibres having diameters in the same range as the dimension of the mesh opening.

Fibre development during mechanical refining, and its effect on the fracture energy of paper sheets of different pulp mixes, has been studied in detail (Lidbrandt et al. 1980; Mohlin et al. 1995; Mohlin 1997; Hiltunen et al. 2000; Hiltunen et al. 2002). However, these studies looked into the effect of refining on the strength of the paper structure directly, rather than focusing on the generation of microfibres.

The process of delamination of fibre walls by beating and refining has been studied in considerable detail (Page et al. 1967). As elucidated by Karnis (1994), the forces acting on the fibres in refining are assumed to act along the fibre length. As a result, the fibres are peeled off the surface in refining, as opposed to being chopped off perpendicular to the fibre length. This mechanism suggests that fibre length remains unchanged. The paper further noted that microscopic observations substantiated the above assumption. However, in practice, there is some fibre shortening associated with refining. Models on such comminution of fibres have been developed by Roux and Mayade (1997), who examined the change of the mean fibre length during refining. In this model, the potential of fibre cutting under given conditions was predicted to be a function of the energy consumed by the solid phase and of the average impact intensity, i.e., the ratio between the net machine power and the "cutting" length of bars per unit time. Corte and Agg (1980) used a comminution model to compare the shortening rate of fibres in a disc refiner and a laboratory beater. They found that the disc refiner cuts longer fibres more rapidly than the short fibres, while the laboratory beater was found to cut long and short fibres at the same rate. Olson et al. (2003) found that the probability of a fibre being selected for cutting during refining is proportional to the applied energy and fibre length, and was independent of pulp consistency. Corson (1972) mathematically modeled the refining of wood chips into individual fibres using a comminution approach. This approach was more recently expanded by Strand and Mokvist (1989) to model the operation of a chip refiner employed in mechanical pulping of wood chips.

However, these studies all used comminution models to predict the cutting of fibres perpendicular to the fibre axis, rather than the peeling action assumed to be predominant in refining (Karnis, 1994). The objective in this present study, therefore, is to model the energy consumed in peeling of a cellulose fibre to yield microfibres of smaller diameter

To study the effects of refining of pulp on papermaking in a laboratory scale, a PFI mill is commonly used. The PFI mill is used to pulp beat fibres to increase fibre flexibility and improve the properties of the resulting handsheet. In the process, the refiner causes fibrillation generating fibres of smaller diameter, and also produces fines.

The components of a PFI mill are shown in Fig. 1. During the operation of the PFI mill, the head containing the bars is pushed to one side of the casing, as shown in Fig. 1. As elaborated by Murphy (1962), the stock in a PFI mill is centrifuged against the wall of the mill house. It is carried around in a narrow band toward the beating gap where it converges with the moving bars of the roll. The mill house at that point forms a smooth bedplate. The fibres are subjected to impact by rotating bars against the bedplate. The action of any refiner is determined by shear and compression forces in the refining zone, and by their distribution on single fibres. These forces are more evenly distributed in a laboratory beater such as the PFI mill than in industrial refiners. In over-simplified terms, the beating action resembles a plunger moving down into the pulp mass (Watson, Phillips 1964). The primary effects of the beating process are:

(a) intra-fibre bond breaking (internal fibrillation)
(b) external fibrillation
(c) fibre cutting and the production of fines

Studies of handsheet properties and microscopic examination of fibres have shown that all these effects take place in a PFI mill (Stationwala et al. 1996).

The dynamics of a single bar are shown pictorially in Fig. 2. The forces applied to the fibres in the beating gap can be resolved into two components – the compression force normal to the bar surface directly due to the load, and a tangential stress due to the resistance of pulp to shear imposed by the relative motion between the roll and the housing. Although the terms "shear" and "compression" are used to describe two components, the compression of the fibres in the gap in itself may involve a small component of shear.

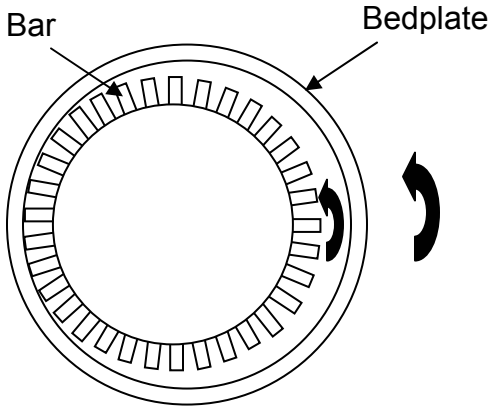

Fig. 1. Components of a PFI mill

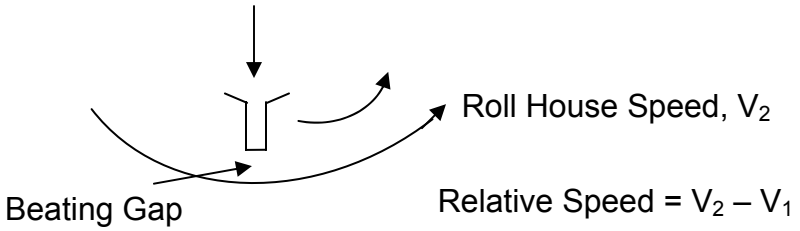

Fig. 2. Parameters related to the beating gap in a PFI mill

The aim of this work was to develop a quantitative model for microfibre generation from bleached kraft pulp through refining in a PFI mill. Theoretical studies on refining action noted earlier for other kind of refiners have estimated only the energy needed for fibre shortening. Thus, no work done so far provides any quantitative measure of the energy needed to generate microfibres from fibres by the reduction of diameter without any fibre shortening.

The goal of the refining modeled in this work is not merely to achieve better fibrillation on the cell wall surface, but also to separate microfibres as discrete entities with high aspect ratios. Therefore, the total energy imparted to the fibres needs to be much greater than what is usually employed in refining. This is substantiated by the conclusion drawn by Stationwala et al. (1996) that the peeling-off mechanism described earlier demands a relatively high amount of energy. Variations in the operating conditions of the PFI mill (load, consistency, temperature, nature of fibre, mill speed, etc.) may lead to an increase in the energy obtained in refining. But these variations alone may not be sufficient to substantially increase the generation of microfibres.

One simple way to substantially increase the energy imparted to the fibres is to keep the operation running for a much longer period of time. This implies that the number of revolutions employed has to be far greater than commonly used in laboratory conditions. As Kerekes (2001) noted, the extent of refining is most commonly expressed in terms of the number of revolutions. This forms the basis of the theory presented in this work, where bleached softwood kraft pulp was subjected to 125,000 revolutions in a PFI mill, as opposed to about 1,000 revolutions commonly used to study the effect of refining on fibre properties.

EXPERIMENTAL DATA

Developing a model for the energy consumption in generating microfibres requires some experimental data. These data form the basis for evaluating two of the assumptions used in the model development, as described in this section.

Generating Refined Fibres

The experimental methods for generating these data are based on a process detailed by Chakraborty et al. (2005) for producing wood microfibres from bleached northern black spruce kraft pulp. In summary, 24 g of pulp fibres of 10% consistency was charged in a PFI mill, which was then rotated for 125,000 revolutions. In the original study, this refining step was followed by an additional stage of crushing the fibres under liquid nitrogen to obtain high yield of microfibres 1 μm in diameter. For the purpose of the present work, however, the fibres were characterized right after the refining stage at the end of 125,000 revolutions of the PFI mill, before they were subjected to cryocrushing.

Fibre Characterization

SEM studies: A Hitachi S2500 Scanning Electron Microscopy (SEM) instrument was used to characterize the fibres after 125,000 revolutions. The refined fibres were dispersed in water to form a suspension of 0.1% fibres in water. A drop of this suspension was placed on the SEM stub, and allowed to dry before analyzing in the SEM. Each sample was gold coated, and a voltage of 10 kV was used during imaging with the SEM. Samples of the bleached kraft pulp (BKP) were also prepared in the same manner.

25 such samples were prepared for both BKP and the refined fibres generated thereof, and the SEM images of 200 fibres of each were analyzed. Analysis of these images (Fig. 3) showed an average BKP fibre diameter of 13 μm. Moreover, image analysis revealed that more than 90% of the fibres generated in this way were in the range between a few nanometers and 2 μm in diameter (Fig. 4). The distribution was centred around a diameter 1.3 μm. Therefore, for modeling purposes, an average final fibre diameter of 1.3 μm was assumed at the end of 125,000 revolutions.

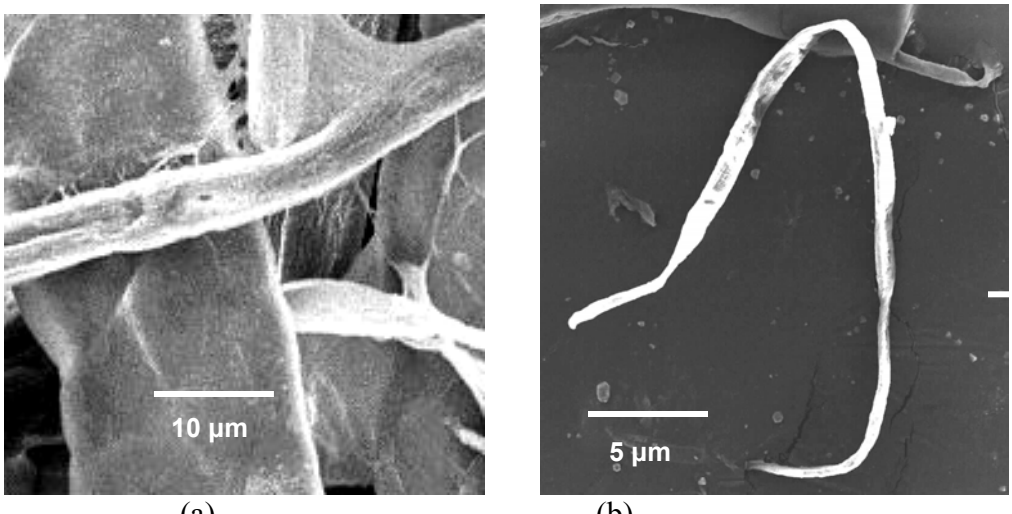

(a) (b)

Fig. 3. Typical SEM images of (a) bleached kraft pulp (BKP) and (b) BKP after 125,000 revolutions in a PFI mill

Study of Tensile Property of Single Fibres

The energy spent in elastic deformation of the fibres is critical in modeling the energy consumed in refining, for reasons described later. Therefore, the energy consumed in elastic deformation needed to be calculated as a fraction of the total energy consumed by the fibres before fracture. For this purpose, understanding of load-elongation (or stress-strain) behaviour of single fibres was important.

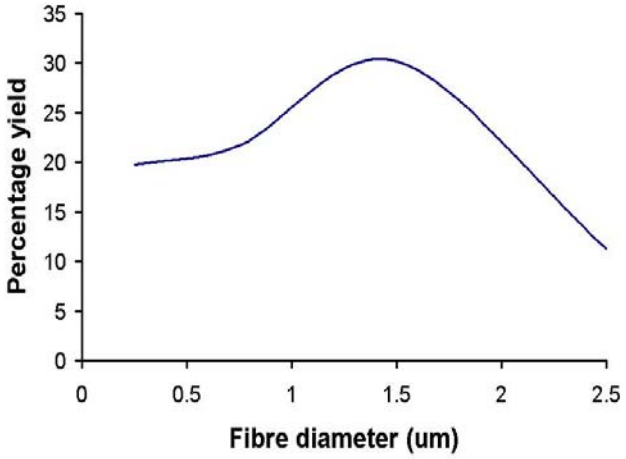

Fig. 4. Number yield of microfibres generated after refining

Previous studies (Page and EL-Hosseiny 1983) on tensile strengths of single pulp fibres indicated non-linear deformation behaviour especially with fibres having high micro fibril angle. The initial linear elastic region (following Hooke's law) was small compared to the total area under the stress-strain curve. In a recent study, Gilani (2006) also reported the tensile behaviour of isolated single pulp fibre. The study suggested that the nature of stress-strain curve and the fracture strength is strongly dependent on the isolation technique (mechanical or chemical) and on the micro fibril angle. While the mechanically isolated fibres failed at comparatively low strain in a rather brittle manner, chemically isolated (acid or alkali treated) fibres, which more closely resembles the BKP fibres used in this study, had large non-linear deformation region associated with high strain compared to small elastic deformation.

However, given the small length of ~ 2 mm of the BKP fibres, it was practically impossible to clamp a single fibre in between the two clamps of a tensile tester. The strong tendency to twist in chemically isolated pulp fibres also add to uncertainties in the stress-strain results (Gilani 2006). Additional complications like were also reported in handling the short length pulp fibres.

Therefore, some other natural fibre had to be chosen that had similar properties as that of BKP fibres. The criteria that were matched were cellulose content and percentage crystallinity. These predominantly dictate the chemical and mechanical properties of the fibres. The cellulose content and crystallinity of BKP fibres were 90% and 55% respectively (Chakraborty et al. 2006). It was noted that the cellulose content of hemp fibres after acid and alkali treatment was 94%, and the crystallinity was 55% (Bhatnagar 2004).

Therefore, chemically treated single hemp fibres were used for tensile property studies. The acid and alkali treatments are described briefly as follows:

Acid treatment was performed to remove pectin and hemicellulose from hemp. Alkali treatment completes this removal process and also disrupts the lignin structure by separating the linkages between lignin and carbohydrates. For this purpose, hemp fibres were submerged in a 1M hydrochloric acid solution in a beaker at 80ºC ± 5ºC for two hours with constant stirring. Subsequently, 2% w/w sodium hydroxide solution was added to the sample at 80°C ± 5ºC for two hours with constant stirring for better impregnation of alkali into the fibres. The treated fibres were then cooled and washed with abundant distilled water until it became neutral, and vacuum filtered.

Single fibres were isolated from the chemically treated hemp. The mechanical strength and modulus of the single fibres were analyzed with a Sintech-1 machine model 3397-36 in tensile mode with a load cell of 5 lb using a gauge length of 15 mm. The tensile tests were performed at a crosshead speed of 2.5 mm/min. 20 chemically treated fibres were studied in this manner.

A typical stress-strain curve for a chemically treated hemp fibre is shown in Fig. 5. Energy taken up during tensile stress is given by the area under the stress-strain curve. The results indicated that the energy absorbed before breaking the fibres was predominantly in the non-linear deformation zone. The energy spent in elastic deformation, i.e., deformation up to the point where Hooke's Law holds good, ranged between 3% and 5% of the total energy.

Therefore, in view of the small proportion of energy transferred to the chemically isolated BKP fibre during elastic deformation, the elastic component of energy supplied to the fibres in tensile mode was neglected for modeling purposes.

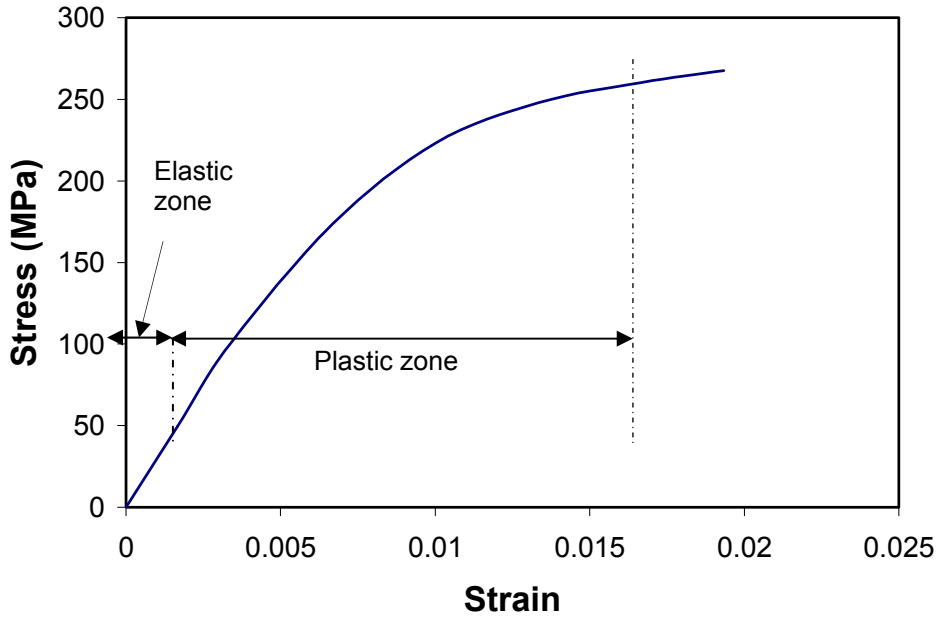

Fig. 5. Energy consumed during elastic and plastic deformations of chemically treated hemp fibres in tensile mode

MODEL ASSUMPTIONS

In summary, the following assumptions were made in the model:

(i) Initial and final fibre diameters before and after refining are 13 μm and 1.3 μm respectively.

(ii) The deformation of the fibres in the elastic zone is minimal. Therefore, the work of elastic deformation is negligible. This forms the basis of Rittinger's law, as discussed below.

(iii) A charge of 24 g of bleached kraft pulp of 10% consistency is used, which is the standard charge for a PFI mill (Tam Doo, Kerekes 1989).

LAWS OF COMMINUTION

Although comminution theory has been applied to the refining of fibres previously, there still exists substantial theory on comminution, correlating fibre size reduction to energy consumption, that has not been used by researchers studying pulp fibres. In this study, standard comminution theory has been used to determine the refining energy required to produce microfibres from bleached softwood kraft pulp fibres. For this purpose, some of the most common laws of comminution were considered.

Rittinger's Law

This law states that the energy input into a comminution process is proportional to the quantity of new surface produced. In the mathematical form

$$E = C\,(A_2 - A_1) \qquad (1)$$

where E = specific energy (i.e., energy per unit mass) input, J/kg
A_1 = initial specific surface (i.e., initial surface per unit volume), m^{-1}
A_2 = final specific surface, m^{-1}
C = Rittinger's constant, J.m/kg

The value of C depends on the material being crushed. In this case, C is primarily a function of the hydrogen bond density among the different microfibres of cellulose.

Kick's Theory and Bond's Theory

Rittinger's formula only accounts for the decomposition of molecular bond forces. In practice, most materials elongate elastically before breakage, but the work of elastic deformation preceding fracture is neglected in Rittinger's formula. It has, however, been incorporated in other comminution laws, such as *Kick's "volume" theory* and by *Bond's theory*, referred to as "*third theory*" (Beke 1981). Kick's theory, however, considers only this elastic deformation energy, and neglects the work done in breaking a material into small particles. Bond's theory, on the other hand, accounts for the energy required in both elastic deformation, and the final breakage of the materials.

It is worth mentioning that Kick's and Bond's theory are more appropriate with larger particles, while Rittinger's law is applied to fine grinding (Holdich 2002) as in PFI mill used in this study.

Rationale for Using Rittinger's Law to Characterize Microfibre Generation from Fibres

The energy imparted to the fibres during refining produces both elastic deformation and plastic deformation before breakage. However, the experiments on hemp discussed previously revealed that the energy for elastic deformation was negligible, and BKP fibre fracture occurs primarily by the decomposition of molecular bond forces (thereby creating new surfaces) in the plastic zone. Therefore, Rittinger's Law characterizes the process under investigation quite well. This is also substantiated by a study by Wisconsin (1957) who demonstrated experimentally that Rittinger's Law holds almost perfectly for ball mill beating of pulp.

ENERGY AND COST ASSOCIATED WITH MICROFIBRE GENERATION

The average initial diameter of each fibre of the starting material (BKP) is assumed to be 13 μm, as noted earlier. The refining action generated microfibres 1.3 μm in diameter. Hence, the energy used in refining reduced the size of the fibres from 13 μm to 1.3 μm.

Energy Consumed by Fibres according to Rittinger's Law

We consider a fibre of length l, m. For a fibre of diameter d, A_1 in equation (1) has a value of $[(\pi d l)/(\pi d^2 l/4)] = 4/d = 4/(13\times10^{-6})$ m^{-1} $= 3.1X10^5$ m^{-1}. Similarly, $A_2 = 4/(1.3\times10^{-6})$ $m^{-1} = 3.1\times10^6$ m^{-1}.

Putting these values of A_1 and A_2 in equation (1) gives the specific energy to generate microfibres of 1.3 μm diameter from fibres 13 μm in diameter as

$$E = C\,(3.1\times10^6 - 3.1\times10^5) = 27.9\times10^5\ C,\ J/kg \qquad (2)$$

For the present work, the energy expressed in equation (2) is provided by a PFI mill. The charge in a PFI mill in this case consists of 24 g of fibres. Thus, for a charge of 24 g of fibres, equation (2) can be written as

$$E' = 27.9X10^5\ C \times (24/1000),\ J = 66960\ C,\ J \qquad (3)$$

where E' is the energy required for microfibre production for a sample size of 24 g of fibres.

Energy Consumed by Fibres in Refining

The operations of a PFI mill have been previously described by various researchers, but theoretical modeling relating the product properties to the operating parameters have been scarce. The most relevant studies in this direction have been

performed by Kerekes and coworkers (reference?). The specific energy (E) on pulp in a PFI mill is expressed as

$$E = N\,I \tag{4}$$

where N = number of bar impacts per unit mass of fibres, and I is the energy/impact, also called refining intensity (Welch and Kerekes, 1994)

. Welch and Kerekes (1994) deduced that the specific energy consumption in PFI refining of bleached softwood kraft pulp lies within the range of 0.59 to 0.68 J/g.rev. In accordance with the approximate average value adopted by Kerekes (2001), a value of 0.63 J/g.rev was assumed in the present case.

For a 24 g charge of BKP, and a number of revolutions = N_r, this gives the value of the total energy consumed as

$$E' = 0.63 \text{ J/g.rev} \times 24 \text{ g} \times N_r \text{ rev., i.e, } E' = 15\,N_r, \text{ J} \tag{5}$$

Equating Refining Energy to Energy Consumed by Fibres According to Rittinger's Law

Equating equations (3) and (5) gives

$$66960\ C = 15\,N_r \tag{6}$$

$$\text{i.e., } N_r = 4464\ C \tag{7}$$

Hence, with the knowledge of the value of Rittinger's constant C, the number of PFI revolutions to generate microfibres 1 μm in diameter can be estimated.

Net Energy Required for Microfibre Generation and Rittinger's Constant

Considering 125,000 as the number of revolutions for generating fibres in the range of 1.3 μm in diameter, equation (5) shows that 1875 kJ of energy is needed by a 24 g batch in a PFI mill to reduce the fibre diameter from 13 μm to 1.3 μm.

Putting 125,000 as the number of revolutions in equation (7) gives a value of 28 J.m/kg for the Rittinger's constant.

Energy Required to Generate Microfibres 1 μm in Diameter

Knowledge of the value of the Rittinger's constant for a given material makes it possible to deduce the energy required to reduce its diameter from any initial diameter to any final diameter. Therefore, if microfibres 1 μm in diameter are to be generated by refining alone, the energy consumed in the process can be calculated by putting 1 μm as the final diameter. This gives a value of A_2 (i.e., 4/diameter) as $4/1\times10^{-6} = 4\times10^{6}$.

Therefore equation (1) gives

$$E = C\,(4X10^{6} - 3.1X10^{5}) = 28 \text{ (J.m/kg) X } 36.9X10^{5}\ m^{-1} = 103.3 \text{ MJ/kg} \tag{8}$$

Hence, if microfibres 1 μm in diameter are generated solely by refining in a PFI mill, each 24 g charge would consume an energy of about 2480 kJ.

The number of revolutions needed for microfibre generation in a PFI mill may be calculated by putting the value of the energy per 24 g charge (E') = 2480 X 10^3 J in equation (5)

$$2480 \text{ X } 10^3 = 15\ N_r \quad \text{i.e., } N_r = 165333 \tag{9}$$

Therefore, each 24 g of pulp charged in a PFI mill should be rotated for 165,333 revolutions to generate microfibres 1 μm in diameter starting with fibres 13 μm in diameter.

It should be recognized that the value of 103.3 MJ/kg obtained in equation (8) represents the energy requirement for microfibre generation from softwood bleached kraft pulp fibres through any size reduction process, not only for refining in a PFI mill.

Cost of Microfibre Generation

Considering the cost of electricity as 6 cents per kWh, i.e., 6 cents per 3600 kJ, the cost of supplying 103.3 MJ of energy to the pulp is calculated as $1.72. This implies that the generation of microfibres 1 μm in diameter starting with bleached softwood kraft pulp costs $1.72/kg. Moreover, the price of northern bleached softwood kraft pulp, although variable, is roughly in the range of $650 per metric ton, i.e., 65 cents/kg. This indicates that the total cost of the cellulose microfibres is about $2.37/kg, which is the sum of prices of the bleached kraft pulp, and of generating the microfibres thereof. This may be compared to the price of conventional polymers, most of which cost around $1/kg. Since cellulose microfibres act as reinforcing agents, and contribute to an increase in mechanical properties of the matrix, a price of $2.37/kg of the reinforcing agents may be considered reasonable.

CONCLUSIONS

The energy required in generating microfibres 1 μm in diameter from bleached kraft wood pulp was successfully modeled. The average diameter of each initial fibre before refining was considered as 13 μm. Rittinger's Law was used to characterize the energy requirement in generating the microfibres. Considering the experimental evidence that 125,000 revolutions in a PFI mill gave a high yield of fibres 1.3 μm in diameter, Rittinger's constant for the given system was found out to be 28 J.m/kg. Using this value of Rittinger's constant, the refining energy needed for generating microfibres 1 μm in diameter was estimated as 103.3 MJ/kg. For unit electricity cost of 6 cents per kWh, this corresponds to a cost of $1.72/kg, which brings the total cost of the microfibres to $2.37/kg. Given that the price of conventional polymers is in the range of $1/kg, the price of microfibres used as reinforcing agents may be feasible.

ACKNOWLEDGEMENTS

The authors would like to acknowledge BIOCAP/NSERC Strategic Projects and Ontario Graduate Scholarship for providing financial assistance for this project.

REFERENCES CITED

Beke, B. (1981). "The process of fine grinding," Joint publication by: Martinus Nijhoff/Dr W. Junk Publishers, The Hague, The Netherlands, and Akademiai Kiado, Budapest, Hungary, pp. 10-12.

Bhatnagar, A. (2004). "Isolation of cellulose nanofibres from renewable feed stocks and root crops," Ph.D. thesis, Faculty of Forestry, University of Toronto.

Brecht, W., and Klemm, K. (1953). "The mixture of structures in a mechanical pulp as a key to knowledge of its technological properties," *Pulp Pap. Mag. Can.* 54(1), 72.

Chakraborty, A., Sain, M., and Kortschot, M. (2005). "Cellulose microfibrils: A novel method of preparation using high shear refining and cryocrushing," *Holzforschung* 59(1), 102-107.

Chakraborty, A., Sain, M., and Kortschot, M. (2006). "Reinforcing potential of wood pulp derived microfibres in PVA matrix", *Holzforschung* 60(1), 53-58.

Corson, S. R. (1972). "Probabilistic model of the disk refining process", *Svensk Papperstidn*. 75(2), 57-64.

Corson, S. R. (1980). "Fibre and fines fraction influence strength of TMP", *Pulp Pap. Can.* 81(5), 69-70, 73, 75-76.

Corte, H., and Agg, S. (1980). "Shortening of pulp fibres during beating", IPC Intern. Symp. Fundam. Concepts Refining 1980, Appleton, WI, 149-157.

Courchene, C. E., McDonough, T. J., and Page, D. H. (2002). "Effect of bleach plant processing on fiber strength", Tappi Fall Technical Conference and Trade Fair 2002, 93-101.

Gilani, M. S. (2006). "A micromechanical approach to the behaviour of single wood fibers and wood fracture at cellular level", Ph.D. thesis, École Polytechnique Fédérale de Lausanne.

Hiltunen, E., Kettunen, H., Laine, J. E., and Paulapuro, H. (2000). "Effect of softwood kraft refining on a mechanical-chemical mixture sheet," *Tappi J.* 83(10), 67-75.

Hiltunen, E., Kettunen, H., Laine, J. E., and Paulapuro, H. (2002). "Effect of softwood kraft pulp refining on fracture behaviour of TMP-based paper," *Appita* 55(6), 494.

Holdich, R. (2002). "Fundamentals of particle technology", Midland information technology and publishing, UK, pp. 113-122.

Karnis, A. (1994). "The mechanism of fibre development in mechanical pulping," *J. Pulp Paper Sci.* 20(10), J280-J288.

Kerekes, R.J. (2001). "Characterization of refining action in PFI mills," PIRA 6th International Conference, Toronto, Canada, 2001.

Lidbrandt, O., and Mohlin, U.-B. (1980). "Changes in fiber structure due to refining as revealed by SEM", IPC Intern. Symp. Fundam. Concepts Refining 1980, 61-74.

Luukko, K. (1998). "On the characterization of mechanical pulp fines," *Paperi Puu* 80(6), 411-448.

Luukko, K., and Paulapuro, H. (1997). "Mechanical pulp fines: effect of particle size and shape," Engineering & Papermakers: Forming Bonds for Better Papermaking Conference 1997, 131-136.

Mohlin, U.-B. (1977). "Mechanical pulp properties – the importance of fines retention," *Svensk Papperstidn*. 80(3), 84-88.

Mohlin, U.-B. (1997). "Fiber development during mechanical pulp refining," *J. Pulp Paper Sci.* 23(1), J28-J3.

Mohlin, U.-B., and Miller, J. (1980). "Industrial refining – Effects of refining conditions on fiber properties," Refining 95: Third Intern. Refining Conference 1995, 13.

Murphy, D. C. (1962). "Mechanical factors in beating," *Appita* 16(1), 16-30.

Olson, J. A., Drozdiak, J., Martinez, M., Garner, R., Robertson, A. G., and Kerekes, R. (2003). "Characterizing fibre shortening in low-consistency refining using comminution model," *Powder Technol.* 129, 122-129.

Page, D. H., Seth, R. S., and DeGrace, J. H. (1967). "Delamination of fiber walls by beating and refining," *Tappi* 50(10), 489.

Page, D. H., and El-Hosseiny, F. (1983). "The mechanical properties of single wood pulp fibers. Part VI. Fibril angle and the shape of stress-strain curve," *J. Pulp Paper Sci.* 9, 99-100.

Roux, J. C., and Mayade, T. L. (1999). "Modeling of the particle breakage kinetics in the wet mills for the paper industry", *Powder Technol.* 105, 237-242.

Stationwala, M. I., Mathieu, J., and Karnis, A. (1996). "On the interaction of wood and mechanical pulping equipment. Part I: fibre development and generation of fines," *J. Pulp Paper Sci.* 22(5), J155-J160.

Strand, B. C., and Mokvist, A. (1989). "Application of comminution theory to describe refiner performance", *J. Pulp Paper Sci.* 15(3), J100-J105.

Tam Doo, P. A., and Kerekes, R .J. (1989). "The effect of beating and low-amplitude flexing on pulp fibre flexibility", *J. Pulp Paper Sci.* 15(1), J36-J42.

TAPPI, "Fines Fraction of Paper Stock by Wet Screening," Tappi Testing Method T 261 pm-80.

Watson, A. J., and Phillips, F. H. (1964). "Beating characteristics of the PFI mill III. Observations related to the beating mechanism", *Appita* 18(3), 84-102.

Welch, L. V., and Kerekes, R. J. (1994). "Characterization of the PFI mill by the C-factor," *Appita* 45(5), 387-390.

Wisconsin, A., (1957). "Factors contributing to the strength properties of a sheet of paper," *Project Report* (*Project* 1513), 1-179.

Article submitted: Dec. 3, 2006; Resubmitted after format change: Dec. 5, 2006; First cycle of reviewing completed: January 9, 2007; Revised article submitted: April 20, 2007; Article accepted April 22, 2007; Published: April 24, 2007

EFFECT OF PULP DELIGNIFICATION DEGREE ON FIBER LINE PERFORMANCE AND BLEACHING EFFLUENT LOAD

Jorge L. Colodette*, José L. Gomide, Dalton L. Júnior, and Cristiane Pedrazzi

Industrially made kraft pulps obtained by a modified cooking process may contain 60-75 mmol/kg of hexenuronic acids (HexAs), which represents 6-7.5 kappa units. HexAs do not react with oxygen and very little of it is actually removed across the oxygen delignification stage, causing low efficiencies in the range of 25-35%. In this study, an economical evaluation of the ECF bleaching processes was carried out, having none and double-stage oxygen delignification, when applied to eucalyptus pulps of kappa varying in the range of 14-21. The bleaching processes included sequences containing specific stages for HexAs removal (Z, A/D and D_{HT}). Results indicated that the use of oxygen delignification was not economically attractive, particularly for HexA-rich low-kappa pulps, but processes without oxygen delignification present significant environmental challenges.

Keywords: Kraft pulp, Delignification degree, Bleaching, HexA, Effluent load

Contact information: Pulp and Paper Laboratory, Federal University of Viçosa, Av. Peter H. Rolfs, s/n, Viçosa, MG Brazil 36.570-000; phone:55-31-3899 2086, fax: 55-31-3899 2490, colodett@ufv.br

INTRODUCTION

Eucalyptus kraft pulps produced by kinetically modified pulping processes contain very high amounts of hexenuronic acids (HexAs), in the range of 60-75 mmol/kg pulp (Almeida and Silva Júnior 2004; Lanna et al. 2002; Colodette et al. 2001). This HexA concentration range is roughly equivalent to 6-7.5 kappa units (Vuorinen et al. 1996). Considering that the out-of-digester kappa number varies in the range of 14-18 for eucalyptus pulps and that, purportedly, the HexA contents of the pulps at this kappa number range tend to be rather constant (Almeida and Silva Júnior 2004; Lanna et al. 2002; Chakar et al. 2000), the significance of HexAs in the overall kappa number may vary sharply, depending upon the pulp's initial kappa number. For example, kappa 14 and 18 pulp samples containing equal amounts of HexAs (e.g. 7.5 units kappa) will have 53.4 and 41.2% of their kappa represented by these acids, respectively. Thus, the impact of HexAs on overall kappa number is more significant for the kappa 14 pulp.

Oxygen delignification efficiency is rather low for low-kappa pulps containing high HexA concentrations (Colodette et al. 2006; Eiras and Colodette 2003) since oxygen does not react with HexAs (Vuorinen et al. 1996). As a matter of fact, it is doubtful whether or not oxygen delignification is worth implementing at all for HexA-rich eucalyptus kraft pulps having low kappa number.

The objective of this study was to evaluate bleachability of HexA-rich (derived from modified cooking) eucalyptus kraft pulps of kappa number 14, 17.5 and 21, with sequences containing specific stages for removal of hexenuronic acids such as D_{HT}, A/D,

and Z. Note that the kraft pulping modifications were made to simulate the Andritz Lo-solids™ cooking process, within the limitations of laboratory equipment available.

EXPERIMENTAL

Materials

Five trees of a 7-years old hybrid *Eucalyptus grandis x Eucalyptus urophylla* clone were used. The trees were obtained from commercial plantations and they derived from progeny of a first generation cross of the aforementioned species. The average characteristics of the five samples were as follows: 532 kg/m^3 density, 42.5% cellulose, 27.3% total lignin, 17.4% hemicelluloses, 5.1% uronic acids, 2.4% acetyl groups, 3.2% ethanol/toluene extractives, and 2.0 lignin syringyl/guayacyl (S/G) ratio.

Methods

Pulping was carried out by a modified kraft pulping method to kappa numbers 14, 17.5 and 21. Conditions were kept constant, except that active alkali charges were varied to achieve the desired kappa number. The following cooking conditions were used on 500 g (dry weight basis) pre-steamed chips: (1) impregnation zone: 112°C, 60 minutes, 45% of total active alkali, liquor-to-wood ratio (L/W) = 3.5/1; (2) upper cooking zone: 155°C, 60 minutes, 30% of active alkali, L/W = 3.5/1; (3) lower cooking zone: 156°C, 120 minutes, 25% of total active alkali, L/W = 3.5/1 L/kg. A total sulfidity of 37% and an H-factor of 680 were used in all cases. Total active alkali values of 21.8, 18.7 and 16.6%, expressed as NaOH, were required for kappa number 14, 17.5, and 21, respectively. Bleaching of pulps was carried out to 90% ISO brightness with the sequences D_{HT}(PO)DP, A/D(PO)DP, Z/ED(PO), O/OD_{HT}(PO)DP, O/OA/D(PO)DP, and O/OZ/ED(PO), whereby: O/O refers to a double stage oxygen delignification without inter-stage washing; D_{HT} refers to a long (120 min) and unusually high temperature chlorine dioxide stage (90-95 °C); (PO) refers to a fully pressurized hydrogen peroxide stage in the presence of oxygen; D refers to conventional chlorine dioxide stage; P refers to atmospheric peroxide stage; A/D refers to a hot (90-95 °C) acid hydrolysis (pH 2.5-3) followed by a hot chlorine dioxide stage without inter-stage washing; Z/E refers to a high consistency ozone stage followed by an alkali extraction without inter-stage washing.

General oxygen delignification and bleaching conditions are listed in Table 1. In the O/O stage the alkali charges of 1.7, 1.8, and 1.9 % on o.d. pulp weight were used for the kappa 14, 17.5 and 21 pulps, respectively. These charges were all applied in the first stage and in the form of oxidized white liquor (OWL). The oxygen charge was kept constant and equal to 2.3 % for all three pulps, with 1.8 % being applied in the first O-stage and 0.5% applied in the second O-stage. For the D_{HT}(PO)DP and A/D(PO)DP sequences, a kappa factor of 0.15 was applied to the first chlorine dioxide stage, regardless of pulp kappa number. The balance chlorine dioxide was applied to the second D-stage of the sequence. For the Z/ED(PO) sequence the fixed charge of 1.52% ClO_2 was applied in the single D-stage, regardless of pulp kappa number. The same approach was followed for the O/OD_{HT}(PO)DP, O/OA/D(PO)DP and O/OZ/ED(PO) sequences, except that only 0.57% of ClO_2 was applied in the single D-stage of the latter sequence.

Except where otherwise stated, the following standard analytical procedures were used: viscosity - Tappi T 230, kappa number - Tappi T 236, residual alkali - Tappi T 625, carbohydrates - Tappi T 249, black liquor solids - Tappi T 650, pulp yield and rejects - gravimetric, COD - Paptac H3, color - Paptac H5, AOX - Scan P 69:94, forming handsheets for reflectance testing - Tappi T 272, diffuse brightness of pulp - Tappi T 525 and brightness reversion - Tappi UM 200. The analyses of bleach chemical solutions and residuals were carried out according to Kraft (1967). Pulp hexenuronic acids were measured according to Vuorinen et al. (1996). The pulp cellulose and hemicelluloses (xylans) contents were determined, indirectly, from the carbohydrate analytical data. Bleaching chemical costs were calculated in US$/odt of bleached pulp, using market chemical prices (US$/ton of product 100% pure) as follows: O_2 = 100, ClO_2 = 1000, H_2O_2 = 850, O_3 = 1500, NaOH 500, oxidized white liquor 190, H_2SO_4 = 80, $MgSO_4$ = 270.

Table 1. General oxygen delignification and bleaching conditions

Stage	Consistency %	Time, min	Temp., ºC	Pressure, kPa	End pH
O/O	10/10	15/45	100/105	600/500	12/11.5
D_{HT}	10	120	95	-	2.8
A/D	11/10	120/10	95/90	-	2.8/3.0
Z/E	40/10	1/30	30/60	-	2.5/10
(PO)	10	120	95	500	10.5
D	10	120	85	-	4.5
P	10	120	85	-	10.5

RESULTS AND DISCUSSION

Pulping Results

It was observed that extending cooking from kappa number 21 to 17.5 resulted in a screen yield drop of 2%, from 53.4 to 51.4%, and increased active alkali demand by about 2%, from 16.6 to 18.7% as NaOH (Table 2). Rejects decreased from 0.3 to 0.1%. The pulp viscosity decreased from 87.1 to 54.7 mPa.s, and the xylan content dropped from 19.4 to 17.2%. Pulp HexAs content increased from 48.5 to 69.7 mmol/kg pulp, in spite of the fact that xylan content decreased. This trend has been observed in other studies with eucalyptus pulps (Almeida and Silva Júnior, 2004). The residual active alkali increased from 4.3 to 6.7 g/L and the black liquor pH increased from 11.9 to 12.3. Extending cooking even further from kappa number 21 to 14 resulted in a yield drop of 4.1%, from 53.4 to 49.3%, and an increase in effective alkali demand of 5.2%, from 16.6 to 21.8%. The pulp viscosity decreased from 87.1 mPa.s to 40.5 mPa.s and the pulp xylan level decreased 3.7%, from 19.4 to 15.7% in spite of the HexAs content increase from 48.5 to 68.5 mmol/kg. Thus, it is apparent that a significant part of the yield difference between kappa 21 and 14 derives from xylan losses. The residual active alkali increased from 4.3 to 10.9 g/L, and the black liquor pH increased from 11.9 to 12.5. No rejects

were observed at kappa 14. The aforementioned results confirmed the very well known concept that higher kappa pulps present higher yield and viscosity. The question which remains is: Is the wood savings derived from this improved yield sufficient to pay for the additional chemicals cost required to bleach the higher kappa pulps, considering the low cost of eucalyptus wood in Brazil?

Table 2. Pulping Results

Target Kappa No.		14.0	17.5	21.0
Active Alkali, % NaOH		21.8	18.7	16.6
Brown Pulp Characteristics	Measured Kappa **No.**	14.1	17.4	20.9
	Viscosity, mPa.s	40.5	54.7	87.1
	Xylans, %	15.7	17.2	19.4
	Screened Yield, %	49.3	51.4	53.4
	Rejects, %	0.0	0.1	0.3
	HexAs, mmol/kg	68.5	69.7	48.5
Black Liquor	Solids, %	15.8	14.9	14.2
	Active alkali, g/L NaOH	10.9	6.7	4.3
	Final pH	12.5	12.3	11.9

Oxygen Delignification Results

The main factors affecting eucalyptus kraft pulp oxygen delignification efficiency are kappa number, HexAs content, and carryover to the bleach plant. The overall oxygen delignification efficiency, as measured by the kappa drop across the O/O stage, increased with increasing kappa number, but the efficiency based only on the "true lignin kappa number" tended to decrease (Table 3). "True lignin kappa number" is the one derived only from lignin, after subtraction of the kappa number due to hexenuronic acids, considering the ratio 10 mmol/kg HexA equals to 1 kappa number unit. The lignins from higher kappa pulps tend to contain less free phenolic hydroxyl groups (Gellerstedt 1996), which are the main sites for oxygen reactions, and this may explain the slightly lower efficiency based solely on lignin. However, the higher kappa pulps contained, proportionally, more lignin available for reaction than the lower kappa ones because of their similar or lower HexAs contents. Therefore, the higher kappa pulps produced higher overall oxygen delignification efficiency than the lower kappa ones, given that HexAs do not react with oxygen (Vuorinen et al. 1996). In this work, the influence of HexAs on kappa number was calculated assuming that 10 mmol/kg pulp of HexAs is equivalent to 1 kappa unit (Vuorinen et al. 1996). This ratio has been somewhat questioned in a later work by Li and Gellerstedt, 1997 who claim a ratio of 11.6-11.9 mmol/kg pulp of HexAs per kappa unit.

Table 3. Characteristics of the brown and oxygen-delignified pulps of kappa 14, 17.5 and 21

Pulp Characteristics	Brown			Oxygen Delignified		
Total Kappa No.	14.1	17.4	20.9	10.2	11.9	12.8
Lignin Kappa No.	7.3	10.4	16.1	3.4	5.0	8.0
HexA´s Kappa No.	6.8	7.0	4.8	6.8	6.9	4.8
Overall O/O Stage efficiency, %	-	-	-	27.6	31.6	38.7
True Lignin O/O Stage Efficiency, %	-	-	-	53.4	51.9	50.3
COD, kgO_2/odt	10	10	10	10	10	10

Bleaching Results

Current best available technologies to bleach eucalyptus kraft pulps include sequences such as D_{HT}(PO)DP, A/D(PO)DP and Z/ED(PO). The eleven bleach plants installed or rebuilt in South America in the last 10 years have chosen among these technologies. These choices stem from the fact that aforementioned sequences contain a first bleaching stage adapted to remove HexAs, which are abundant in eucalyptus pulps produced by modified cooking processes, and a last stage adapted to prevent pulp brightness reversion, which is a common problem for eucalyptus kraft pulps bleached to high brightness (Colodette et al, 2006). These sequences were compared for kappa 14, 17.5 and 21 pulps untreated or previously treated with double-stage oxygen delignification. For the sake of a fair comparison, all bleaching sequences were carried out under similar operating conditions (Table 1), maintaining a constant kappa factor of 0.15 in the first chlorine dioxide stage and varying chlorine dioxide and peroxide doses in subsequent stages in order to achieve the target brightness of 90% ISO. For the sequence initiating with the Z/E stage, a fixed ozone charge of 0.6% on oven dried pulp weight was applied in the ozone treatment.

Sequences

The lowest and highest bleaching chemical costs were obtained with the sequences D_{HT}(PO)DP and Z/ED(PO), respectively, for both brown (Table 4) and oxygen-delignified (Table 5) pulps. Note that chemical costs include all oxidants, acid, base and additives used in each bleaching sequence. The D_{HT} stage is highly efficient for bleaching eucalyptus pulps derived from modified cooking. Such pulps contain large amounts of HexAs and the chlorine dioxide stage run at high temperature (D_{HT}) easily removes them by acid hydrolysis while simultaneously oxidizing the lignin. The D_{HT} stage is not effective for bleaching pulps containing no or low HexAs such as Soda/AQ, sulfite, softwood kraft and even hardwood kraft produced by conventional cooking procedures. On the other hand, the sequence containing the ozone stage has one less stage than the others and tends to consume more chemicals. As should be expected, the bleaching cost increased with increasing kappa number of the brown pulp, regardless of the bleaching sequence. The impact was much more significant for the pulps not treated with oxygen delignification and bleached with the Z/ED(PO) sequence (Table 4). For the brown pulp bleached with the D_{HT}(PO)DP and A/D(PO)DP sequences, an increase of about US$5/odt was observed when the kappa number was increased from 14.1 to 17.4 or from 17.4 to 20.9, whereas for the Z/ED(PO) sequence this increase reached US$7.5/odt when the kappa was raised from 14.1 to 17.4, and US$13.7/odt when it was raised from

17.4 to 20.9 (Table 4). For the oxygen-delignified pulps bleached with the D_{HT}(PO)DP sequence, an increase of only about US$2/odt was observed by raising kappa number from 14.1 to 17.4 or from 17.4 to 20.9, while for the Z/ED(PO) sequence an additional US$8/odt was required. Thus, the ozone-based sequence has low tolerance for high-kappa pulps, particularly those not treated with oxygen. It is worth noting that the oxygen delignification stage largely reduced the kappa number differences among the various pulps. Hence, the kappa number of the original pulp had a smaller effect on the bleaching cost for the oxygen delignified than for the brown pulps.

In this work bleachability has been defined as the ratio between kappa number entering the bleach plant and total active chlorine (TAC) required for attaining the target brightness of 90% ISO. Total active chlorine was defined by the following equation: TAC = (ClO_2*2.63 + H_2O_2*2.09 + O_3*2.5). The factors 2.63 and 2.09 are simple conversions of ClO_2 and H_2O_2 into active Cl_2 based on their oxidation equivalents. On the other hand, the factor 2.5 is not a simple conversion of O_3 into active Cl_2 based on oxidation equivalents, but rather a result that has been reported in-mill experiences with ozone (Munro and Griffiths, 2000). Based on simple oxidation equivalent conversion this factor would be 4.3 for the ozone case. For the brown pulp, bleachability tended to increase with increasing kappa number, with the exception of the kappa 20.9 pulp bleached with the sequence Z/ED(PO), which presented an unusually low bleachability in relation to all other samples. This kappa number value is probably excessively high for a three stage bleaching sequence initiating with an ozone stage. However, for the oxygen-delignified samples bleachability tended to increase with increasing kappa number only for the D_{HT}(PO)DP sequence, while decreasing for the other two. This result may be explained by the high efficiency of the D_{HT} stage in reducing kappa number, a fact that is reflected by the much higher bleachability values achieved by the D_{HT}(PO)DP sequence (2.19-2.49 kappa units/ kg active Cl), as compared to the other two sequences (1.84-2.10). The only exception to this basic tendency was the unusually high bleachability (2.52) achieved by the Z/ED(PO) sequence with the kappa 14.1 pulp previously delignified with oxygen. This is an indication that ozone bleaching with a three-stage sequence is well fitted to lower kappa pulps.

Pulp brightness reversion was not significantly affected by pulp kappa number, oxygen delignification, or bleaching sequence. Suitable reversion values in the range of 1.6 to 2.4 were obtained in the whole spectrum of treatments, and no clear trend was possible to derive. Note that brightness reversion values for eucalyptus pulps may vary from 1-5% ISO (by Tappi UM 200 standard) depending upon the pulping and bleaching procedures. One explanation for the good brightness stability of these pulps is the presence of a final hydrogen peroxide stage in all sequences evaluated. Previous work (Eiras and Colodette 2005) carried out with eucalyptus pulps using the same brightness reversion procedure used in this work (Tappi UM 200) have indicated better brightness stability for pulps bleached with sequences ending with a final peroxide stage in relation to those ending with a final D stage. Final viscosities tended to be acceptable regardless of kappa number and bleaching sequence for both brown and oxygen-delignified pulps, but the A/D(PO)DP sequence delivered the highest viscosities. As expected, pulps cooked to lower kappa numbers and oxygen delignified showed the lowest final viscosities. Bleaching yield tended to be slightly higher for the pulps bleached with the

Z/ED(PO) sequence in relation to the other two, but differences were small, in the range of 0.3-0.5%. As should be expected, higher kappa pulps presented the lowest bleaching yields. There was a clear trend towards slightly lower yields for pulps treated with oxygen in relation to the brown ones.

Table 4. Performance of the D_{HT}(PO)DP, A/D(PO)DP and Z/ED(PO) Sequences for Bleaching Kappa 14-21 Brown Eucalyptus Kraft Pulps to 90% ISO Brightness

Sequence	D_{HT}(PO)DP			A/D(PO)DP			Z/ED(PO)		
Brown Kappa No.	**14.1**	**17.4**	**20.9**	**14.1**	**17.4**	**20.9**	**14.1**	**17.4**	**20.9**
H_2O_2, %	0,5	0,5	0,5	0,5	0,5	0,5	0,8	1,5	2,7
O_2, %	0,5	0,5	0,5	0,5	0,5	0,5	0	0	0
O_3, %	0	0	0	0	0	0	0,6	0,6	0,6
OWL for O_2 delig, % NaOH	0	0	0	0	0	0	0	0	0
NaOH for Bleaching, %	1,5	1,5	1,6	1,8	1,9	2,0	1,8	2,1	2,8
H_2SO_4, %	0,6	0,6	0,6	0,9	0,9	0,9	1,0	1,0	1,0
$MgSO_4$, %	0,15	0,15	0,15	0,15	0,15	0,15	0,15	0,15	0,15
*ClO_2, %	2,1	2,6	3,0	2,5	3,0	3,4	1,52	1,52	1,52
[1]Total Active Chlorine (TAC), %	6.45	7.85	9.05	7.65	8.85	9.95	7.17	8.64	11.14
Bleachability, Brown K # / TAC	**2.19**	**2.22**	**2.31**	**1.84**	**1.97**	**2.10**	**1.97**	**2.02**	**1.88**
Chemical Cost, US$/odt	**33.7**	**39.0**	**44.1**	**40.0**	**45.0**	**49.7**	**41.2**	**48.7**	**62.4**
Final Brightness, % ISO	90.2	90.2	90.0	90.1	90.0	90.0	90.1	90.0	90.1
Reversion, % ISO	2.0	1.9	1.9	1.8	2.4	2.1	2.2	2.8	2.1
Final Viscosity, mPa.s	16.5	22.8	28.1	17.8	25.8	30.2	15.9	20.7	26.9
[2]Bleaching Yield, %	97.3	96.7	96.0	97.5	96.9	96.3	97.7	97.1	96.4

[1]Total Active Chlorine (TAC) = (ClO_2*2.63 + H_2O_2*2.09 + O_3*2.5);
[2]Includes yield loss across O/O stage.

Incoming Kappa Number

The ideal kappa number to terminate pulping and start bleaching has always been a matter of debate. The controversy is only natural, since it depends on a large number of factors that include not only the type of wood, pulping process, type and number of bleaching stages, presence of oxygen delignification, but foremost on the price of the wood and bleaching chemicals. Kappa ranges of 25-30 and 17-20 have been considered ideal for softwood and hardwood kraft pulps, respectively. However, with the advent of modified cooking associated with elemental chlorine free and totally chlorine free bleaching, there has been a trend towards lower kappa numbers. When oxygen delignification is brought into the picture, the ideal kappa to terminate the cook is very much affected by the efficiency of the oxygen stage installed. Furthermore, the hexenuronic acid content of hardwood pulps is another important factor. The establishment of an ideal kappa number for terminating pulping can be properly done, taking into account bleaching and wood costs.

Table 5. Performance of the D_{HT}(PO)DP), A/D(PO)DP and Z/ED(PO) Sequences for Bleaching Kappa 14-21 Oxygen Delignified Eucalyptus Kraft Pulps to 90% ISO Brightness

Sequence	O/O D_{HT}(PO)DP			O/O A/D(PO)DP			O/O Z/ED(PO)		
Brown Kappa No.	**14.1**	**17.4**	**20.9**	**14.1**	**17.4**	**20.9**	**14.1**	**17.4**	**20.9**
O/O Stage Kappa No.	**10.2**	**11.9**	**12.8**	**10.2**	**11.9**	**12.8**	**10.2**	**11.9**	**12.8**
H_2O_2, %	0,5	0,5	0,5	0,5	0,5	0,5	0,5	0,8	1,2
O_2, %	2,8	2,8	2,8	2,8	2,8	2,8	2,5	2,5	2,5
O_3, %	0	0	0	0	0	0	0,6	0,6	0,6
OWL for O_2 delig, % NaOH	1,7	1,8	1,9	1,7	1,8	1,9	1,7	1,8	1,9
NaOH for Bleaching, %	1,1	1,1	1,2	1,4	1,5	1,6	1,4	1,7	2,0
H_2SO_4, %	0,6	0,6	0,6	0,9	0,9	0,9	1,0	1,0	1,0
$MgSO_4$, %	0,15	0,15	0,15	0,15	0,15	0,15	0,15	0,15	0,15
*ClO_2, %	1,2	1,5	1,6	1,4	1,8	2,1	0,57	0,95	1,14
[1]Total Active Chlorine (TAC), %	4.25	4.88	5.15	4.75	5.75	6.55	4.05	5.67	7.01
Bleachability, O/O Stage K #/ TAC	**2.40**	**2.44**	**2.49**	**2.15**	**2.07**	**1.96**	**2.52**	**2.10**	**1.83**
Chemical Cost, US$/odt	**28.8**	**31.4**	**33.1**	**32.5**	**37.0**	**40.7**	**32.9**	**40.9**	**47.9**
Final Brightness, % ISO	90.2	90.2	90.3	90.0	90.0	89.8	90.0	90.1	90.0
Reversion, % ISO	2.0	1.9	2.0	1.6	1.8	1.8	2.0	1.9	1.8
Final Viscosity, mPa.s	14.8	19.4	22.8	16.5	21.3	24.7	13.9	18.1	20.9
[2]Bleaching Yield, %	96.5	96.0	95.4	96.8	96.2	95.6	96.9	96.4	95.8

[1]Total Active Chlorine (TAC) = (ClO_2*2.63 + H_2O_2*2.09 + O_3*2.5);
[2]Includes yield loss across O/O stage.

Table 6 shows the effect of incoming kappa number on overall fiber line economics for brown and oxygen-delignified pulps, respectively. A wood cost of US$45/odt of wood was used for the calculations, since this cost is currently typical for the Brazilian market (spot market). For brown pulp, increasing kappa number results in a prediction of increased overall bleaching costs regardless of the bleaching process chosen, and that is in line with the fact that the wood cost savings due to increasing kappa number are not sufficiently high to override the large impact of the kappa number on bleaching chemical costs. However, for the oxygen-delignified pulp this trend is somewhat changed, at least for the D_{HT}(PO)DP bleaching technology, due to its high efficiency. The oxygen delignification stage brings the kappa number of the high kappa pulps to values sufficiently low for the efficient operation of the D_{HT}(PO)DP sequence and, consequently, the chemical costs for this sequence is rather low even for the high kappa pulps. Therefore, in this particular case, the yield gains benefit from terminating the cook at a higher kappa number more than offset the slight increase in bleaching chemical costs (Table 6) caused by the high kappa. In other words, the D_{HT}(PO)DP sequence accommodates better the potential bleaching cost increase derived from a high incoming kappa than the other sequences. The lower tolerance of the Z/ED(PO) sequence to high kappa numbers is clearly seen, whereby a sharp increase in wood plus bleaching

costs occurs when kappa number is increased above 14 both for brown and oxygen-delignified pulps.

Table 6. Wood and Bleaching Chemical Costs for Production of 90% ISO Brightness Pulp using Modified Cooking Technology to Kappa Nº 14-21 and Bleaching with the Sequences D_{HT}(PO)DP, A/D(PO)DP and Z/ED(PO), with and without Oxygen Delignification

Operational Costs	D_{HT}(PO)D			A/D(PO)DP			Z/ED(PO)		
Brown Kappa No.	**14.1**	**17.4**	**20.9**	**14.1**	**17.4**	**20.9**	**14.1**	**17.4**	**20.9**
Bleaching costs, US$/odt pulp	33.7	39.0	44.1	40.0	45.0	49.7	41.2	48.7	62.4
Bleaching Yield, %	97.3	96.7	96.0	97.5	96.9	96.3	97.7	97.1	96.4
Pulping Yield, %	49.3	51.4	53.4	49.3	51.4	53.4	49.3	51.4	53.4
Fiber line Yield, %	48.0	49.7	51.3	48.1	49.8	51.4	48.2	49.9	51.5
Wood Costs, US$/odt pulp	93.8	90.5	87.8	93.6	90.3	87.5	93.4	90.2	87.4
Wood + Bl. costs, US$/odt pulp	**127.5**	**129.5**	**131.8**	**133.6**	**135.4**	**137.2**	**134.6**	**138.8**	**149.8**
Operational Costs	**O/O D_{HT} (PO)DP**			**O/O A/D(PO)DP**			**O/O Z/ED(PO)**		
Bleaching costs, US$/odt pulp	28.8	31.4	33.1	32.5	37.0	40.7	32.9	40.9	47.9
Bleaching Yield, %	96.5	96.0	95.4	96.8	96.2	95.6	96.9	96.4	95.8
Pulping Yield, %	49.3	51.4	53.4	49.3	51.4	53.4	49.3	51.4	53.4
Fiber line Yield, %	47.6	49.3	50.9	47.7	49.4	51.1	47.8	49.5	51.2
[1]Wood Costs, US$/odt pulp	94.6	91.2	88.3	94.3	91.0	88.1	94.2	90.8	88.0
Wood + Bl. costs, US$/odt pulp	**123.4**	**122.6**	**121.5**	**126.8**	**128.0**	**128.8**	**127.1**	**131.7**	**135.9**

[1]At a wood price of US$45/odt.

Economy of Oxygen Delignification

Oxygen delignification is currently a standard technology for production of bleached eucalyptus kraft pulps. The overall understanding is that such a stage is paramount to decrease operational costs and foremost to improve pulp mill environmental performance. Considering that oxygen delignification is highly inefficient for eucalyptus kraft pulps derived from modified cooking, the need for such a stage has been questioned. Table 6 shows that there is always an operational cost benefit derived from the installation of the oxygen delignification technology, regardless of incoming kappa number and bleaching sequence. However, this benefit is not very large, varying from 4 to 14 US$/odt pulp, depending upon the bleaching technology and kappa number considered. If one takes into account the D_{HT}(PO)DP sequence, which was the most efficient among all those considered in this study, the operational cost benefits of oxygen delignification are even less significant, 4 to 10 US$/odt pulp, depending upon the incoming kappa number. The most significant operational cost comes from wood, which is not largely affected by oxygen delignification. The price of wood is a major factor influencing operational costs. As an example, for the 14.1 kappa pulp a decrease in wood

price from US$45/odt (Table 6) to US$30/odt reduces operational costs from US$127.5/odt to US$ 96.2/odt, for the D_{HT}(PO)DP sequence and from US$123.4/odt to US$ 91.9/odt, for the O/OD_{HT}(PO)DP sequence. This shows that that oxygen delignification has a slight positive impact on cost, but the major effect comes from wood price.

The capital required to install oxygen delignification is quite high. It is unlikely that an operational cost saving of US$4/odt pulp caused by oxygen delignification is sufficient to adequately remunerate a capital investment of over 20 million US$. Therefore, the justification for installing the O-stage for bleaching eucalyptus kraft pulp is indeed an environmental one. Among the sequences evaluated, the D_{HT}(PO)DP and Z/ED(PO) presented the highest and lowest effluent loads, respectively (Table 7). The D_{HT}(PO)DP sequence is particularly problematic when it comes to effluent color, with the color derived from this sequence being 1.5-2.5 fold higher than that of the A/D(PO)DP and Z/ED(PO) sequences. The lowest AOX values were observed for the Z/ED(PO) sequence, followed by the D_{HT}(PO)DP and A/D(PO)DP ones. Effluent load increased with increasing kappa number, as expected. This effect was much more significant with brown pulp. Oxygen delignification substantially decreased effluent load. It decreased COD in the range of 20-40%, with the most significant benefit occurring for the higher kappa pulps. Among the various sequences, no clear trends on COD were observed as far as the impact of oxygen delignification is concerned. The largest impact of the oxygen delignification was on effluent color, causing a reduction of 65-75%. The large influence of oxygen delignification on color was not significantly affected by pulp incoming kappa number and/or bleaching sequence. The oxygen delignification stage caused a decrease of 50-70% on effluent AOX load with the most significant drops occurring for the D_{HT}(PO)DP sequence and the least significant for the Z/ED(PO) one. The benefits were more significant for the higher kappa pulps. Further investigations in our research program will focus on effluent treatability and pulp strength properties, considering these two scenarios.

Note that the costs related to increased effluent load and loss in energy (fewer solids to burn) for the processes without oxygen delignification was not taken into account in the economical analyses (Table 6). This matter will be addressed in another publication where a more in depth economical evaluation of the various approaches is presented. For example, the average costs for effluent treatment using aeration stabilization basins or activated sludge systems in Brazilian eucalyptus mills is in the range of 2-3 US$/$m^3$ effluent. Such treatments manage to decrease COD by 60-70% from raw effluents containing 30-40 kg O_2/odt pulp COD. Thus, it is possible to derive an estimate for increased effluent treatment cost based on increased effluent COD. On the other hand, the energy losses due to fewer solids to burn can be easily calculated on the basis of decreased solids to recovery, which in the case of eucalyptus kraft pulp mills vary in the range of 3-4%. It is worth noting that for mills having a bottleneck in the recovery area the decreased solids may result in increased mill throughput. Therefore, the economical analyses must take this matter also into account.

Table 7. Bleaching Effluent Load for Production of 90% ISO Brightness Pulp using Modified Cooking Technology to Kappa No. 14-21 and Bleaching with the D_{HT}(PO)DP, A/D(PO)DP, and Z/ED(PO) Sequences, with and without Oxygen Delignification

Brown Kappa No.	14.1	17.4	20.9	14.1	17.4	20.9	14.1	17.4	20.9
Effluent Load	**D_{HT}(PO)DP**			**A/D(PO)DP**			**Z/ED(PO)**		
Bleaching Filtrate COD, kg O_2/bdt	32,5	42,1	51,1	31,5	37,5	40,4	18,9	23,9	29,3
Bleaching Filtrate Color, kg Pt/bdt	64,0	77,2	85,4	32,3	41,6	50,5	14,1	27,3	41,9
Bleaching Filtrate AOX, kg Cl/bdt	0,45	0,64	0,81	0,47	0,73	1,03	0,17	0,24	0,30
Effluent Load	**O/O D_{HT}(PO)DP**			**O/O A/D(PO)DP**			**O/O Z/ED(PO)**		
Bleaching Filtrate COD, kg O_2/bdt	25,7	29,1	30,8	24,5	25,2	26,9	14,2	17,1	20,0
Bleaching Filtrate Color, kg Pt/bdt	16,6	20,3	25,8	9,1	12,3	14,8	4,9	9,1	13,1
Bleaching Filtrate AOX, kg Cl/bdt	0,16	0,20	0,24	0,19	0,22	0,30	0,09	0,10	0,12

CONCLUSIONS

- Eucalyptus fiberlines already equipped with oxygen delignification will benefit from terminating the cook at higher kappa numbers (17.5-21) and proceeding with the sequence D_{HT}(PO)DP, which gives the lowest operating costs.
- For new fiberlines, the most attractive economy to manufacture bleached eucalyptus kraft pulp is achieved by terminating the cook at kappa number ~14 and bleaching with the D_{HT}(PO)DP sequence, without oxygen delignification. The great economical advantage derives from the significant capital savings. But this approach leads to significant effluent load challenges.

ACKNOWLEDGEMENT

This article first appeared in the procedings of the 4th Congreso Iberoamericano de Investigación en Celulosa y Papel, CIADICYP-2006, which was held in Santiago and Valdivia, Chile between October 23 and 27, 2006. By agreement with the organizers, selected articles from the conference were submitted to *BioResources*, subject to the usual peer-review process.

REFERENCES CITED

Almeida, F. S., and Silva Júnior, F. G. (2004). "Influence of alkali charge on hexenuronic acid formation and pulping efficiency for Low-Solids cooking of Eucalyptus," In: *Proc. Tappi Fall Technical Conference*. TAPPI Press, Atlanta.

Chakar, F., Allison, L., Ragauskas, A., Mcdonough, T., and Sezgi, U. (2000). "Influence of hexenuronic acids on U. S. bleaching operations. *Tappi J*. 83(11), 62. (digital document).

Colodette, J. L., Gomide, J. L., Girard, R., Jaaskelainen, A. S., and Argyropoulos, D. (2001). "Influence of pulping conditions on eucalyptus kraft pulp yield, quality, and bleachability," *Tappi J.* 1(1), 14-19.

Colodette, J. L., Gomes, C. M., Mounteer, A. H., Rabelo, M. S., and Eiras, K. M. M. (2006). "Modern high brightness low impact bleaching of eucalyptus kraft pulp," *Papier*, *IPW* 1, T14 - T17.

Colodette, J. L., Gomes, C. M., Rabelo, M. S., Eiras, K. M. M, Gomes, A. F., and Oliveira, K. D. (2006). "Eucalyptus kraft pulp bleaching: State-of-the-art and new developments," *O Papel* 67(9): 88 -111.

Eiras, K. M. M., and Colodette, J. L. (2003). "Effect of pulp bleachable lignin and hexenuronic acids contents on O-stage," *El Papel* 179(106), 32-36.

Eiras, K. M. M., and Colodette, J. L. (2005), "Investigation on eucalyptus kraft pulp brightness stability," *J. Pulp Paper Sci*. 31(1), 13-18.

Gellerstedt, G. (1996). "The chemistry of bleaching and brightness reversion," In: *Pulp Bleaching: Principles and Practice*. C. W. Dence, and D. W. Reeve (eds.), Atlanta: TAPPI Press, 91-111.

Kraft, P. (1967). In: *Pulp & Paper Manufacture*, McDonald, R. G. (ed.), 2nd Ed., McGraw-hill Book Company, New York, Vol.1, p. 628-725.

Lanna, A. E., Costa, M. M., Fonseca, M. J., Fonseca, S. M., Mounteer, A. H., Colodette, J. L., and Gomide, J. L. (2002). "Maximizing pulp yield potential for a eucalypt kraft pulp mill´s wood supply - A case study from Brazil," *Appita J.* 55(6), 439-443.

Li, J., and Gellerstedt, G. (1997). "The contribution to kappa number from hexeneuronic acid groups in pulp xylan," *Carbohydrate Research* 302, 213-180.

Munro, F., and Griffiths, J. (2000). Operating experience with an ozone-based ECF bleaching sequence. In *Proc Int. Pulp Bleaching Conf*., Atlanta: Tappi Press, Oral Presentations, 225-230.

Vuorinen, T., Teleman, A., Fagerstrom, P., Buchert, J., and Tenkanen, M. (1996). "Selective hydrolysis of hexenuronic acid groups and its application in ECF and TCF bleaching of kraft pulps," In *Proc. Int. Pulp Bleaching Conf*., Atlanta: TAPPI Press, Vol. 1, 43-51.

Article translation submitted: March 6, 2007; First round of reviewing completed: April 14, 2007; Revised version received: April 21, 2007; Revision accepted: April 22, 2007; Published: April 24, 2007.

GROWTH STRESSES AND CELLULOSE STRUCTURAL PARAMETERS IN TENSION AND NORMAL WOOD FROM THREE TROPICAL RAINFOREST ANGIOSPERM SPECIES

Julien Ruelle,[a, b*] Hiroyuki Yamamoto,[b] and Bernard Thibaut [a]

Few studies have been conducted about relation between cellulose parameters and biomechanical properties of wood in tropical angiosperms species. For this purpose, on 13 trees from 3 species of French Guyana tropical rainforest in a clear active process of restoring verticality, *i*) growth strains were measured in situ in order to determine the occurrence of tension wood within samples and *ii*) cellulose structural parameters were estimated on all the samples using X-ray diffraction method. Crystallite size was estimated from the full-width at half-maximum of the Miller index (002) arc diffraction and angle *T* was measured following Cave's method. Relationships between these parameters and growth stresses were good and the variations between normal and tension wood were significant, i.e. a lower angle *T* and a larger crystallite size in tension wood. In order to have a good estimation of the microfibril angle in the main layer of the secondary wall for each species, an experimental calibration was done between angle *T* and microfibril angle observed with scanning electron microscopy.

Keywords: Cellulose, Microfibril angle, Crystallite size, Tension wood, Tropical rainforest, Growth stresses

*Contact information: a: UMR EcoFoG, Campus agronomique - BP 709, 97387 Kourou cedex, Guyane Française, b: School of Bioagricultural Sciences, Nagoya University, Chikusa, Nagoya 464-8601, Japan; *Corresponding author: ruelle_j@kourou.cirad.fr*

INTRODUCTION

In order to restore verticality, trees are able to bend their trunk by the formation of a highly stressed wood, called reaction wood, producing a biomechanical dissymmetry between the upper and lower side of the axis. In gymnosperms the wood of the lower side of the axis is highly compressed and is called compression wood. On the contrary angiosperms will produce a highly tensile-stressed wood on the upper side called tension wood (Archer 1986). Reaction wood is generally associated with marked changes in anatomical structure. Compression wood shows rounder cells, intercellular spaces and cracks in the cell wall (Dadswell and Wardrop 1949). Tension wood is characterised in some species by the occurrence of fibres with a particular morphology and chemical composition due to the development of the so-called gelatinous layer (G-layer). This layer is essentially made up of strongly crystalline cellulose with a very low microfibril angle.

In both strategies a parameter involved in this biomechanical state is the geometry and structure of cellulose, one of wood's main constituents. Orientation of the microfibrils of cellulose in the main layer of the secondary wall of wood cell plays an important role in the generation mechanism of growth stresses (Yamamoto 1998; Yamamoto et

al. 1998) and also strongly affects many wood properties as longitudinal modulus of elasticity or longitudinal shrinkage (Barnett 2004; Washusen et al. 2001). Other cellulose structural parameters vary from normal to reaction wood; Andersson et al. (2003) and Washusen and Evans (2001) showed a variation of cellulose crystallite size respectively in compression wood of *Picea abies* and tension wood of *Eucalyptus globulus*.

Few studies have been done on tropical species so that, in this work, we try to highlight relationships between some cellulose structural parameters, i.e. microfibril angle and crystallite size measured by X-ray diffraction method, and growth stresses in 13 trees among 3 species from French Guyana tropical rainforest. X-ray diffraction method allows a rapid assessment of wood microstructure, but in the case of microfibril angle estimation a calibration is needed between the angle *T*, a parameter from X-ray diffractogram defined by Cave (1966), and microfibril angle (MFA) observed with optical techniques. Meylan (1967) made an empirical calibration on *Pinus radiata* using Cave's method and Yamamoto et al. (1993) made the same on two gymnosperms and two angiosperms species whose normal wood shows thin fibre cell walls and tension wood does not show G-layer. In this study we decided to make a calibration for the three studied species in order to see if the existing calibration could provide a good estimation for microfibril angle in tropical species with G-layer and/or with thick fibre cell walls.

EXPERIMENTAL

Plant Material

Three species in the tropical rainforest distributed in three families (Table 1) were selected. This selection was based on the anatomical aspect of tension wood observed from previous experiments (Fig. 1), in order to study various types of tension wood:

- *Eperua falcata* Aublet for tension wood with G layer,
- *Laetia procera* (Poepp.) Eichler for the multilayered feature in tension wood,
- *Simarouba amara* Aublet for the lack of difference in normal vs. tension wood.

Table 1. List of Trees Studied and their Diameter at Breast Height

Family	*Genus species*	Trees	Diameter at Breast Height (cm)
Caesalpinaceae	*Eperua falcata* Aublet	Ef 1	21.96
		Ef 2	24.19
		Ef 3	22.60
Flacourtiaceae	*Laetia procera* (Poepp.) Eichler	Lp1	19.10
		Lp2	22.92
		Lp3	28.33
		Lp4	21.80
		Lp5	26.42
Simaroubaceae	*Simarouba amara* Aublet	Sa1	23.87
		Sa2	25.78
		Sa3	16.87
		Sa4	27.00
		Sa5	40.00

Trees were selected in the same zone in French Guyana, near Kourou. Trees diameter at breast height ranged between 16.8 and 40 cm (Table 1). All the trees were in a clear active process of restoring verticality after some accidental inclination. This was verified in situ by mechanical measurement of growth strains (GS) by the "single hole" method (Almeras et al. 2005; Fournier et al. 1994). This method gives the value of the displacement between two pins hammered onto the trunk (after local debarking) at a 45 mm distance from each other. A hole (20 mm depth and 20 mm diameter) is drilled at the mid-point between the two pins. A displacement is measured (in µm) and converted into a strain (in %) using a calibration factor: 9.6×10^{-4} corresponding to a calibration made on *Eperua Falcata* (Fournier et al. 1994). Eight measures (every 45°) were realised at breast height on each tree, Position 1 corresponding to the upper side of the leaning trunk.

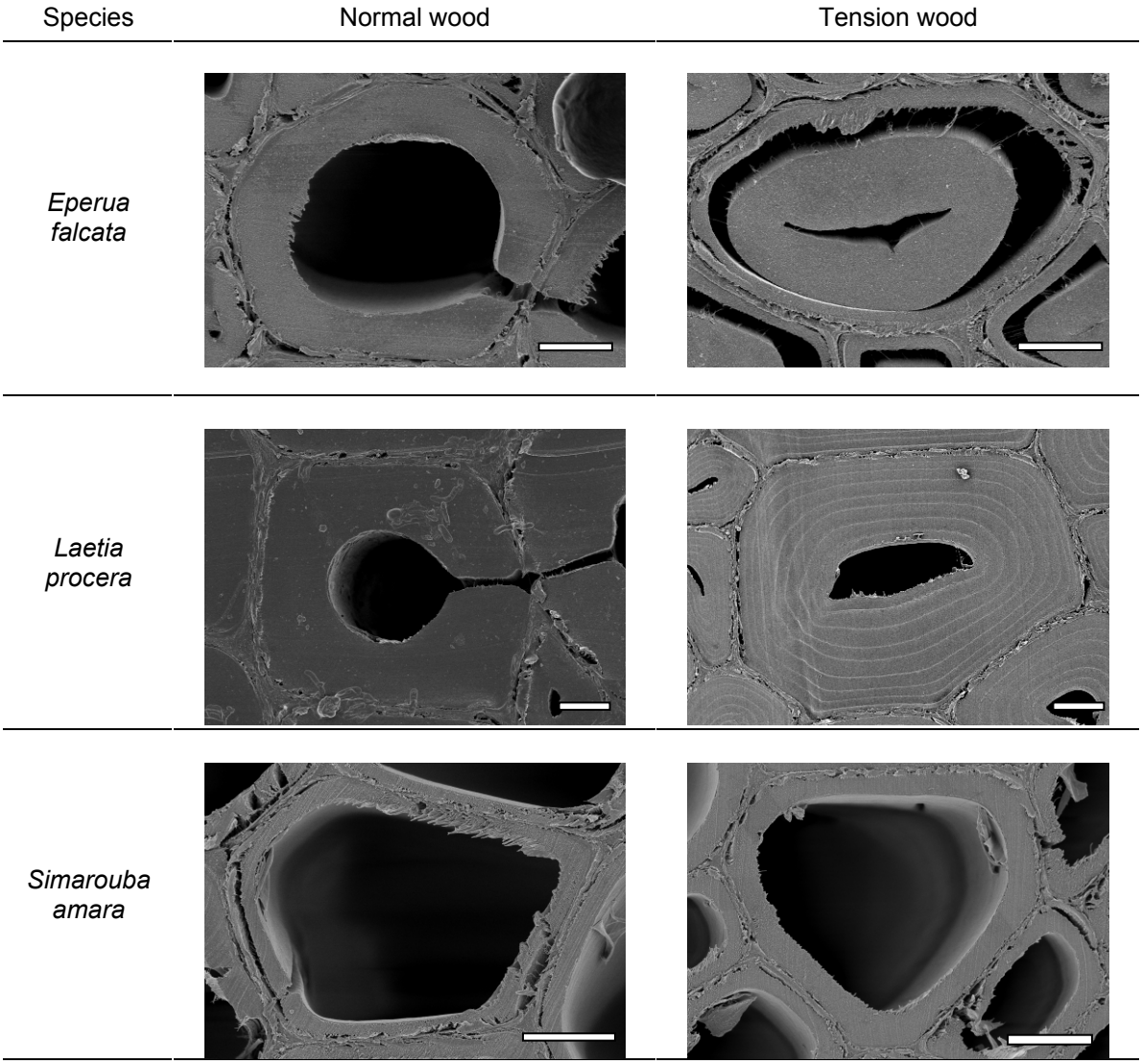

Fig. 1. Cross section of normal wood (on the left) and tension wood (on the right) of the three species studied observed with Scanning Electronic Microscopy. *Bars*, 5 µm

Normal wood of the three species has a typical secondary wall as shown in Fig. 2. Tension wood from *Simarouba amara* and *Laetia procera* has a S_3 layer in the secondary wall.

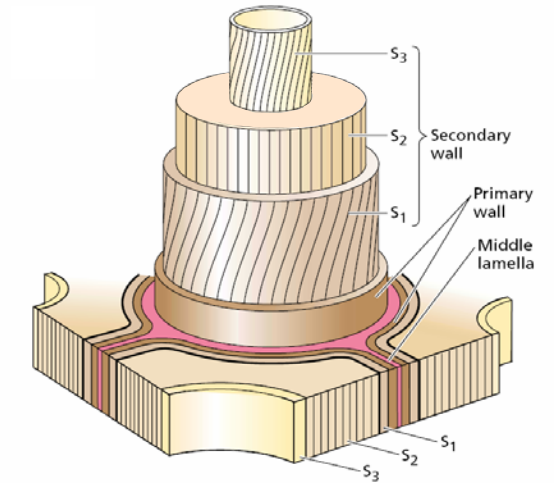

Fig. 2. Diagram of the cell wall organization often found in cells with thick secondary wall (Taiz and Zeiger 2002)

Two wood samples were taken, as close as possible to the GS measurement zone, above and below the hole. Observations were made on both samples to ensure the homogeneity of the studied wood above and below the GS measurement zone (Fig. 3).

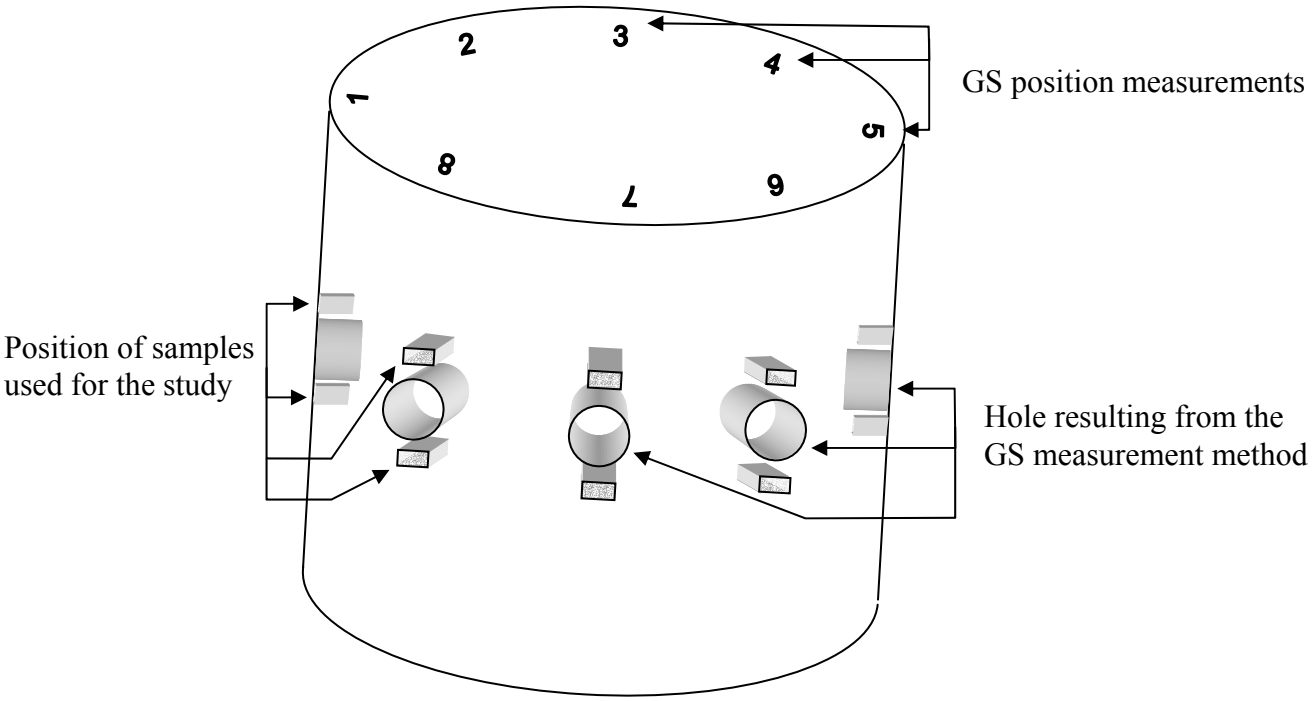

Fig. 3. Localization of specimen used for the experiments

Measurements show clearly that wood layers on the upper side exhibited a very much higher tensile stress than in all other places (Table 2) including lower side, which does not present significant difference in mechanical stressing with side places. Upper wood positions with very high growth strains are called tension wood in the next paragraphs, while all other locations are named normal wood.

Table 2. Growth Strains (X 10^{-6}) mean value and number of positions used for upper and lower side for each tree

Trees	Tension wood (TW) growth strains values		Normal wood (NW) growth strains values		Upper / lower side ratio means
	Mean of the upper side	Number of positions	Mean of the lower side	Number of positions	
Ef 1	1312	3	429	3	3
Ef 2	2282	3	710	3	3
Ef 3	2122	3	582	3	4
Lp1	2714	3	666	3	6
Lp2	2035	2	515	3	4
Lp3	2701	3	666	3	4
Lp4	1590	3	582	3	3
Lp5	2592	3	446	3	6
Sa1	1302	3	480	3	3
Sa2	1648	3	426	3	4
Sa3	954	3	285	3	3
Sa4	3219	3	179	3	18
Sa5	1616	3	502	3	3

From the data reported by Archer (1986) and from more recent studies (Clair et al. 2006; Yoshida et al. 2002), these growth strains values in tension wood are in the high range of reported values.

Method Used for Cellulose Structural Parameters Measurement

MFA estimation with X-ray diffraction method

Measurements were made using an X-ray diffractometer (Shimadzu XD-D1w) under the following conditions. A point-focused X-ray beam (Cu-Kα X-ray, beam diameter 1 mm) was applied to tangential sections: 1 mm thick x 15 mm long. An X-ray diffraction apparatus with a symmetrical transmission mode was used. The scattered X-ray was detected by a Na-I scintillation counter behind a receiving slit of width and length of 1 mm x 1 mm. Each sample was rotated around its normal axis at a rotation speed of six degrees per minute in a position of $2\theta = 22.4$ degrees and the diffraction intensity was recorded on a chart at a speed of 2 cm per minute.

As show in Fig. 4 angle *T* was obtained from the diffraction intensity around (002) arc (Cave 1966). Cave's (1966) (Eq. 1) and Yamamoto's (1993) (Eq. 2) formula gives an estimation of the mean MFA using this angle *T*:

$$MFA = 0.6T \quad (1)$$

$$MFA = 1.575x10^{-3}T^3 - 1.431x10^{-1}T^2 + 4.693T - 36.19 \quad (2)$$

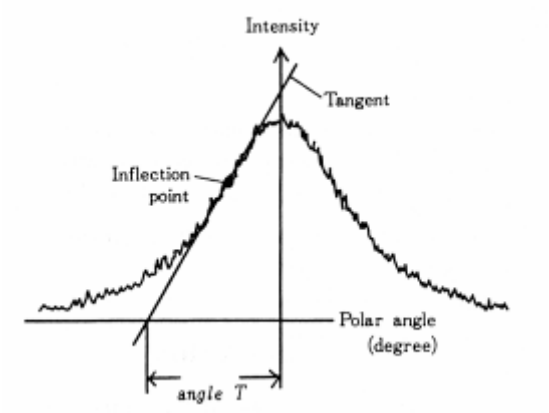

Fig. 4. Measurement procedure of angle *T* from a (002) arc diffraction

Crystallite size estimation with X-ray diffraction method

Measurements were made with the reflection technique using an X-ray diffractometer (Shimadzu XD-D1w) under the following conditions. The incident X-ray radiation was from the Cu Kα band (λ= 0.154nm) with a power of 35kV and 35mA passed through a Ni filter and collimated by a slit of 0.1 degree. The wood samples were fixed in a sample holder so that the fibre axis was vertical. The diffraction intensity for (200) was registered in the angular range from 10 to 40 degrees.

The crystallite size in the direction perpendicular to the 002 crystal plane was calculated using the Scherrer equation (Washusen and Evans 2001):

$$L = 0.9\frac{\lambda}{H\cos\theta} \quad (3)$$

where L is the crystallite size (in nm) perpendicular to the plane; λ is X-ray wavelength; H is the full-width at half-maximum (FWFM) in radian; and θ is the Bragg angle.

A Kolmogorov-Smirnov test was performed to compare crystallite size and angle *T* value between tension and normal wood.

Microfibril angle measurement with Field-Emission Scanning Electron Microscopy (FE-SEM)

Many techniques exist for the direct observation of MFA in wood. During previous experiments we tried to observe MFA in tropical species by use of the iodine crystal technique (Senft and Bendtsen 1985), but only few results were obtained on *Simarouba amara*. This fact may be linked to the thickness of the wall fibre; *Simarouba amara* is the only thin-walled tropical species we studied in these previous experiments. The application of the iodine crystal technique seems to be very difficult to apply on

thick-walled species, so that we choose to directly observe MFA with Field-Emission Scanning Electron Microscopy (FE-SEM).

Observations were made in axial planes. Sample geometry was 5×1×7 mm^3 (R×T×L). Samples were dehydrated through a graded ethanol series and then processed using the *t*-butyl alcohol freeze-drying method. In order to observe the cellulose fibrils of some layers, a lignin extraction treatment ($NaClO_2$ 0.6%, CH_3COOH 0.13% in distilled water during 40 hours) (Wise et al. 1946) was performed on longitudinal sections. The dried samples were mounted on aluminium stubs and lightly sputter-coated with platinum. Samples were observed by FE-SEM (Hitachi, S-4500) at an accelerating voltage of 3 kV.

Microfibril angle (MFA) measurements were made from direct longitudinal observations by FE-SEM on samples from various trees. The choice of samples used for this measurement was based on the results from X-ray diffraction method results, in order to scan a wide range of angle T value in each species (Fig. 9). We had to look at samples where the S_3 layer was removed during sample preparation in order to observe microfibril angle from the S_2 layer or the G-layer. As the direct observation of MFA is very tedious we had to take a limited number of samples. These measurements were made on about 20 fibrils per picture. Images used for this measurement are shown in Fig. 5.

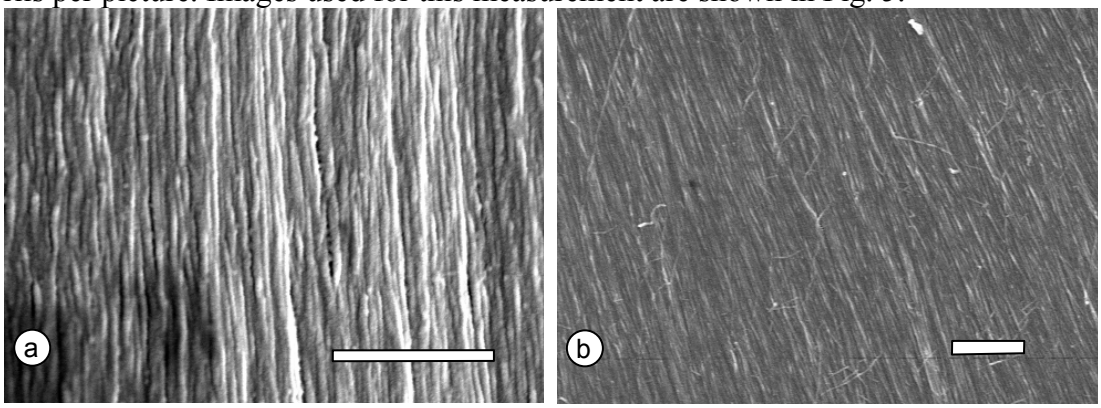

Fig. 5. Example of images used for the measurements of microfibril angle on tension wood (a) and normal wood (b) of *Laetia procera*. *Bars*, 500 nm

RESULTS AND DISCUSSION

Growth Strains and Cellulose Structural Parameters

Results from crystallite size measurement show that the crystallite size was larger in tension wood sample ($p<0.001$) (Fig. 6). The relationship between growth stress and crystallite size (Fig. 7) shows that both parameters increased in the same way, even though the tendency is less clear for *Eperua falcata*. This variation observed for *Eperua falcata* is mainly due to the large value of crystallite size observed in sample showing low growth strain values. These samples correspond to lateral wood, located between the lower and the upper side of the trunk. They could actually contain both tension and normal wood, which can explain the discrepancy between growth strain values and crystallite size.

The means for crystallite size were 3.31 nm and 2.65 nm for tension and normal wood, respectively (Fig. 6). Washusen and Evans (2001) also highlight wider crystallite size in the tension wood of *Eucalyptus globulus* Labill. Jahan and Mun (2005) showed an increasing of crystallite size on *Trema orientalis* wood samples after a selective removal of lignin and hemicelluloses. Tension wood is known to contain less lignin and a different content of hemicelluloses compared to normal wood (Timell 1967). Thus we can observe from literature and our results that the evolution of cellulose crystallite size usually goes with a modification of the matrix composition. This fact was already observed (Fahlen and Salmen 2003), and authors hypothesized that this evolution of crystallite size was due to a modification of the interaction existing between cellulose microfibrils and components of the matrix. But this variation remains unexplained, and we would consider a modification at the level of cellulose biosynthesis to explain it.

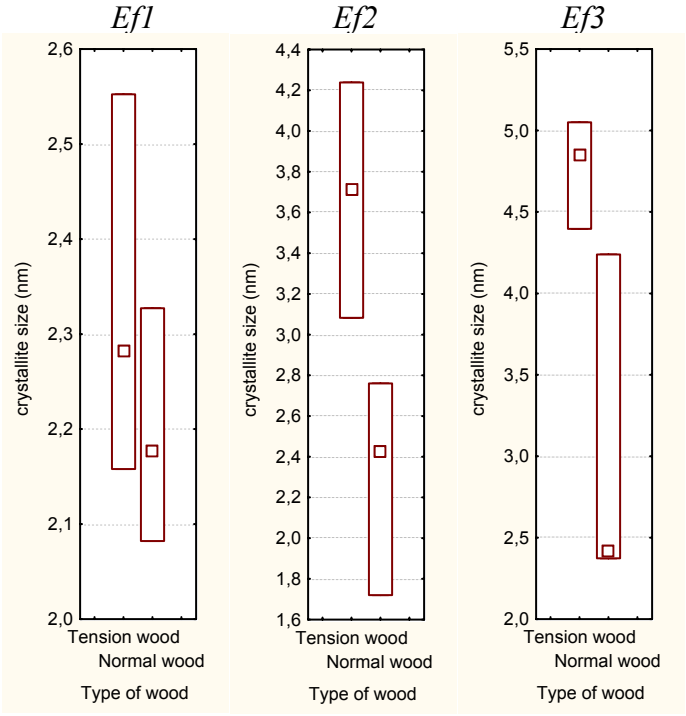

Fig. 6A. Box-and-whisker plots of crystallite size values of each kind of wood for each studied tree

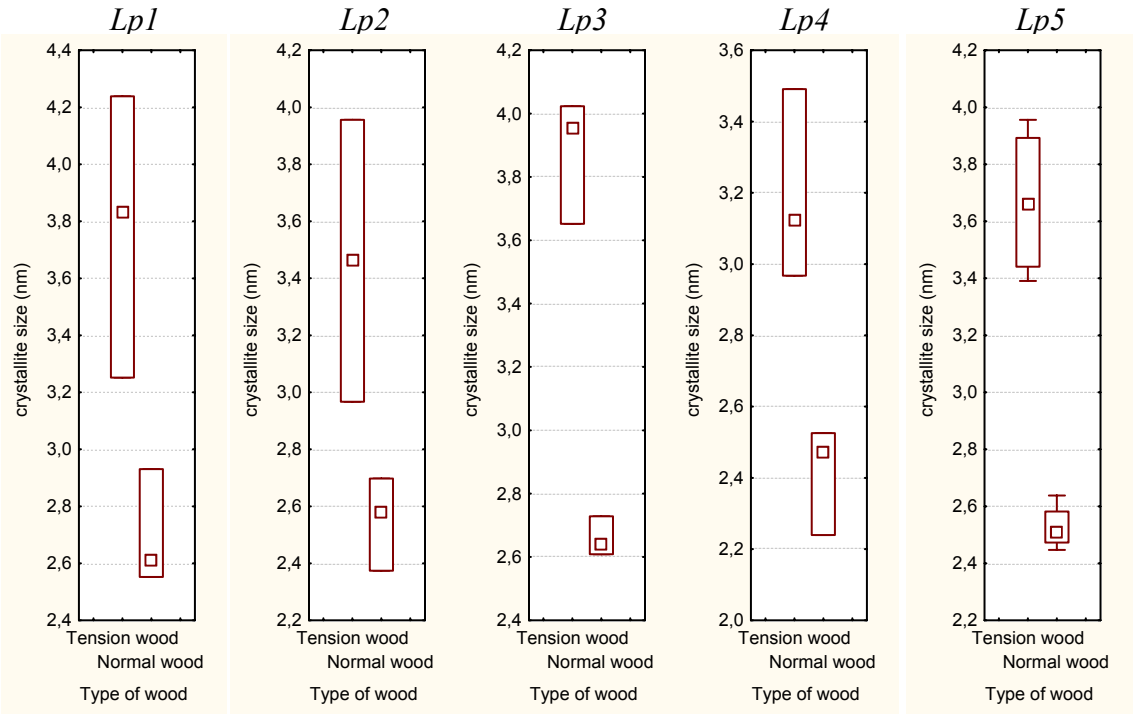

Fig. 6B. Box-and-whisker plots of crystallite size values of each kind of wood for each studied tree

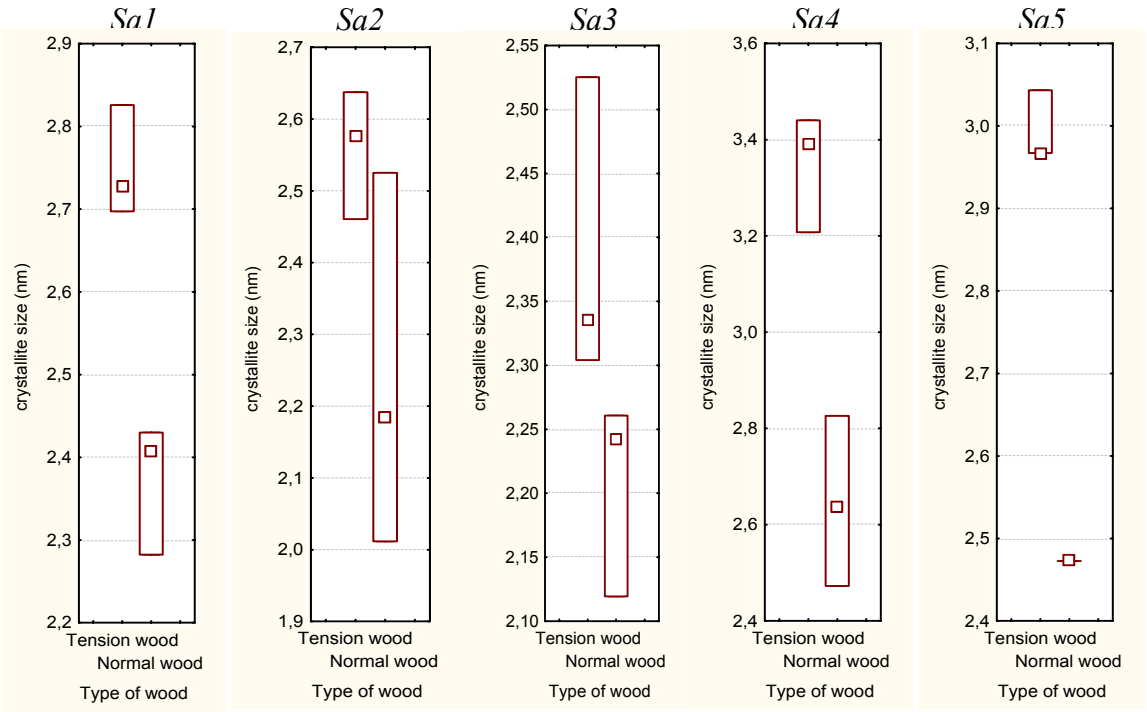

Fig. 6C. Box-and-whisker plots of crystallite size values of each kind of wood for each studied tree

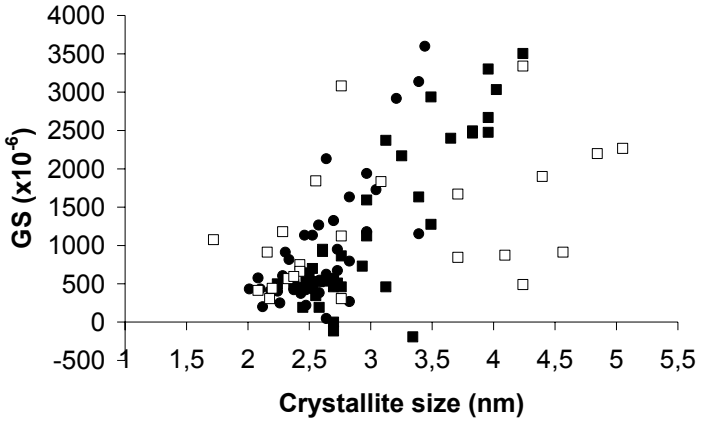

Fig. 7. Relationship between growth strains (x10^{-6}) and crystallite size (nm).
□; *Eperua falcata*, ■; *Laetia procera*, ●; *Simarouba amara*

Usually the angle *T* is used to estimate average MFA in wood (Abasolo et al. 2000; Cave 1966; Lofty et al. 1973; Yamamoto et al. 1993). In this study we checked the relationship between this parameter and the growth stress measured on samples (Fig. 8). The observed relationship was good, i.e. $r^2 = 0.5178$ for *Eperua falcata*, 0.7011 for *Laetia procera* and 0.4697 for *Simarouba amara*. The general tendency, i.e. a decreasing of angle *T* in high tensile stress wood, was the same for the three studied species.

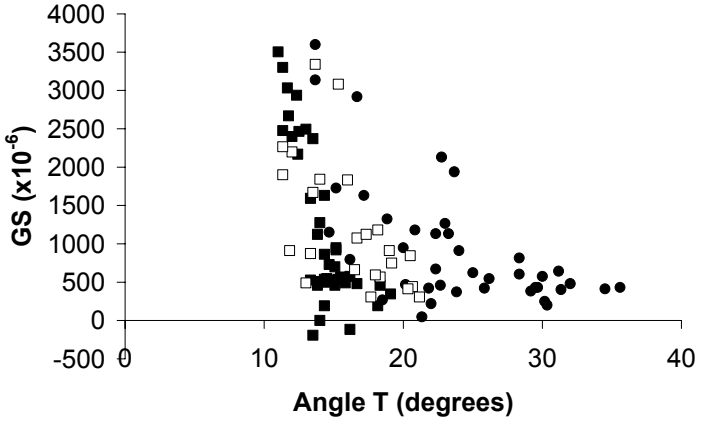

Fig. 8. Relationship between growth strains (x10^{-6}) and angle T values (degrees).
□; *Eperua falcata*, ■; *Laetia procera*, ●; *Simarouba amara*

At an interspecific level the mean values of angle *T* were 15.85° and 19.91° in tension and normal wood, respectively, showing that angle *T* was lower in tension wood samples ($p<0.001$). The value range for angle *T* (Fig. 9) in *Eperua falcata* and *Laetia procera* were very similar, with a minimum close to 11° and a maximum close to 20°. In *Simarouba amara* the range was larger than in other species, starting at about 14° and with a maximum at about 35°. The main difference that exists between the two first species and *Simarouba amara* is the density, directly linked with the cell wall thickness.

Without a true calibration of angle T value with average MFA we cannot tell if these differences between species reflect MFA variation.

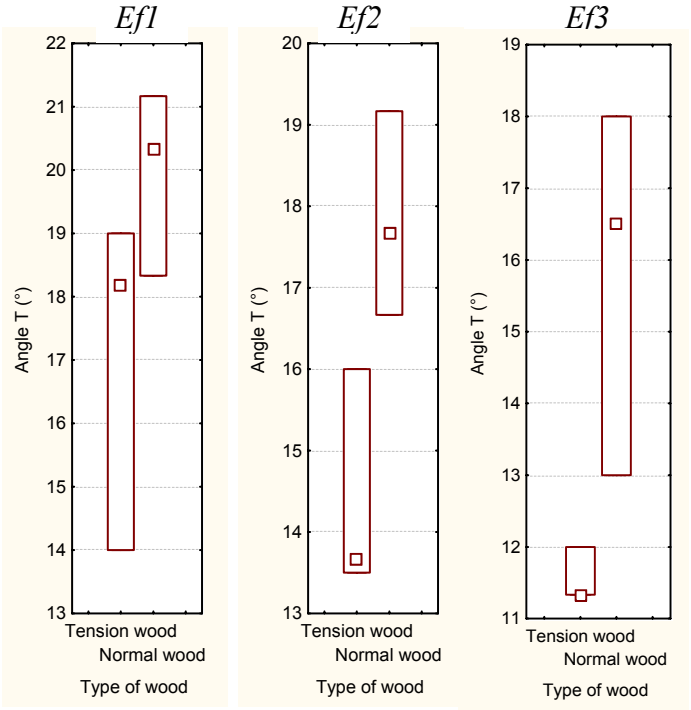

Fig. 9A. Box-and-whisker plots of angle T values of each kind of wood for each studied tree

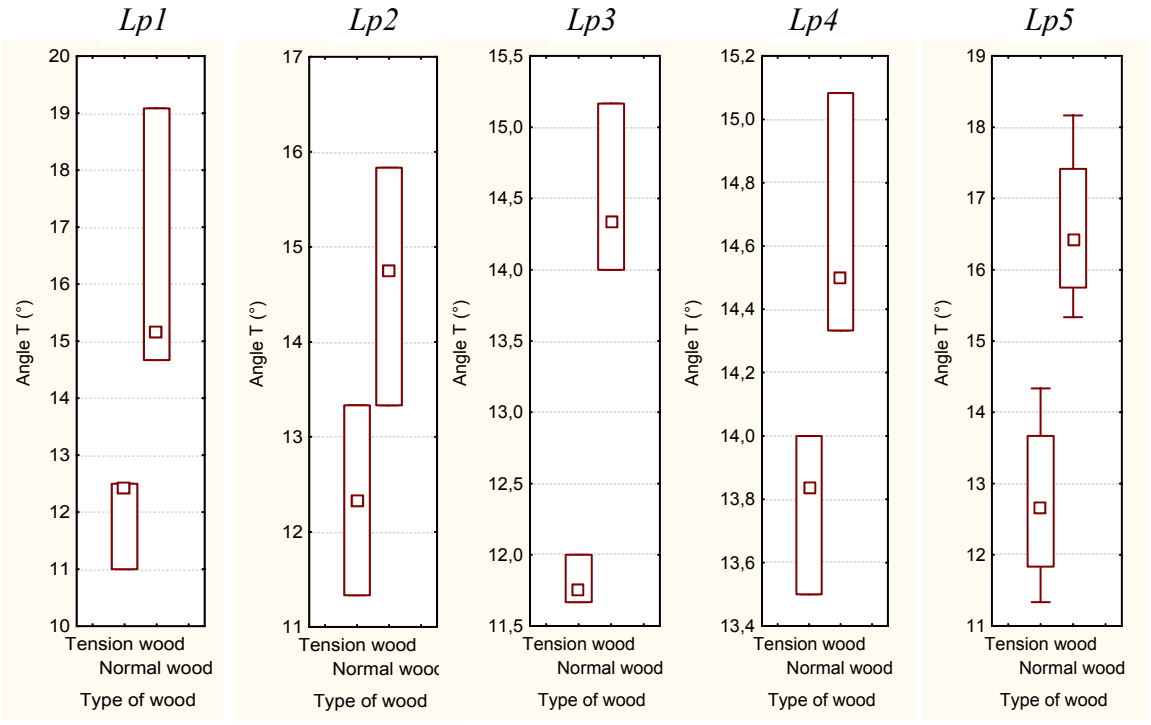

Fig. 9B. Box-and-whisker plots of angle T values of each kind of wood for each studied tree

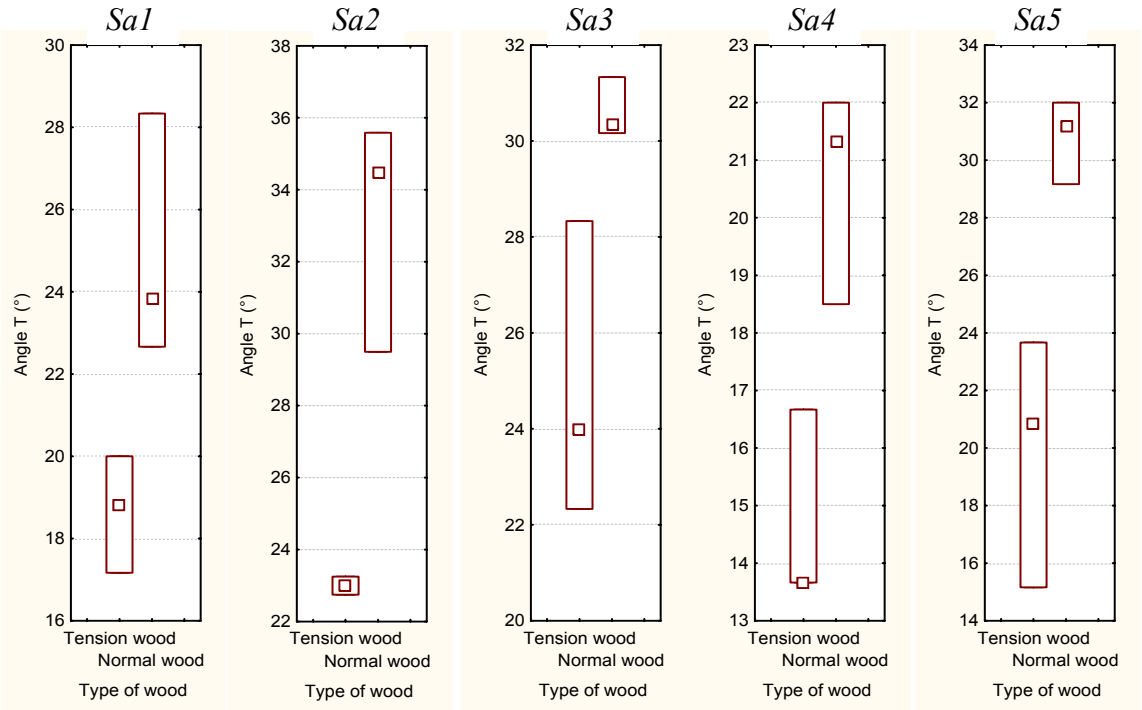

Fig. 9C. Box-and-whisker plots of angle T values of each kind of wood for each studied tree

Relationship between Angle *T* and Direct Observation of MFA

Fig. 10 shows the relationships between angle *T* and MFA measured with SEM observations for each species. Representations of Cave's (Eq. 1) and Yamamoto's formula (Eq. 2) are represented in order to make a comparison between these various calibrations.

First of all we see that relationships between angle *T* and directly observed MFA were very good for every studied species. This fact shows that the X-ray method is a really efficient tool to estimate MFA in wood, as long as a calibration is available for the interpretation of the (002) peak diffraction pattern. Observation of results in Fig. 10 and Fig. 11 indicates that the range of values for MFA is almost the same for all the species. This point leads us to think that thickness of cell wall has, with cell wall shape (Sarén and Serimaa 2005), a strong influence on results from X-ray diffraction method. Such influence can be seen in the relationships between angle *T* and directly observed MFA in thick-walled species, which deviate from thin-walled species and from Cave's findings. Cave assumed that the state of cellulose crystal is invariable when MFA changes; we observed that cellulose crystallite size varies from tension to normal wood. This also explains the observed deviation from Cave's relationships for all the species.

The real aim of this calibration was not to estimate more accurately the average MFA of the sample, but to find a relation between the MFA of the main layer of the secondary wall of samples, considered by many authors as a critical factor in the mechanical behaviour of wood (Barnett 2004; Megraw et al. 1998) and the criteria given by the application of Cave's method i.e. angle T.

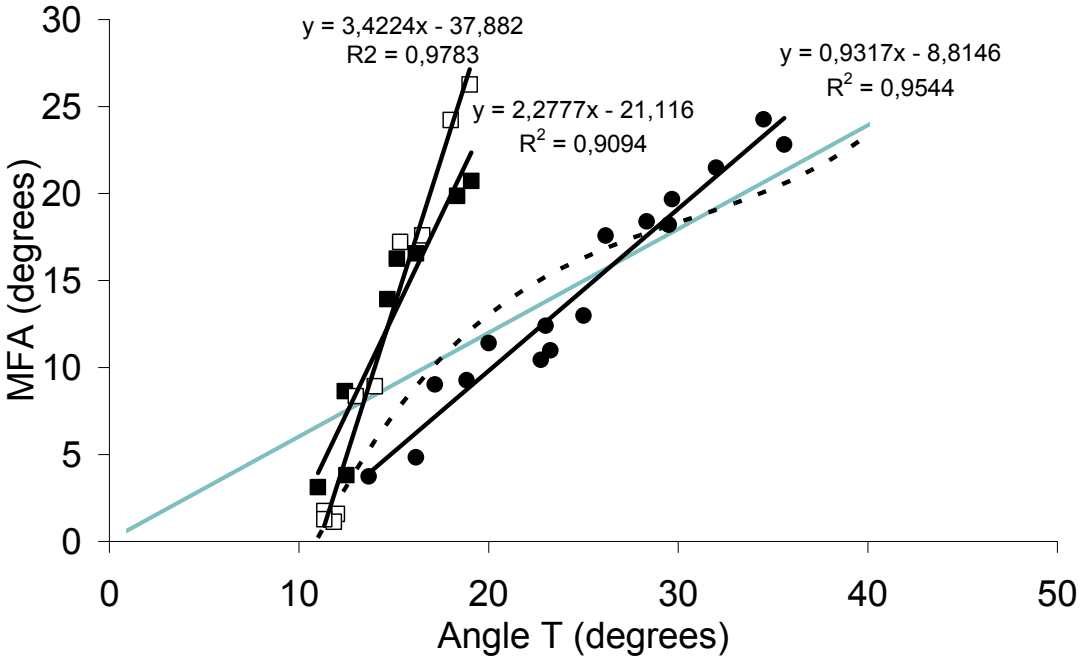

Fig. 10. Relationships between MFA measured with SEM observations and angle T from X-ray diffraction method. □; *Eperua falcata*, ■; *Laetia procera*, ●; *Simarouba amara*. Light gray line is Cave's formula (Eq. 1) and dashed curve is Yamamoto's formula (Eq. 2)

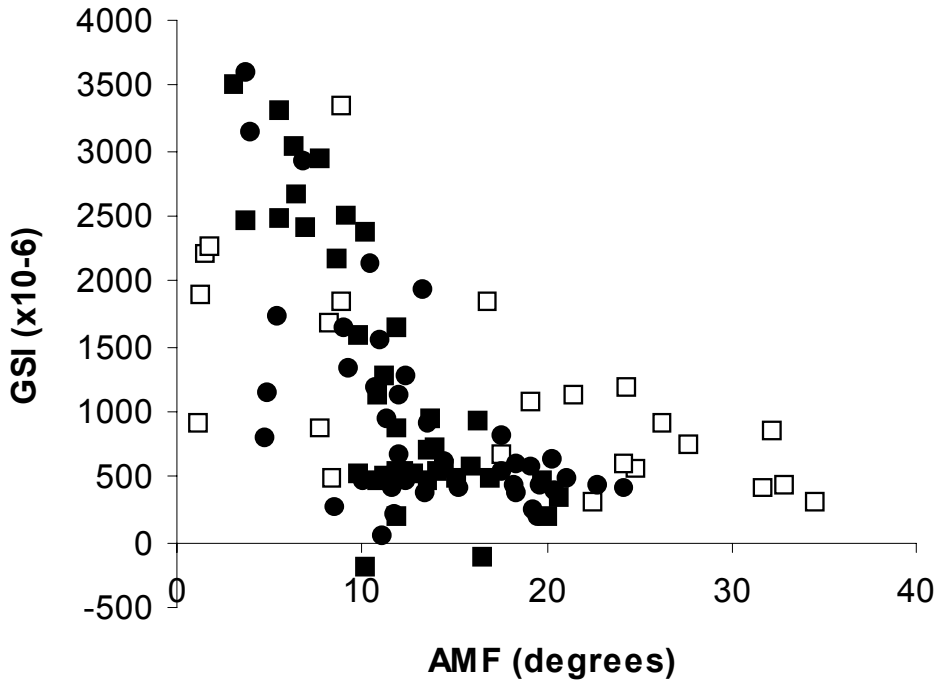

Fig 11. Relationship between growth strains (x10^{-6}) and angle T values (degrees). □; *Eperua falcata*, ■; *Laetia procera*, ●; *Simarouba amara*

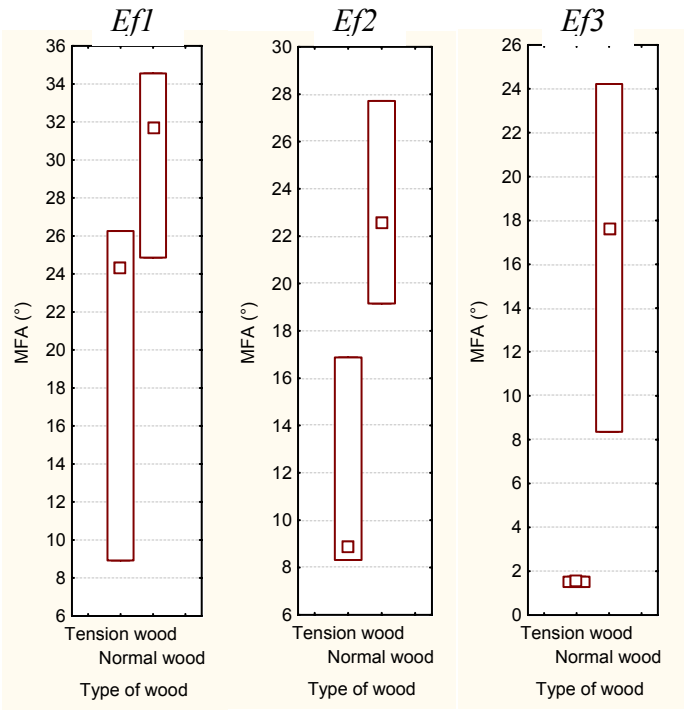

Fig. 11A. Box-and-whisker plots of MFA values of each kind of wood for each studied tree

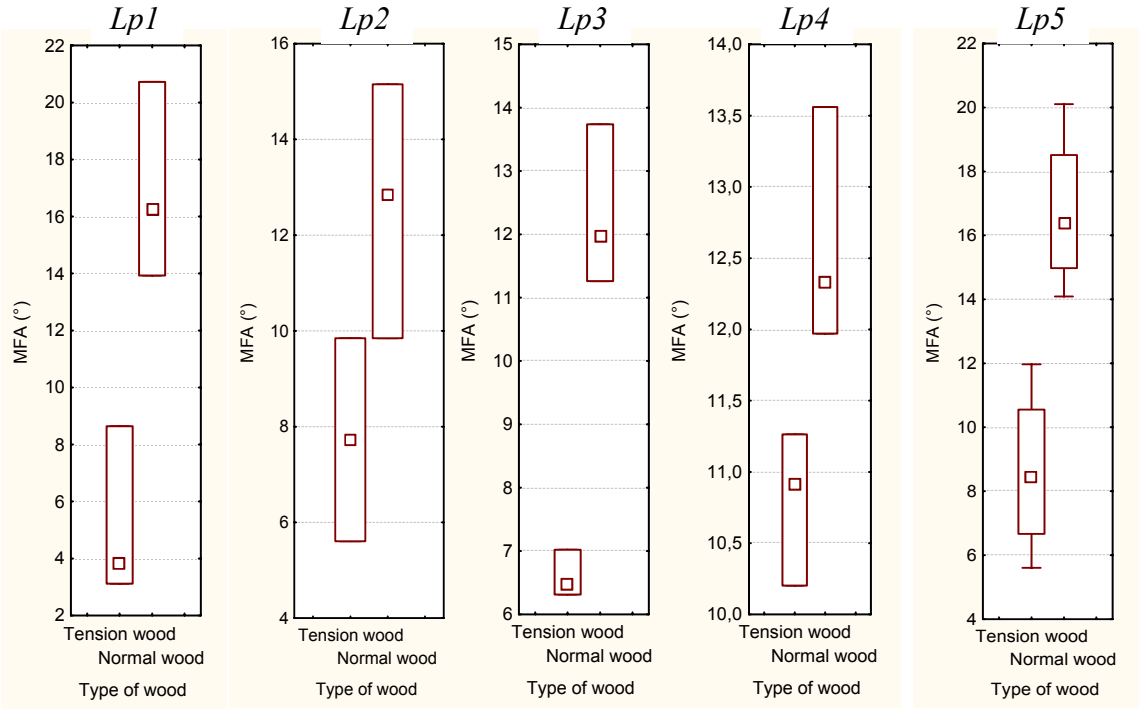

Fig. 11B. Box-and-whisker plots of MFA values of each kind of wood for each studied tree

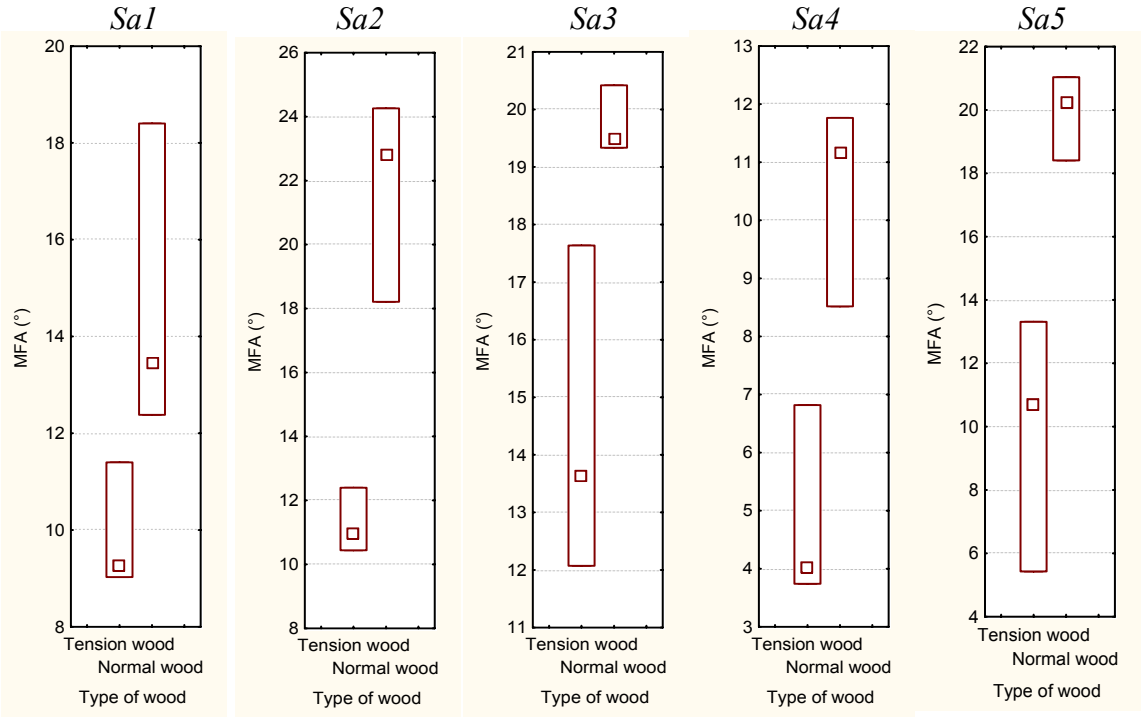

Fig. 11C. Box-and-whisker plots of MFA values of each kind of wood for each studied tree

It follows from these results that MFA estimation of *Simarouba amara* by means of Cave's and particularly Yamamoto's formula is not so far from the present observations. Yamamoto's formula was calculated in order to estimate MFA from X-ray diffraction method for a wide range of angle *T* values, in softwood species and hardwood species with thin-walled fibres and with tension wood that does not show gelatinous layer. This explains the good approximation of *Simarouba amara* MFA.

CONCLUSIONS

1. The cellulose structural parameters estimated during this work show good relationships with growth stresses: cellulose crystallite size increases in tension wood while angle *T*, which shows a strong relationship with directly observed MFA, decreases. The modification of the state of cellulose in the cell wall of fibres is a key for the explanation of growth stress generation, but the phenomena leading to these modifications still remains unclear. An important step in the understanding of the impact of cellulose structure variation on properties is the collection of data from various species and various kind of wood. This work was dedicated to this first step of understanding.
2. X-ray diffraction can provide lot of information on wood ultrastructure. The relationship between angle T and directly observed MFA was very good but a calibration is needed, especially for thick-walled fibres species, in order to estimate

the mean MFA of the main layer of the secondary wall. The deviations from Cave's (Eq. 1) and Yamamoto's (Eq. 2) formula observed for these species confirm the influence of cell wall geometry on X-ray diffraction measurements. Many authors discussed the influence of the method used and cell shape on X-ray diffraction results, but from an empirical point of view, a study devoted to calibration for many hardwood species would provide a useful tool for the analysis of cellulose microfibril orientation influence on growth stress generation.

REFERENCES CITED

Abasolo, W. P., Yoshida, M., Yamamoto, H., and Okuyama, T. (2000). "Microfibril angle determination of Rattan fibers and its influence on the properties of the Cane," *Holzforschung* 54(4), 437-442.

Almeras, T., Thibaut, A., and Gril, J. (2005). "Effect of circumferential heterogeneity of wood maturation strain, modulus of elasticity and radial growth on the regulation of stem orientation in trees," *Trees* 19, 457-467.

Andersson, S., Serimaa, R., Paakkari, T., Saranpää, P., and Pesonen, E. (2003). "Crystallinity of wood and the size of cellulose crystallites in Norway spruce (*Picea abies*)," *J. Wood Science* 49, 531-537.

Archer, R. R. (1986). *Growth stresses and strains in trees*, Springer-Verlag, Berlin Heidelberg New-York.

Barnett, J. R. (2004). "Cellulose microfibril angle in the cell wall of wood fibres," *Biol. Rev*. 79, 461-472.

Cave, I. D. (1966). "Theory of X-Ray measurement of microfibril angle in wood," *Forest Products J.* 16(10), 37-42.

Clair, B., Ruelle, J., Beauchêne, J., Prevost, M. F., and Fournier, M. (2006). "Tension wood and opposite wood in 21 tropical rainforest species. 1. About the presence of G layer," *IAWA J.* 27(3), 329-338.

Dadswell, H. E., and Wardrop, A. B. (1949). "What is reaction wood?" *Australian Forestry* 13(1), 22-33.

Fahlen, J., and Salmen, L. (2003). "Cross-sectional structure of the secondary wall of wood fibers as affected by processing," *J. Mater. Sci*. 38, 119-126.

Fournier, M., Chanson, B., Thibaut, B., and Guitard, D. (1994). "Mesure des déformations résiduelles de croissance à la surface des arbres, en relation avec leur morphologie. Observation sur différentes espèces," *Ann. Sci. For*. 51(3), 249-266.

Jahan, M. S., and Mun, S. P. (2005). "Effect of tree age on the cellulose structure of Nalita wood (Trema orientalis)," *Wood Science and Technology* 39, 367-373.

Lofty, M., El-osta, M., Kellog, M., Foschi, R. O., and Butters, R. G. (1973). "A direct X-ray technique for measuring microfibril angle," *Wood and Fiber* 5, 118-127.

Megraw, R. A., Leaf, G., and Bremer, D. (1998). "Longitudinal shrinkage and microfibril angle in Loblolly pine," *In Microfibril Angle in Wood: Proceedings of the IAWA/IUFRO International Workshop on the Significance of Microfibril Angle to*

Wood Quality (ed. B. G. Butterfield), Westport, N.Z. University of Canterbury Press, Canterbury, N.Z., 27-61.

Meylan, B. A. (1967). "Measurement of microfibril angle by X-ray diffraction," *Forest Products J.* 17, 51-58.

Sarén, M. P., and Serimaa, R. (2005). "Determination of microfibril angle distribution by X-ray diffraction," *Wood Science and Technology*, Online.

Senft, J. F., and Bendtsen, B. A. (1985). "Measuring microfibrillar angles using light microscopy," *Wood and Fiber science* 17(4), 564-567.

Taiz, L., and Zeiger, E. (2002). *Plant Physiology, Third Edition*, Sinauer Associates.

Timell, T. E. (1967). "Recent Progress in the Chemistry of Wood Hemicelluloses," *Wood Sci. Technol.* 1, 45-70.

Washusen, R., Ades, P., Evans, R., Ilic, J., and Vinden, P. (2001). "Relationships between density, shrinkage, extractives content and microfibril angle in tension wood from three provenances of 10-year-old Eucalyptus globulus Labill," *Holzforschung* 55(2), 176-182.

Washusen, R., and Evans, R. (2001). "The association between cellulose crystallite width and tension wood occurrence in *Eucalyptus globulus*," *IAWA J.* 22(3), 235-243.

Wise, L. E., Murphy, M., and D'Addieco, A. A. (1946). "Chlorite holocellulose, its fractionation and bearing on summative wood analysis and on studies on the hemicelluloses," *Paper Trade J.* 122(2), 35-43.

Yamamoto, H. (1998). "Generation mechanism of growth stresses in wood cell walls : roles of lignin deposition and cellulose microfibril during cell wall maturation," *Wood Sci. Technol.* 22(1).

Yamamoto, H., Okuyama, T., and Yoshida, M. (1993). "Method of determining the mean microfibril angle of wood over a wide range by the improved Cave's method," *Mokuzai Gakkaishi* 39, 118-125.

Yamamoto, H., Okuyama, T., and Yoshida, M. (1998). "Growth stress generation and microfibril angle in reaction wood," *Microfibril Angle in Wood. The proceedings of the IAWA / IUFRO international workshop on the Significance of microfibril angle to wood quality*, 225-239.

Yoshida, M., Ohta, H., Yamamoto, H., and Okuyama, T. (2002). "Tensile growth stress and lignin distribution in the cell walls of yellow poplar, *Liriodendron tulipifera* Linn," *Trees* 16, 457-464.

Article submitted: January 18, 2007; First round of reviewing completed: March 4, 2007; Revised version received: May 1, 2007; Accepted: May 2, 2007; Published: May 4, 2007

ANTI-SCALING AGENTS IN KRAFT PULPING

Fernando E. Felissia,[1] María C. Area,[2] Olga M. Barboza,[1] and Dora I. Bengoechea[1]

Scale formation in the digester during kraft pulping represents a great problem in pulp mills. Scaling reduces pulping control and efficiency, increasing energy costs and leading to cleaning breakdowns, with subsequent losses in productivity. The kraft process promotes $CaCO_3$ scaling due to high calcium ion and carbonate concentrations, as well as high alkalinity and temperature levels, which increase the speed with which liquors reach a state of supersaturation. This work examines the action of diethylene triamine penta(methylene phosphonic acid) (DTPMPA), either alone or combined with commercial anti-scaling agents, as an inhibitor of calcium carbonate precipitation in the kraft pulping of *Pinus taeda*. The theoretical amount of calcium deposited in the digester was obtained by mass balance. Soluble calcium was stable throughout cooking when using the phosphonates alone or combined with anti-scaling agents. When adding only DTPMPA, calcium stays in the pulp, rather than forming deposits.

Keywords: *Anti-scaling agents, Pinus taeda, Kraft cooking, Calcium - Phosphonates*

Contact information: [1] *Investigators.* [2] *Directora. Programa de Investigación de Celulosa y Papel - FCEQyN – Universidad Nacional de Misiones - Félix de Azara 1552, (3300) Posadas, Misiones, Argentina. Tel/Fax: 54-3752- 422198. Contact: m_c_area@fceqyn.unam.edu.ar*

INTRODUCTION

Scale formation in the digester during kraft pulping reduces productivity, since it reduces the efficiency of pulping, increases energy costs, and increases the duration of downtime taken for cleaning of equipment (Guo and Severtson 2004). Dissolution of saline compounds in water forms solvated cations and anions. Generally, an increase in water temperature produces an increase in solubility in most salts. Important and noticeable exceptions are $CaCO_3$, $CaSO_4$, and $Mg(OH)_2$, which turn less soluble when temperature increases (Kemmer and McCallion 1993). The main source of calcium is wood, followed by white liquor. The quantity of calcium released in cooking depends principally on the wood species and the quantity of bark entering the system. In the washing of brown pulp, only a 5% reduction of calcium in the pulp is obtained. Carbonate comes from various sources, from the decomposition of lignin-carbohydrate complexes, from the decarboxylation of hemicelluloses during pulping, from black and white alkaline liquors, from the incomplete clarification of liquor, from fresh water, and from the atmosphere (Barata and Candelas 1997). The kraft process, due to its operating conditions of high alkalinity, high temperatures, and high pressures, promotes $CaCO_3$ scaling. As the pH of a solution containing carbonate anion increases above 8, the predominant species in the solution is the carbonate ion (Manji, A., and Kaagiannis, J. 2005). Deposits are produced due to the fact that the saturation limit of $CaCO_3$ is

exceeded in the aqueous medium of the process, due to changes in temperature and pressure (Severtson et al. 1999).

Practically all of the materials present in the process (wood, water, limestone, others) contribute to the formation of deposits. Wood is a source of calcium, potassium, magnesium, silica, manganese, iron, aluminum, and sodium. Limestone possesses calcium, magnesium, strontium, etc. An analysis of the scaling in a white liquor preheater showed deposits containing 13 and 87% inorganic and organic materials, respectively. The inorganic portion included 41% of calcium and magnesium carbonates. Caustic deposits in the pipes contained more than 74% of inorganic materials (Stopka et al. 1987).

Scaling in the kraft pulping processes occurs as a result of the presence of organic ligands (Fader et al. 2005). Lignin fragments formed during pulping (especially those containing phenolic hydroxyls groups) have a high tendency to interact with the calcium, increasing its solubility in the black liquor. As long as the temperature increases, the pH tends to decrease, and the calcium ions are partially displaced from the lignin by the hydrogen ions. Thus, these react with the carbonate ions, resulting in calcium carbonate scaling.

In addition to lignin, different organic species are found that also complex the calcium in the black liquor (Fader et al. 2005). Together with the calcium and carbonate, black liquor normally contains other ions, such as sulfate, which can precipitate and form scale. Scale formation mechanisms of calcium carbonate include nucleation, crystal growth, and the addition of particles, which form the deposit.

For the treatment of pulping and bleaching process streams, the performances of additives in the presence of other dissolved organics are important because these liquors contain extracted wood polymers that can also interact with calcium and carbonate to affect nucleation and crystallization processes (Guo and Severtson 2004).

A study of the behavior of metallic ions in kraft pulping shows that the Mg and Mn concentrations increase continually in the liquors, while Ca concentrations increase to a maximum value and decrease rapidly, probably due to the precipitation of $CaCO_3$ in fibers and on metallic surfaces. Authors have suggested that as temperature increases, the concentration of Ca increases up to the supersaturation level necessary to initiate the precipitation, followed by a rapid fall in the Ca concentration up to its solubility limit. This shows that when the Na_2CO_3 concentration increases in white liquors, the calcium maximum concentration necessary for the precipitation decreases. Moreover, the $CaCO_3$ precipitation is produced even if initially there is no $CaCO_3$ in the white liquor. This is due to the carbonate generated by the uronic acids formed by the decarboxylation of hemicelluloses soluble in water (Guo and Severtson 2002).

Chemical treatments known as antiscalants impede mechanisms that result in the formation of crystalline deposits (Guo and Severtson 2004). Chelants or sequestering agents have been usually used to prevent the deposition, precipitation, and crystallization of calcium carbonate in water systems. Other types of reagents have been studied as threshold inhibition agents. These include water-soluble organic polymers, phosphonates, and polyphosphates. Organic polymer anti-scalants include products derived from acrylamide, maleic acid, vinyl acetate, vinyl alcohol, and acrylic acid. The list also

includes polyarilamines, with phosphonic, carboxylic, or sulfonic groups (Fader et al. 2005).

Guo and Severtson (2003) have described the influence of both molecular and polymeric carboxylic acid containing additives on the nucleation of $CaCO_3$ in solutions representative of process liquors found in the production of wood pulp. Studying aminocarboxylic acids as ethylenediaminetetraacetic acid (EDTA) and diethylene-triaminepentaacetic acid (DTPA), they found that parameters for the fit of nucleation data in the presence of these chelants where the same as those found when no additive was present.

In addition to the apparent requirement of regularly spaced acid groups, the efficacy of a polyacid in inhibiting nucleation and growth of crystalline phases appears strongly dependent on molecular weight (Loy et al 2004).

Polymeric anti-scalants work primarily by one or more of the following three mechanisms: threshold inhibition, crystal dispersion, and crystal modification (Duggirala 2005). Threshold inhibition occurs when an adsorbed anti-scalant blocks the active sites of crystal growth. Crystal dispersion is a mechanism by which agglomeration and growth of microcrystals is avoided by an increase in the surface anionic charge. Crystal modification is produced when the absorbed anti-scalant alters the morphology of the microcrystal in the process of growing, resulting in crystals with irregular shape. These deformed crystals inhibit the growth of a regular crystalline lattice. In all cases, polymers avoid the formation of a layer of adherent scale.

The ability of aminophosphonates to inhibit $CaCO_3$ nucleation and crystal growth kinetics under high temperature and high pH conditions is based on adsorption, as these species are known to adsorb strongly to a wide variety of mineral surfaces including $CaCO_3$ (Guo and Severtson 2004).

This work studied the diethylene triamine penta(methylene phosphonic acid) (DTPMPA) chelant and commercial anti-scaling agents (alone or combined with the chelant), as inhibitors of $CaCO_3$ precipitation. The evolution of the content of total and soluble calcium in the black liquor during cooking was followed. The theoretical calcium deposited in the digester was obtained by mass balance.

MATERIALS AND METHODS

Raw Materials

Pinus taeda chips supplied by Alto Paraná S.A. were screened, accepting the fraction retained on a 5x5 mm screen and the fraction passing through a 25x25mm screen. The bark and the knots were manually discarded. White liquor was prepared using NaOH, $Na_2S.9H_2O$, and Na_2CO_3 (all of analytical grade) to control the quantity of Ca introduced to the system.

The anti-scalant polymers Dequest 9020 (modified polyacrylic acid, sodium salt), Dequest 9030 (sulphonated polyacrylic acid copolymer), and DTPMPA (sodium salt of diethylene triamine penta(methylene phosphonic acid)) in aqueous solution were supplied by Solutia Inc. (St. Louis, Missouri). All products assayed were commercial anti-scaling agents. They were cataloged as: A (Dequest 9020), B (Dequest 9030), C and D (both

sodium acrylate / maleic anhydride copolymer from different manufacturers). The concentration of DTPMPA (diethylene triamine penta(methylene phosphonic acid), Q) tested (2kg/t dry wood, or 0.2 %) is given in terms of active acid. The other products were added according to recommendations of the manufacturers.

Cooking

Kraft cooks were carried out in a 7L MK digester using a condenser for sample taking, with the system under pressure. Before cooking, the digester was washed with acid, circulating a solution of H_2SO_4 (10% v/v) during 10 minutes, and rinsing with deionized water. The cooking conditions were: liquor-wood relationship (5:1), active alkali: 24% OD wood (NaOH basis), sufidity: 35 % (relative to active alkali), maximum temperature: 170ºC, impregnation time: 60 min; H Factor: 2000, and Na_2CO_3: 10g/L.

The time 0 to 70ºC was recorded, and a 20 ml sample was extracted from the digester, corresponding to the beginning of cooking. Every 20 minutes the temperature was recorded, and 20 ml liquor samples were taken in plastic flasks. A complete condenser relief was carried out after each sampling. Ten samples were extracted per cook. Pulps were washed with deionized water.

Pulps were screened by a 0.15 mm slit width screen and they were characterized by viscosity (Tappi T236 om-99) and kappa number (Tappi T230 om-99).

Calcium Monitoring

The method of calcium determination was adapted from the work of Guo and Severtson (2002). For the total calcium determinations, 2mL of samples were transferred to centrifugal tubes, adding 10 ml of an HCI 4% solution, stirring and centrifuging during 15 min at 2900 rpm. The supernatant (a solution of $CaCl_2$), was collected in a 10 ml test tube (acid washing, rinsing, and drying). For the determination of soluble calcium, 5 ml samples were filtered using a nylon mesh (0.45 μm pore), when calcium insoluble salts are retained (such as $CaCO_3$ and $CaSO_4$), passing the soluble Ca into alkali. Over the filtrate, the process was similar to that used for the determination of total calcium. Suspended calcium was obtained through the difference between total calcium and soluble calcium.

Metals in Pulp

For the determination of the Ca, Mg, Fe, Cu, and Mn contents in pulp, 4% HCl was added to a fraction of 5 grams pulp of 2% consistency, during one hour. Subsequently, the pulp was filtered with a Büchner funnel, and the filtrate was analyzed.

Calcium Balance

Calcium concentrations were determined in white liquor, wood, pulp, black liquor, pulp wash-water, and in the acid solution with which the digester was washed. All metals were determined by atomic absorption spectroscopy with a Perkin Elmer Analyst 200 model (Perkin Elmer web page).

Results

Cooking results are presented in Table 1.

Table 1: Results of Cooking With and Without Anti-Scaling Polymers

	Total yield	Screened yield	Rejects	kappa nº	Viscosity
	(%)	(%)	(%)		(cp)
Control*	46.8	46.1	0.68	23.6	32.4
A (0.05 %)	45.6	44.6	0.99	26.4	32.4
B (0.05 %)	45.1	44.9	0.18	24.9	32.2
C (0.012 %)	45.1	44.4	0.65	24.6	31.0
D (0.12 %)	46.3	45.7	0.68	25.6	32.1
D (0.012 %)	46.8	46.0	0.80	26.0	30.5
Q (0.2 %)	46.6	45.5	1.03	23.8	33.0
A (0.05 %) + Q 0.2	46.7	46.2	0.53	24.4	33.0
B (0.05 %) + Q 0.2	46.3	45.8	0.49	27.0	33.4

*Control = Cooking without anti-scaling nor chelant polymer aggregate

It can be appreciated that the presence of A, B and C polymers produced a slight yield loss. The chelant alone did not affect the characteristics of delignification and degradation of pulps, while polymers decreased delignification. C and D polymers produced a viscosity decrease. The main source of calcium entering the system was wood (750 ppm), followed by white liquor (6 ppm). The metal content in pulps is presented in Table 2.

It was observed that polymer D in the 0.012% dosage level did not modify the content of Ca in the pulp, when compared to cooking without additives. When the dose was increased to 0.12%, a reduction in the content of Ca of about 270 ppm was produced, comparable to the reduction produced by polymer C, but with a 0.012% charge (230 ppm). A similar reduction was obtained with polymers A and B (292 and 353 ppm respectively). A significant reduction was obtained when the chelant was added together with polymers A and B (722 and 928 ppm respectively). The polymers analyzed decreased the content of Mg, Fe, and Cu in pulps, as compared with those of the control pulp. On the other hand, Mn levels decreased solely in presence of the chelant. This can be of great importance if there are subsequent bleaching stages with oxygen and hydrogen peroxide.

Table 2: Metal Ion Content in Pulps (Cooking With and Without Anti-Scaling Polymers)

	Ca	Mg	Cu	Fe	Mn
	(ppm)	(ppm)	(ppm)	(ppm)	(ppm)
Control*	1322	329	4.75	20.2	38.4
A (0.05 %)	1030	216	3.53	10.2	45.0
B (0.05 %)	969	214	2.91	10.8	43.1
C (0.012 %)	1089	213	2.55	9.91	47.8
D (0.12 %)	1048	207	1.92	5.23	44.7
D (0.012 %)	1323	139	1.42	14.0	48.7
Q (0.2 %)	1043	426	2.35	5.29	17.0
A (0.05 %) + Q 0.2	600	243	3.58	8.52	14.1
B (0.05 %) + Q 0.2	394	160	n.d.	8.10	15.7

*Control = cooking with and without anti-scalant nor chelant polymers aggregate

Figures 1 and 2 show the evolution over time of total and soluble calcium in the cooking liquors.

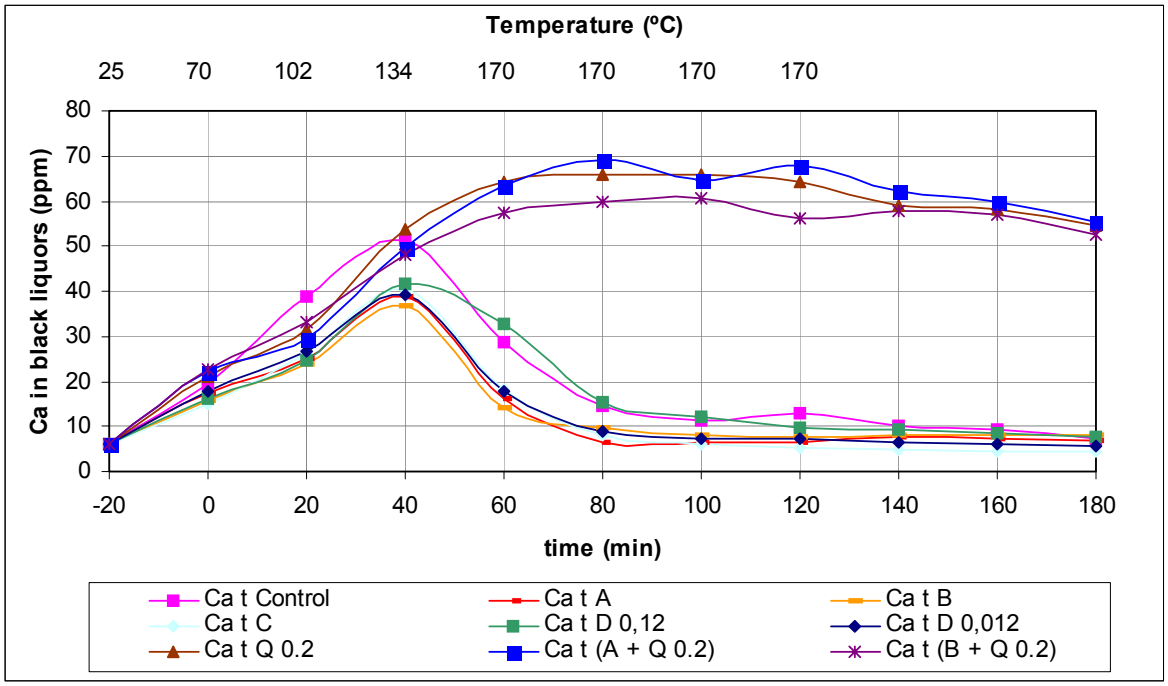

Figure 1: Total calcium content in the samples of black liquors obtained in cookings with DTPMPA and polymers

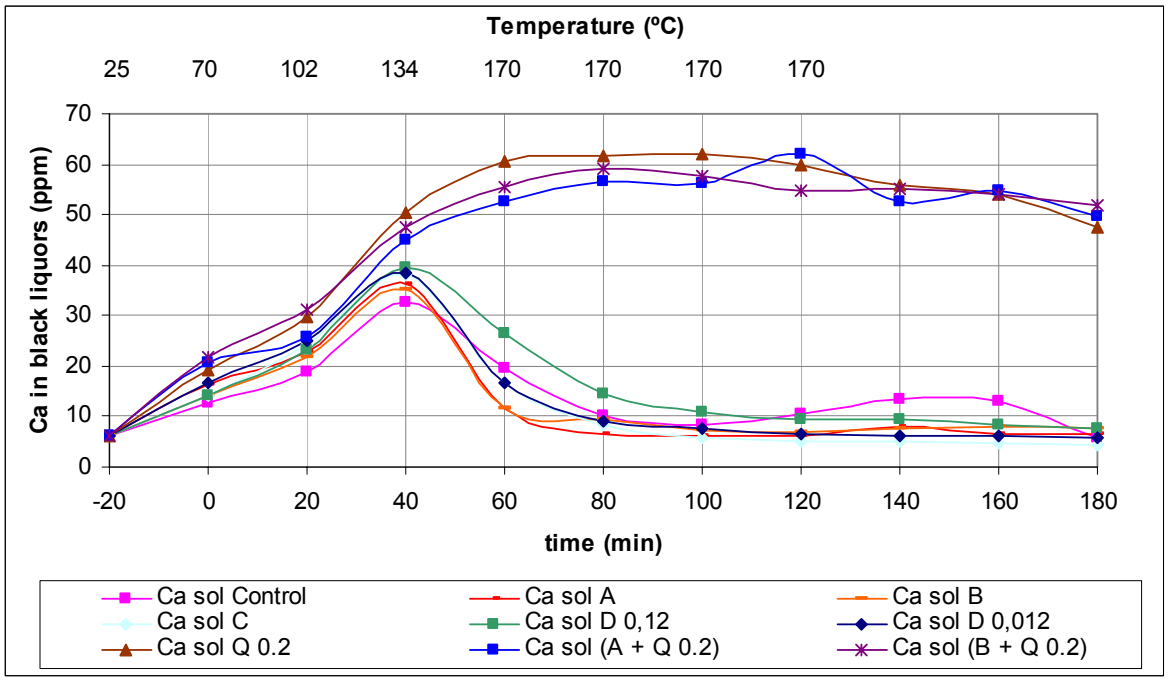

Figure 2: Soluble calcium content in the black liquor samples obtained from cookings with DTPMPA and polymers

Figure 1 shows two different behaviors of the evolution of total calcium in the liquor extracted during cooking. The first group included all the cooks incorporating DTPMPA. In this case, total calcium was observed to increase during the first 60 minutes, and then to remain practically constant, staying in the liquor during the entire process.

Soluble calcium showed similar behavior (Fig. 2), with a difference of approximately 5% in the total calcium (in most cases), which represents the suspended calcium. Curves appear similar to those reported by Severtson (1999) for similar products having comparable concentrations. The behavior of magnesium is presented in Fig. 3.

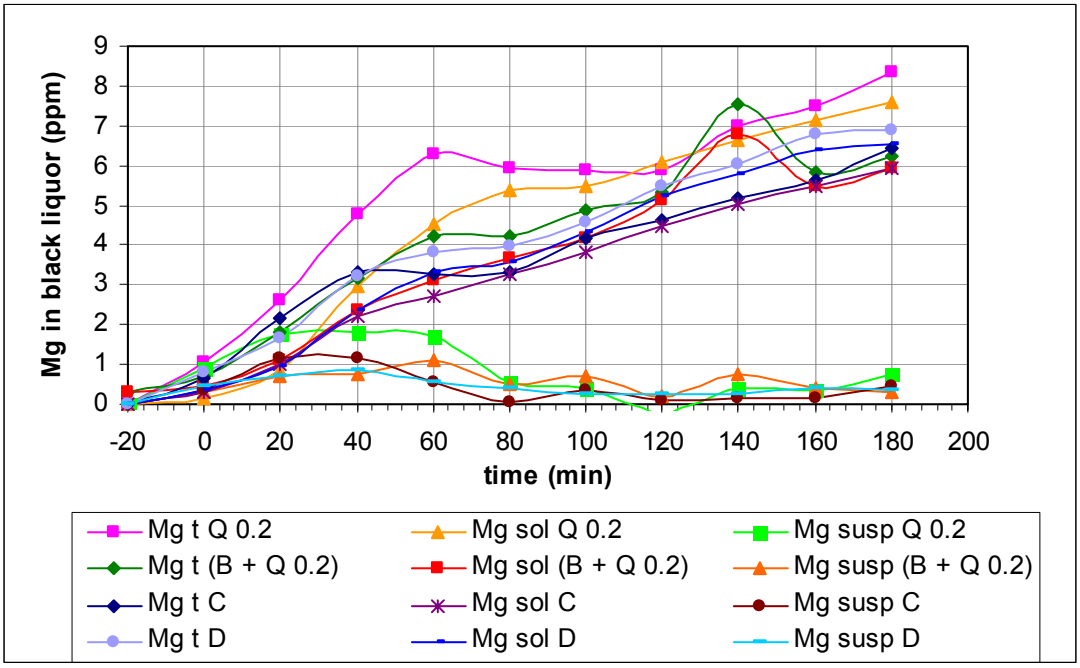

Figure 3: Total, soluble, and suspended magnesium in liquor samples (cookings with DTPMPA and polymers)

The second group comprised the control cooks (without additives) and cooks with the A, B, C, and D polymers. It was observed that total calcium increased, with a maximum after 40 minutes (135ºC). After this point, it decreased until it almost disappeared from the liquor. This behavior can be explained through two hypotheses. Either the calcium re-precipitates onto the chips, or it is deposited onto the walls of the digester. In the latter case, it might be a hard deposit, or rather it might have a soft nature, not forming adherent scaling.

It can be observed that magnesium values were proportionally very low in the liquor samples, and suspended Mg, in a form susceptible of generating scaling, was minimal during the cooking. Figure 4 presents the final concentration of Ca (ppm) in pulps and final black liquors of all cooks.

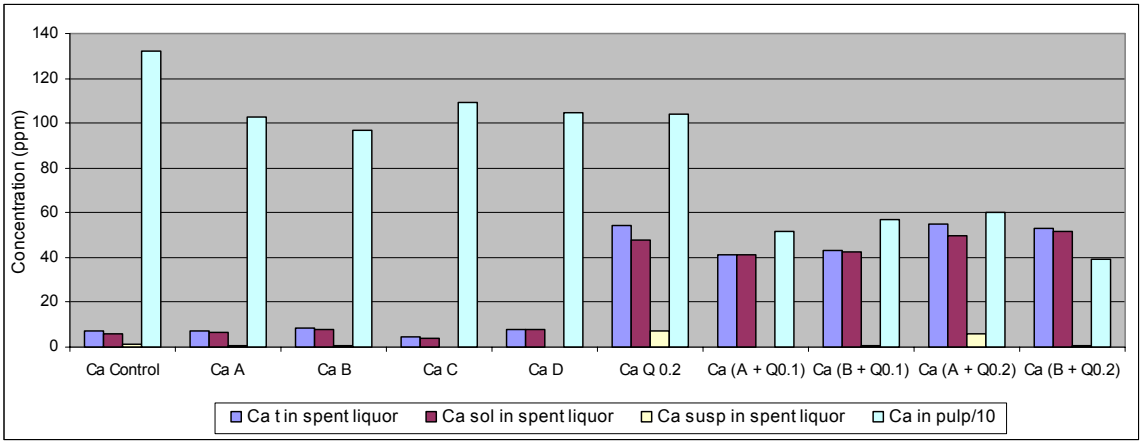

Figure 4: Concentration of Ca (ppm) in pulps and black liquors of all cooks

It can be seen that the chelant alone and the chelant combined with polymers A or B polymers increased the calcium concentration in the final black liquor. The quantity of suspended calcium reached a significant stage with the use of DTPMPA alone and of polymer A with 0.2% of DTPMPA.

Figure 5 shows the mass balance for the total calcium in all cooks. To perform this, the concentration of Ca in the liquor, within and outside of the chips after 180 minutes of cooking was assumed to be similar.

The calcium balance depended on whether the different products were applied alone or combined (Fig. 5). The calcium content of the pulps treated with DTPMPA alone and with all the polymers applied individually was approximately 22% less than the control (except for the case of polymer D at 0.012% concentration). On the other hand, the combination of anti-scaling products with DTPMPA extracted a great quantity of calcium from the pulps, transferring it to the liquor. This effect indicates an important interaction between the polymers and the chelant.

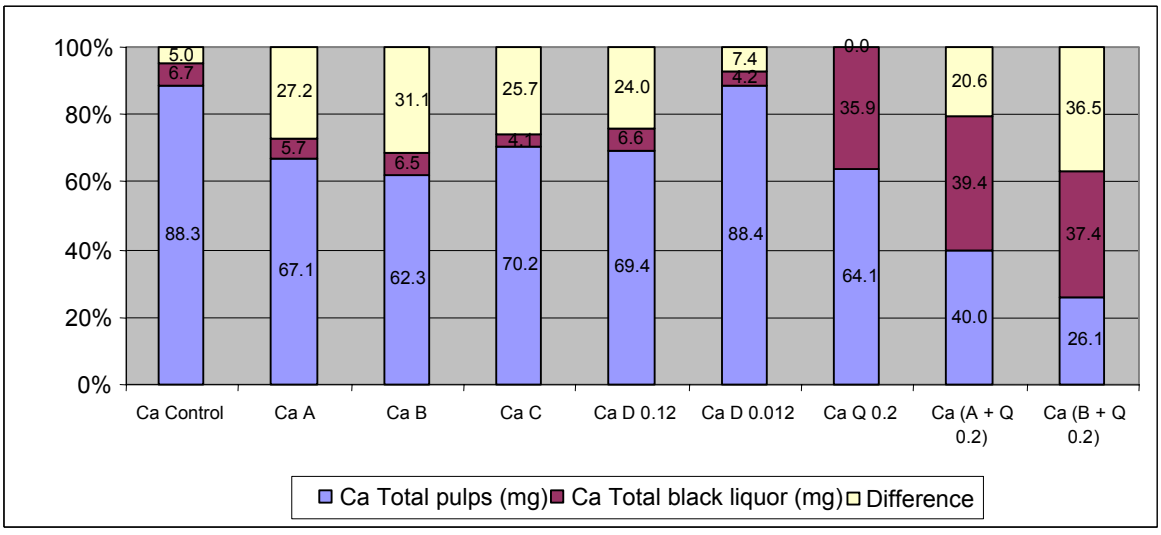

Figure 5: Mass balance for the total calcium in cooking with DTPMPA and anti-scaling polymers

This behavior can produce some practical implications. When DTPMPA is present, a great part of the calcium and also other metallic ions are extracted from the pulps. This is beneficial to the bleaching system, mainly the oxygen stage. Most of the calcium passes then to the recovery system. As the structure of the $CaCO_3$-polymer complex is assumed to be stable, no problems are expected to occur in the evaporators. Theory indicates that phosphonates act as polymers, inhibiting the growth of the crystals through adsorption on the nuclei and the crystals under development (Guo and Severtson 2002). Hence, we can presume that the stability of the $CaCO_3$-DTPMPA particles is similar to that of the $CaCO_3$- polymer.

When DTPMPA alone was added, the non-detected calcium fraction was minimized ("difference" in the pulp or in the liquor). When polymers were combined with DTPMPA, the greatest extraction of calcium from the pulp occurred, indicating an important interaction between both types of additive.

Since a similar behavior was observed in the cases in which polymers were used alone, or were combined with DTPMPA, we tried to identify the destination of the non-detected calcium (difference). To verify the calcium losses in the laboratory washing system, after extracting black liquor, the cooked chips were disintegrated at 6% consistency, filtered, and rewashed twice, at 6 and 2% consistency. Table 3 and Fig. 6 present the mass balance of total calcium in the cooking carried out with 0.012% of anti-scalant polymer D. It should be made clear these results are valid only in our laboratory system. This is because, due to the absence of a blow-tank, the quantity of remaining liquor inside the chips is important.

Table 3: Calcium Balance in Cooking with Anti-Scaling Polymer D (0,012%)

Balance/ kg wood*	mg Ca
Black liquor	14,6
Pulp washing	140,3
Pulp	608,6
Acid washing digester	5,4
Difference	4,1

* Ca Entry = 773 mg (wood: 750 mg; liquor: 24mg)

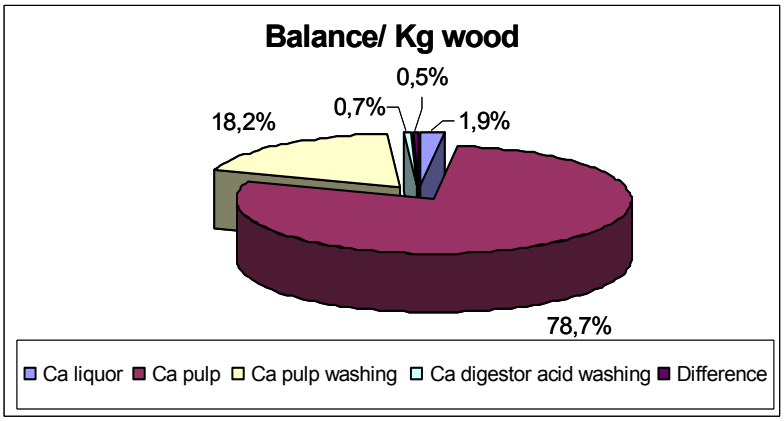

Figure 6. Pie chart of calcium balance in cooking with anti-scaling polymer D (0,012%)

It is clear that in the absence of chelant during the cooking, most of the calcium remains in the pulp. Going back to the hypothesis of disappearance of the liquor calcium (Figures 1 and 2), it is observed that 18% approximately is found on the pulp, and is easily extracted by water washing, whereas a 0.7% was deposited on the walls of the digester (probably, an adherent scaling), being susceptible to extraction solely by acid washing.

Another experiment simulated a system with high calcium content, without pulp. The system comprised black and white liquor and Ca until an initial concentration of 88 ppm. The concentrations of polymer D and chelant (24 and 200 mg/L respectively) were the same ones used in the previous experiences (calculated as if there had been pulp in the system). Samples were extracted every 20 minutes, to evaluate total, soluble and suspended calcium in the liquor. At the end of the experiment, the digester was washed with water and acid. The balance shows the quantification of the total calcium present in the liquor, water and acid (figure 8).

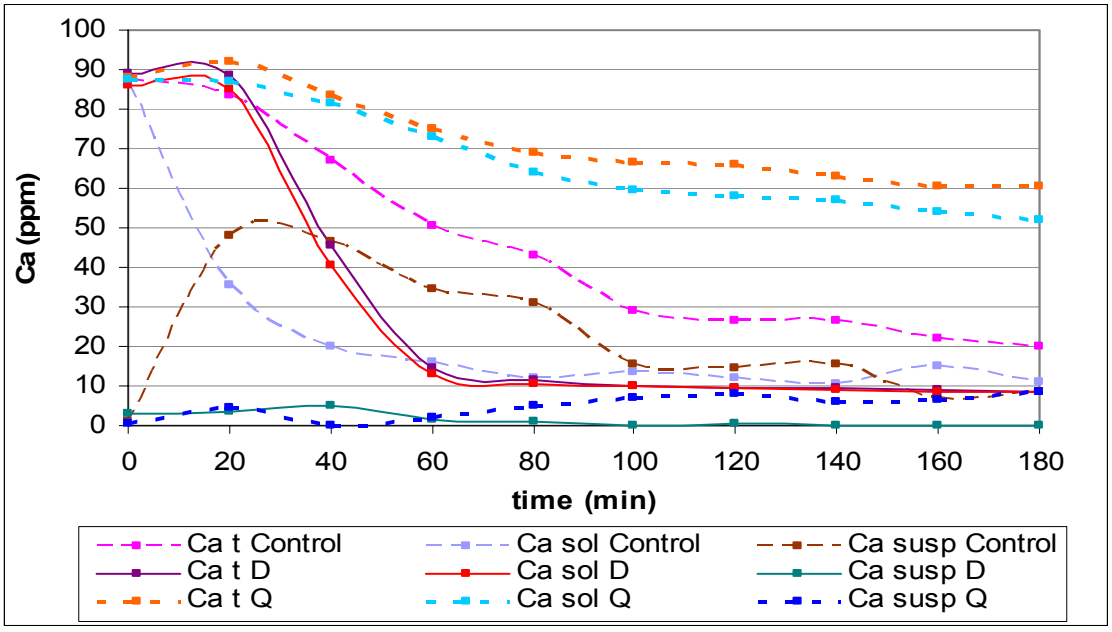

Figure 7. Total, soluble, and suspended calcium in liquor samples (cookings without pulp, with DTPMPA and D polymer)

Total and soluble calcium concentrations decreased in the period between 20 and 60 minutes (maximum temperature). The similarity of the two curves indicates that there was no suspended calcium in the system. A similar behavior, although less intense, was observed in the control experiment, but with an important amount of suspended Ca. In the treatment with chelant, total and soluble calcium decreased at the end of the treatment. The suspended Ca was similar to the control treatment.

Table 4 shows thee Total calcium balance at the end of the experiences.

Table 4: Calcium Balance in the Simulated Experiment with Anti-Scaling Polymer D (24 mg/L) and chelant (200 mg/L)

Balance/ kg wood*	Control (% Ca)	Polymer (% Ca)	Chelant (% Ca)
Black liquor	52,7	15,9	73,3
Water washing	21,2	6,0	11,8
Acid washing digester	26,0	78,1	14,9

* Ca Entry = 88 mg/L

It is clear that chelant maintained calcium in the liquor phase, while polymer D resulted in deposition on the digester walls.

CONCLUSIONS

1. Using laboratory techniques, the operation of anti-scaling products can be evaluated. However, other methodology is required to determine the nature of the suspended calcium and its participation in the cumulative process leading to the formation of a layer of adherent scale.

2. Diethylene triamine penta(methylene phosphonic acid) (DTPMPA) acts also as anti-scaling agent in a way similar to that of polymers.

3. Without additives (control), most of the calcium remained in the pulp, in a way similar to that in the presence of polymers or with DTPMPA alone, however at a lower proportion.

4. In cooking without additives (control) and with polymers alone, it was observed that total calcium in the liquor increased up to a temperature of 135ºC (where supersaturation occurs) and then decreased (due to the precipitation of $CaCO_3$), keeping at very low concentrations during the rest of the process. Soluble calcium showed a similar behavior, with an approximate difference of 5% in most of the cases (attributed to suspended calcium).

5. When polymers were combined with DTPMPA, an important interaction was observed, increasing noticeably the quantity of calcium extracted from the pulps. Final pulps presented no differences in yield and viscosity with respect to the control.

6. When using the phosphonate alone or combined with the anti-scaling agents studied, soluble calcium remained stable during the pulping. This could allow us to suppose that the highest Ca concentration in black liquor going to evaporation will not produce scaling in the system. On the other hand, the reduction of Ca content in the pulp could reduce the calcium oxalate deposits in subsequent stages of pulp bleaching.

7. The quantity of calcium suspended in the liquor became significant only with the use of DTPMPA alone or polymer A with 0.2% DTPMPA.

ACKNOWLEDGEMENTS

The authors wish to acknowledge Ind. Chemist Isabel C. Silva and Pablo Pezzano from Solutia Inc., as well as Dr. Alberto Venica and Alto Paraná S.A. The technical team was represented by Ing. Julieta Benítez. Chem Eng. Students included Mirta Morrone and Cristian Alfonso.

This article first appeared in the procedings of the 4th Congreso Iberoamericano de Investigación en Celulosa y Papel, CIADICYP-2006, which was held in Santiago and Valdivia, Chile between October 23 and 27, 2006. By agreement with the organizers, selected articles from the conference were submitted to *BioResources*, subject to the usual peer-review process.

REFERENCES CITED

Barata, P. A., and Candelas, C. F. (1997). "Calcium and magnesium balance in an unbleached fibre line: A mill case," *Appita J.* 50(6), 505-508.

Duggirala, P. Y. (2005). "Formation of calcium carbonate scale and control strategies in continuous digesters", CD del II Coloquio Internacional sobre Celulosa de Eucalipto, Concepción, Chile, Mayo.

Fader, M. K., Nguyen, D. T., Wang, X. H., Zhang, F., and Ling; T-F. (2002). "Methods of preventing scaling kraft involving inorganic compositions, and inorganic compositions therefore" *United States, HERCULES INCORPORATED 20020071783*, Url: http://www.freepatentsonline.com/20020071783.html (Consulted: 22/02/2005).

Guo J., and Severtson S. J. (2002). "Influence of organic additives on calcium carbonate precipitation during kraft pulping," *Tappi J*. 1(8), 21-27.

Guo J., and Severtson, S. J., (2003). "Application of classical nucleation theory to characterize the influence of carboxilate-containing additives on $CaCO_3$ nucleation at high temperature, pH, and ionic strength" *Ind. Eng. Chem. Res*. 42, 3480-3486.

Guo J., and Severtson, S. J., (2004). "Inhibition of calcium carbonate nucleation with aminophosphonates at high temperature, pH and ionic strength," *Ind. Eng. Chem. Res.* 43, 5411-5417.

Kemmer, F. N., and McCallion, J. (1992). *Manual del Agua. Su Naturaleza, Tratamiento y Aplicaciones*. Nalco Chemical Company. Tomo I. (ed.) McGraw-Hill. Capítulo 3, 4-5.

Loy, J. E., Guo, J., and Severtson, S. J. (2004). "Role of adsorption fractionation in determining the $CaCO_3$ scale inhibition performance of polydisperse sodium polyacrylate" *Ing. Eng. Chem*. 43, 1882 – 1887.

Manji, A., and Kaagiannis, J. (2005). "Inorganic scale buildup in a bleach plant-a mill study," *Tappi J.* 4(11), 29-32.

Perkin Elmer, Inc., AAnalyst 200, Url: http://las.perkinelmer.com/Catalog/FamilyPage.htm?CategoryID=AAnalyst+200+Spectrometer+Family. (Consulted: 17/04/2007).

Severtson, S. J., Duggirala, P. Y., Carter, P. W., and Reed, P.E. (1999). "Mechanism and chemical control of $CaCO_3$ scaling in the kraft process" *Tappi J.* 82(6), 167-174.

Stopka, F., Kmet, L., and Gasparec, P. (1987). "Undesirable elements and deposits in a kraft pulp mill," *Papir Celuloza* 42(10), 241-244, 255.

Article submitted to journal: March 8, 2007; April 7, 2007; Revised version received: May 2, 2007; Accepted: May 2, 2007; Published May 4, 2007.

CHEMICAL COMPOSITION AND CONTENT OF ESSENTIAL OIL FROM THE BUD OF CULTIVATED TURKISH CLOVE (*Syzygium aromaticum* L.)

M. Hakkı Alma,[a*] Murat Ertaş,[a] Siegfrie Nitz,[b] and Hubert Kollmannsberger[b]

In this study, clove bud oil, which was cultivated in the Mediterranean region of Turkey, was provided from a private essential oil company in Turkey. Essential oil from clove (*Syzygium aromaticum* L.) was obtained from steam-distillation method, and its chemical composition was analyzed by GC and GC-MS. The results showed that the essential oils mainly contained about 87.00% eugenol, 8.01% eugenyl acetate and 3.56% *β*-Caryophyllene. The chemical composition of the Turkish clove bud oil was comparable to those of trees naturally grown in their native regions.

Keywords: Syzygium aromaticum, Turkish Clove, Essential oil, Eugenol, Chemical composition

*Contact information: a: Department of Industrial Engineering of Forest, University of Kahramanmaras Sutcu Imam, 46100 Kahramanmaras, Turkey; b: Lehrstuhl für Chemisch-Technische Analyse und Chemische Lebensmitteltechnologie, Technische Universität München, 85350 Freising-Weihenstephan, Germany; *Corresponding author: alma@ksu.edu.tr*

INTRODUCTION

Essential oils of plants and their other products from secondary metabolism have had a great usage in folk medicine, food flavoring, fragrance, and pharmaceutical industries (Alma et al. 2004; Satil et al. 2003; Kusmenoglu et al. 1995; Dıgrak et al. 1999)

Cloves (*Syzygium aromaticum* L.) are the aromatic dried flower buds of a tree in the family *Myrtaceae.* The clove tree is an evergreen which grows to a height ranging from 10-20 m, having large oval leaves and crimson flowers in numerous groups of terminal clusters. The flower buds are at first of a pale color and gradually become green, after which they develop into a bright red, when they are ready for collecting. Cloves are harvested when 1.5-2 cm long, and consist of a long calyx, terminating in four spreading sepals, and four unopened petals which form a small ball in the centre (Kim et al. 1998).

Clove is native to Indonesia and used as a spice in virtually all of the world's cuisine. The name derives from French *clou*, a nail, as the buds vaguely resemble small irregular nails in shape. Cloves are harvested primarily in Indonesia and Madagascar; it is also grown in Zanzibar, India, Sri Lanka, and the "Spice Islands" (Moluccas, Indonesia known as the Bandas Islands). Cloves can be used in cooking, either whole or in a ground form, but as they are extremely strong, they are used sparingly. The spice is used throughout Europe and Asia and is smoked in cigarettes (also known as kreteks) in Indonesia and in occasional coffee bars in the West, mixed with marijuana to create marijuana spliffs. Cloves are also an important incense material in Chinese and Japanese culture. Clove essential oil is used in aromatherapy, and oil of cloves is widely used to treat toothache in dental emergencies (Kim et al. 1998).

It was reported that *Syzygium aromaticum* have been successfully used for asthma and various allergic disorders by oral administration (Kim et al. 1998).

The essential oil of cloves has anesthetic and antimicrobial qualities and is sometimes used to eliminate bad breath or to ameliorate the pain of a bad tooth. Sesquiterpenes, found in clove, were investigated as potential anticarcinogenic agents (Zheng et al. 1992).

The whole essential oil or its main component eugenol ($C_{10}H_{12}O_2$; 4-allyl-2-methoxy phenol), is used by dentists to calm the nerve inside a tooth after the removal of deep decay, and is the characteristic odor of a dentist's office. When mixed with zinc oxide, eugenol forms a cement used in dentistry (Lee and Shibamoto 2001). Clove oil is used in the traditional blend of choji (1% clove oil in mineral oil) and is applied to Japanese sword blades to prevent tarnishing of the polished surface (Cai and Wu 1996; Baytop 1999). Also, eugenol derivatives or methoxyphenol derivatives in wider classification are used in perfumery and flavoring. They are used in formulating insect attractants and UV absorbers, analgesics, biocides and antiseptics. They are also used in manufacturing stabilizers and antioxidants for plastics and rubbers (Lee and Shibamoto 2001).

Three essential oils are available from clove species: clove bud oil, clove stem oil, and clove leaf oil. Each has different chemical composition and flavour. Clove bud oil, the most expensive and the best quality product, contains eugenol (80-90%), eugenol acetate (15%), and beta caryophyllene (5-12%). It is well known that the amounts of secondary compounds like essential oils are affected by genetic factors, climate, soil and cultivation techniques (Pitarevic et al. 1985; Verzar-Petri et al. 1985; Arslan et al. 2004).

More recently, the clove species has been started to be cultivated in the Mediterranean part of Turkey. So far, no study has been done on the chemical composition of clove cultivated in Turkey. Therefore, in this study it was aimed at determining the chemical composition of the clove cultivated in Turkey.

EXPERIMENTAL

Preparation of Essential Oil

In this study, Clove bud essential oil was provided from a private plant (the so-called "OZDROG") in Hatay province, located in the southern of Turkey. The essential oil of clove, cultivated in Antalya province of Turkey, was obtained by a steam-distillation method by using an industrial type distiller for 3 h. The essential oil was dried over anhydrous sodium sulfate (Na_2SO_4) and stored at -18 ºC.

Chemical Analysis

Qualification of the essential oil (11.5 mg) diluted in diethyl ether (Et_2O) (1 mL) was analyzed on a Finnigan- MAT 8200 Mass Spectrometer coupled with a Hewlett-Packard GC- 5890II series GC by using An SE-54 fused silica capillary column (30 m x 0.25 mm i.d.; 0.25 μm film thickness). Helium (He), having a flow rate of 1.15 mL/min, was used as carrier gas. The GC oven temperature was kept at 60 °C for 5 min and programmed to 260 °C at a rate of 2 °C/min and then kept at 260 °C. The injector temperature was 250 °C. The amount of injection was 1 μL. The carrier gas was delivered at a constant pressure of 5 kg/cm^2. MS spectra were taken at El ion source of 70 eV. The split ratio was 1:5. Retention indices for all the components were determined according to the Van Den Dool method (Dool and Kratz 1963), using *n-alkanes* as standard. Identification of the components was based on comparison of their mass spectra

with those of internal (computer) library, NIST libraries and some reference compounds, and those described by Adams (1995).

Quantification of the essential oil was conducted by gas chromatography with a flame ionization detector (GC-FID) on a Hewlett-Packard GC-589011 series GC. A 1 μL aliquot of oil was injected into the same column under the same GC conditions as described for the GC-MS study. However, the split ratio was 1:14.

RESULTS AND DISCUSSION

Table 1 represents the chemical composition of the essential oil from the bud of clove (*Syzygium aromaticum*). As can be seen from this table, 18 compounds, representing about 99.95% of the essential oil from clove, were characterized. The major components are as follows: eugenol (87.00%), eugenyl acetate (8.01%) and *β*-Caryophyllene (3.56%).

A typical gas chromatogram of Turkish clove buds is shown in Fig. 1.

Table 1. Chemical Composition of the Essential Oil from Turkish Clove Buds

Compounds	RI	%
2-Heptanone	889	0.04
α-Pinene	921	0.01
p-Cymene	1023	Tr*
Limonene+1,8 Cineole	1029	0.01
2-Heptyl acetate	1046	0.04
(E)-*β*-Ocimene	1051	0.33
2-Nonanone	1092	0.02
Linalool	1098	0.01
Methyl salicylate	1189	0.07
p-Allyl phenol	1260	0.19
Eugenol	1361	87.00
α-Copaene	1372	0.10
β-Caryophyllene	1412	3.56
α-Humulene	1446	0.40
Δ-Cadinene	1518	0.04
Eugenyl acetate	1526	8.01
Caryophyllene oxide	1573	0.10
2(12),6(13)-Caryophyllen-dien-5-ol	1627	0.02

*Tr < 0.01

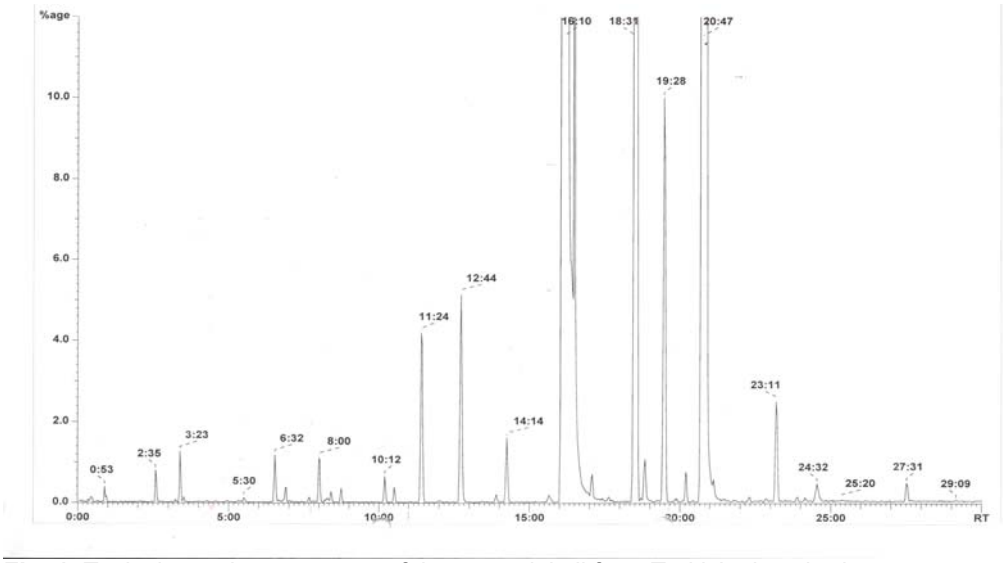

Fig. 1. Typical gas chromatogram of the essential oil from Turkish clove buds.

In previous studies, the essential oil contents of clove (*Syzygium aromaticum*) were reported by Tomaino et al. (2005); Lee and Shibamoto (2001) and Porta et al. (1998) as eugenol (82.6%); eugenol (89.2%), eugenyl acetate (8.6 %); and eugenol (77.4%), eugenyl acetate (19.5%) and caryophyllene (2.01%), respectively. Our results were between the lowest and the highest values reported.

CONCLUSIONS

The chemical composition of clove bud oil provided from private Turkish company in Turkey was investigated. Essential oil from clove (*Syzygium aromaticum* L.), cultivated in the Mediterranean region of Turkey, was obtained from steam-distillation method, and its chemical composition was determined by GC and GC-MS. The findings indicated that the essential oils mainly had about 87.00% eugenol, 8.01% eugenyl acetate and 3.56% *β*-Caryophyllene. The chemical composition of the Turkish clove bud oil was found to be comparable to those from clove trees naturally grown in its native regions.

REFERENCES CITED

Adams, R. (1995). *Identification of Essential Oil Components by Gas Chromatography/Mass Spectroscopy*, Allured Publishing Co., Carol Stream, Illinois, USA.

Alma, M. H., Nitz, S., Kollmannsberger, H., Dığrak, M., Efe, F. T. and Yılmaz, N. (2004). "Chemical Composition and Antimicrobial activity of the essential oils from the gum of Turkish Pistachio (*Pistacia vera* L.)," *J. Agric. Food Chem.* 52, 3911-3914.

Arslan, N., Gürbüz, B. and Sarıhan, E. O. (2004). "Variation in essential oil content and composition in Turkish anise (*Pimpinella anisum L.*) populations," *Turk. J. Agric. For.* 28, 173-177.

Baytop, T. (1999). "*Therapy with medicinal plants in Turkey (Past and Present)*," No. 3255, 2nd ed., Istanbul Publications of the Istanbul University, Istanbul.

Cai, L., and Wu, C. D. (1996). "Compounds from *Syzygium aromaticum* possessing growth inhibitory activity against oral pathogens," *Journal of Natural Products*. 59, 987–990.

Dığrak, M., Alma, M. H., and İlçim, A. (1999). "Antibacterial and antifungal effects of various commercial plant extracts," *Pharm*. *Biol*. 37, 216-220.

Dool, V. D., and Kratz, P. D. (1963). "A generalization of the retention index system including linear temperature programmed gas-liquid partition chromatography," *J. Chromatogr*. 11, 463-471.

Kim, H. M., Lee, E. H., Hong, S. H., Song, H. J., Shin, M. K., Kim, S. H., and Shin, T. Y. (1998). "Effect of *Syzygium aromaticum* extract on immediate hypersensitivity in rats," *Journal of Ethnopharmacology* 60, 125–131.

Kusmenoglu, S., Baser, K. H. C., and Ozek, T. (1995). "Constituents of the essential oil from the hulls of *Pistacia vera L*.," *J. Essent*. *Oil Res*. 7, 441-442.

Lee, K. G., and Shibamoto, T. (2001). "Antioxidant property of aroma extract isolated from clove buds [*Syzygium aromaticum (L.) Merr. Et Perry*]," *Food Chemistry*. 74, 443–448.

Pitarevic, I., Kustrak, D., Kuftinec, J., and Blazevic, N. (1985). "Influence of ecological factors on the content and composition of the essential oil in *Salvia officinalis*," In: *Proceedings of the 15th International Symposium on Essential Oils*, Svendsen, A. B. and Scheffer, J. J. C. (eds.). Martinus Nijhoff/Dr W. Junk Publishers, Boston, 199-202.

Porta, G. D., Taddeo, R., D'Urso, E., and Reverchon, E. (1998). "Isolation of clove bud and star anise essential oil by supercritical CO_2 extraction," *Lebensm.-Wiss. u.-Technol.* 31, 454-460.

Satil, F., Azcan, N., and Baser, K. H. C. (2003). "Fatty acid composition of Pistachio nuts in Turkey," *Chem*. *Nat*. *Comput*. 39, 322-324.

Tomaino, A., Cimino, F., Zimbalatti, V., Venuti, V., Sulfaro, V., De Pasquale, A., and Saija, A. (2005). "Influence of heating on antioxidant activity and the chemical composition of some spice essential oils," *Food Chemistry*. 89, 549-554.

Verzar-Petri, G., Then, M., and Meszaros, S. (1985). "Formation of essential oil in clary sage under different conditions," In: *Proceedings of the 15th International Symposium on Essential Oils*, Svendsen, A. B. and Scheffer, J. J. C. (eds.). Martinus Nijhoff/Dr W. Junk Publishers, Boston, 19-21.

Zheng, G. Q., Kenny, P. M., and Lam, K. T. (1992). "Sesquiterpenes from clove (*Eugenia caryophyllata*) as potential anticarcinogenic agents," *Journal of Natural Products* 55, 999–1003.

Article submitted: January 16, 2007; First round of reviewing completed: February 12, 2007; Revised version received: May 17, 2007; Article accepted: May 17, 2007; Article published: May 23, 2007.

CHARACTERIZATION OF A NOVOLAC RESIN SUBSTITUTING PHENOL BY AMMONIUM LIGNOSULFONATE AS FILLER OR EXTENDER

Juan Manuel Pérez[a], Francisco Rodríguez[a], M. Virginia Alonso[a], Mercedes Oliet[a,*], and Juan M. Echeverría[b]

In this work two types of lignin-novolac resins have been formulated, partially substituting phenol by softwood ammonium lignosulfonate as filler or extender (methylolated) to study the viability of that substitution when resins will be employed as adhesives in textile felts. A commercial novolac resin was used as reference. Free phenol, free formaldehyde, water content, softening point, and flow distance values were determined in all cases to verify whether the material fulfills specifications. In addition, FTIR and NMR spectroscopic techniques were employed for the characterization of three resins samples tested to discuss their structural differences and similarities. The results obtained have shown that the substitution proposed is feasible from the point of view of the resins synthesis to get the pre-polymer.

Keywords: Phenolic Resins, Ammonium Lignosulfonate, Methylolation, Synthesis

*Contact information: a: Departamento de Ingeniería Química, Facultad de Ciencias Químicas, Universidad Complutense de Madrid, Avda. Complutense s/n. 28040 Madrid. Spain; b: Hexion Speciality Chemicals Ibérica S.A.,Ctra. a Navarra, Epele 39, 20120 Hernani, Spain; *Corresponding author: moliet@quim.ucm.es*

INTRODUCTION

There are two types of phenolic resins: resol and novolac. The first one is synthesized under basic pH conditions with excess of formaldehyde, and the latter is carried out at acidic pH (with an excess of phenol). They are widely used in industry because of their chemical resistance, electrical insulation, and dimensional stability (Gardziella et al. 2000). There are some published works involving lignin-resol resins (Kou et al. 1991; Vázquez et al. 1997; Danielson et al. 1998; Alonso et al. 2001), fewer employing lignin-novolac for different applications (El-Saied et al. 1984; Ysbrandy et al. 1992), but there has not been any work involving lignin-novolac combinations for textile-felts applications, which is the focus of the present paper. Phenolic resin-bonded textile felts can be considered to be fiber-reinforced plastic with a high level of fibers. These fibers are derived from textile scraps recycled from the textile industry.

Due to the increase of phenol cost, researchers have been working to partially substitute this monomer by natural polymers that present similar structure in the resin without modification of resin properties (Gardziella et al. 2000). One of these possible substitutes, among other natural compounds, is lignin, a polydisperse natural polymer constituted mainly of phenyl propane units, which present a structure close to that of phenolic resin (Forss et al. 1979).

Lignin is a by-product of the pulp and paper industry that can be present in many different forms. The choice of the type of lignin to incorporate into resin synthesis has been based on cost and availability (Alonso et al. 2001). The kraft process consumes most of the lignin in the process of recovering the reagents used in pulping. Organosolv lignins are not available in great amounts. So, the best possible substitutes of phenol by lignin-derived chemicals at an industrial scale are the lignosulfonates, which are obtained from the sulphite process. Among the different types of lignosulfonate, the ammonium lignosulfonate is the most suitable to substitute phenol, because final properties of phenolic resins are better (Calvé et al. 1988; Allan et al. 1989). In a previous work it has been verified that the lignosulfonate that better adapts as copolymer in the formulation of resol type phenolic resins was the ammonic type from coniferous wood (Alonso et al. 2001). The results of that study make it possible to deduce that this type of lignin also can be useful for novolac resins. In addition, ammonium ion is used as an intermediate in the first stage of the curing reaction of the formulated resin, which favors this process (Zhang et al. 1997).

Lignosulfonates are not very reactive with phenol and formaldehyde; hence it is also usual to modify their structure. The most common ways of lignin modification are methylolation (Dolenko et al. 1978; Peng et al. 1994; Alonso et al. 2001) and phenolation (Nada et al. 1987; Alonso et al. 2005). Both processes are able to activate lignin, but phenolation is less studied because of the high cost of this process. On the other hand, methylolation does not need an expensive installation.

Novolac oligomers are prepared in acidic media, using an excess of phenol over formaldehyde. The mechanism associated with this reaction can be described in four steps. First, a methylene glycol is protonated by an acid from the reaction medium, which then releases water to form a hydroxymethylene carbonium ion. This ion acts as a hydroxyalkylating agent by reacting with phenol via electrophilic aromatic substitution. A pair of electrons from the benzene ring attacks the electrophile, forming a carbocation intermediate, followed by deprotonation and a regain of aromaticity. The methylol group of the hydroxymethylated phenol is unstable under acidic conditions and loses water readily to form a benzylic carbonium ion. This ion then reacts with another phenol to form a methylene bridge in another electrophilic aromatic substitution in the *ortho* and *para* positions. This major process repeats itself until the formaldehyde is exhausted (Knop and Pilato 1985). These pre-polymers are thermally stable and can be stored effectively. Novolac crosslinking is usually achieved by introducing a source of methylene groups to form additional methylene bridges between aromatic rings. Hexamethylenetetramine (HMTA) is the most widely used curing agent (source of formaldehyde) for these reactions.

The reaction mechanism associated with the formulation of lignin-novolac is similar to that of the conventional approaches previously described. Considering the particular case of the lignosulfonates employed in this work, the α-carbon of the lateral chain of the phenyl-propane units is occupied by the sulfonate group. Lignosulfonates may be reacting by itself or with phenol adding to the β-carbon of the lateral chain. The proposed mechanism for the reaction among the lignosulfonate with phenol and formaldehyde in acid medium is exhibited in Fig. 1 (Dos Santos, 1996). The first step consists of the condensation between lignin fragments and the phenol present with

formaldehyde. After that, in a second step, vacuum distillation is employed to adjust the content of free phenol in accordance with the required specifications for textile felt applications. The addition of a curing agent (HMTA) with methylene groups is also necessary for the crosslinking.

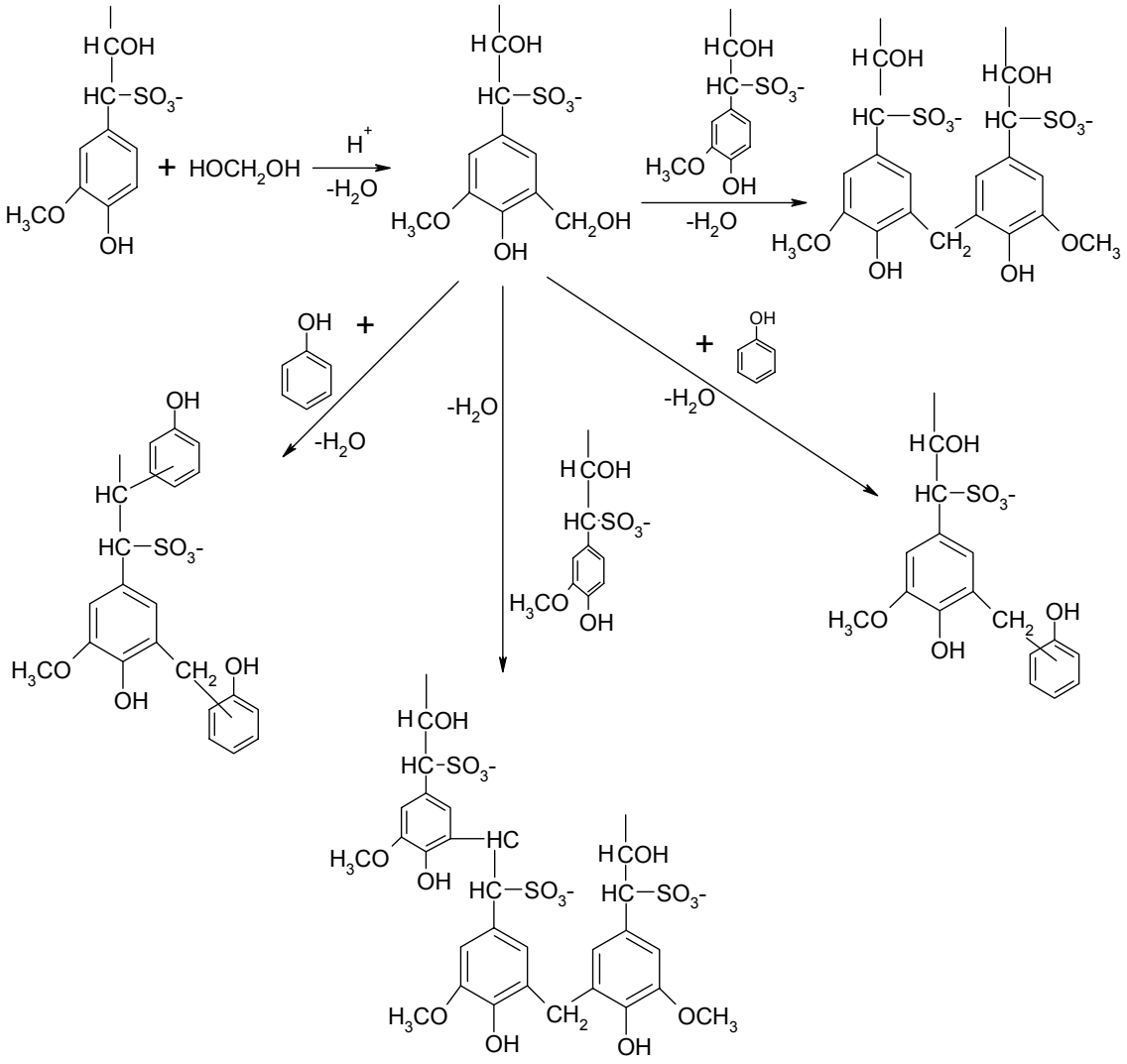

Figure 1. Mechanism of lignin-novolac resins synthesis substituted with lignosulfonates

In this work, two types of lignin-novolac resins were synthesized in the laboratory and compared with a commercial novolac. One lignin-novolac resin was formulated incorporating softwood ammonium lignosulfonate directly, as filler, and the other one incorporated ammonium lignosulfonate modified by methylolation. Formulated resins were characterized in terms of free phenol, free formaldehyde and water contents, softening point, and flow distance to compare with properties of commercial resin. The structural differences among resins were established spectroscopically by Fourier Transform Infra-Red (FTIR) spectroscopy and ^{1}H and ^{13}C Nuclear Magnetic Resonance

(NMR) techniques. The aim of this work was to study whether the partial substitution of phenol by lignin is feasible, attending to their chemical structure and the specifications for the final applications.

EXPERIMENTAL

Materials

Commercial novolac resin and hexamethylenetetramine were supplied by Hexion Speciality Chemicals Ibérica, S.A. The softwood ammonium lignosulfonate used was supplied by Borregaard Deutschland as Borresperse AM 320. This product resembles a spray-dried powder containing 80 wt% of lignosulfonate, 6% of ash, 4.22% of moisture, and 1.93% of phenolic hydroxyl groups. Lignin-novolac resins were synthesized by using commercial grades of phenol, formaldehyde, and oxalic acid.

Procedure

A commercial novolac resin (PF) was tested in this study as reference material. This product is obtained by the polymerization between formaldehyde and phenol in acidic medium. Lignin-novolac (LN) was formulated in the laboratory, substituting phenol by lignosulfonate at the beginning of the pre-polymer synthesis (Fig. 1). Methylolated lignin-novolac (MLN) resin was synthesized under the same operating conditions as LN resin, but using lignosulfonate modified by methylolation. The details of this modification were reported in a previous article (Alonso et al. 2001). The substitution of phenol by ammonium lignosulfonate has been 30 wt% in both samples, because of higher amounts do not produce suitable resins (Ysbrandy et al. 1992; Kharade et al. 1998). The phenol/lignosulfonate (P/L) and phenol- lignosulfonate/formaldehyde (PL/F) molar ratios were 1/0.27 and 1/0.76, respectively.

The resins syntheses (LN and MLN) were carried out in a laboratory glass reactor (2 l) equipped with a stirrer, thermometer, and reflux condenser (Fig. 2.a), and were accomplished in four stages. First was the addition step, where lignosulfonate (modified or non-modified), phenol, and oxalic acid (0.5 wt% in relation to phenol) were dissolved and heated up to a temperature of 100 ºC. Then, the formaldehyde (37 wt%) was added, with heating continued during 90 min. Second, the condensation reaction took place for 90 min (Fig. 2.a.). After the second stage, the installation was changed by a distillation system, as shown in Fig. 2.b. The water was removed by atmospheric pressure distillation followed by vacuum distillation to remove most of phenol and water. Finally, the resin was washed with distillated water to remove the phenol and achieve the required specifications.

Pre-Polymers Analysis

The parameters analyzed in the formulated samples were free phenol, free formaldehyde, water content, softening point, and flow distance. The values for these parameters must be in agreement with commercial resin specifications.

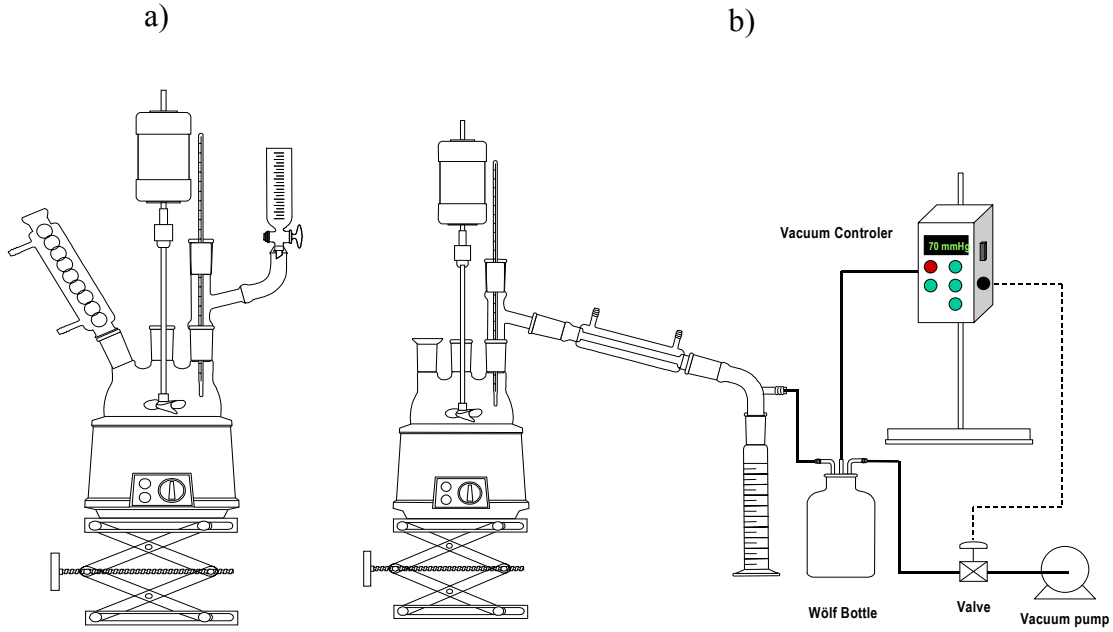

Figure 2. Scheme of experimental set-up of resins synthesis. a) Formaldehyde addition and reaction condensation; b) Atmospheric and vacuum distillations

Free phenol (P_f) was determined by gas chromatography, using a Varian 3400 chromatograph with a flame ionization detector (FID) and helium as carrier gas. An HP-INNOWax (crosslinked polyethylene glycol) high-performance capillary column of 0.2 μm film thickness, 50 m length, and 0.2 mm internal diameter was used. The internal standard employed was *p*-cresol, which was added to the methanol dissolved samples.

Free formaldehyde (F_f) was analyzed by the hydroxylamine hydrochloride method with endpoint titration (ISO 9397) by using a METTLER TOLEDO titrator DL-50. Free formaldehyde was also analyzed in the methylolated lignosulfonate in order to determinate its conversion in the reaction and formulation of prepolymer.

The resin or methylolated lignosulfonate (1 g) was dissolved in 60 mL of an isopropanol–water mixture (2:1, v/v); hydrochloric acid was added until the pH was between 2 and 3. Then, 0.1 N sodium hydroxide was used to adjust the pH to 3.5. Finally, 10 mL of the 10% hydroxylamine–hydrochloride solution was added. After 10 min, the solution was retitrated with 0.1 N sodium hydroxide up to pH = 3.5.

Water content (W_f) was determined according to DIN 51 777.1 and DIN 53 715 by using a Karl-Fischer Titrator (DL-31 Mettler-Toledo).

Softening point (SP) was performed in a Mettler-Toledo FP-900 with a FP83 measurement cell according to DIN 51920.

Flow distance (FD). From the powdered resin (mixture of sample novolac resin and 11 wt% HMTA), a tablet was formed. This tablet was placed on a pre-heated horizontal glass plate at 125 ºC in an oven (ISO 8619). After 3 min, the plate was tilted to an angle of 60º. The flow distance was measured after 30 min and given in mm.

FTIR/NMR Spectroscopy

The commercial novolac, lignin-novolac, and methylolated lignin-novolac resins were characterized by FTIR and ^{1}H and ^{13}C NMR spectroscopic techniques in order to analyze the structural differences. In addition, the lignosulfonates (modified and without modifying) employed were also analyzed by using these techniques.

FTIR spectra were recorded with a Mattson Satellite spectrophotometer, using the potassium bromide pellet method. The pellet was prepared from a mixture of 300 mg potassium bromide and 5 mg of resin sample (or lignosulfonate). The operating conditions were: 4000-400 cm^{-1} spectral width, 32 accumulations, 1 gain, 4 cm^{-1} resolution, and signal processing by triangular apodization. Band asignments were based on cited studies (Morterra et al. 1985; Costa et al. 1997; Nada et al. 1998; Carotenuto et al. 1999; Sun et al. 2001).

^{1}H and ^{13}C NMR spectroscopy. The ^{1}H spectra were recorded on a 200 MHz NMR spectrometer (BRUKER AC 200). The conditions used were: 4000.000 Hz sweep width, 7.2 μs pulse width, and a temperature of 297 K. Samples (0.1 g) and 10 μL of tetramethylsilane (TMS) were dissolved in 1 ml of deuterated-dimethylsulfoxide ($DMSO_{d6}$). ^{1}H chemical shifts were measured with respect to TMS as internal standard {($DMSO_{d6}$) = 2.5 ppm}. ^{13}C spectra were recorded on a 500 MHz NMR spectrometer (BRUKER AMX 500). In this case, the conditions used were: 90º pulse width, 6 s pulse time, 323 K, and 26000 sweeps. Peaks assessments were based on cited literature (Lundquist et al. 1989; Faix et al. 1994; Gardziella et al. 2000; Sun et al. 2001; Wang et al. 2005).

RESULTS AND DISCUSSION

Characterization of Novolacs

The required specifications for commercial (PF) resins and the results obtained in the characterization of lignin-novolac (LN) and methylolated lignin-novolac (MLN) are shown in Table 1. The free formaldehyde amounts of different samples fulfilled the specifications because these polymers are formulated with formaldehyde by default. In relation to free phenol content, lignin-resin (LN), and methylolated lignin resin (MLN) also conformed to the required values according to commercial resins specifications. Note that the methylolated lignin-novolac showed a free phenol content superior to that of the lignin-novolac resin. Methylolated lignin resin reduces the permeability in relation to LN and commercial resins, and therefore the pre-polymer offers resistance to the removal of phenol during the formulation.

Water content is also an important specification in the final application of these resins because it has a remarkable influence on the plasticity of novolacs. The effect on the melt viscosity is even more pronounced. For example, a buildup of the water content from 0.1 to 3% reduces the melt viscosity up to 90% (Knop and Pilato 1985). The reactivity of novolac to HMTA increases when water content increases, and the flow distance is reduced in spite of decreasing melt viscosity (Gardziella et al. 2000). The influence of free phenol is similar to water content but is less severe.

Table 1. Lignin-Resin Characteristics and Commercial Resin Specifications.

Resin	P_f (%)	F_f (%)	W_f (%)	SP (ºC)	FD (mm)
LN	0.14	0.19	0.23	119	27
MLN	0.19	0.02	0.28	118	26
Commercial*	< 0.20	< 0.30	< 0.40	115-125	25-40

P_f: Free phenol; F_f: Free formaldehyde; W_f : Water content; SP: Softening point; FD: Flow distance. * Required specifications supplied by Hexion Ibérica, S.A.

In addition, curing reaction of novolacs is carried out over 100 ºC, water forms vapor, and so the final material can present a porous structure with reduced mechanical properties. Therefore, a resin with low initial water content will achieve better final properties after curing. Note that all resins studied had less water than the maximum commercial specification, and lignin-novolac had less water than MLN because less water was used during formulation of LN resin (Table 1).

The softening point is a critical parameter in order to determine the feasibility of resins in textile-felt applications. If the softening point of lignin-resins is not in the commercial resin range (115-125 ºC), then these pre-polymers would not be employed for textile-felts, because the resin could not penetrate into the fibers. In this case, the softening point temperatures of synthesized resins with ammonium lignosulfonate were in the specified range, as shown in Table 1.

Lignin-novolac and methylolated lignin-novolac resins had a flow distance within the commercial range, but these results were near the lower limit. This fact is due to the presence of lignin in the samples, which reduced chain mobility of the resins. In short, these two lignin-resins fulfilled the specifications required by the textile-felts manufacture.

The FTIR spectra of lignin-novolac, methylolated lignin-novolac, and commercial resins are shown in Fig. 3. The highest wavenumber zone did not offer any difference among the three resins assayed. However, the spectra showed more information about resins structure within the 2000 to 400 cm^{-1} zone. The broad absorbance at 1701-1692 cm^{-1} corresponding to C=O stretching was observed in MLN spectra, but not in the commercial spectrum (Faix et al. 1994; Nada et al. 1998). The most typical band of lignin structures is 1600 cm^{-1}. In this case, it was not present in commercial resin, but a 1610 cm^{-1} band was able to overlap it. In addition, the 1470-1460 cm^{-1} band was not very intensive, which indicates that methylolated lignin molecule incorporates hydroxylmethyl groups in the MLN resin (Nada et al. 1998; Alonso et al. 2001). The main objective of methylolation was to incorporate hydroxylmethyl groups into the lignin aromatic ring. Note that LN resin also showed the same band (1470-1460 cm^{-1}), which implies that even without methylolation this group can be incorporated into the aromatic ring of lignin. In addition, this band (1470-1460 cm^{-1}) overlapped with a 1430 cm^{-1} band (methylene bridge), which is typical of novolac resins and in this case is not well resolved (Costa et al. 1997). The 819 cm^{-1} band corresponds to out-of-plane aromatic ring deformation by 1, 2, and 4 links. The band at 754 cm^{-1} is the 1, 2, and 6 substitutions of this aromatic ring. These two bands are quite similar in all resins due to great similarity of the substitutions,

as shown in Fig. 3. On the other hand, lignin-novolac and methylolated lignin-novolac had a predominance of 1, 2, and 6 links. This means that lignin aromatic rings have steric hindrance (Ŝebenik et al. 1974; Costa et al. 1997). The 655 cm^{-1} band in LN and MLN resins spectra indicates the presence of sulfonic groups from lignosulfonate.

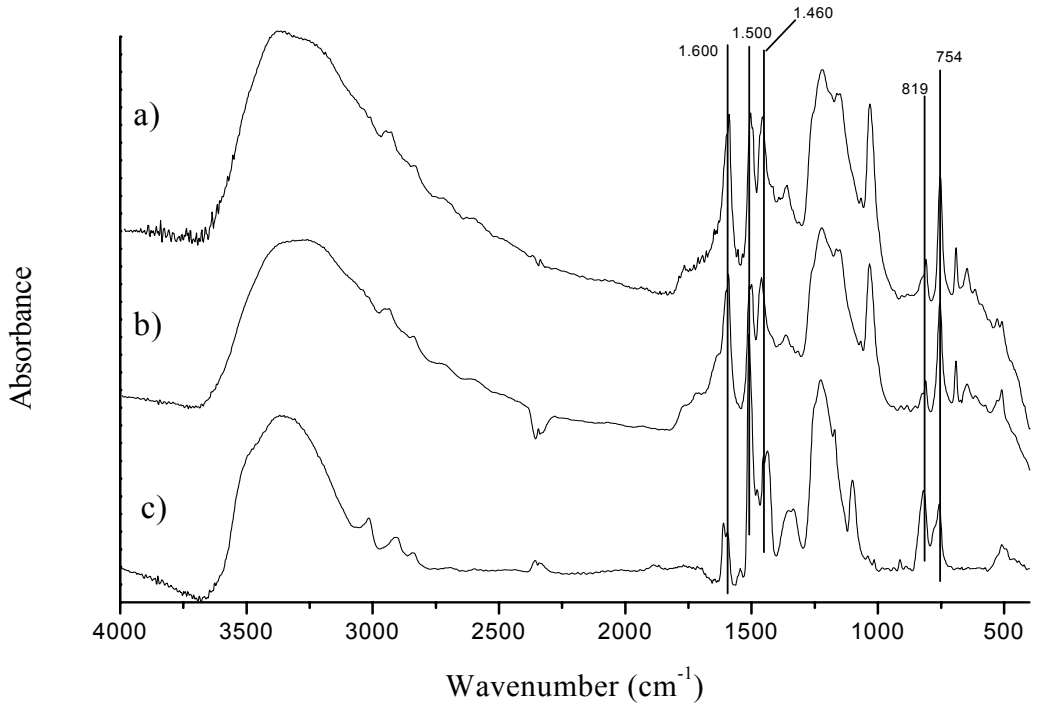

Figure 3. FTIR spectra of a) LN, b) MLN and c) Commercial novolac resins

The three resins studied also showed important differences in ^{1}H NMR spectra (Fig. 4). For instance, the 9 ppm zone corresponds to aldehyde protons linked to aromatic ring substitutions of the type -CHO. This signal did not appear in MLN, which implies that in this pre-polymer there were higher levels of substitutions than in the others resins. In addition, it supposes more steric hindrance to -CHO group incorporation into the MLN aromatic rings. Signals corresponding to aromatic protons (6.5-7.0 ppm) showed the presence of more free positions in the aromatic rings of resins. An absence of signals in the range of 7.0 to 7.5 ppm for commercial resin spectrum showed that the aromatic rings were less substituted. The lignin-novolac and methylolated lignin-novolac resins exhibited a higher level of replacement at the aromatic ring, which indicates that crosslinking reactions will be favored during the curing stage. In lignin-novolac resins the decrease of protons signal of hydroxylmethyl groups coming from lignin (4.5-4.6 ppm) demonstrated the dehydration of these groups to form methylene links with phenyl groups; this dehydration did not happen in commercial resins, which explain higher reactivity of lignin-novolac with the phenol. Thus, these circumstances are desirable for

resin-curing reactions. 3.80-3.90 ppm signals appeared in the MLN resin spectrum, which indicates the presence of -CH_2OH groups coming from the methylolation reaction. This group could promote greater crosslinking of MLN resin during the curing reaction.

The resins' ^1H NMR spectra did not reveal the complexity of the chemical structure of these polymers, due to the overlapping of signals (Fig. 4). The ^{13}C NMR technique, in general, allows identification of a greater number of functional groups. Lignin-novolac spectra have a great many signals due to presence of lignin functional groups, which have a very complex structure. ^{13}C NMR spectra give an idea of the difficulty in understanding the resins structure, as shown in Fig. 5.

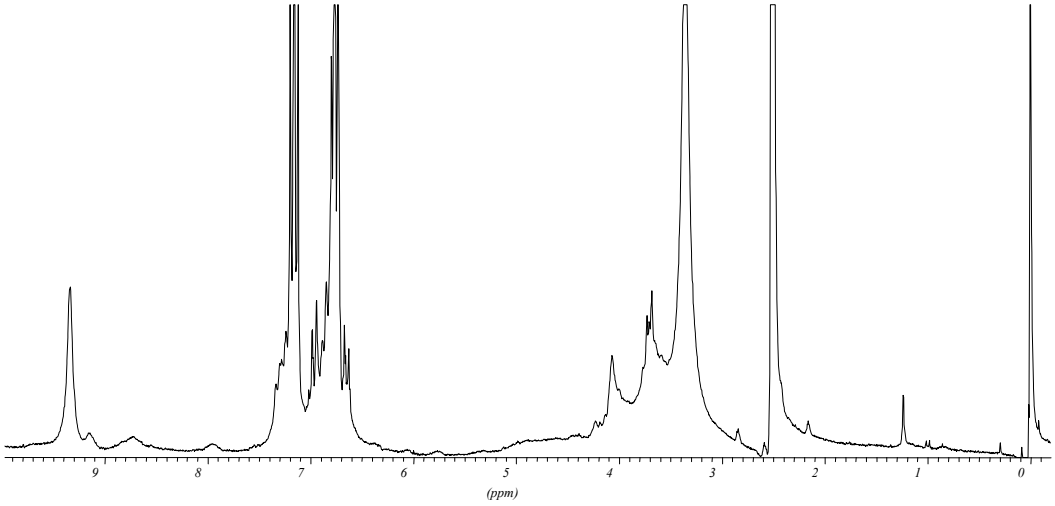

Figure 4 a. ^1H NMR spectrum of LN resin

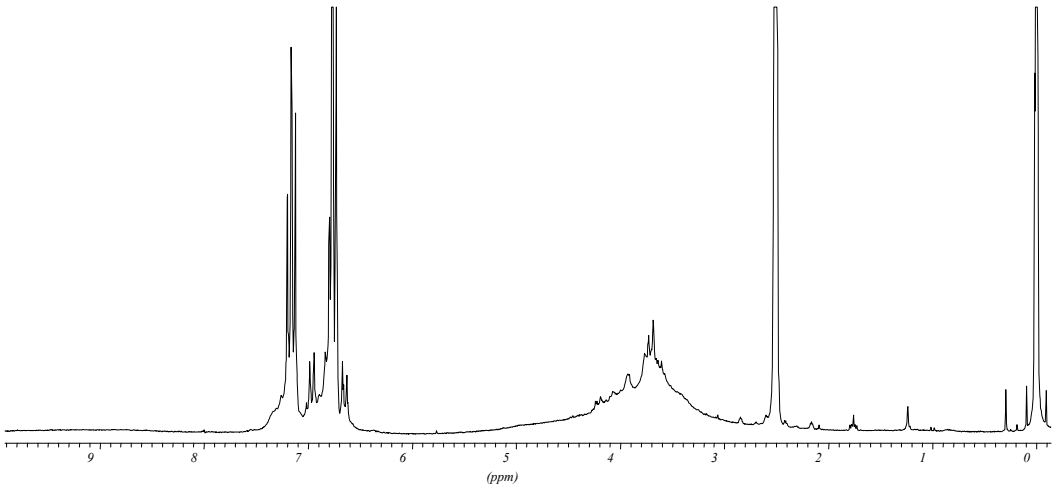

Figure 4 b. ^1H NMR spectrum of MLN resin

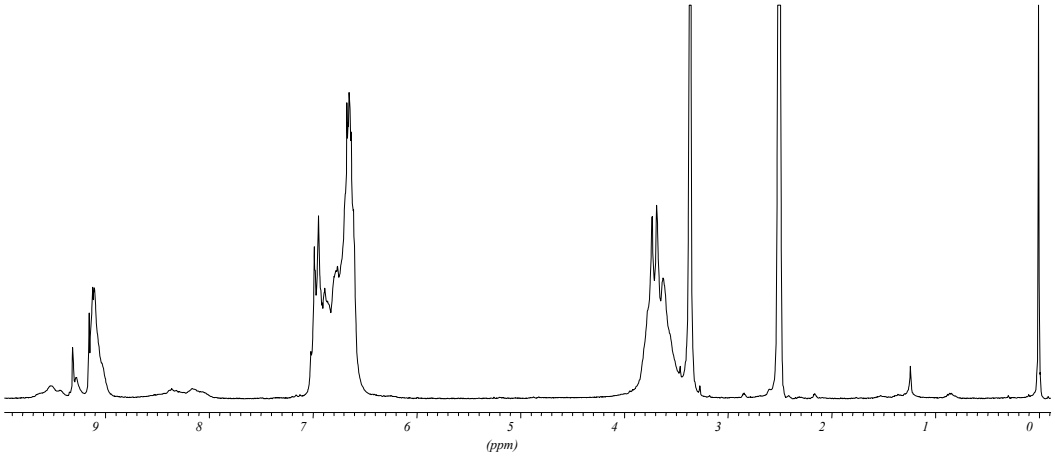

Figure 4 c. ^{1}H NMR spectrum of commercial novolac resins

An absence of peaks at 170-180 ppm implies that the aliphatic carboxylic acids were not formed in any of the three resins studied, which could make the resin curing reactions more difficult. The 166.5 ppm peak, which appears in the MLN spectrum, corresponds to the C=O link. This feature was also observed in the FTIR spectrum (Fig. 3.b), and it can be assigned to ester group linked to aromatic ring. The spectrum of commercial resin showed a signal at 150 ppm corresponding to OH linked to aromatic carbon, and this signal was unsubstituted in the *ortho* position by a CH_2 in LN and MLN. The same happens around 130 ppm, which is also a typical signal of novolac resins, due to C3 and C5 carbons of the phenolic ring substituted in its *ortho* position by a CH_2 (Holopainen et al. 1997). This signal, in novolac resins, is masked by resonances coming from lignosulfonate incorporated during polymer synthesis. The zone of 60-80 ppm (α, β and γ carbons of the (β)- aliphatic-O-(4)-aromatic links) was present only in the lignin-substituted resins. This range is consistent with the presence of a lignin structure. The zone of 35 ppm, characteristic of phenolic resins, is due to CH_2 in an *ortho* position with respect to the hydroxylmethyl carbon group of phenolic ring (Holopainen et al. 1997).

Note that the incorporation of methylolated lignin instead of lignosulfonate presents a reaction mechanism similar to that shown in Fig. 2, with the exception that the formaldehyde cannot occupy *meta* sites in an aromatic ring. Although both mechanisms are similar in lignin samples, methylolated lignin presents methylene groups which will react with the phenol, while lignosulfonate (without modification) competes with methylene links between phenolic rings.

Summary of Results

Summarizing, despite a great number of signals and unavoidable overlapping, it was possible to distinguish novolac's typical signals by means of the three techniques employed. Identification of these signals implies that the lignin-novolac and methylolated lignin-novolac resins had similar links relative to commercial resin; however, resins synthesized with lignin showed a more complicated structure, due to lignin incorporation. Thus, LN and MLN would substitute for commercial resins in textile felt applications.

In the future an extensive characterization would be needed to determine and optimize cure process conditions for these polymers. In addition, other tasks should include evaluation of curing agent content (HMTA) during the cure process of the resins. Processing knowledge and kinetic methods developed for epoxy and unsaturated polyester resins should also benefit the manufacture of similar systems based on different polymers (Kenny et al. 1995; Boey et al. 2000; Lee et al. 2000).

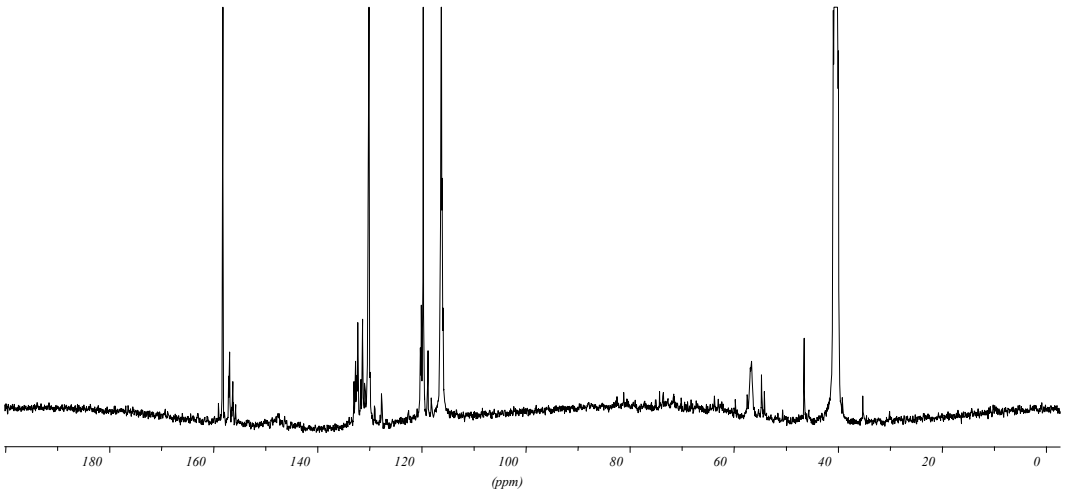

Figure 5 a. ^{13}C NMR spectrum of LN resin

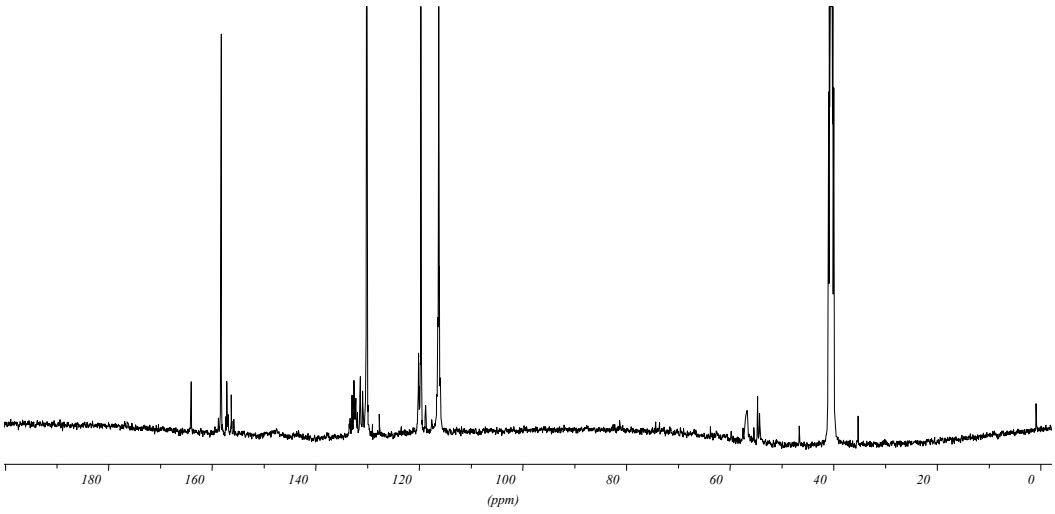

Figure 5 b. ^{13}C NMR spectra of MLN resin

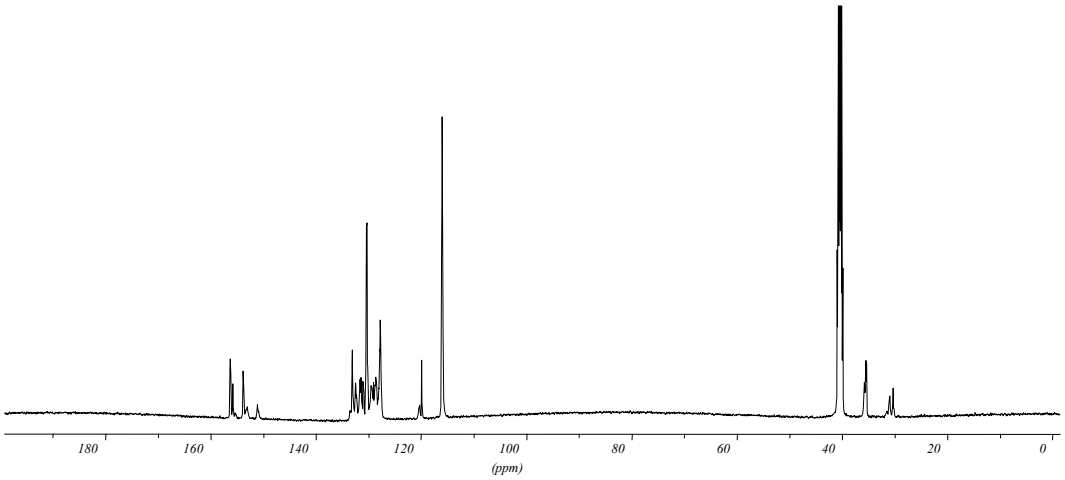

Figure 5 c. ^{13}C NMR spectra of commercial novolac resin

CONCLUSIONS

1. Phenol, formaldehyde, and water contents, as well as softening point and flow distance values of LN and MLN resins synthesized were in range with specifications that have been established for use of commercial novolac resins. Therefore, these samples conform to the specifications required for the textile felt applications.
2. FTIR and NMR spectroscopies showed that the chemical structure of lignin-novolac and methylolated lignin-novolac resins were more complicated than that of a commercial novolac resin due to the functional groups of the incorporated ammonium lignosulfonate.
3. Although the LN and MLN resins are structurally complex, the high variety of functional groups in relation to commercial resin could favour the curing reaction.

ACKNOWLEDGEMENTS

The authors gratefully acknowledge the support of "Ministerio de Ciencia y Tecnología" (project CTQ2004-02031/PPQ).

REFERENCES CITED

Alonso, M. V., Rodríguez, J. J., Oliet, M., Rodríguez, F., García, J., and Gilarranz, M. A. (2001). "Characterization and structural modification of ammonic lignosulfonate by methylolation," *J. Appl. Polym. Sci*. 82(11), 2661-2668.

Alonso, M. V., Oliet, M., Rodríguez, F., García, J., Gilarranz, M. A., and Rodríguez, J. J. (2005). "Modification of ammonium lignosulfonate by phenolation for use in phenolic resins," *Bioresource Technol.* 96(9), 1013-1018.

Allan, G. G., Dalan, J. A., and Foster, N. C. (1989). "Modification of lignins for use in phenolic resins," *J. Am. Chem. Soc. Symp.* Ser. 385, 55-57.

Boey, F. C. Y., and Qiang, W. (2000). "Experimantal modeling of the cure kinetics of an epoxy hexaanhydro-4-methylphatalic anhydride (MHHPA) system," *Polymer* 41, 2081-2094.

Calvé, L. R., Shields, J. A., Blanchette, L., and Fréchet J. M. J. (1988). "A practical lignin-based adhesive for waferboard/OSB," *Forest Prod. J.* 38(5), 15-20.

Carotenuto, G., and Nicolais, L. (1999). "Kinetic Study of Phenolic Resin Cure by IR Spectroscopy ," *J. Appl. Polym. Sci.* 74(11), 2703-2715.

Chow, S., and Steiner, P. R. (1979). "Comparisons of the Cure of Phenol-Formaldehyde Novolac and Resol Systems by Differential Scanning Calorimetry ," *J. Appl. Polym Sci*. 23, 1973-1985.

Costa, L., Rossi di Monterela, L., Camino, G., Weil, E. D., and Pearce, E. M. (1997). "Structure-charring relationship in phenol-formaldehyde type resins," *Polym. Degrad. Stabil.* 56, 23-25.

Danielson, B., and Simonson, R. (1998). "Kraft lignin in phenol formaldehyde resin. Part 1. Partial replacement of phenol by Kraft lignin in phenol formaldehyde adhesives for plywood," *J. Adhesion Sci.* 12(9), 923-939.

Dolenko, A. J., and Clarke, M. R. (1978). "Resin blinders from Kraft lignin," *For. Prod. J*. 28(8), 41-46.

Dos Santos, F. (1996). "Utilizaçao de Lignossulfonatos na preparaçao de resinas fenólicas tipo novolaca e pós de moldagem fenólicos". Universidade de Sao Paulo, Maestria, 1996.

El-Saied, H., Nada, A. M. A., Ibrahem, A. A., and Yousef, M. A. (1984). "Waste liquors from cellulosic industries. III. Lignin from soda-spent liquor as a component in phenol-formaldehyde resin ," *Angew. Makromolek. Chem.* 122, 169-181.

Faix, O., Argyropoulos, D. S., Robert, D., and Neirink, V. (1994). "Determination of Hydroxyl Groups in Lignins Evaluation of ^{1}H-, ^{13}C-, ^{31}P-NMR, FTIR and Wet Chemical Methods," *Holzforschung.* 48(5), 387-394.

Forss, K. G., Fuhrmann, A. (1979). "Finnish plywood, particleboard, and fireboard made with a lignin-base adhesive," *Forest Prod J.* 29(7), 39-43.

Gardziella, A., Pilato, L. A., and Know, A. (2000). *Phenolic Resins: Chemistry, Applications, Standardization, Safety and Ecology*. New York: Springer

Holopainen, T., Alvila, L., Rainio, J., and Pakkanene, T. T. (1997). "Phenol-Formaldehyde Resol Resins Studied by ^{13}C-NMR Spectroscopy, Gel Permeation Chromatography, and Differential Scanning Calorimetry," *J. Appl. Polym. Sci.* 66, 1183-1193.

Ishida, H., and Rodriguez, Y. (1995). "Curing kinetics of a new benzoxazine-based phenolic resin by differential scanning calorimetry," *Polymer.* 36(16), 3151-3158.

Kenny, J. M., Pisaniello, G., Farina, F., and Puzziello, S. (1995). "Calorimetric analysis of the polymerisation reaction of a phenolic resin," *Thermochim. Acta,* 269/270, 201-211.

Kharade, A. Y., and Kale, D. D. (1998). "Effect of Lignin on phenolic Novolac Resins and Moulding Powder," *Eur. Polym. J*. 34(2), 201-205.

Knop, A., Pilato, L. A. (1985). *Phenolic Resins*. Springer-Verlag, New York.

Kou, M., Hse, C.-Y., and Huang, D.-H. (1991). "Alkali treated Kraft lignin as a component in flakeboard resins ," *Holzforschung* 45, 47-51.

Lee, S. H., Yoshioka, M., and Shiraishi, N. (2000). "Preparation and properties of phenolated corn bran (CB)/phenol/formaldehyde cocondensed resin," *J. Appl. Polym. Sci.* 77, 2901-2907.

Lundquist, K., and Stern, K. (1989). "Analysis of lignins by ^{1}H NMR spectroscopy," *Nordic Pulp Pap. Res. J.* 4(3), 210-213.

Matuana, L.M., Riedl, B., and Barry, A.O. (1993). "Caracterisation cinetique per analyse enthalpique differentielle des resins phenol-formaldehyde a base de lignosulfonates," *Eur Polym J*. 29(4), 483-490.

Morterra, C., and Low, M. J. D. (1985). "I.R. studies of carbons-VII. The pyrolysis of a phenol-formaldehyde resin," *Carbon*. 23(5), 525-530.

Nada, A. M. A., El-Saied, H., Ibrahem, A. A., and Yousef, M. A. (1987). "Waste liquors from cellulosic industries. IV. Lignin as component in phenol formaldehyde resol resin," *J. Appl. Polym. Sci.* 33, 2915-2924.

Nada, A. M. A., El-Sakhawy, M., and Kamel, S. M. (1998). "Infra-red spectroscopy study of lignins," *Polym. Degrad. Stabil*. 60, 247-251.

Ozawa, T. B. (1965). "A new method of analysing thermogravimetric data," *Chem. Soc. Jpn*. 38(1), 1881-1886.

Peng, W., and Riedl, B. (1994). "The chermorheology of phenol-formaldehyde thermoset resin and mixtures of the resin with lignin fillers," *Polymer* 35(6), 1280-1286.

Ŝebenik, A., Vizovisek, I., and Lapange, S. (1974). "Determination of kinetic parameters form the reaction between phenol and formaldehyde by differential scanning calorimetry ," *Eur. Polym. J*. 10, 273-278.

Sun, R. C., Lu, Q., and Sun, X. F. (2001). "Physico-chemical and thermal characterization of lignins from *Caligonum monogoliacum* and *Tamarix* spp," *Polym. Degrad. Stabil.* 72, 229-238.

Vázquez, G., González, J., Freire, S., and Antorrena, G. (1997). "Effect of chemical modification of lignin on the gluebond performance of lignin-phenolics resins," *Biores. Technol.* 60, 191-198.

Wang, M., Wei, L., and Zhao, T. (2005). "Cure study of addition-cure-type and condensation-addition-type phenolic resins," *Eur. Polym. J*. 41, 903-912.

Wolfrum, J., and Ehrenstein, G.W. (1999). "Interdependence Between the Curing Structure, and the Mechanical Properties of Phenolic Resins," *J. Appl. Polym. Sci.* 74, 3173-3185.

Ysbrandy, R.E., Sanderson, R.D., and Gerischer, G.F.R. (1992). "Adhesives from autohydrolysis bagasse lignin. Part I ," *Holzforschung* 46(3), 249-252.

Zhang, X., Looney, M. G., and Solomon, D. H. (1997). "The chemistry of novolaca resins: 3. ^{13}C and ^{15}N n.m.r. studies of curing with hexamethylenetetramine," *Polymer* 38(23), 5835-5848.

Article submitted: March 19, 2006; First round of reviewing completed: April 12, 2007; Revised version received May 5, 2007; Corrected version approved: May 23, 2007; Article published May 25, 2007.

IN SITU DETECTION OF CELL WALL POLYSACCHARIDES IN SITKA SPRUCE (*PICEA SITCHENSIS* (BONG.) CARRIÈRE) WOOD TISSUE

Clemens Altaner[a]*, J. Paul Knox[b] and Michael C. Jarvis[a]

Wood cell wall polysaccharides can be probed with monoclonal antibodies and carbohydrate-binding modules (CBMs). Binding of monoclonal antibodies to β-1-4-xylan, β-1-4-mannan, β-1-3-glucan, and α-1-5-arabinan structures were observed in native Sitka spruce (*Picea sitchensis* (Bong.) Carrière) wood cell walls. Furthermore CBMs of different families, differing in their affinities for crystalline cellulose (3a) and amorphous cellulose (17 and 28), were shown to bind to the native wood cell walls with varying intensities. Resin channel forming cells exhibited an increased β-1-4-xylan and a decreased β-1-4-mannan content. Focusing on severe compression wood (CW) tracheids, β-1-3-glucan was found towards the cell lumen. In contrast, α-1-5-arabinan structures were present in the intercellular spaces between the round tracheids in severe CW, highlighting the importance of this polymer in cell adhesion.

Keywords: α-1-5-Arabinan, Carbohydrate-binding module (CBM), Cellulose, β-1-3-Glucan, Immunofluorescence, β-1-4-Mannan, Monoclonal antibody, Sitka spruce (Picea sitchensis (Bong.) Carrière), β-1-4-Xylan

*Contact information: a: Chemistry Department, University of Glasgow, Glasgow G12 8QQ, Scotland, UK, b: Centre for Plant Sciences, University of Leeds, Leeds LS2 9JT, England, UK; *Corresponding Author: C.Altaner@chem.gla.ac.uk*

INTRODUCTION

The chemical composition of wood varies not only at the tissue level between wood types but also at the cellular level between cell wall layers. Cell wall components at these levels determine not only the unique mechanical properties of certain wood types but also their chemical reactivity and accessibility to pulping and bleaching agents. The analysis of the chemical wood structure at cellular levels is difficult to achieve. Although advances have been made in the miniaturisation of classical wet-chemical wood analysis, their capacity for spatial resolution is not adequate for investigations at the cellular level (Dahlman et al. 2000; Pranovich et al. 2006). Infrared micro-spectroscopy has the potential to determine the chemical wood composition on the cellular level (Hori and Sugiyama 2003; Dokken et al. 2005). Unfortunately, spectroscopic techniques only yield a limited amount of structural information on the polysaccharides present.

Antibody labelling of plant cell wall polysaccharides has a long history of successful use on primary cell walls (Vreeland 1970), and a wide range of monoclonal antibodies directed to cell wall polymers is now available (Knox 1997). Another type of molecular probe recently used for the detection of polysaccharides in plant cell walls is carbohydrate-binding modules (CBMs) (Din et al. 1991; Taylor et al. 1996; McCartney et

al. 2004; McCartney et al. 2006; Blake et al. 2006; Filonova et al. 2007). CBMs are classified into families (http://afmb.cnrs-mrs.fr/CAZY/ (Coutinho and Henrissat 1999)), which display different affinities to cell wall polysaccharide structures such as amorphous or crystalline cellulose. Recombinant his-tagged forms of CBMs can be used as selective probes in a manner similar to that used for monoclonal antibodies (McCartney et al. 2004).

Apart from the use of molecular probing techniques for cell wall polysaccharides in differentiating vascular wood tissue (Baba et al. 1994; Guglielmino et al. 1997; Ermel et al. 2000; Maeda et al. 2000; Samuels et al. 2002; Lafarguette et al. 2004), some reports of their application towards mature wood tissues or processed wood products like pulp can be found (Duchesne et al. 2003; Hafrén and Daniel 2003; Hildén et al. 2003; Lappalainen et al. 2004; Brändström et al. 2005; Hafrén 2005; Daniel et al. 2006; Filonova et al. 2007; Altaner et al. 2007). Here we report the potential of molecular probes, which have up to now not been applied to wood, to locate cell wall polysaccharides in untreated Sitka spruce (*Picea sitchensis* (Bong.) Carrière) cross-sections.

EXPERIMENTAL

Anti-mouse-IgG FITC, anti-rat-IgG FITC, anti-rabbit-IgG FITC, and anti-mouse-His were obtained from Sigma. The β-1-3-glucan and β-1-4-mannan antibodies were obtained from Biosupplies Australia. Details of the anti-α-1-5-arabinan monoclonal antibody LM6 (Willats et al. 1998), anti-β-1-4-xylan LM11 (McCartney et al. 2005), and the microbial CBMs designated CBM3a (*Clostridium thermocellum*), CBM17 (*Clostridium cellulovorans*), and CBM28 (*Bacillus sp. 1139*) have been described elsewhere (Carrard et al. 2000; Boraston et al. 2000; Boraston et al. 2002; Blake et al. 2006).

Samples were cut from Sitka spruce (*Picea sitchensis* (Bong.) Carrière) trees grown at Kershope, Northumbria, UK and felled when 36 years old. Transverse sections were cut (20 µm thick) with a sliding microtome from the wood blocks (L: 30 mm, T: 5 mm, R: 50 mm) after soaking in cold water for 30 min. This ensured that no extraction of any wood components occurred during sample preparation.

The wood sections were incubated for 1 h at room temperature under gentle shaking with 200 µl primary molecular probe solution dissolved in 800 µl 3% milk powder in phosphate-buffered saline (PBS) (Jones et al. 1997). The liquid was removed and the wood sample was washed 3 times for 5 min with PBS under the same conditions. In case of his-tagged CBMs an additional labelling step using anti-mouse-His before anti-IgG FITC application was needed as described by McCartney et al. (2004). Bound primary molecular probes were then labeled with the corresponding anti-IgG FITC (Sigma), using 750 µl of a 1:100 dilution in 3% milk powder in PBS. Incubation lasted 1 h at room temperature under gentle shaking in the dark. The samples were again washed 3 times for 5 min in PBS. Finally the wood sections were mounted onto microscope slides in the presence of Citifluor anti-fade reagent (Agar Scientific). The labeled samples were examined with an Olympus BH6 microscope equipped with epifluoresc-

ence irradiation. Alternatively, a Zeiss CLSM510-UV microscope, fitted with a 488 nm laser and 505-550 nm band-pass filter, was used to acquire higher resolution images by confocal laser scanning microscopy. Bright-field images were collected with a transmitted light detector.

RESULTS AND DISCUSSION

Cellulose

Three different CBMs directed to cellulose were tested for their potential to bind to untreated wood. Whereas the CBM belonging to family 3a binds to crystalline cellulose, the CBMs belonging to family 28 and 17 have an affinity for amorphous cellulose (McCartney et al. 2004; Blake et al. 2006). Figure 1 shows equivalent cross-sections containing a band of compression wood (CW) that appeared brighter in the control than the neighbouring normal wood (NW).

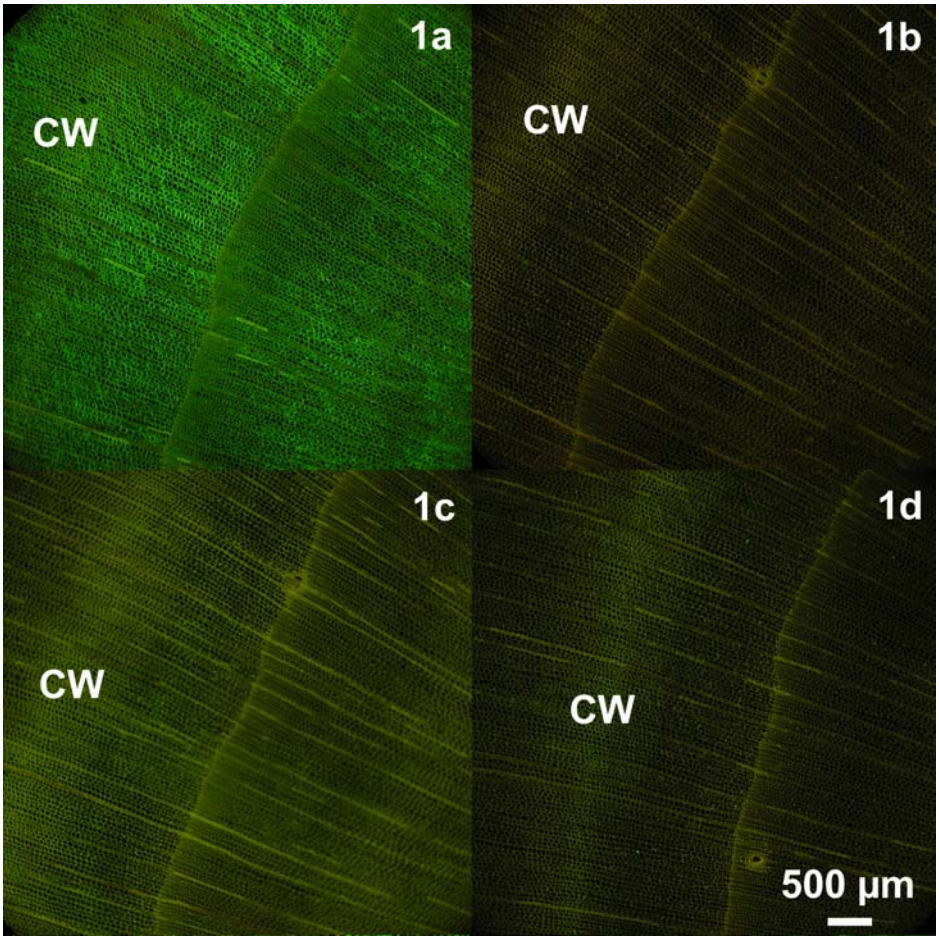

Fig. 1. Equivalent unextracted Sitka spruce cross-sections containing a compression wood (CW) band incubated with CBM3a (a), control (without primary molecular probe) (b), CBM17 (c) and CBM28 (d). The true colour images were obtained with a fluorescence-microscope.

The autofluorescence of the wood cell wall in the control can be attributed to lignin present in wood (Donaldson et al. 1999) (Fig. 1b). Despite the yellowish lignin auto-fluorescence, the bright green fluorescence of antibody-linked FITC could be clearly identified. CBM3a, binding to crystalline cellulose, strongly stained all wood types in the samples similarly (Fig. 1a). CBMs from families 17 and 28, having an affinity to amorphous cellulose, displayed a differential reaction, with CBM17 binding to ray cells and CW (Fig. 1c), whereas CBM28 (Fig. 1d) was almost equivalent to the control (Fig. 1b), with a negligible amount of binding. The obvious difference in affinity to xylem tissue of the CBMs, showing a much stronger binding of the CBM recognising crystalline cellulose, is comparable with literature reports of other species, e.g. tobacco stems (Blake et al. 2006).

Due to the differences in the affinity of the individual CBMs towards their ligands, it is not possible to draw conclusions from the staining intensity on the amount of the corresponding cellulose types in the cell walls. If it is assumed that all the molecular probes bind only to cellulose of one form or another, then this premise leads to the interpretation that whereas crystalline cellulose is abundantly present in all cell types, amorphous cellulose is predominately present in ray cells and CW tracheids. However, it has to be mentioned that the staining for CW may be due to the presence of β-1-3-glucan (callose) structures, which are present in severe CW (Hoffmann and Timell 1972, Fig. 4), since recognition of callose by this CBM has been reported (Boraston et al. 2000; Boraston et al. 2002).

Apart from the aforementioned factors, affinity and selectivity, the accessibility of the ligands can have a significant influence on the results of immunolabelling studies. Indeed variations in the accessibility of the polymers have been exploited to visualise damages in spruce pulp fibres using a CBM (Hildén et al. 2003). In the case of our study, differences in accessibility between NW and CW are not expected due to sample preparation. First, this is because the tissue types are present within the same sections, ruling out an influence of the microtome knife. Secondly although variations in the microfibril angle could result in additional variations in the accessibility on the tissue level due to alterations in the surface roughness of the section, this seems unlikely, since we used juvenile wood which like CW has a high microfibril angle. At the cell wall level we found indications that CBM3a bound more strongly to the inner and outer secondary cell wall layers (data not shown). This is consistent with the findings of Hildén et al. (2003).

Solid-state NMR spectroscopy (Hult et al. 2000; Andersson et al. 2004; Newman 2004) and x-ray diffraction (Andersson et al. 2003; 2004; Thygesen et al. 2005) have been used to study the cellulose structure in wood. X-ray diffraction yields data on the crystallinity index and size cellulose crystals. Solid-state NMR spectroscopy gives insights into the various forms of crystalline cellulose (i.e. Iα, Iβ, and para-crystalline), as well as the amount of accessible and inaccessible surface chains. Based on the assumption that CBMs bind selectively to individual forms of cellulose, it can be expected that they posses the potential to validate the above-mentioned methods for the analysis of cellulose structures. Especially with respect to the more disordered cellulose structures, which are inaccessible to x-ray diffraction, CBMs promise to be powerful in gaining information. This is because the affinity of CBMs towards cellulose can be

expected not only to be dependent on the crystallinity index, but also the size of the individual fibril aggregates. Furthermore the application of CBMs has the potential to increase the resolution from the tissue level to the level of the individual cell wall layers. The average cellulose crystallinity for Norway spruce (*Picea abies* (L.) Karst.), Scots pine (*Pinus sylvestris* L.), and Radiata pine (*Pinus radiata*) was reported to be slightly above 50%. This value is fairly constant for the individual wood types (namely juvenile wood, mature wood, early wood, late wood, opposite wood, and CW) with the tendency to higher values for slow grown tracheids (Newman 2004). To the best of our knowledge, information on the crystal size of cellulose in conifers is only available on NW for Norway spruce and Scots pine (Andersson et al. 2004). Although this data does not show any difference between the two species it cannot be ruled out that a difference between individual wood tissues, in particular for CW, does exist. Indeed increased lateral dimensions of the cellulose crystals in tension wood compared to NW have been reported (Washusen and Evans 2001). Hult et al. (2000) found indications of an unique cellulose structure in CW by solid-state NMR spectroscopy. A higher proportion of para-crystalline cellulose in CW was accompanied by an increased amount of accessible cellulose fibril surface. These results are consistent with a selective staining of CW by CBM17 as seen in Figure 1c. To our knowledge no data on the cellulose structure of parenchymatic ray cells of conifers exists.

Mannan

In native wood, mannans were detected by the antibody binding to linear β-1-4-mannan structures. Staining was consistent for all examined wood types, namely early wood, late wood, NW, and CW, although cells forming resin channels were less stained than the surrounding tracheids (Fig. 2).

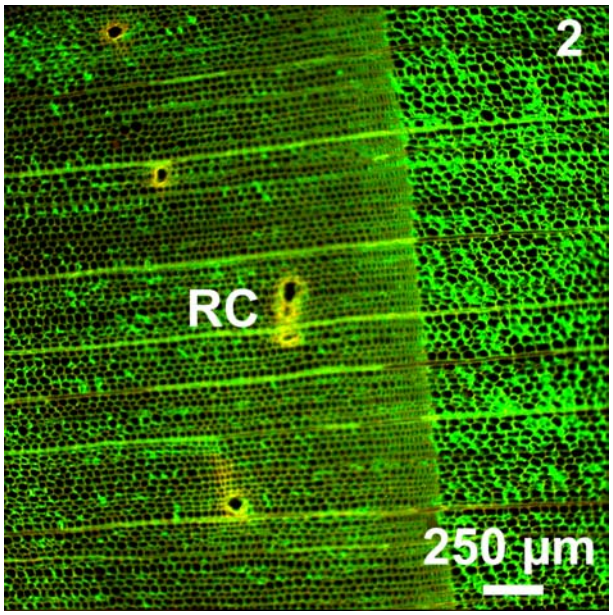

Fig. 2. Unextracted Sitka spruce cross-sections labelled for linear β-1-4-mannan structures including resin channels (RC). The images were obtained with a fluorescence-microscope and contrast enhanced.

It is unlikely that the reduced labelling of the resin channel forming cells is caused by a decreased accessibility of the β-1-4-mannan antibody to its epitope due to a high resin content of the cells, since labelling with LM11 for β-1-4-xylan (Fig. 3) showed the opposite effect. On the cellular level immunofluorescence labelling indicated differences in the mannan content between the individual cell wall layers (data not shown). Electron microscopy in combination with immuno-(gold)labelling is required to confirm this.

Xylan

Strong binding of the anti-β-1-4-xylan LM11 antibody was found for all wood types. Cells forming the resin channels showed a stronger fluorescence than the surrounding tissue (Fig. 3). Labelling of cells forming resin channels clearly differed for xylan and mannan. A reduced mannan content (Fig. 2) seemed to be accompanied by an increased xylan content of those cells (Fig. 3). Binding of anti-β-1-4-xylan antibody to wood resins seemed unlikely, due to their different chemical structures. As in the case of mannan immunofluorescence, labelling indicated differences in the xylan content between the individual cell wall layers (data not shown), but higher resolution microscopy is required to draw clear conclusions.

To the best of our knowledge no experiments have been reported which investigate the chemical composition of epithelial cell walls of wood. Studies on the chemical composition of resin ducts have focused on the cell contents and not the cell walls (Nagy et al. 2000). A deviation in the chemical composition of those cell walls from ordinary tracheids would support the distinctive biological function of resin channels in either facilitated secretion of the resin or increased resistance against microbial attack.

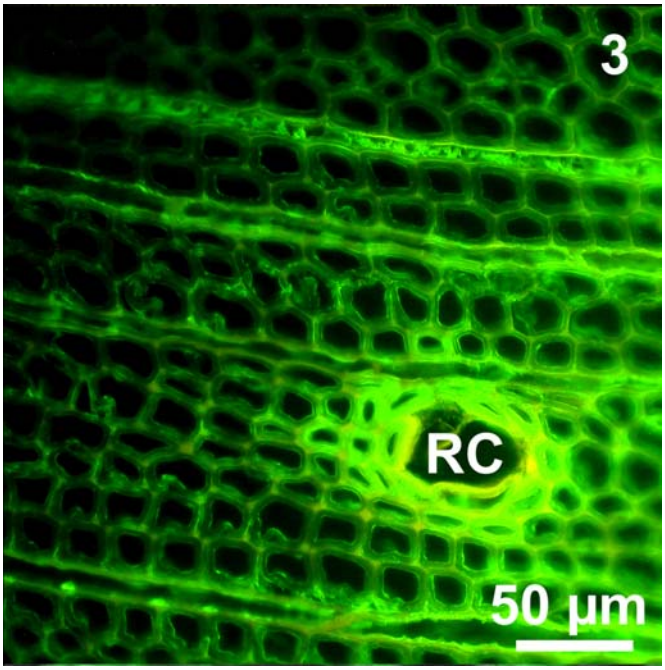

Fig. 3. Unextracted Sitka spruce cross-sections labelled for linear β-1-4-xylan structures using LM11 including resin channels (RC). The images were obtained with a fluorescence-microscope and contrast enhanced.

Callose

Callose was detected in severe CW. A patchy staining pattern of the β-1-3-glucan monoclonal antibody was observed on cell wall surfaces towards the lumen in CW tracheids (Fig. 4). Hoffmann and Timell (1972) identified small amounts of callose in severe CW by classical wet-chemical wood analysis. Furthermore Waterkeyn et al. (1982) as well as Włoch and Hejnowicz (1983) located β-1-3-glucan structures in or between the helical cavities of severe CW tracheids with aniline blue staining. These findings are consistent with observations made using the β-1-3-glucan binding monoclonal antibody.

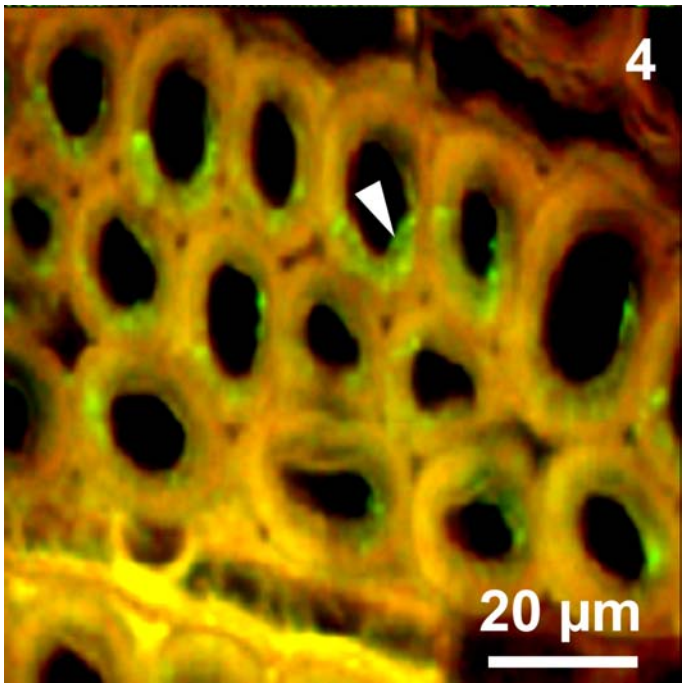

Fig. 4. Unextracted severe CW Sitka spruce cross-section labelled for β-1-3-glucan (callose) structures. Arrow indicates callose in or between the helical cavities. The image was obtained with a fluorescence-microscope and contrast enhanced.

Arabinan

A monoclonal antibody to α-1-5-arabinan indicated that this polysaccharide structure was located in the linings of intercellular spaces between tracheids of severe CW and in the walls of parenchymatic ray cells (Fig. 5). Ermel et al. (2000) detected a constant decrease of α-1-5-arabinan in differentiating poplar tissue from phloem to xylem, indicating its importance during cell differentiation. Whereas these authors were not able to obtain information on the distribution of LM6 epitope in poplar wood cell walls by electron microscopy, primary cell walls showed an absence or reduced abundance of α-1-5-arabinan structures in the middle lamella and cell corners compared to the homogenously labelled primary cell wall (Serpe et al. 2002; Guillemin et al. 2005). Because wood contains only minor amounts of arabinose (Côté et al. 1968) it seems likely that the α-1-5-arabinan structures are concentrated in the primary wall.

Therefore one might speculate that Sitka spruce shows active control of cell separation when forming CW, by digestion of the middle lamella and exposing the α-1-5-arabinan containing primary wall.

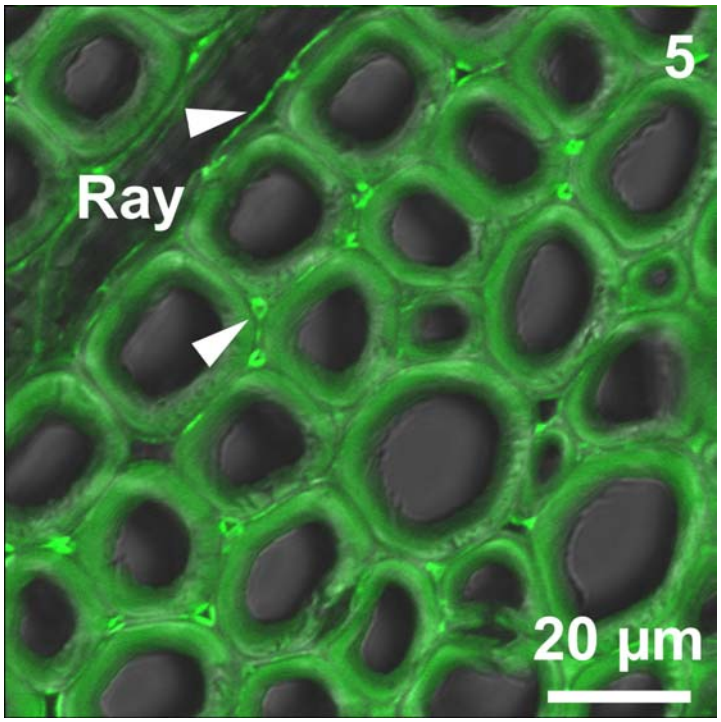

Fig. 5. Confocal laser scanning image of an unextracted severe CW Sitka spruce cross-section labelled for α-1-5-arabinan structures using LM6. Bright field (a) and florescence signal (b). Arrows indicates arabinan lining the intercellular spaces between the tracheids in severe CW and in parenchymatic ray cells.

CONCLUSIONS

A wide range molecular probes (monoclonal antibodies and cellulose-directed recombinant his-tagged forms of CBMs) have proven to yield information on the distribution of cell wall polysaccharides in untreated wood tissue. Fluorescence labelling revealed differences in the chemical composition of wood on the tissue level. Resin channel forming cells exhibited a decreased mannan and an increased xylan content compared to the surrounding tracheids. CBMs directed to amorphous cellulose bound more intensively to ray cells and CW tracheids than normal wood tracheids. On the cellular level this technique indicated clear structures for α-1-5-arabinan and callose. While in severe CW α-1-5-arabinan is located in the intercellular spaces, callose is found towards the cell lumen. For the other molecular probes only indications of variable abundance of the corresponding epitopes in the different cell wall layers were found. Electron microscopy in conjunction with immuno-(gold) labelling would be needed to obtain images of the necessary resolution to provide unambiguous information on their distribution within the individual cell wall layers.

ACKNOWLEDGMENTS

We thank Harry Gilbert (University of Newcastle Upon Tyne) for CBMs, S. Mochan and B. Gardiner (NRS Forest Research UK) for the provision of timber, A. Hapca (Napier University) for support with sample sectioning, S. Marcus for the help with the antibody labelling, M. Blatt (University of Glasgow) for granting access to a confocal laser scanning microscope and SHEFC for financial support.

REFERENCES CITED

Altaner, C., Hapca, A., Knox, J. P., and Jarvis, M. C. (2007). "Antibody labelling of galactan in Sitka spruce (*Picea sitchensis* (Bong.) Carrière)," *Holzforschung.* 61, 311-316.

Andersson, S., Serimaa, R., Paakkari, T., Saranpää, P., and Pesonen, E. (2003). "Crystallinity of wood and the size of cellulose crystallites in Norway spruce (*Picea abies*)," *J. Wood Sci.* 49, 531-537.

Andersson, S., Wikberg, H., Pesonen, E., Maunu, S. L., and Serimaa, R. (2004). "Studies of crystallinity of Scots pine and Norway spruce cellulose," *Trees.* 18, 346-353.

Baba, K., Sone, Y., Kaku, H., Misaki, A., Shibuya, N., and Itoh, T. (1994). "Localization of hemicelluloses in the cell-walls of some woody-plants using immonugold electron-microscopy," *Holzforschung* 48, 297-300.

Blake, A. W., McCartney, L., Flint, J. E., Bolam, D. N., Boraston, A. B., Gilbert, H. J., and Knox, J. P. (2006). "Understanding the biological rationale for the diversity of cellulose-directed carbohydrate-binding modules in prokaryotic enzymes," *J. Biol. Chem.* 281, 29321-29329.

Boraston, A. B., Chiu, P., Warren, R. A. J., and Kilburn, D. G. (2000). "Specificity and affinity of substrate binding by a family 17 carbohydrate-binding module from Clostridium cellulovorans cellulase 5A," *Biochemistry* 39, 11129-11136.

Boraston, A. B., Ghaffari, M., Warren, R. A. J., and Kilburn, D. G. (2002). "Identification and glucan-binding properties of a new carbohydrate-binding module family," *Biochemical J.* 361, 35-40.

Brändström, J., Joseleau, J. P., Cochaux, A., Giraud-Telme, N., and Ruel, K. (2005). "Ultrastructure of commercial recycled pulp fibers for the production of packaging paper," *Holzforschung* 59, 675-680.

Carrard, G., Koivula, A., Soderlund, H., and Beguin, P. (2000). "Cellulose-binding domains promote hydrolysis of different sites on crystalline cellulose," *Proc. Nat. Acad. Sci. USA* 97, 10342-10347.

Côté, W. A., Kutscha, N. P., Simson, B. W., and Timell, T. E. (1968). "Studies on compression wood. VI. Distribution of polysaccharides in cell wall of tracheids from compression wood of Balsam fir *Abies balsamea* (L) Mill," *Tappi* 51, 33-40.

Coutinho, P. M., and Henrissat, B. (1999). "Carbohydrate-active enzymes: an integrated database approach." In: *Recent Advances in carbohydrate bioengineering*. Eds. Gilbert, H. J., Davies, G., Henrissat, B., Svensson, B. The Royal Society of Chemistry, Cambridge. pp. 3-12.

Dahlman, O., Jacobs, A., Liljenberg, A., and Olsson, A. I. (2000). "Analysis of carbohydrates in wood and pulps employing enzymatic hydrolysis and subsequent capillary zone electrophoresis," *J. Chromatogr. A* 891, 157-174.

Daniel, G., Filonova, L., Kallas, A. M., and Teeri, T. T. (2006). "Morphological and chemical characterisation of the G-layer in tension wood fibres of *Populus tremula* and *Betula verrucosa*: Labelling with cellulose-binding module CBM1(HjCel7A) and fluorescence and FE-SEM microscopy," *Holzforschung* 60, 618-624.

Din, N., Gilkes, N. R., Tekant, B., Miller, R. C., Warren, A. J., and Kilburn, D. G. (1991). "Non-hydrolytic disruption of cellulose fibers by the binding domain of a bacterial cellulase," *Bio-Technol*. 9, 1096-1099.

Donaldson, L. A., Singh, A. P., Yoshinaga, A., and Takabe, K. (1999). "Lignin distribution in mild compression wood of Pinus radiata," *Can. J. Bot.* 77, 41-50.

Dokken, K. M., Davis, L. C., and Marinkovic, N. S. (2005). "Use of infrared microspectro-scopy in plant growth and development,' *Appl. Spectrosc. Rev.* 40, 301-326.

Duchesne, I., Takabe, K., and Daniel, G. (2003). "Ultrastructural localisation of glucomannan in kraft pulp fibres," *Holzforschung* 57, 62-68.

Ermel, F. F., Follet-Gueye, M. L., Cibert, C., Vian, B., Morvan, C., Catesson, A. M., and Goldberg, R. (2000). "Differential localization of arabinan and galactan side chains of rhamnogalacturonan I in cambial derivatives," *Planta* 210, 732-740.

Filonova, L., Kallas, A. M., Greffe, L., Johansson, G., Teeri, T. T., and Daniel, G. (2007). "Analysis of the surfaces of wood tissues and pulp fibers using carbohydrate-binding modules specific for crystalline cellulose and mannan," *Biomacromolecules* 8, 91-97.

Guglielmino, N., Liberman, M., Jauneau, A., Vian, B., Catesson, A. M., and Goldberg, R. (1997). "Pectin immunolocalization and calcium visualization in differentiating derivatives from poplar cambium," *Protoplasma* 199, 151-160.

Guillemin, F., Guillon, F., Bonnin, E., Devaux, M. F., Chevalier, T., Knox, J. P., Liners, F., and Thibault, J. F. (2005). "Distribution of pectic epitopes in cell walls of the sugar beet root," *Planta* 222, 355-371.

Hafrén, J. (2005). "Antibody-based assay for galacturonan deesterification on wood pulp fibers during bleaching," *J. Wood Sci.* 51, 655-658.

Hafrén, J., Daniel, G. (2003). "Distribution of methyl-esterified galacturonan in chemical and mechanical pulp fiber," *J. Wood Sci.* 49, 361-365.

Hildén, L., Daniel, G., and Johansson, G. (2003) "Use of a fluorescence labelled, carbohydrate-binding module from *Phanerochaete chrysosporium* Cel7D for studying wood cell wall ultrastructure,". *Biotechnol. Lett.* 25, 553-558.

Hoffmann, G. C., and Timell, T. E. (1972). "Polysaccharides in ray cells of compression wood of Red pine (*Pinus resinosa*)," *Tappi* 55, 871-873.

Hori, R., and Sugiyama, J. (2003). "A combined FT-IR microscopy and principal component analysis on softwood cell walls," *Carbohydr. Polym.* 52, 449-453.

Hult, E. L., Larsson, P. T., and Iversen, T. (2000). "A comparative CP/MAS C-13-NMR study of cellulose structure in spruce wood and kraft pulp," *Cellulose* 7, 35-55.

Jones, L., Seymour, G. B., and Knox, J. P. (1997) "Localization of pectic galactan in tomato cell walls using a monoclonal antibody specific to (1->4)-beta-D-galactan," *Plant Physiol.* 113, 1405-1412.

Knox, J. P. (1997). "The use of antibodies to study the architecture and developmental regulation of plant cell walls." In: *International review of cytology - a Survey of Cell Biology*, Academic Press, San Diego, Vol. 171 pp. 79-120.

Lafarguette, F., Leple, J. C., Dejardin, A., Laurans, F., Costa, G., Lesage-Descauses, M. C., and Pilate, G. (2004). "Poplar genes encoding fasciclin-like arabinogalactan proteins are highly expressed in tension wood," *New Phytologist* 164, 107-121.

Lappalainen, A., Tenkanen, M., and Pere, J. (2004). "Specific antibodies for immunochemical detection of wood-derived hemicelluloses." In: *Hemicelluloses: Science and technology*, ACS, Washington. Vol. 864 pp. 140-156.

Maeda, Y., Awano, T., Takabe, K., and Fujita, M. (2000). "Immunolocalization of glucomannans in the cell wall of differentiating tracheids in *Chamaecyparis obtuse*," *Protoplasma* 213, 148-156.

McCartney, L., Blake, A. W., Flint, J., Bolam, D. N., Boraston, A. B., Gilbert, H. J., and Knox, J. P. (2006). "Differential recognition of plant cell walls by microbial xylan-specific carbohydrate-binding modules," *Proc. Nat. Acad. Sci. USA* 103, 4765-4770.

McCartney, L., Gilbert, H. J., Bolam, D. N., Boraston, A. B., and Knox, J. P. (2004). "Glycoside hydrolase carbohydrate-binding modules as molecular probes for the analysis of plant cell wall polymers," *Anal. Biochem.* 326, 49-54.

McCartney, L., Marcus, S. E., and Knox, J. P. (2005). "Monoclonal antibodies to plant cell wall xylans and arabinoxylans," *J. Histochem. Cytochem.* 53, 543-546.

Nagy, N. E., Franceschi, V. R., Solheim, H., Krekling, T., and Christiansen, E. (2000). "Wound-induced traumatic resin duct development in stems of Norway spruce (Pinaceae): Anatomy and cytochemical traits," *Am. J. Bot*. 87, 302-313.

Newman, R. H. (2004). "Homogeneity in cellulose crystallinity between samples of *Pinus radiata* wood," *Holzforschung* 58, 91-96.

Pranovich, A., Konn, J., and Holmbom, B. (2006). "Methodology for chemical microanalysis of wood." In: *Proceedings of the 9th European Workshop on Lignocellulosics and Pulp (EWLP)*. University of Natural Resources and Applied Life Sciences (BOKU),Vienna. pp. 436-439.

Samuels, A. L., Rensing, K. H., Douglas, C. J., Mansfield, S. D., Dharmawardhana, D. P., and Ellis, B. E. (2002). "Cellular machinery of wood production: differentiation of secondary xylem in Pinus contorta var. latifolia," *Planta* 216, 72-82.

Serpe, M. D., Muir, A. J., and Driouich, A. (2002). "Immunolocalization of beta-D-glucans, pectins, and arabinogalactan-proteins during intrusive growth and elongation of nonarticulated laticifers in *Asclepias speciosa* Torr.," *Planta* 215,357-370.

Taylor, J. G., Haigler, C. H., Kilburn, D. G., and Blanton, R. L. (1996). "Detection of cellulose with improved specificity using laser-based instruments," *Biotechnic & Histochem*. 71, 215-223.

Thygesen, A., Oddershede, J., Lilholt, H., Thomsen, A. B., and Ståhl, K. (2005). "On the determination of crystallinity and cellulose content in plant fibres," *Cellulose* 12, 563-576.

Vreeland, V. (1970). "Localization of a cell wall polysaccharide in a Brown alga with labeled antibody," *J. Histochem. Cytochem.* 18, 371-373.

Washusen, R., and Evans, R. (2001). "The association between cellulose crystallite width and tension wood occurrence in *Eucalyptus globules*," *Iawa J.* 22, 235-243.

Waterkeyn, L., Caeymaex, S., and Decamps, E. (1982). "Callose in compression wood tracheids of Pinus and Larix," *Bull. Soc. R. Bot. Belg.* 115, 149-155.
Willats, W. G. T., Marcus, S. E., Knox, J. P. (1998). "Generation of a monoclonal antibody specific to (1->5)-alpha-L-arabinan," *Carbohydr. Res.* 308, 149-152.
Włoch, W., and Hejnowicz, Z. (1983). "Location of Laricinan in Compression Wood Tracheids." *Acta Soc. Bot. Pol.* 52, 201-203.

Article submitted: February 20, 2007; First round of revisions completed: April 2, 2007; Revised version received: May 5, 2007; Article accepted: May 10, 2007; Article published: May 25, 2007.

FLOCCULATION AND REDISPERSION OF CELLULOSIC FIBER SUSPENSIONS: A REVIEW OF EFFECTS OF HYDRODYNAMIC SHEAR AND POLYELECTROLYTES

Martin A. Hubbe

Cellulosic fibers in aqueous suspensions are subject to flocculation effects that involve two contrasting scales of dimension. The net effect of flocculation determines how uniformly fibers can become formed into a sheet during the manufacture of paper. At a macroscopic level, the highly elongated shape of typical wood-derived fibers in agitated suspensions can give rise to frequent inter-fiber collisions and the formation of fiber flocs. At a submicroscopic scale, surfaces of suspended materials can become joined by macromolecular bridges. Although such bridges tend to reduce paper's uniformity, polyelectrolyte flocculants are used in most paper machine systems to achieve relatively high retention efficiencies of fine particles as paper is being formed. By adjusting the papermaking equipment, judiciously selecting points of addition of chemicals, and by managing chemical dosages, papermakers employ a variety of strategies to achieve favorable combinations of retention and uniformity. This review considers scholarly work that has been directed towards a greater understanding of the underlying mechanisms.

Keywords: Flocculation, Cellulose, Fibers, Pulp, Suspensions, Polyelectrolytes, Hydrodynamic shear, Paper formation, Retention aids, Uniformity, Crowding, Selective detachment

Contact information: Department of Forest Biomaterials Science and Engineering, North Carolina State University, Campus Box 8005, Raleigh, NC 27695-8005 USA; hubbe@ncsu.edu

INTRODUCTION

The subject of flocculation of cellulosic fibers in aqueous suspensions is both fascinating and economically important. Certain aspects of the process have been called "paradoxical" (see Hubbe and Rojas 2005). Fiber flocculation appears to depend on phenomena occurring within two markedly different ranges of size. At a molecular scale, suspensions of cellulosic materials and fine particles are affected by short-range electrostatic, dispersion, and polymer bridging forces acting between surfaces. At a macroscopic scale, cellulosic fibers are sufficiently long, relative to their thickness, so that they tend to collide with each other in stirred suspensions. Though agitation also can play a role in separating fibers from one another, the distribution of cellulosic fibers in an agitated suspension is typically less uniformly distributed in space, compared to what would be predicted by a random number generator.

The term "flocculation" can be defined differently in each of the two size regimes just mentioned. At a molecular scale, where the focus is on the interactions between objects within about 100 nm of each other, "flocculation" can refer to the role of high-molecular-mass polyelectrolytes in forming bridges between surfaces. In this article the

word "colloidal" also will be used to refer to events occurring at a scale of nanometers. The words "agglomeration," and "deposition" will be used to refer to solid objects coming and remaining in contact, regardless of the cause. The word "coagulation" will be used to describe the effects of water-soluble chemicals such as aluminum sulfate or low-mass polyelectrolytes, which can bring about agglomeration as a result of charge neutralization or by means of localized electrostatic effects (Hogg et al. 1966; Hunter 1987). The term "flocculation," when it is used in reference to chemical effects, is usually reserved to describe the action of high-mass polyelectrolytes that can form strong bridges between surfaces (La Mer and Healy 1963; Gregory 1973, 1976). As will be described in greater detail, such bridges appear to break irreversibly, if the suspension encounters hydrodynamic forces of sufficient intensity and duration.

At a macroscopic scale the term "flocculation" can be used as a synonym for "the formation of clumps of fibers," regardless of the cause. As will become clear in the course of this review, macro-scale flocculation can occur for mechanical and hydrodynamic reasons, even if there is a net repulsion between the surfaces at a colloidal scale. Chemical treatments often can make macroscopic flocculation more intense than it would have been otherwise. This is especially true in the case of "flocculants" or "retention aids," which are other names used for the very-high-mass polyelectrolytes capable of forming macromolecular bridges.

Why Papermakers Care

Papermaking technologists have economic and practical reasons to be interested in flocculation. During conventional paper production, as well as during production of wet-laid non-woven fabrics, the papermaker attempts to avoid excessive flocculation or entanglement of the fibers (Rojas and Hubbe 2004). Paper that contains a lot of thick areas, due to the presence of flocs, also must contain a lot of thin, weak areas, adjacent to those flocs. Correlations between paper's strength and its uniformity have been predicted or shown in various studies (Linhart et al. 1987; Waterhouse 1993; Korteoja et al. 1997, 1998; Nazhad et al. 2000). Nonuniform paper also can hurt paper's appearance and adversely affect subsequent operations, such as coating (Hua et al. 1996). Various methods have been developed to quantify paper's uniformity (Norman and Wahren 1972; Peters 1997; Keller and Pawlak 2001; Bernié and Douglas 2001).

At the same time that papermakers are attempting to produce highly uniform paper, they also have a strong incentive to maintain a high efficiency of retention of fine particles. Such particles can include mineral "fillers," which often make up 10-25% of the mass of paper intended for printing. The diameters of typical filler particles lie in the range of about 0.25 to 5 μm, a size that is much too small to be retained by filtration by the forming fabrics used in paper manufacture (Van de Ven 1984). Other small particles in papermaking furnish can include fiber fines (*e.g.* parenchyma cells), and emulsion particles used for hydrophobizing or "internal sizing" of the paper. The chemical efficiency of such sizing agents can fall significantly if they are not retained during the first pass through the forming section of a paper machine. Unretained sizing agents can spend several additional minutes in contact with the aqueous solution or "white water" used in papermaking, causing the chemicals to become hydrolyzed (Savolainen 1996). In addition, non-retained fine materials can be wasteful, contributing to costs of wastewater

treatment and sludge disposal, as well as contributing to deposits that form on the wetted surfaces of process equipment.

The most common strategies used by papermakers to retain fine particle at high efficiency all involve very-high-mass polyelectrolytes, *i.e.* "retention aids" (Allen and Yaraskavitch 1989; Horn and Linhart 1991; Swerin and Ödberg 1997; Alfano et al. 1998; Norell et al. 1999; Tripattharanan et al. 2004a). The most commonly used retention aids consist of water-soluble cationic or anionic copolymers of acrylamide, having mean molecular masses in the range of about 4 million to 20 million Daltons. Use of such polymers can cause significant decreases in paper's uniformity, especially at excessively high retention aid dosages or when hydrodynamic shear forces are inadequate to break up the resulting flocs (Lindström et al. 1977; Jokinen and Ebeling 1985; Jokinen and Palonen 1986; Eisenlauer et al. 1987; Wågberg and Lindström 1987ab; Adamski et al. 1991; Horn and Linhart 1991; Swerin and Ödberg 1993, 1997; Swerin et al. 1996a; Swerin et al. 1997; Swerin 1998; Alfano et al. 1998; Clemençon and Gerli 2000; Hubbe 2000; Gruber and Müller 2001; Anker 2002; Solberg and Wågberg 2003). Chemically-induced increases in flocculation also tend to reduce the strength of the resulting paper (Roberts et al. 1986, 1987; Linhart et al. 1987).

An order-of-magnitude estimate can be made of the economic loss that results from paper's nonuniformity (see Hubbe 2005a). Nazhad et al. (2000) prepared laboratory sheets of paper having different uniformity. Uniformity was evaluated in terms root-mean-squared variations in basis weight of small areas, and compared to the tensile force required for breakage. By comparing their laboratory results to typical machine-made papers, it can be estimated that there is potential to achieve about 30% higher strength, if only the sheets were more uniform. According to Dodson and Serafino (1993), the variation of local basis weight of typical machine-made paper, on a scale of 1 mm, is about twice what would be obtained if the fiber had been laid in random positions. Using a more conservative number, let's suppose that it were possible to improve formation to such a degree that it was possible to reduce the basis weight of paper by 10% in a typical case. Since worldwide paper sales are in the neighborhood of 200 billion dollars per year, and because materials can make up a substantial part of the cost of paper (Diesen 1998), it follows that the annual value of improved formation might be in the range of 10-20 billion dollars.

A Working Hypothesis

The goals of this review can be stated in the form of a hypothesis, as follows: It is proposed that papermakers' success in meeting their goals within both size ranges of flocculation – molecular and macroscopic – requires optimization of sequential events. These events are affected by polyelectrolyte interactions, the ionic charges on various macromolecules and surfaces, hydrodynamic shear, and the effects of time. Though it is possible for paper technologists to optimize such parameters in an evolutionary manner, through incremental adjustments, a goal of this review is to show that the net results can be explained in mechanistic terms.

A second hypothesis will be proposed in order to answer the question, "In light of the complexity of papermaking systems, why have papermakers usually been quite successful in achieving favorable combinations of efficient fine-particle retention and

uniform formation?" The following two-part explanation will be supported by the literature:

1. Chemically-induced attachments between fibers can be broken at much lower levels of hydrodynamic shear stress compared to similar attachments of fine particles to fiber surface.
2. Attachments resulting from very-high-mass polyelectrolytes typically are somewhat irreversible, not capable of being formed again with the same strength after breakable of the initial contact.

Before evaluating the two hypotheses, as just given, one needs to understand something about the solid materials, the unit operations through which the fibers pass during the manufacture of paper, and various ways that fiber suspensions are affected by flow. These issues are considered in the following two sections.

CELLULOSE FIBER SUSPENSIONS – A PAPERMAKER'S PERSPECTIVE

Fibers from Wood

From a historical perspective the statement that "paper is made from trees" reflects relatively recent developments. Prior to 1775 most fibers used for papermaking originated from such sources as cotton, linen, or bark (Hunter 1947). To save costs, papermakers often used recycled textile fibers, *i.e.* rags. Rags continued to be a dominant source of papermaking fibers until about 1860, when wood pulp began to displace the dwindling rag supply. Advantages of wood as a fiber source for paper include its abundant supply, year-round availability, relatively high density, good storage stability, relative uniformity, and favorable ratio of fiber length to thickness. Issues related to the length-to-thickness ratio will be considered in a later section of this review.

Ways in which cellulosic fibers are separated from wood can play a significant role with respect to flocculation. Two main approaches, mechanical pulping and chemical pulping, are used to convert wood into its component fibers. Mechanical pulping most often involves abrading fibers from wood chips in the presence of water. The process is called "refining" when it takes place between the surfaces of steel plates, one of which is rotating (Smook 1992; Baker 1995). Raised rectangular bars on the plates squeeze and shear the woody material, causing fibers to separate. Considerable damage to the fibers occurs during mechanical pulping, yielding a broad range of sizes in the resulting suspension.

In an effort to preserve more of the initial fiber length of fibers, as was present originally in the wood, much of the mechanical pulping nowadays is done at raised temperatures. By carrying out the refining operation under pressure in the presence of steam, during so-called "thermo-mechanical pulping" (TMP), the lignin that holds fibers together in wood becomes softened (Back and Salmén 1982; Salmén et al. 1985), and the fibers can be separated with less shortening. Advantages of mechanical fibers, from a papermaker's standpoint, include their high yield, retaining over 90% of the solid material from wood chips. Disadvantages include a high requirement of electrical energy, relatively poor brightness stability, and limited strength characteristics. Factors

that limit the strength of paper made from TMP fibers include their relative non-conformability, shortened fiber length, and the presence of hydrophobic materials on the fiber surfaces. Fatty acids and esters, rosin acids (in the case of softwood fibers), and various unsaponifiable oils from wood are known to interfere with the development of hydrogen bonds between fibers when paper is dried.

Chemical pulping of wood chips, especially by means of the kraft process, has become the leading source of fibers for papermaking. From the standpoint of flocculation, some distinguishing characteristics of kraft fibers, relative to TMP fibers, include greater preservation of fiber length, less debris, greater flexibility (especially after refining), and a more hydrophilic surface. Tam Doo and Kerekes (1982) observed that chemical pulp fibers were 20 to 30 times more flexible that mechanical pulp fibers from the same wood source. The sodium hydroxide and sodium sulfide used in a kraft cook tend to solubilize lignin, the phenolic glue that holds fibers together in wood. Most of the extractable, relatively hydrophobic components of wood are likewise removed, partly by saponification and partly in the formation of soap-stabilized emulsion droplets. Subsequent multi-stage bleaching of kraft fibers with such materials as chlorine dioxide, oxygen, ozone, and hydrogen peroxide, usually with at least one alkaline extraction stage and several washing operations, results in a purification of the fibers, leaving behind mainly the relatively hydrophilic polysaccharide components of the fiber. Despite the removal of carboxylic acid species during kraft pulping and various types of bleaching operations, cellulosic fibers upon their arrival at paper mills typically still have a weak negative charge when they are placed in water (Herrington and Petzold 1992; Lloyd and Horne 1993).

To achieve an optimum balance of the paper's strength, apparent density, and appearance characteristics, kraft fibers are subjected to different levels of refining after the pulping process is completed. The mechanical compression and shearing of kraft fibers in a refiner results in internal delamination, making the fibers more flexible (Paavilainen 1993). Whereas the cross-section of an unrefined kraft fiber often can be described as rectangular or "rounded," refining allows the fibers to collapse into a ribbon-like form. A broad contact between fibers in paper yields greater density and higher strength.

Fiber length is a key factor related to fiber flocculation (see next section). Refining can affect fiber length in two ways. First, refining sometimes straightens bent or kinked fibers, increasing their end-to-end distance (Ny and Messmer 2004). The effect can be compared to the straightening that occurs when a long balloon becomes filled with air. However, unlike such a balloon, fibers remain relatively constant in length due to the predominantly length-wise orientation of most of the cellulose fibrils. As it is being refined, the fiber takes up increasing amounts of water, becoming more swollen. Second, depending on the intensity of refining, some of the fibers may be broken or "cut" (Baker 1995). The word "intensity" refers to the quotient of mechanical energy expended during a given time period, divided by the number of individual impacts between fibers and the edges of the bars within the refiner. A relatively high intensity of refining is more likely to result in forces that exceed the tensile strength of a fiber. By refining fibers at a lower intensity it is usually possible to develop bonding strength with less reduction in fiber length (Corson 2002; McDonald et al. 2004).

Unit Operations of Papermaking

During a typical papermaking operation, a suspension of fibers passes through a series of unit operations. Table 1 describes the main function of such operations in a typical, but relatively simple paper machine system. The table also lists an estimated level of hydrodynamic shear stress, and a statement about how the operation is likely to affect the uniformity of the resulting paper.

Table 1. Unit operations of a typical paper machine, their functions, hydrodynamic shear levels, and expected effects on paper uniformity

Unit Operation	Function	Hydrodynamic Shear (Pa)	Effects on Paper Uniformity
Machine chest	Provide and mix a supply of papermaking materials	"Low"	Chemicals added early in the process have less effect on paper uniformity.
Tickle refiner	Allow operators to shorten fibers and slow rate of dewatering	"Highest"	Shorted fibers have a reduced tendency to form flocs.
Fan pump	Dilute the stock from about 4% solids to about 0.5% solids	20,000 *	The diluted stock has a much reduced tendency to form flocs.
Hydrocyclone cleaners	Remove heavy grit, sand, *etc.*	"Very high"	Intense shear can break down high molecular mass polyelectrolytes.
Pressure screens	Remove large objects, e.g. incompletely pulped fiber bundles	10,000 *	Fibers have to pass individually through the screen slots.
Headbox tube expansions	Deflocculate the suspension	"High"	Extensional flow is effective in disrupting fiber flocs.
Headbox slice	Accelerate the jet of stock onto the forming fabric	100 *	The shear flow results in some fiber alignment in the machine direction.
Free jet of stock	Fibers in web start to become immobilized	"Very low"	Fiber flocs partly re-form within the free jet.
Jet impingement onto forming fabric(s)	Adjustments in relative speed of jet and fabric can affect web structure	"High"	"Rushing" or "dragging" can break up fiber flocs. **
Hydrofoils of forming blades	Vacuum and pulsations cause more rapid release of water from paper web	500 *	Foils under forming fabric can moderately improve formation uniformity. ***

* Tam Doo et al. (1984)
** Svensson and Österberg 1965; Parker 1972; Manson 1996; Swerin and Mähler 1996; Swerin and Ödberg 1996
*** Walser et al. 1970; Kiviranta and Paulapuro (1992); Eames 1993; Schiher and Getman 1994; Manson 1996; Condon 1996; Södergren and Neun (2000); Norman 2000; Keller and Lucas (2002)

The item called "pressure screens" in Table 1 deserves comment. As stated in the table, only individual fibers can pass through the openings of a typical pressure screen used in a paper machine system. However, such fibers can have various fine particles attached to them. For example, a fiber with attached calcium carbonate particles would not be disadvantaged in any way from passing through the screen. On the other hand, the

hydrodynamic shear might cause some of the fine particles to be dislodged. Papermakers can fine-tune the results of their operation by choosing to add a high-mass flocculant either before or after a pressure screen (Hubbe and Wang 2002). Issues of this nature will be considered in detail later in this article (see Selective Detachment).

In addition to the functions listed in Table 1, the unit operations of papermaking also provide the operators with numerous potential points of addition for chemical additives. By selecting different points of addition, the operator can, in effect, choose the conditions of mixing, the length of time that each chemical will be exposed to the fiber suspension before formation of paper, and also the maximum shear stress to which the additives are likely to be exposed. An optimum sequencing of the chemical additives, relative to existing unit operations, can have large influences on process efficiency and product quality (Wågberg and Lindström 1987; Swerin et al. 1993; Åsselman and Garnier 2001; Hubbe and Wang 2002; Hubbe 2005b).

What All Has to Come Together

Let's suppose that you are on a team that has been asked to improve the recipe and addition points for chemical additives needed to make certain grade of paper. The team's assignment is to improve the paper's uniformity, while still maintaining good retention and keeping other properties the same. In such a situation it can be useful to imagine an ideal, exceptionally high-quality wet-web of paper coming off of a forming fabric. Next, one works backwards and thinks about the preceding steps that must have occurred in order to reach that point. The following list summarizes some attributes of the wet web of a typical grade of paper or paperboard that might have earned it the description of "exceptionally high quality:"

1. A near-random (or better) spatial distribution of fibers in the X-Y plane
2. Suitably low levels of either fiber clumps or void areas associated with fiber flocculation (especially in size range of 1-10 mm)
3. A high percentage of attachment to long fibers by any fine, particulate material present in the mixture, ensuring efficient retention in the web of paper
4. A fine, porous structure of the wet web that allows relatively rapid release of water by gravity and hydrofoil action, while avoiding large pinholes that would adversely affect the efficiency of vacuum dewatering

In order for any papermaking strategy to achieve all four of the listed objectives simultaneously, it would need to take into account factors acting at both the colloidal and the macroscopic ranges of size. The complexity of the situation can be appreciated if one examines a statement such as "let's just apply sufficient hydrodynamic shear just before the slurry leaves the headbox so that all of the solids are dispersed from each other and the paper is completely random." As described in the following section, one of the problems with the previous statement is that flocs in a fiber slurry can form again within milliseconds (Farnood et al. 1993; Condon 1996), though details of the shear-history of the fibers can affect the results. Another issue to be concerned with is that complete dispersion of all of the fine particulate matter from fiber surfaces and from agglomerates of particles can be expected to reduce the efficiency of retention during the forming

process (Van de Ven 1984). Further issues related to the statement in quotes will be considered in subsequent sections.

Developers of papermaking chemicals might consider a different possibility while reading the remaining parts of this article. Suppose that it were possible to design a chemical additive that selectively causes agglomeration or deposition of very fine materials, such as sizing agent particles and filler particles, and suppose that the chemical has very little tendency to aggravate the flocculation of fibers. Such a strategy would be expected to achieve at least the first three objectives of the preceding list. All that remains to be done is to invent that chemical.

Yet another scenario to keep in mind, especially when reading the later parts of this article, is whether it is possible to design chemical treatments that allow the solid components of paper to come back together efficiently and remain attached just as the paper sheet is in the process of dewatering. As will be described, such a scenario may be important with respect to item 4 of the preceding list. However, before considering such possibilities, the next section will consider factors that affect fiber flocculation in the absence of chemical treatments.

UNAVOIDABLE, BUT MANAGEABLE: FLOCCULATION AS A MECHANICAL PHENOMENON

Crowding

Imagine a single, straight fiber of length l suspended in a fluid undergoing laminar shear flow. The word shear implies a steady gradient of velocity as one moves in a direction perpendicular to the streamlines of flow. As has been shown (Adler et al. 1981; Takamura et al. 1981), such a fiber will tend to rotate about its center as it responds to the flow around it. Next, imagine a suspension composed of such fibers. As one might anticipate, the rotating motions of adjacent fibers easily can result in mutual collisions.

As a first attempt at predicting how the attributes of fiber suspensions might affect the likelihood of inter-fiber collisions, Mason (1954) defined a critical fiber concentration (CFC). The concept is illustrated in Fig. 1. As shown, at the CFC each fiber has just enough surrounding space so that it can rotate about its center in any direction without experiencing any collisions. The regular, non-overlapping spacing depicted in Fig. 1 is not intended to be realistic. Nevertheless, the concept has been shown to be useful in predicting volume-concentration C_V for which inter-fiber collisions are either relatively rare ($C_V < CFC$) or increasingly frequent ($C_V > CFC$).

A further logical step, still based on the situation described in Fig. 1, involves the concept of a crowding factor, N_c (Kerekes and Schell 1992; Kerekes 1995). If two fiber suspensions have the same value of N_c, then they are expected to have about the same tendency to form flocs resulting from flow-induced collisions. The crowding factor has been defined as follows,

$$N_c = 2/3\ C_v\ (L/d)^2 \quad (1)$$

where C_v is the volume fraction of fibers, L is fiber length, and d is fiber diameter.

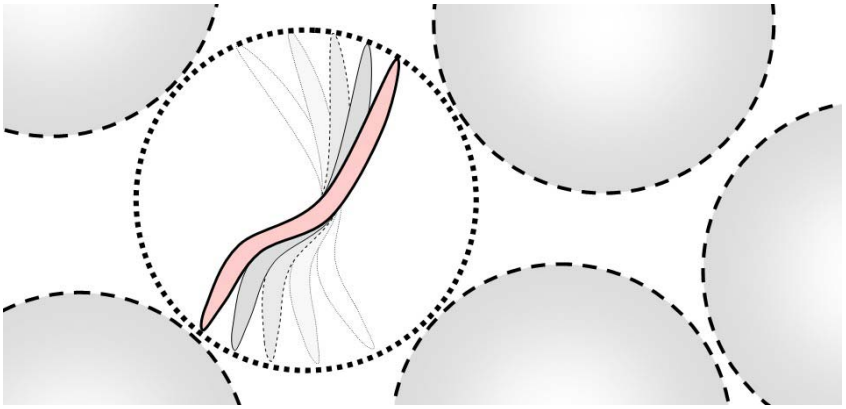

Fig. 1. Schematic illustration of the volume required for individual fibers to rotate freely without colliding with neighboring fibers

Based on Eq. (1) it would be expected that flocculation ought to increase as the first power of the solids content and as the second power of the ratio of length to thickness of the fibers. It has been found that with increasing values of N_c within the range 1 to 60, the frequency of collisions increases from occasional to frequent, and for $N_c > 60$, the contact amount fibers in a stirred suspension becomes almost continuous and persistent flocs become apparent. To place these numbers into context, the value of N_c in the approach flow to most paper machine forming sections is in the upper quadrant of the "occasional to frequent" collision range (Kerekes and Schell 1992). In other words, papermakers face the challenge of preparing a relatively uniform product *despite* the fact that the component fibers are frequently colliding with their neighbors as a result of flow. Though it is theoretically possible for papermakers to form paper from much more highly dilute suspensions, the amount of pumping and the size of equipment required for such practices is usually considered to be cost-prohibitive. Recent efforts have been aimed at applying Eq. (1) in the case of mixtures of different sizes of fibers with improved precision (Huber et al. 2003).

Fiber Collisions in Real Systems

Given the simplifying assumption that were made in the derivation of Eq. (1), one should not be too surprised to find ways in which real fiber slurries show deviations, *e.g.* cases where suspensions having equal values of N_c show different flocculation tendencies. Table 2 lists some characteristics of fiber suspensions that either increase or decrease the tendency of a fiber suspension to flocculate, relative to what would be predicted based on the N_c value of a typical fiber suspension.

Locking of Fibers into Persistent Flocs

Only on a rare occasion would a paper machine superintendent permit a visitor to lean over the moving fabric upon which paper is being formed. Not only is the situation dangerous, but anything falling from the visitor's pocket might tear a hole in the fabric or damage a press roll, causing thousands of dollars in repair costs, plus the value of lost production time. We are all very fortunate that such permission was granted to Farnood *et al.* (1993). These researchers used dual-laser light backscattering to observe the state

Table 2. Factors that tend to Increase of Decrease Flocculation in Comparison to the Predictions of the Crowding Factor Equation

Increased Flocculation	**Literature References**
Persistent curl in the fibers	Beghello and Eklund 1997
Unusually high length-to-thickness ratio	Beghello and Eklund 1997
Long fibers present in a mixture	Egelhof 1972; Kerekes and Schell 1992
Wider length distribution with same mean	Kropholler and Sampson 2001
High level of surface fibrillation	Stoere et al. 2001
Increased fiber stiffness	Kerekes and Schell 1995; Dodson 1996
Increased temperature (lower viscosity)	Egelhof 1972
Decreased Flocculation	
Increased fiber flexibility	Beghello and Eklund 1997; Kerekes 1995; Ross and Klingenberg 1998; Wikström and Rasmuson 1998
Unusually low length to thickness ratio	Kerekes and Schell 1992; Kerekes 1995
Presence of debris, acting as a lubricant	Peterson 1994; but see also Beghello 1998
Unequal sized objects	Mason 1954; Van de Ven and Mason 1981
Increased fluid viscosity	Kerekes 1995

of flocculation within the jet of papermaking furnish at different locations between the headbox slice opening and the early parts of a forming fabric. As the suspension emerged from the slice opening, the fibers appeared to be well dispersed. But when the researchers moved the laser just 100 cm downstream from the slice opening (less than 0.1 seconds later in the process), the fibers already had become substantially flocculated. Condon (1996) reported similar observations in which the fibers in a jet of stock became substantially reflocculated within 75 mm of the slice opening, corresponding to about 12 milliseconds of elapsed time.

When explaining the observations just described, it is usual first to refer to the frequencies of inter-fiber collisions, as summarized in the previous subsection. However, the crowding factor, by itself, cannot explain how flow-induced fiber flocs can be strong enough to persist through the forming operation and end up in the finished paper. The dramatic change from a high state of dispersion to a state in which the fibers appear to be "locked" into flocs calls for a more complete explanation.

As proposed by Meyer and Wahren (1964), Chang and Robinson (1967), and Parker (1972), a fiber subjected to hydrodynamic shear becomes momentarily bent, and an instant later it can become locked together with other fibers while trying to straighten itself out. Floc structures formed in this manner appear to be held together by the stored elastic energy in the partially bent fibers, in combination with inter-fiber friction (Kerekes et al. 1985; Farnood et al. 1994; Andersson et al. 1999; Schmid and Klingenberg 2002; Björkman 2003; Gosz et al. 2003; Swerin and Ödberg 1997). The validity of the mechanism is supported by the fact that flocs do not form readily when the solution phase viscosity is increased (Beghello 1998); higher viscosity presumably prevents fibers from snapping back into shape quickly enough to interlock the system. In addition, fiber flocs tend to form most prominently just beyond a point where shear stresses are reduced (Jacquelin 1968; Björkman 2003; Kerekes et al. 1985).

Figure 2 illustrates some of the simplest flocs that could be formed by this "bend and then lock into flocs" mechanism (Parker 1972). While the simple structures shown in Fig. 2 can help illustrate the mechanism, observations of stirred fiber suspensions make it clear that typical flow-induced fiber flocs can involve large numbers of fibers. Yeung et al. (1997) envisioned a process in which structural members of a floc rearrange themselves and gradually densify under continued hydrodynamic shear.

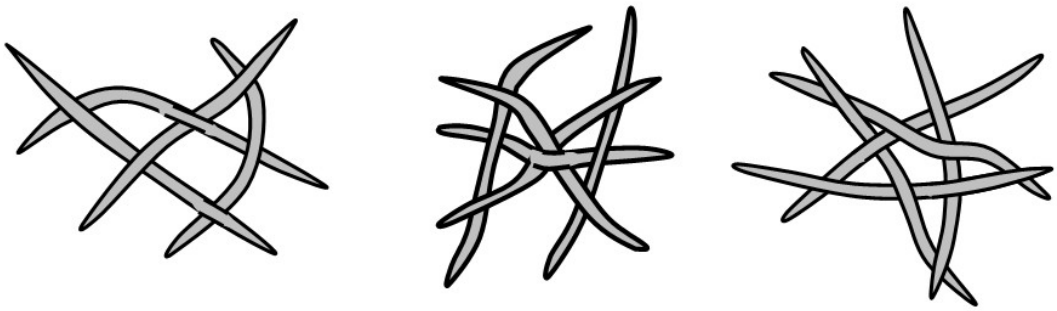

Fig. 2. Illustration of three of the simplest self-locking flocks, according the Parker (1972).

Healing

Though less obvious in comparison to the flocculation and locking mechanisms described in the previous two subsections, a phenomenon called "healing" or "smoothing" tends to make the resulting paper somewhat more uniform than it would have been otherwise (Gorres et al. 1986; Norman et al. 1995; Norman 2000). Imagine a paper test sheet being formed on a screen from a highly dilute slurry of flocculated fibers. Already there are some fibers resting on the screen surface. As other fibers and fiber flocs approach the screen, the flow veers around the already occupied areas of screen surface (Sampson 1997). Relatively few fibers "land" on the part of the screen already occupied by fiber flocs, due to the greater flow resistance in those locations. In the case of handsheets, some authors have suggested that such a healing effect can result in paper that is significantly more uniform than would have resulted from a completely random placement of fibers (Norman et al. 1995; Norman 2000). Under typical machine-made papermaking conditions, it appears that healing effects usually are obscured by the fore-mentioned flocculation effects (Sampson et al. 1995).

Flow and the Transient Breakdown of Flocs

If one thinks in terms of the "spring-loaded" nature of fiber flocs, resulting from the flow-induced bending and subsequent straightening, then it stands to reason that continuing exposure to hydrodynamic forces of similar intensity ought to be able to overcome the bending forces that hold flocs together. Studies have identified two main ways in which shear flow tends to break down fiber flocs (Pandya and Spielman 1982; Lee and Brodkey 1987). On the one hand, fibers may be eroded from the surface of a floc (Healy and La Mer 1964; Spicer and Pratsinis 1996). On the other hand, a floc may be split in two (Kolmogorov 1949; Hinze 1955; Higashitani et al. 1989). Investigators have proposed quasi-equilibrium states in which the rates of floc formation and destruction are balanced (Kaji et al. 1991; Spicer and Pratsinis 1996).

Because shear flow results when fluid flows parallel to a surface, *e.g.* in the case of flow within a pipe, it is important to consider how effectively shear flow can break up fiber flocs. Two main disadvantages can be expected if one relies just on shear flow to break up flocs. First, as already has been described, the "bend, straighten and lock" mechanism will continue to produce additional flocs, possibly resulting in a dynamic equilibrium. Another problem is that shear flow, instead of "pulling" directly on a floc, will tend to make it rotate (Adler et al. 1981: Takamura et al. 1981), a factor that tends to lessen the tensile force exerted by the flow.

Much more effective disruption of fiber flocs can occur if a fiber suspension experiences extensional flow, a condition in which there is a gradient of velocity *parallel* to the streamlines of flow (Kerekes 1983; Higashitani et al. 1989; Li et al. 1995; Li and Ödberg 1997; Shah 2002). Extensional flow can manifest itself, for instance, when fluid passes into an opening or at an expansion in a tube. Kerekes (1983) showed that fiber flocs passing into a tube tended to become greatly elongated, almost to the breaking point. Contractions in flow channels also have been found to be extremely effective for stretching and breaking macromolecules (Nguyen and Kausch 1992), an effect that is attributed to extensional flow. Transient extensional flow events also occur within turbulent flow (Liu and Glasgow 1997); however such events appear to be of too brief duration to be highly effective in fragmenting flocs (Wagle et al. 1988).

There are three critical points in the papermaking process at which papermakers take particular advantage of extensional flow effects in ways that tend to pull fiber flocs apart.

1. The pressure screens in a typical paper machine system give rise to extensional flow as the suspension is forced to pass through small slots or holes (Bliss 1996). Flow accelerates and then decelerates as an element of liquid enters and emerges from an opening in the screen. The effect on fiber flocs is further enhanced by the fact that the openings in the screen are designed to be just large enough to permit passage of individual fibers, due to their size and flexibility.
2. Extensional flow effects are imposed upon fiber suspensions within the tube banks on the intake side of certain hydraulic headboxes (Kiviranta and Paulapuro 1990; Bonfanti et al. 2000). The tubes are intended to deliver uniform flow, pressure, and velocity across the width of a paper machine forming section. By designing sudden expansions within such tubes, fiber flocs can be pulled apart more effectively.
3. Perhaps most importantly, the velocity of flow becomes accelerated considerably as it passes through the headbox slice, which functions something like a nozzle. The strong alignment of fibers (Ulmar and Norman 1997), as well as the elongation of flocs (Praast et al. 1998), in the direction of manufacture of machine-made papers appears to originate partly due to extensional flow during passage through the slice. The observations, cited earlier, of substantial absence of fiber flocs immediately after the slice opening can be viewed as a testament to the effectiveness of such extensional acceleration in disrupting fiber flocs. One has to be careful, however, since acceleration of flow within a nozzle *also* imparts hydrodynamic shear, which is maximized at the fixed surfaces, and it was noted

earlier that such shear flow will tend to bend fibers, making it more probable that they become locked together as flocs a moment later.

"Passive" is perhaps the best adjective to describe the approach that paper machine operators take with respect to the three phenomena mentioned above. Once a paper machine has been installed, there is no easy way to make significant adjustments to the workings of a certain pressure screen, the design of the tubes entering the headbox, or the shape of the slice. Papermakers can take a more active roll when they adjust the relative angle and velocity at which the jet of furnish lands on the surface of a forming fabric. A relatively shallow angle of impact, often described as "velocity forming," is least disruptive to the nascent fiber mat structure within the jet. A relatively steep impact, often called "pressure forming," gives the papermaker an opportunity to break up fiber flocs, though there is no guarantee that the net effects of pressure forming will be favorable in terms of customer requirements.

By adjustments of the fan pump flow, as well as adjustments in the pressure within the headbox system, papermakers can fine-tune the jet velocity. Many papermakers prefer to "drag" the jet of fiber, meaning that the forming fabric velocity is a few percent higher than that of the jet (Svensson and Österberg 1965; Parker 1972; Manson 1996; Swerin and Mähler 1996; Swerin and Ödberg 1996). The velocity difference not only tends to reduce the flocs in the paper, but also, there is an increased tendency for fibers to become aligned in the direction of manufacture. Such alignment of fibers in shear flow has been documented in a variety of systems (Stover et al. 1992; Orts et al. 1995). The same effects often can be achieved by "rushing" the sheet, a condition in which the jet velocity is faster than that of the fabric. Similar principles apply in the case of so-called "twin-wire" or "gap former" paper machines (Swerin and Mähler 1996), especially when one takes into account the fact that, for reasons of stability, the jet usually first impinges onto one fabric surface, before it comes into contact with the other.

Management of Vortex Flow

Before turning to chemical aspects of fiber flocculation, there is one more physical effect that can give papermakers a degree of control over the uniformity and structure of a paper sheet. That is, one needs to be aware of a tendency for vortex cells of flow to form having their axis in the direction of manufacture (Aidun 1996, 1998). Such vortices arise spontaneously in response to such factors as the abrupt cessation of shear at the upper and lower surfaces of the jet of suspended fibers as it emerges from a headbox slice (Söderberg and Alfredsson 1997). Such vortices can interact with adjacent vortices in complex ways as a paper web gradually becomes dewatered on a Fourdrinier paper machine. It is sometimes possible to minimize machine-directional basis weight or moisture streaks by adjusting the position on the forming table at which sufficient water has been removed to essentially "freeze" the basic structure of the sheet. Alternatively, more serious streakiness may persist in the product in cases where the structure becomes immobilized at a point where certain vortices having different wavelengths happen to reinforce each other.

The fact that shear flow tends to align fibers in the direction of manufacture has important implications relative to flocculation. If there were a way to choreograph fibers

such that they all rotated in parallel orbits, then the frequency of inter-fiber collisions would be reduced considerably. This is, of course, an idealization. Turbulent components of flow, which are expected to cause chaotic fiber motions, are unavoidable within the ranges of jet velocities and jet dimensions associated with modern papermaking. Waterhouse (1993) observed that handsheets formed under oriented flow conditions, presumably leading to fiber alignment, had much more uniform formation, compared to standard handsheets formed from suspensions of similar consistency. Recent progress has been demonstrated by a system in which a degree of twist is imposed upon the flow within the inlet tubes to a hydraulic headbox (Islek et al. 2004). Reported improvements in formation uniformity in such systems supports the idea that inter-fiber collisions and floc development were somehow decreased by controlling the orientations of fiber rotation.

FLOCCULATING EFFECTS OF CHEMICAL ADDITIVES

Evidence that Polyelectrolytes Can Act like Bridges

As mentioned in the introduction, adding polyelectrolytes having very high molecular mass to a suspension of cellulosic fibers often increases the observed degree of flocculation. Increased strength of flocs and fiber networks also has been demonstrated, resulting from such treatments (Swerin et al. 1992). Commercial acrylamide-based retention aid products can be describes as "huge," having molecular masses generally in the range of about 4 to 20 million Daltons. Acrylamide copolymers having up to 10% cationic monomer groups are especially popular, since they adsorb readily onto the negatively charged surfaces of cellulosic fibers. Given the fact that most papermakers add either aluminum compounds, polyamines, or cationic starch at some point in the process, anionic copolymers of acrylamide also function very well as retention aids in many papermaking systems.

Use of the term "bridging" to describe the action of very-high molecular mass polyelectrolytes goes back to work by La Mer and Healy (1963) and Gregory (1976). These investigators noted that the very large molecules were able to agglomerate suspended solids even in cases where the average electrostatic repulsions between predominantly negatively charged surfaces would have been sufficient to inhibit inter-particle collisions. Observed agglomeration rates were consistent with a model in which each suspended particle was only partly covered by polyelectrolyte at the point of maximum agglomeration (Fleer and Lyklema 1974; Gregory 1976). In certain cases it was possible to observe rates of flocculation in excess of what could be achieved by simple ions; these effects were attributed to the extension of polymer tails out from the solid surfaces (Gregory 1973). Flocculation was found to decrease with time, following addition of the polyelectrolyte solution (Gregory and Sheiham 1974; Forsberg and Ström 1994). This effect was attributed to macromolecular fragmentation or gradual flattening of the adsorbed conformations. The fact that flocculating ability increased markedly with molecular mass was taken as further evidence that the mechanism involved the ability of single macromolecules to bridge the space between pairs of suspended objects, essentially adsorbing onto two surfaces at once.

Figure 3, an illustration of macromolecular bridging flocculation, emphasizes certain aspects of the process. First, there tends to be more attachment of fine particles on fibrils of a cellulosic fiber, rather than onto the main part of the fiber (Haslam and Steele 1936; McNeal et al. 2005). One way to understand this trend is based on a hydrodynamic lubrication effect, whereby particles of unequal size that are on a collision course in shear flow tend to deviate from their undisturbed streamlines, due to the viscosity of the fluid between them (Mason 1954; Brenner 1968; Adler et al. 1981; Van de Ven and Mason 1981). Another way to picture what is happening is that the fibrils tend to intercept strands of the polyelectrolytes due to relative flow past the fiber surface. The entrapped macromolecules or strands of macromolecules then can act like a sort of fishnet, trapping fine particles (Lindström and Glad-Nordmark 1984). Whatever the explanation, it can be shown that the resulting attachments, in the wet state, are much stronger in comparison to what can be achieved by simple ions (Hubbe 1987ab).

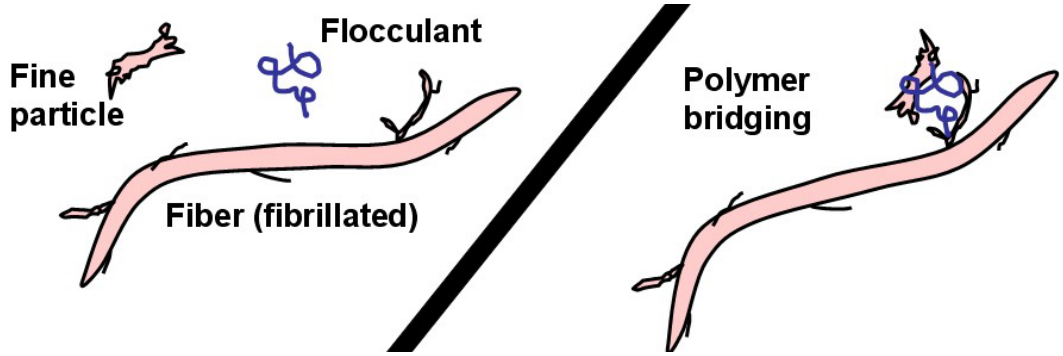

Fig. 3. Illustration of the term "bridging" as it is applied to the flocculating action of polyelectrolytes having very high mass

In addition to "strong," the word "brittle" also can be used to describe the macromolecules that form polymeric bridges. Studies have shown that agitation of fiber suspensions flocculated by very-high-mass polyelectrolytes tends to reduce the mean molecular mass substantially (Sikora and Stratton 1981; Tanaka et al. 1993; Forsberg and Ström 1994). Once bridge-type attachments are broken, any fiber flocs that form subsequently will not be of as high strength (Unbehend 1976; Hubbe 2000a). Unbehend (1976) defined the term "hard flocs" to describe the structures formed as a result of very-high-mass polyelectrolyte addition. The brittle nature of such polymer bridges can be rationalized based on the very large chain lengths of the polyelectrolyte molecules that can adsorb simultaneously onto two surfaces in an extended, three-dimensional manner. To place things into perspective, if a retention aid molecule were as thick and angel-hair spaghetti, its fully extended length would span a football field.

Paper that is formed from flocculated fiber suspensions tends to be weak. In a revealing set of experiments, Roberts et al. (1986, 1987) observed that paper's tensile strength either decreased, increased, or stayed about the same, depending on how long a fiber suspension was mixed following treatment with cationic starch, a well-known dry-strength agent. To explain the results, it was noted that initial introduction of the cationic starch solution produced extensive flocculation. Continued agitation appeared to

gradually break the chemical-induced attachments between fibers, resulting in a well-dispersed suspension.

Various factors affect both the efficiency of cationic acrylamide copolymer retention aids and their tendency to flocculate fiber suspensions. The effectiveness of such polyelectrolytes can be significantly reduced if substantial amounts of negatively charged colloidal materials are present in the process water (Krogerus 1993; Dunham et al. 2000). The cationic macromolecules appear to form complexes with the anionic colloidal material, rather than interacting efficiently with fiber and particle surfaces. In such cases, retention aid efficiency often can be substantially improved by pretreating the system with a high-charge cationic additive (Wågberg and Ödberg 1991; Swerin et al. 1996b; Dunham et al. 2000). In addition to neutralizing the colloidal material in the mixture, the high-charge cationic additives also can cause the subsequently added cationic retention aid molecules maintain more extended conformations in the adsorbed state (Swerin et al. 1996b). When papermakers employ anionic acrylamide copolymers as retention aids, retention performance similarly can be enhanced by pretreating the system with something that is strongly cationic (Allen and Yaraskavitch 1989; Petzold et al. 1996; Petzold 1999). The cationic additives, after becoming adsorbed, appear to provide sites on the solid surfaces, to which the subsequently added anionic retention aid molecules can attach. Retention aid efficiency also tends to decrease as the salt concentration becomes relatively high (Buontempo et al. 1996), an effect that most likely can be attributed to decreased molecular extension in the adsorbed state (Fleer et al. 1993; Wågberg 2000).

Effects of Charged Patches Formed by Polyelectrolytes

Given the evidence that bridging-type flocculants can markedly decrease paper's uniformity, papermakers have had a strong incentive to consider additives that function in a somewhat different way, while still contributing to the retention of fine particles. Studies have shown that the highly branched, highly cationic macromolecule polyethyleneimine (PEI) tends to adsorb onto surfaces in a patch-like manner (Pfau et al. 1999; Horn 2001). As suggested by Fig. 4, such patches on cellulosic fibers, latex binders, and other negatively charged matter would be expected to act as isolated areas of positive charge. In theory, the presence of oppositely charged patches on surfaces within a suspension can be expected to promote agglomeration of the suspension (La Mer and Healy 1963; Kasper 1971; Gregory and Sheiham 1974; Sandell and Luner 1974). To the degree that the term "patch" is valid, one would expect such agglomeration to be reversible in the presence of varying degrees of hydrodynamic shear. In other words,

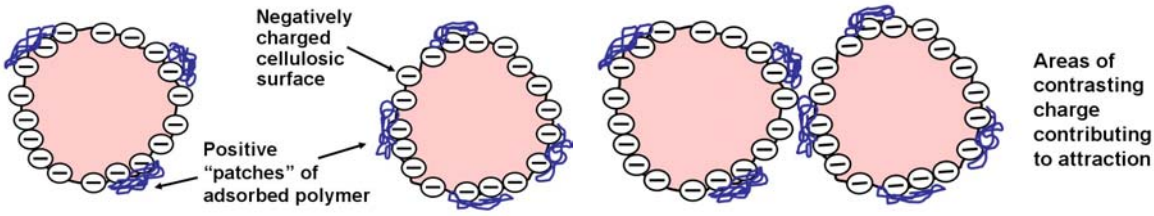

Fig. 4. Illustration of the "charged patch" mechanism of polyelectrolyte adsorption and subsequent coagulation of suspended solids by electrostatic attraction

vigorous agitation might be expected to redisperse solids that had become agglomerated due to a charged-patch mechanism, but the suspension would be expected to agglomerate again when hydrodynamic forces are reduced.

In support of the "charged patch" mechanism of agglomeration, Goossens and Luner (1976) flocculated microcrystalline cellulose (MCC) by addition of poly-ionene, having a molecular mass of 60,000 Daltons. Based upon the fact that the maximum in flocculation did not correspond to zero zeta potential, these authors, as well as others (Beck et al. 1977; Petzold 1999), have concluded that charged patches must be involved. The tendency for the MCC to agglomerate decreased with continued agitation, consistent with a process of gradual spreading out of the polymer over the available surfaces. In an indirect demonstration of the same concept, Das and Lomas (1973) treated some of the fine matter from a papermaking system with moderate-mass PEI, essentially making those particles into solid patches of charge, and having the opposite charge compared to other surfaces in the suspension. The resulting flocs were much stronger than would have been expected based on neutralization of charges.

Jokinen and Palonen (1986) found that high-charge, moderate-mass cationic polyelectrolytes were able to retain fine materials with relatively little adverse effect on paper's uniformity. However, such additives were not able to achieve the high levels of retention efficiency that were obtained with very-high-mass retention aids. More recently, Tripattharanan et al. (2004b) observed efficient retention of fiber fines and precipitated calcium carbonate filler particles following treatment of a fiber suspension with a copolymer of ethyleneimine (modified PEI) having a molecular mass of approximately 2 million Daltons. Such molecular masses are considerably lower than those that have been proposed for bridging interactions between surfaces.

Charge Neutralization and Retention of Colloidal Matter

There is abundant evidence to support a "charge neutralization" mechanism of agglomeration, *i.e.*, coagulation (Hogg et al. 1966; Alince and Robertson 1974; Walkush and Williams 1974; Stratton and Swanson 1981). However, the ways in which coagulation affects papermaking operations can be subtle (Bjellfors et al. 1965). The idea is that elimination of electrostatic forces of repulsion allows the ever-present and attractive London dispersion forces to become dominant (Hunter 1987). Studies suggest that charge neutralization, by itself, as well as suppressing of charge effects by salt addition, usually has little effect on the uniformity of machine-made paper (Mason 1950; Beghello and Eklund 1999). Pelton (1993) suggested that the apparent ineffectiveness of London dispersion forces in flocculating cellulosic suspensions may be due to a high level of fibrillation of the surfaces, on a nanometer scale. The water-loving polysaccharide chains at the cellulosic surfaces would be expected to offer a very low Hamaker coefficient, and also tend to sterically stabilize the systems. Nevertheless, charge neutralization may play a critical role in the retention of colloids, including the very small filler particles, droplets of hydrophobic sizing agents, macromolecules, and the like.

One can envision the retention of colloidal matter during papermaking as a two-step process. In the first step, the very small particles become agglomerated together into larger entities or become deposited onto cellulosic surfaces. Marton (1974) showed that

the effective surface area per unit mass of cellulosic fines within typical papermaking furnish can be about 3 to 5 times larger than that of the longer fibers. Because cellulosic fines often make up between 5 and 25% of the mass of paper, depending on the pulping and refining processes, one can expect a charge neutralization strategy to result in large proportion of colloidal matter becoming deposited onto the surfaces of cellulosic fines. Thus, the second step of the process of retaining colloidal matter involves retaining the fiber fines. Some fiber fines can be retained by mechanical filtration during paper formation; however, papermakers increasingly are relying upon the use of retention aid polymers, as described in the previous two subsections.

To back up the statement that charge neutralization has relatively little effect on fiber flocculation and fines retention, Tripattharanan et al. (2004b) conducted experiments with a refined bleached hardwood kraft suspension that contained 45% fiber fraction, 25% fiber fines, and 30% precipitated calcium carbonate (PCC) by mass. The electrical conductivity was adjusted to 1000 μS/cm using sodium sulfate. Fine-particle retention efficiency was evaluated under a variety of hydrodynamic conditions, simulating different aspects of the papermaking process. A neutral charge condition was obtained, as confirmed by microelectrophoresis, by addition of 0.1% moderate-mass poly-DADMAC, dry basis. No significant differences were observed in the turbidity of filtrate when comparing results in the presence or absence of poly-DADMAC addition.

In another set of tests, a suspension was prepared with 0.5% bleached chemithermomechanical pulp (BCTMP) pulp solids and 0.05% ground calcium carbonate (Hubbe 2000). The suspension was treated at different levels of poly-DADMAC, except that the molecular mass was higher than in the previous instance. Relatively weak fiber flocs were observed, using an optical method; however the strength of the flocs was too low to detect by means of a viscometric method. There was a maximum in the degree of flocculation if the poly-DADMAC dosage was just enough to achieve a zeta potential of zero. The relative weakness of the flocs, as well as the fact that they were maximized at the neutral point, suggests either a charged patch mechanism or a charge neutralization mechanism.

SELECTIVE DEFLOCCULATION

Papermakers appear to benefit from a kind of natural selection. As stated earlier (see "A Working Hypothesis"), it has been proposed that chemically induced linkages between fibers tend to be broken at lower levels of hydrodynamic force, compared to similar linkages between fibers and small particles, or between small particles attached to other relatively small objects. In view of the concepts outlined in the previous section, the hypothesis given earlier now can be stated in chemical, as well as mechanical terms. Thus, it can be proposed that when papermakers use very-high-mass retention aids under optimum conditions, the macromolecular bridges are strong enough to hold fine particles onto other various surfaces, but bridges between pairs of fibers become irreversibly broken. Before considering how different types of chemical effects and surface forces might or might not be compatible with this concept, the following subsection will

consider some mechanical factors that appear to favor this kind of mechanism in the case of typical papermaking fiber suspensions.

Implications of Sizes, Shapes, and Flows

Several authors have explained the general principle that fibers in an agitated suspension are more susceptible to becoming separated by hydrodynamic forces, in comparison to smaller objects that are attached to fibers or to each other (McKenzie 1968; King and Williams 1975; Stratton 1983; Hubbe 1984, 1986; Hubbe and Wang 2002). To rationalize this effect in quantitative terms it is necessary to consider both the sizes and the shapes of different solid entities present in a typical papermaking furnish. Realizing that mechanical pulp mixtures can comprise an extremely diverse range of sizes, the following analysis will be based on a typical hardwood kraft pulp furnish. Let us further assume that this furnish also contains calcium carbonate filler particles having a mean diameter of 2 μm.

Before considering the extent to which the elongated shapes of papermaking fibers affects their susceptibility to be separated by hydrodynamic forces, it is already possible to make some initial estimates based on the contrasting sizes of fibers *vs.* fine material. Consider the situation diagrammed in Fig. 5. The figure depicts a spherical particle adhering to a rough, planar surface that is exposed to shear flow. Even if the prevailing flow environment can be described as turbulent, it makes sense to envision flow adjacent to a surface as being part of a viscous sublayer, in which the momentary fluid motion can be described in terms of a laminar shear field (Cleaver and Yates 1973; Hubbe 1984).

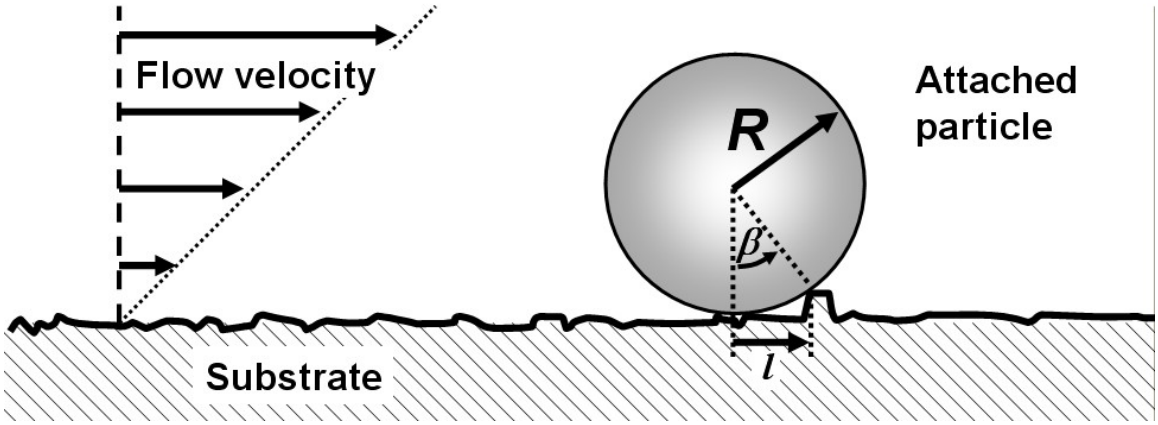

Fig. 5. Geometric model of spherical particle exposed to shear flow, to account for minimum hydrodynamic shear stress needed to cause detachment by a rolling mechanism

According to one theory, the ability of a particle to resist becoming rolled from its point of attachment depends on (a) the maximum attractive force between the particle and substrate during the process of detachment, (b) the particle size, and (c) the size of the area of contact, which is assumed to be governed by the scale of roughness on each of the solid surfaces (Hubbe 1984). Assuming that the origin of the interactive forces holding particles onto the substrate are independent of particle size, it can be shown that the attractive force ought to be proportional to the diameter of the object that is being

modeled as a sphere (Hogg et al. 1966). The hydrodynamic force, acting to push the particle parallel to the substrate is given by the following equation (Goldman et al. 1967; O'Neill 1968),

$$F = 32.06\, R^2\, \tau_o\,, \qquad (2)$$

where R is the particle radius and τ_o is the hydrodynamic shear stress at the substrate surface. Because we are interested in determining the minimum shear stress at which an attached particle begins to roll, it is also possible to estimate the torque that will result from a given level of hydrodynamic shear stress. The hydrodynamic torque can be expressed as follows:

$$T = 43.92\, R^3\, \tau_o \qquad (3)$$

To complete the analysis, it is necessary to make a reasonable estimate of a length scale of the contact region, as indicated by the parameter l in Fig. 5 (Hubbe 1984). It follows from the figure that l is given by

$$l = R \sin \beta = R\, [\, (2H/R) + (H^2/R)\,]^{1/2}\,, \qquad (4)$$

where β is the angle shown in the figure and H is the height of a typical bump on the substrate that defines the length of the "level arm" l, tending to resist a rolling motion of the particle. At the limit of low roughness, the second term within the brackets can be neglected, and the expression can be combined with (3) to give a critical shear stress corresponding to detachment by rolling,

$$\tau_o^* = F_{adhesive}\, l\, /\, (43.9\, R^3) \propto R\, R^{1/2} / R^3 \propto R^{-3/2} \qquad (5)$$

Experimental verification of Eq. (5) was obtained in the case of different uniformly sized populations of spherical titanium dioxide particles being detached from cellulosic film and glass substrates (Hubbe 1985). The results support the statement that higher shear stress is required to cause rolling detachment of smaller particles from a surface.

The next step is to consider the shapes of entities that are to be detached by flow. Figure 6 compares two objects. The first is a roughly spherical object having the same radius as that of the cross-section of a typical hardwood fiber. The second object represents a hardwood fiber having one end projecting outwards into the solution phase. Let us suppose, for example, that the fiber is about 50 times as it is wide and that the tip of the fiber projects ten fiber widths away from the "crossing point" at which it is in contact with another fiber. The hydrodynamic torque exerted on the fiber, in comparison to that exerted on the spherical object, can be estimated from

$$T_{fiber} = T_{sphere} \int_0^{10} L\, dL = \tfrac{1}{2}\, 10^2\, T_{sphere} = 50\, T_{sphere} \qquad (6)$$

To estimate the ratio of shear stress required to detach the fiber, shown in Fig. 5, in comparison to a typical filler particle having a radius of 1 μm, one combines the results expressed in equations (5) and (6).

$$\text{Ratio} = (20\ \mu\text{m} / 2\ \mu\text{m})^{1.5} \times 50 \approx 1600 \quad (7)$$

This result, though very approximate, suggests that a much more intense flow would be required to detach a filler particle from a fiber surface, in comparison to the flow event required to detach two fibers from one another, assuming that the forces holding the objects together have similar origin.

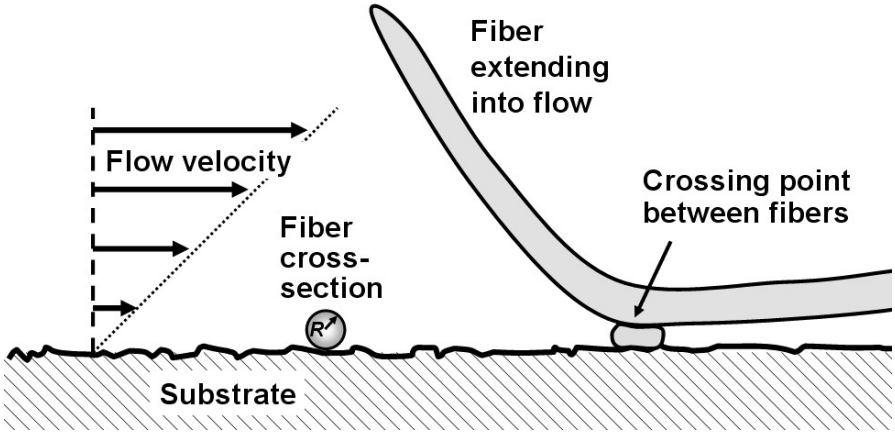

Fig. 6. Geometric diagram to compare the torque exerted by hydrodynamic shear on a particle of radius *R* versus a fiber having a similar cross-section

Evidence of Selective Deflocculation

Relatively little research has been published to demonstrate that fine particles are indeed less likely to be detached by hydrodynamic shear, compared to the separation of pairs of fibers. An exception is one study in which a slurry of bleached chemithermomechanical pulp and ground calcium carbonate filler was treated with a very-high-mass cationic acrylamide copolymer (Hubbe 2000). It was shown that fiber flocs were substantially broken down by passing the suspension through a peristaltic pump. After exposing the fibers to a kitchen blender, the chemically-induced flocs were irreversibly broken, and the degree of fiber flocculation was not significantly different than that of an untreated suspension. However, even the high level of shear stress in the blender apparently was not sufficient to dislodge the filler particles from the fiber surfaces under the conditions of treatment. Measurements of filtrate sampled with a 100-mesh screen before or after shearing in the blender, showed essentially the same strong reduction in turbidity with increasing dosage of the cationic flocculant added to the system.

FLOC REVERSIBILITY

Near the beginning of this article it was proposed to envision an ideal web of paper. It might seem, following the discussion in the previous section, that many of the preconditions required for producing an ideal web might be achieved by judicious use of a high-mass flocculating polymer, followed by a well-chosen level of hydrodynamic shear. However, such a strategy still does not fully address the fourth precondition on the earlier list, *i.e.* "a fine, porous structure of the wet web that allows relatively rapid release of water by gravity and hydrofoil action, while avoiding large pinholes that can adversely affect the efficiency of vacuum dewatering." Lindström (1989) suggested that the key to achieving this further goal involves reversibility of the chemical-induced attachments among solid surfaces in the papermaking suspension. In other words, one makes use of colloidal attractions between the solids to increase the effect of friction between the wetted surfaces (Andersson et al. 2000; Zauscher and Kingenberg 2000). Then, during the formation and initial dewatering of the wet web of paper, the surfaces will tend to remain joined at the points of initial contact, rather than sliding around to form a dense, relatively impermeable mat.

Experimental Verification of Floc Reversibility

Hedborg and Lindström (1996) carried out pioneering work showing that the reversibility of chemically-induced flocculation can depend on the type of chemical treatment. Tests were carried out according to the "Dynamic Drainage/Retention Jar" method of Britt and coworkers (Britt 1973; Britt and Unbehend 1976), with some key modifications. In a departure from the original procedure, Hedborg and Lindström compared the solids level of the filtrate obtained when the fiber mixture was first agitated at a higher speed, versus the solids level obtained after the agitation speed had been decreased. A reversibility index was defined as

$$I_{\text{rev}} = (B - A) / (C - A) \quad (8)$$

where A is the fine particle retention efficiency at the higher agitation level, B is the retention efficiency after a combined exposure to high shear, followed by lower shear, and C is the retention efficiency in the case of steady agitation at a lower level. In each case the agitation scheme was applied after the suspension had been treated with one of more chemical additive.

Based on analyses of this type it was concluded that certain microparticle retention aid treatment programs yielded more reversible flocculation, in comparison to treatment just with very-high-mass polyelectrolyte flocculants. In other words, it was concluded that the solid surfaces were able to come back together and "stick," after being separated, in the case of treatments that included microparticles or nanoparticles, such as colloidal silica. Other researchers similarly have documented a greater ability of microparticle-type additive systems to reflocculate fiber suspensions after dispersion in shear (Swerin et al. 1993; Swerin et al. 1997; Hubbe 2001). Mechanisms related to the use of such microparticles have been described in other publications (Langley and Litchfield 1986; Anderson and Lindgren 1996; Wågberg et al. 1996; Åsselman and Garnier 2000, 2001; Hubbe 2005b). Briefly stated, it appears that sequential treatment by

polymeric flocculants, high levels of hydrodynamic shear, and then addition of highly negatively charged colloidal particles can result in systems that favor gentle reattachment of the solid surfaces after shear, without causing excessive re-flocculation of the fibers.

In the case of treatment with cationic acrylamide copolymers, work by Ericksson and Alm (1993) showed that the degree of reversibility of flocculation can depend on the polyelectrolyte's charge density (Ericksson and Alm 1993). Bridge-type behavior, including irreversible breakdown of the flocs by shear, was found for copolymers having 10% or less of cationic monomeric groups. Systems treated with higher-charge flocculants came together again after being mechanically dispersed. Results can be interpreted in terms of a more extended adsorbed conformation of the lower-charged polyelectrolytes (Fleer et al. 1993; Wågberg 2000).

Though less attention has been paid recently to such issues, it is also well known that the "charged patch" and "charge neutralization" mechanisms of chemically-induced agglomeration also display characteristics of reversibility (Blanco et al. 2002). As noted by Horn and Linhart (1991), the ability of relatively low-mass, high-charge cationic polymers to agglomerate suspensions of negatively charged particles usually is maximized at a zeta potential near to zero. By contrast, increasing levels of very-high-mass flocculants usually achieve very high levels of agglomeration long before the neutral point of surface charge has been reached.

Inter-fiber Friction and Forces of Attraction

The relationship between friction and colloidal forces was studied in detail by Zauscher and Klingenberg (2000, 2001). The goal of the study was to account for the ability of carboxymethylcellulose (CMC) to prevent excessive entanglement during extrusion of mixtures containing long fibers at relatively high solids levels. Results showed that adsorption of CMC not only reduced friction between cellulosic surfaces to a low level, but it also resulted in long-range forces of repulsion. In effect, the big, water-loving molecules prevented close approach of the surfaces. These results help to explain the function of "formation aids" of the type often used during the production of paper and wet-laid nonwoven fabrics (Erspamer 1940; Swanson 1950; Wasser 1978; Lee and Lindström 1989; Keith 1994; Hutton 1995; Giri et al. 2000). Such additives can make it possible to achieve well-formed sheets from fibers having much higher length-to-thickness ratios compared to wood fibers. However, the high cost of formation aids, as well as their adverse effect on dewatering rates has been enough to discourage papermakers from employing similar strategies for conventional paper production.

Another way to quantify effects related to inter-fiber friction is by measuring the volume occupied by a specified quantity of fibers that are allowed to freely settle in an unstirred graduated cylinder (Kline 1967; Alince and Robertson 1974; Gruber et al. 1997). Studies of this nature have shown repeatedly that maximum sediment volumes tend to be associated with levels of chemical treatment that are just sufficient to neutralize the effect of electrostatic repulsions between the solids. It has been proposed that charge neutralization can increase the dewatering rate of papermaking furnish by allowing fine particles to coagulate onto the surfaces of fibers, rather than being free to move through the web of paper to points where they tend to clog passageways of flow (Hubbe 2002). This mechanism, together with the more bulky structure of the mat,

achieved by the frictional effects, may account for the effectiveness of highly charged cationic polymers when they are used as dewatering aids (Allen and Yaraskavitch 1991).

SUMMARY: A PRESCRIPTION FOR UNIFORMITY AND EFFICIENCY

In summary, there are a variety of strategies that papermakers can employ in order to achieve favorable combinations of product uniformity and efficient retention of fine particles. As noted earlier, an ideal wet web ought to have a highly uniform spatial distribution of fibers, an absence of basis weight variations in the size range of about 1 to 10 mm, efficient attachment of fine particles onto cellulosic surfaces, and a fine-scale, porous structure.

Paper machine systems and chemical additive programs can vary considerably, depending on the vintage of the equipment, the nature of the fibers, and the types of paper being produced. Detailed chemical recipes and preferred addition points and dosages of each additive need to be optimized for each specific case. Nevertheless, the work cited in this review suggests a generalized strategy, as follows:

1. To the degree that paper property requirements permit, employ fiber blends that are rich in hardwood, which tends to have a lower length-to-thickness ratio than softwood. Also, the fibers are smaller, tending to produce smaller flocs at the same value of the crowding factor N_C.
2. Optimize the degree of mechanical refining of pulp to achieve inter-fiber bonding, while increasing fiber flexibility. The level of refining often will be constrained by a tendency for reduced rates of dewatering, higher apparent density of the paper, and other related effects with increased refining.
3. When using very-high-mass retention aids, select the addition point and dosage such that the remaining unit operations before the forming zone (including such items as pressure screens, tube expansions, the slice, and jet impingement) impart just enough shear to substantially disperse the fibers from each other, while failing to dislodge most of the fine particulate matter that may be clinging to fiber surfaces.
4. Employ drainage-aid strategies, possibly allowing an increase of the paper machine's fan pump flow, resulting in a lower consistency at the headbox and a lower crowding factor N_C. A key constraint is whether the headbox can handle the additional flow without producing undesirable wake effects in the forming zone. Also, while the maximum speeds of some paper machines can be limited by the dewatering rate, this is not true of all paper machines. As mentioned in earlier sections, drainage strategies can be based on treatments with high-charge cationic polyelectrolytes or aluminum compounds. Certain microparticle treatment programs have the potential to accelerate dewatering rates significantly.
5. Employ a variety of equipment-related strategies, as mentioned in earlier sections. For example, fine-tune the jet-to-wire speed difference, adjusting the state of rush or drag. Adjustments also can be made to the spacing or types of foils or forming blades over which the forming fabric travels.

6. Continue to optimize the system, based on customer feedback, realizing that there are many cases in which the best running conditions, from the customer's standpoint, may fail to coincide with conditions that produce the paper having the most uniform appearance.

Returning to the two hypotheses given near the start of this article, some summary comments can be made in closing. The first hypothesis stated that papermakers need to optimize a sequence of events involving both submicroscopic and macroscopic scales of action. This statement appears to be well supported by the published literature in those cases where papermakers employ very-high-mass polyelectrolytes as retention aids. There is little doubt that both chemical and mechanical factors play a roll in determining paper's uniformity. In the absence of retention aid use, the situation probably was best summed up by Mason (1950), who stated that mechanical and hydrodynamic factors can overwhelm effects of chemical additives. That statement, however, preceded the development of modern retention aid polymers (Schiller and Suen 1956).

A second hypothesis proposed that papermakers' relative success in achieving quite favorable combinations of product uniformity, in addition to efficient retention of fine particles, is due to the fact that fibers can be detached from each other by flow events that are not sufficiently intense to dislodge fine particles from each other or from the fiber surfaces. This hypothesis was found to agree with some approximate calcula-tions, and also to be consistent with various published findings. The mechanism suggests, however, that it might be possible to develop retention aid systems that are more highly tuned in terms of providing a predictable strength of attachment between solid objects in the papermaking furnish. Such developments can be expected to make future papermakers yet more successful in their quest to retain fine particles efficiently, while producing uniform paper.

REFERENCES CITED

Adamsky, F. A., Gibbon, D. L., Simon, G. L., and Williams, R. H. (1991). "Retention mechanisms using a unique dual polymer approach," *Proc. TAPPI 1991 Papermakers Conf.,* TAPPI Press, Atlanta, 469-479.

Adler, P. M., Takamura, K., Goldsmith, H. L., and Mason, S. G. (1981). "Particle motions in sheared suspensions. 30. Rotations of rigid and flexible dumbbells (theoretical)," *J. Colloid Interface Sci.* 83(2), 502-515.

Aidun, C. K. (1996). "A fundamental opportunity to improve paper forming," *Tappi J.* 79(6), 55-60.

Aidun, C. K. (1998). "Quantitative evaluation of the forming jet delivered from four different hydraulic headboxes using high speed digital imaging," *Tappi J.* 81(4), 172-179.

Alince, B., and Robertson, A. A. (1974). "Aggregation of microcrystalline cellulose with polyethylenimine," *Colloid Polymer Sci.* 252, 920-927.

Allen, L. H., and Yaraskavitch, I. (1989). "Dual polymer retention aids – A review," *TAPPI Retention and Drainage Short Course Notes,* TAPPI Press, Atlanta, 59-63.

Allen, L. H., and Yaraskavitch, I. M. (1991). "Effects of retention and drainage aids on paper machine drainage: A review," *Tappi J.* 74(7), 79-84.

Alfano, J. C., Carter, P. W., and Gerli, A. (1998). "Characterization of the flocculation dynamics in a papermaking system by non-imaging reflectance scanning laser microscopy (SLM)," *Nordic Pulp Paper Res. J.* 13(2), 159-165.

Alince, B., and Robertson, A. A. (1974). "Aggregation of microcrystalline cellulose with polyethyleneimine," *Colloid Polym. Sci.* 252, 920-927.

Andersson, K. and Lindgren, E. (1996). "Important properties of colloidal silica in microparticulate systems," *Nordic Pulp Paper Res. J.* 11(1), 15-21, 57.

Andersson, S. R., Nordstrand, T., and Rasmuson, A. (2000). "The influence of some fiber and solution properties on pulp fiber friction," *J. Pulp Paper Sci.* 26(2), 67-71.

Andersson, S. R., Ringnér, J., and Rasmuson, A. (1999). "The network strength of non-flocculated fiber suspensions," *Nordic Pulp Paper Research J.* 14(1), 61-70 (1999).

Anker, L. S. (2002). "Practical experiences in additive screening using a torque-based flocculation analyzer," *Tappi J.* 1(6), 3-8.

Åsselman, T., and Garnier, G. (2000). "The role of anionic microparticles in a poly (acrylamide)-montmorillonite flocculation aid system," *Colloids Surf. A* 170(2/3), 79-90.

Åsselman, T., and Garnier, G. (2001). "The flocculation mechanism of microparticulate retention aid systems," *J. Pulp Paper Sci.* 27(8), 273-278.

Back, E. L., and Salmén, N. L. (1982). "Glass transitions of wood components hold implications for molding and pulping processes," *Tappi* 65(7), 107-110.

Baker, C. F. (1995). "Good practice for refining the types of fiber found in modern paper furnishes," *Tappi J.* 78(2), 147-153.

Beck, U., Müller, F., Goossens, J. W. S., Rohleff, E., and Tretter, H. (1977). "Theoretical and practical contributions to clearing up retention problems," *Wochenbl. Papierfabr.* 105(11/12), 391-398.

Beghello, L. (1998). "Some factors that influence fiber flocculation," *Nordic Pulp Paper Res. J.* 13(4), 274-279.

Beghello, L., and Eklund, D. (1997). "Some mechanisms that govern fiber flocculation," *Nordic Pulp Paper Res. J.* 12(2), 119-123.

Beghello, L., and Eklund, D. (1999). "The influence of the chemical environment on fiber flocculation," *J. Pulp Paper Sci.* 25(7), 246-250.

Bernié, J.-P., and Douglas, W. J. M. (2001). "Effect of a wet-end additive on the components of formation of tissue," *Proc. TAPPI Papermakers Conf.*, TAPPI Press, Atlanta, electronic document.

Bjellfors, C., Eriksson, K.-E., and Johanson, F. (1965). "Influence of cations on cellulose fiber networks," *Svensk Papperstidn.* 68(24), 865-869.

Björkman, U. (2003). "Break-up of suspended fiber networks," *Nordic Pulp Paper Res. J.* 18(1), 32-37.

Blanco, A., Fuente, E., Negro, C., Monte, M. C., and Tijero, J. (2002). "Focused beam reflectant measurement as a tool to measure flocculation," *Tappi J.* 1(10), 14-20.

Bliss, T. (1996). "Screening in the stock preparation system," *TAPPI Stock Preparation Short Course Notes*, TAPPI Press, 171-193.

Bonfanti, J. -D., Roux, J. -C., and Rueff, M. (2000). "Hydraulic headbox S – Technology and industrial results," *Wochenbl. Papierfabr.* 128(20), 1372-1375.

Brenner, H. (1968). "The slow motion of a sphere through a viscous fluid towards a plane surface," *Chem. Eng. Sci.* 16(3-4), 242-251.

Britt, K. W. (1973). "Mechanisms of retention during paper formation," *Tappi* 56(10), 46-50.

Britt, K. W., and Unbehend, J. E. (1976). "Mew methods of monitoring retention," *Tappi* 59(2), 67-70.

Buontempo, J. T., Sherman, L. M., and St. John, M. R. (1996). "Effects of salts on the performance of cationic flocculants used as retention aids for alkaline fine paper," *Proc. TAPPI 1996 Papermakers Conf.*, TAPPI Press, Atlanta, 49-58.

Chang, M. Y., and Robertson, A. A. (1967). "Flocculation studies of fiber suspensions: Influence of zeta potential," *Pulp Paper Mag. Can.* 68(9), T438-T444.

Cleaver, J. W., and Yates, B. (1973). "Mechanism of detachment of colloidal particles from a flat substrate in a turbulent flow," *J. Colloid Interface Sci.* 44(3), 464-474.

Clemençon, I., and Gerli, A. (2000). "Effect of flocculant/microparticles retention programs on floc properties," *Paper Technol.* 41(8), 25-33.

Condon, M. (1996). "Mechanical aspects of forming and formation," *Proc. TAPPI 1996 Papermakers Conf.*, TAPPI Press, Atlanta, 253-273.

Corson, S. R. (2002). "Process impacts on mechanical pulp fiber and sheet dimensions," *Pulp Paper Can.* 103(2), 20-27.

Das, B. S., and Lomas, H. (1973). "Flocculation of Paper Fines. I. Adsorption of and Flocculation by Polyelectrolytes. II. Study of the Nature of the Solid Surface and Soluble Impurities," *Pulp Paper Mag. Can.* 74(8), 95-100.

Diesen, M. (1998). *Economics of the Pulp and Paper Industry*, Papermaking Sci. Technol. Ser., Book 1, Fapet Oy, Helsinki, Finland.

Dodson, C. T. J. (1996). "Fiber crowding, fiber contacts, and fiber flocculation," *Tappi J.* 79(9), 211-216.

Dodson, C. T. J., and Serafino, L. (1993). "Flocculation, dispersion and dynamic scenarios for formation," *Nordic Pulp Paper Res. J.* 8(2), 264-272.

Dunham, A. J., Tubergen, K. R., Govoni, S. T., and Alfano, J. C. (2000). "The effect of dissolved and colloidal substances on flocculation of mechanical pulps," *J. Pulp Paper Sci.* 26(3), 95-101.

Eames, J. (1993). "Modified foil blade design improves forming table drainage, turbulence," *Pulp Paper* 67(4), 45-48.

Egelhof, D. (1972). "Flocculation in streaming fiber suspensions," *Wochenbl. Papierfabr.* 100(13), 494-499.

Eisenlauer, J., Horn, D., Linhart, F., and Hemel, R. (1987). "Fiber-optic flocculation sensor for on-line control of retention and drainage aids efficiency," *Nordic Pulp Paper Res. J.* 4(4), 132-138.

Ericksson, L., and Alm, B. (1993). "Effects of polyelectrolyte characteristics and flocculation conditions on fine particle floc properties," *Nordic Pulp Paper Res. J.* 8(1), 153-159,175.

Erspamer, A. (1940). "The flocculation and dispersion of papermaking fibers," *Paper Trade J.* 110(June 13), 33-38.

Farnood, R. R., Loewen, R. R., and Dodson, C. T. J. (1993). "Forming and formation of paper," in *Products of Papermaking*, Proc. 10th Fund Res. Symp., Oxford, 1993, C. F. Baker (ed.), Vol. 1, 183-208.

Farnood, R. R., Loewen, S. R., and Dodson, C. T. J. (1994). "Estimation of intra-floc forces," *Appita* 47(5), 391-396.

Fleer, G. J., Cohen Stuart, M. A., Scheutjens, J. M. H. M., Cosgrove, T., and Vincent, B. (1993). *Polymers at Interfaces*, Chapman and Hall, London.

Fleer, G. J., and Lyklema, J. (1974). "Polymer adsorption and its effect on the stability of hydrophobic colloids. II. The flocculation process as studied with the silver iodide-polyvinyl alcohol system," *J. Colloid Interface Sci.* 46(1), 1-12.

Forsberg, S., and Ström, G. (1994). "The effect of contact time between cationic polymers and furnish on retention and drainage," *J. Pulp Paper Sci.* 20(3), J71-J76.

Giri, M., Simonsen, J., and Rochefort, W. E. (2000). "Dispersion of pulp slurries using carboxymethylcellulose," *Tappi J.* 83(10), 58 [electronic document].

Goldman, A. J., Cox, R. G., and Brenner, H. (1967). "Slow viscous motion of a sphere parallel to a plane wall. II. Couette flow," *Chem. Eng. Sci.* 22(4), 653-660.

Goossens, J. W. S., and Luner, P. (1976). "Flocculation of Microcrystalline Cellulose Suspensions with Cationic Polymers: Effect of Agitation," *Tappi* 59(2), 89-94.

Gorres, J., Grant, R., Cresson, T., and Luner, P. (1986). "Effect of drainage on randomly formed papers: Simulation study," *Tappi J.* 69(7), 104-105.

Gosz, M., Nair, S., Cassel, K., and Alkhader, M. (2003). "A computational model for predicting the behavior of pulp fibers in shear-driven flows," *Proc. TAPPI 2003 Spring Tech. Conf.*, electronic doc., TAPPI Press, Atlanta.

Gregory, J. (1973). "Rates of flocculation of latex particles by cationic polymers," *J. Colloid Interface Sci.* 42(2), 448-456.

Gregory, J. (1976). "The effect of cationic polymers on the colloidal stability of latex particles," *J. Colloid Interface Sci.* 55(1), 35-44.

Gregory, J., and Sheiham, I. (1974). "Kinetic aspects of flocculation of a polystyrene latex by cationic polymers," *Br. Polymer J.* 6(1), 47-59.

Gruber, E., Gelbrich, M., and Schempp, W. (1997). "Morphological and chemical factors affecting dewatering," *Wochenbl. Papierfabr.* 125(2), 66-72.

Gruber, E., and Müller, P. (2001). "Investigations of the flocculation behavior of microparticle retention systems," *Proc. TAPPI 2001 Papermakers Conf.*, electronic doc., TAPPI Press, Atlanta.

Haslam, J. H., and Steele, F. A. (1936). "The retention of pigments in paper," *Tech. Assoc. Papers* 19, 249-252.

Healy, T. W., and La Mer, V. K. (1964). "The energetics of flocculation redispersion of polymers," *J. Colloid Sci.* 19(4), 323-332.

Hedborg, F., and Lindström, T. (1996). "Some Aspects on the Reversibility of Flocculation of Paper Stocks," *Nordic Pulp Paper Res. J.* 11(4), 254-259.

Herrington, T. M., and Petzold, J. C. (1992). "An investigation into the nature of charge on the surface of papermaking woodpulps. 2. Analysis of potentiometric titration data," *Colloids Surf.* 64(2), 109-118.

Higashitani, K., Inada, N., and Ochi, T. (1989). "Floc breakup in contraction flow to orifice," presented at AICHE Ann. Mtg., San Francisco.

Hinze, J. O. (1955). "Fundamentals of the hydrodynamic mechanism of splitting in dispersion processes," *AIChE J.* 1(3), 289-295.
Hogg, R., Healy, T. W., and Fuerstenau, D. W. (1966). "Mutual coagulation of colloidal dispersions," *Trans. Faraday Soc.* 62(6), 1638-1651.
Horn, D. (2001). "Exploring the nanoworld of interfaces and their functions during paper manufacturing and upgrading," *Wochenbl. Papierfabr.* 129(23/24), 1589-1596.
Horn, D., and Linhart, F. (1991). "Retention Aids," in *Paper Chemistry*, J. Roberts (ed.), Blackie, Glasgow, Chapter 4, 44-62.
Hua, X., Tanguy, P. A., Li, R., and van Wagner, J. S. (1996). "Effect of basestock formation on paper coating," *Tappi J.* 79(5), 112-115.
Hubbe, M. A. (1984). "Theory of detachment of colloidal particles from flat surfaces exposed to flow," *Colloids Surf.* 12(1-2), 151-178.
Hubbe, M. A. (1985). "Detachment of colloidal hydrous oxide spheres from flat solids exposed to flow. 2. Mechanism of release," *Colloids Surf.* 16(3-4), 249-270.
Hubbe, M. A. (1986). "Retention and hydrodynamic shear," *Tappi J.* 69(8), 116-117.
Hubbe, M. A. (1987a) "Detachment of colloidal hydrous oxide spheres from flat solids exposed to flow. 3. Forces of adhesion," *Colloids Surf.* 25(2-4), 311-324.
Hubbe, M.A. (1987b). "Detachment of colloidal hydrous oxide spheres from flat solids exposed to flow. 4. Effect of polyelectrolytes," *Colloids Surf.* 25(2-4), 325-339.
Hubbe, M. A. (2000). "Reversibility of polymer-induced fiber flocculation by shear. 1. Experimental methods," *Nordic Pulp Paper Res. J.* 15(5), 545-553.
Hubbe, M. A. (2001). "Reversibility of polymer-induced fiber flocculation by shear. 2. Multi-component chemical treatments," *Nordic Pulp Paper Res. J.* 16(4), 369-375.
Hubbe, M. A. (2002). "Fines management for increased paper machine productivity," *Proc. Sci. Tech. Advan. Wet End Chem.*, Vienna, May 2002, Pira, Leatherhead, Surrey, UK, Paper 3.
Hubbe, M. A. (2005a). *Emerging technologies in flocculation*, Pira International, Leatherhead, UK.
Hubbe, M. A. (2005b). "Microparticle programs for retention and drainage," in *Micro and Nanoparticles in Papermaking*, J. Rodriguez (ed.), TAPPI Press, Atlanta, 2005.
Hubbe, M. A., and Rojas, O. J. (2005). "The paradox of papermaking," *Chem. Eng. Education* 39(2), 146-155.
Hubbe, M. A., and Wang, F. (2002). "Where to add retention aid: Issues of time and shear," *Tappi. J.* 1(3), 28-33.
Huber, P., Roux, J.-C., Mauret, E., Belgacem, N., and Pierre, C. (2003). "Suspension crowding for a general fiber-length distribution: Application of flocculation mixtures of short and long papermaking fibers," *J. Pulp Paper Sci.* 29(3), 77-85.
Hunter, D. (1947). *Papermaking: The History and Technique of an Ancient Craft*, 2nd Ed., Alfred Knopf, New York.
Hunter, R. J. (1987). *Foundations of Colloid Science*, Clarendon Press, Oxford.
Hutton, I. M. (1995). "The concerns of forming wet lay nonwovens from long fibers," in *Proc. 1995 Nonwovens Conf.*, TAPPI Press, Atlanta.
Islek, A. A., Parsheh, M., Yoda, M., and Aidun, C. K. (2004). "The impact of turbulence and swirl on the flow in the tube bank part of a paper mill headbox," *Proc. TAPPI 2004 Spring Tech. Conf.*, electronic doc., TAPPI Press, Atlanta.

Jacquelin, G. (1968). "Improvements in or relating to the method of and apparatus for treating suspensions of fibers for the formation of aggregates," *UK Pat. 1,109,895*.

Jokinen, O., and Ebeling, K. (1985). "Flocculation tendency of papermaking fibers," *Paperi Puu* 67(5), 317-325.

Jokinen, O., and Palonen, H. (1986). "Interdependence of retention and formation in the manufacture of SC paper," *Paperi Puu* 68(11), 801-802, 805-808.

Kaji, H., Monma, K., and Katsura, T. (1991). "Fractal analysis of flocculation in pulp suspension," *Proc. TAPPI 1991 Int'l. Paper Physics Conf.,* TAPPI Press, Atlanta, Vol. 1, 291-297.

Kasper, D. R. (1971). "Theoretical and experimental investigations of the flocculation of charged particles in aqueous solutions by polyelectrolytes of opposite charge," Ph.D. Thesis, Cal. Inst. Technol., Pasadena.

Keith, J. M. (1994). "Dispersion of synthetic fiber for wet-lay nonwovens," *Proc. 1994 Nonwovens Conf.*, TAPPI Press, Atlanta.

Keller, D. S., and Pawlak, J. J. (2001). "β-radiographic imaging of paper formation using storage phosphor screens," *J. Pulp Paper Sci.* 27(4), 117-123.

Keller, D. S., and Lucas, R. A. (2002). "The effect of forming element induced energy on the material distribution, structure, and structural properties of the paper web," *Paper Technol.* 43(4), 29-37.

Kerekes, R. J. (1983). "Pulp floc behavior in entry flow to constrictions," *Tappi* 66(1), 88-91.

Kerekes, R. J. (1995). "Perspectives on fiber flocculation in papermaking," *1995 Intl. Paper Phys. Conf.*, TAPPI Press, Atlanta, 23-31.

Kerekes, R. J., and Schell, C. J. (1992). "Characterization of fiber flocculation regimes by a crowding factor," *J. Pulp Paper Sci.* 18(1), J32-J38.

Kerekes, R. J., and Schell, C. J. (1995). "Effects of fiber length and coarseness on pulp flocculation," *Tappi J.* 78(2), 133-139.

Kerekes, R. J., Soszynski, R. M., and Tam Doo, P. A. (1985). "The flocculation of pulp fibers," in *Papermaking Raw Materials*, Proc. Fundamental Res. Symp., Oxford, V. Punton (ed.), Mechan. Eng. Publ. Ltd., London, 265-310.

King, C. A., and Williams, D. G. (1975). "Cellulose fiber-to-fiber and fines-in-fiber flocculation: A dynamic comparison," *IPC Tech Paper Ser. 3*, Inst. Paper Sci. Technol. at Georgia Inst. Technol., Atlanta, available at http://smartech.gatech.edu/dspace/handle/1853/2896?mode=full.

Kiviranta, A., and Paulapuro, H. (1990). "Hydraulic and rectifier roll headboxes in boardmaking," *Paper Technol.* 31(11), 34-40.

Kiviranta, A., and Paulapuro, H. (1992). "The role of Fourdrinier table activity in the manufacture of various paper and board grades," *Tappi J.* 75(4), 172-185.

Kline, J. E. (1967). "The application of the Verwey-Overbeek theory to the relative sediment volume of kaolin-water dispersions," *Tappi* 50(12), 590-596.

Kolmogorov, A. N. (1949). "On the breakup of droplets in turbulent flow," *Doklady Akad. Nauk SSSR* 66(5), 825-828.

Korteoja, M., J., Lukkarinen, A., Kaski, K., and Niskanen, K. J. (1997). "Computational study of formation effects on paper strength," *J. Pulp Paper Sci.* 32(1), J18-J22.

Korteoja, M. J., Salminen, L. I., Niskanen, K. J., and Alava, M. (1998). "Statistical variation of paper strength," *J. Pulp Paper Sci.* 24(1), 1-13.

Krogerus, B. (1993). "Dynamic flocculation studies on fiber fines and filler clay," *Nordic Pulp Paper Res. J.* 8(1), 135-140.

Kropholler, H. W., and Sampson, W. W. (2001). "The effect of fiber length distribution on suspension crowding," *J. Pulp Paper Sci.* 27(9), 301-305.

La Mer, V. K., and Healy, T. W. (1963). "Adsorption-flocculation reactions of macromolecules at the solid-liquid interface," *Rev. Pure Appl. Chem.* 13, 112-133.

Langley, J.G., and Litchfield, E. (1986). "Dewatering aids for paper applications," In *Proc. TAPPI Papermakers Conf.*, TAPPI Press, Atlanta.

Lee, C. W., and Brodkey, R. S. (1987). "A visual study of pulp floc dispersion mechanisms," *AIChE J.* 33(2), 297-302.

Lee, P. F. W., and Lindström, T. (1989). "Effects of high molecular mass anionic polymers on paper sheet formation," *Nordic Pulp Paper Res. J.* 4(4), 61-70.

Li, T.-Q., and Ödberg, L. (1997). "Studies of flocculation in cellulose fiber suspensions by NMR imaging," *J. Pulp Paper Sci.* 23(8), J401-J405.

Li, T.-Q., Ödberg, L., Powell, R. L., Weldon, M., and McCarthy, M. J. (1995). "Quantitative measurements of flow acceleration by means of nuclear magnetic resonance imaging," *Nordic Pulp Paper Res. J.* 10(2), 133-138.

Lindström, T. (1989). "Some fundamental chemical aspects on paper forming." in *Fundamentals of Papermaking,* C. F. Baker and V. W. Punton (eds.), Trans. 9th Fund. Res. Symp., Cambridge, Mech. Eng. Publ., Ltd., London, 311-412.

Lindström, T., and Glad-Nordmark, G. (1984). "Flocculation of latex and cellulose dispersions by means of transient polymer networks," *Colloids Surf.* 8(4), 337-351.

Lindström, T., Söremark, C., and Eklund, L. (1977). "Kinetic aspects of the flocculation of cellulosic fiber dispersions with polyacrylamides," *Tech. Trans. CPPA* 3(4), TR114-TR118.

Linhart, F., Horn, D., Eisenlauer, J., and Hemel, R. (1987). "Monitoring and control of formation by means of a fiber optic flocculation sensor," *Wochenbl. Papierfabr.* 115(8), 331-338.

Liu, S. X., and Glasgow, L. A. (1997). "Aggregate disintegration in turbulent jets," *Water Air Solid Pollution* 95(1-4), 257-275.

Lloyd, J. A., and Horne, C. W. (1993). "The determination of fiber charge and acidic groups of radiata pine pulps," *Nordic Pulp Paper Res. J.* 8(1), 48-52.

Manson, D. W. (1996). "The practical aspects of formation," *Wet End Operations Short Course Notes,* TAPPI Press, Atlanta.

Marton, J. (1974). "Fines and wet end chemistry," *Tappi J.* 57(12), 90-93.

Mason, S. G. (1950). "The flocculation of pulp suspensions and the formation of paper," *Tappi* 33(9), 440-444.

Mason, S. G. (1954). "Fiber motions and flocculation," *Tappi* 37(11), 494-501.

McDonald, D., Miles, K., and Amiri, R. (2004). "The nature of the mechanical pulping process," *Pulp Paper Can.* 105(8), T181-T186.

McKenzie, A. W. (1968). "Structure and properties of paper. XVIII. The retention of wet-end additives," *Appita* 21(4), 104-116.

McNeal, M. R., Nanko, H., and Hubbe, M. A. (2005). "Imaging of macromolecular events occurring during the manufacture of paper," *Proc. XIII Fundamental Research Symposium*, Cambridge, Pira International, Leatherhead, Surrey, UK.

Meyer, R., and Wahren, D. (1964). "On the elastic properties of three-dimensional fiber networks," *Svensk Papperstidn.* 67(10), 432-436.

Nazhad, M. M., Harris, E. J., Dodson, C. T. J., and Kerekes, R. J. (2000). "The influence of formation on tensile strength of paper made from mechanical pulps," *Tappi J.* 83(112), 63 [electronic document].

Nguyen, T. Q., and Kausch, H.-H. (1992). "Chain extension and degradation in convergent flow," *Polymer* 33(12), 2611-2621.

Norman, B. (2000). "Web forming," in *Papermaking Part 1: Stock Preparation and Wet End*, H. Paulapuro (ed.), Fapet Oy, Helsinki, Ch. 6, 191-250.

Norman, B., Sjödin, Y., Alm, B., Björklund, K., Nilsson, F., and Pfister, J.-L. (1995). "The effect of localized dewatering on paper formation," *1995 Int'l. Paper Physics Conf.*, 55-59.

Norman, B., and Wahren, D. (1972). "A comprehensive method for the description of mass distribution in sheet and flocculation in turbulence in suspension," *Svensk Papperstidn.* 75(20), 807-818.

Ny, C. L., and Messmer, M. (2004). "Potential of refining and dispersing to develop recycled fiber properties," *Research Forum on Recycling Proc, 7th*, TAPPI Press, Atlanta, 189-196.

O'Neill, M. E. (1968). "A sphere in contact with a plane in a slow linear shear flow," *Chem. Eng. Sci.* 23(11), 1293-1298.

Orts, W. J., Godbout, L., Marchessault, R. H., *et al.* (1995). "Shear-induced alignment of liquid-crystalline suspensions of cellulose microfibrils," *ACS Symp. Ser. 597*: 335-348.

Paavilainen, L. (1993). "Conformability – flexibility and collapsibility – of sulfate pulp fibers," *Paperi Puu* 75(9-10), 689-702.

Pandya, J. D., and Spielman, L. A. (1982). "Floc breakage in agitated suspensions: Theory and data processing strategy," *J. Colloid Interface Sci.* 92(2), 517-531.

Parker, J. D. (1972). *The Sheet Forming Process*, TAPPI STAP Ser. 9, TAPPI Press, New York.

Pelton, R. (1993). "A model of the external surface of wood pulp fibers," *Nordic Pulp Paper Res. J.* 8(1), 113-119.

Peters, C. E. (1997). "Formation: Questions most often asked by papermakers," *Proc. TAPPI 1997 Eng. Papermakers Conf.*, TAPPI Press, Atlanta, 103-107.

Peterson, D. E. (1994). "Nuclear density consistency meter evaluation," *Proc. TAPPI 1994 Process Control Symp.*, TAPPI Press, Atlanta, 9-18.

Petzold, G., Buchhammer, H.-M., and Lunkwitz, K. (1996). "The use of oppositely charged polyelectrolytes as flocculants and retention aids," *Colloids Surf. A.* 119(1), 87-92.

Petzold, G. (1999). "Dual-addition schemes," in *Colloid-Polymer Interactions: From Fundaments to Practice*, R. S. Farinato and P. L. Dubin (Eds.), Wiley, New York, Ch. 3, 83-100.

Pfau, A., Schrepp, W., and Horn, D. (1999). "Detection of a single molecule adsorption structure of poly(ethylenimine) macromolecules by AFM," *Langmuir* 15(9), 3219-3225 (1999).

Praast, H., Göttsching, L., and Wehrle, J. (1998). "Floc orientation in paper," *Papier* 57(6), 376-384.

Roberts, J. C., Au, C. O., Clay, G. A., and Lough, C. (1986). "The effect of C^{14}-labelled cationic and native starches on dry strength and formation," *Tappi J.* 69(10), 88-93.

Roberts, J. C., Au, C. O., Clay, G. A., and Lough, C. (1987). "Study of the effect of cationic starch on dry strength and formation using carbon-14 labeling," *J. Pulp Paper Sci.* 13(1), J1-J5.

Rojas, O. J., and Hubbe, M. A. (2004). "The dispersion science of papermaking," *J. Dispersion Sci. Technol.* 25(6), 713-732.

Ross, R. F., and Klingenberg, D. J. (1998). "Simulation of flowing wood fiber suspensions," *J. Pulp Paper Sci.* 24(12), 388-392.

Salmén, L., Kolseth, P., and de Ruvo, A. (1985). "Modeling the softening behavior of wood fibers," *J. Pulp Paper Sci.* 11(4), J102-J107.

Sampson, W. W. (1997). "The interdependence of sheet structure and drainage," *Paper Technol. Ind.* 38(8), 45-50.

Sampson, W. W., McAlpin, J., Kropholler, H. W., and Dodson, C. T. J. (1995). "Hydrodynamic smoothing in the sheet forming process," *J. Pulp Paper Sci.* 21(12), J422-J426.

Sandell, L. S., and Luner, P. (1974). "Flocculation of microcrystalline cellulose with cationic ionene polymers," *J. Appl. Polymer Sci.* 18(7), 2075-2083.

Savolainen, R. M. (1996). "The effects of temperature, pH, and alkalinity on ASA sizing in alkaline papermaking," *Proc. TAPPI 1996 Papermakers Conf.*, TAPPI Press, Atlanta, 289-295.

Schiher, S. C., and Getman, D. L. (1994). "Forming pulse effects on papermaking," *Proc. TAPPI 1994 Wet-End Operations Short Course*, 109-126, TAPPI Press, Atlanta.

Schiller, A. M., and Suen, T. (1956). "Ionic derivatives of polyacrylamide," *Ind. Eng. Chem.* 48(12), 2132-2137.

Schmid, C. F., and Klingenberg, D. L. (2002). "Properties and fiber flocs with frictional and attractive interfiber forces," *J. Colloid Interface Sci.* 226(1), 136-144.

Shah, P. N. (2000). "The role of turbulent elongational stresses on deflocculation in paper sheet formation," *Tappi J.* 83(4), 1-8.

Sikora, M. D., and Stratton, R. A. (1981). "The shear stability of flocculated colloids," *Tappi* 64(11), 97-101.

Söderberg, L. D., and Alfredsson, P. H. (1997). "Experiments concerning the creation of streaky structures inside a plane water jet," *Proc. TAPPI 1997 Engineering and Paper Conf.*, TAPPI Press, Atlanta, 1205-1221.

Solberg, D., and Wågberg, L. (2003). "On the mechanism of cationic-polyacrylamide-induced flocculation and re-dispersion of a pulp fiber dispersion," *Nordic Pulp Paper Res. J.* 18(1), 51-55.

Södergren, O. F., and Neun, J. A. (2000). "Developments in activity generation on Fourdriniers," *Tappi J.* 83(10), 62 [electronic document].

Spicer, P. T., and Pratsinis, S. E. (1996). "Shear-induced flocculation: The evolution of floc structure and the shape of the size distribution at steady state," *Water Res.* 30(5), 1049-1056.

Smook, G. A. (1992). *Handbook for Pulp and Paper Technologists*, 2nd Ed., Angus Wilde, Vancouver.

Stoere, P., Nazhad, M., and Kerekes, R. J. (2001). "An experimental study of the effect of refining on paper formation," *Tappi J.* 84(7), electronic document.

Stover, C. A., Koch, D. L., and Cohen, C. (1992). "Observation of fiber orientation in simple shear flow of semi-dilute suspensions," *J. Fluid Mech.* 238, 277-296.

Stratton, R. A. (1983). "Effect of agitation on polymer additives," *Tappi J.* 66(3), 141-144.

Stratton, R. A., and Swanson, J. W. (1981). "Electrokinetics in papermaking: A position paper," *Tappi* 64(1), 79-83.

Svensson, O., and Österberg, L. (1965). "The function of wet suction boxes," *Svensk Papperstidn.* 68(11), 403-418.

Swanson, J. W. (1950). "The effects of natural beater additives on papermaking fibers," *Tappi* 33(9), 451-462.

Swerin, A. (1998). "Rheological properties of cellulosic fiber suspensions flocculated by cationic polyacrylamides," *Colloids Surf.* 133(3), 279-294.

Swerin, A., Glad-Nordmark, G., and Ödberg, L. (1997). "Adsorption and flocculation in suspensions by two cationic polymers – Simultaneous and sequential addition," *J. Pulp Paper Sci.* 23(8), J389-J393.

Swerin, A., and Mähler, A. (1996). "Formation, retention, and drainage of a fine paper stock during twin-wire roll-blade forming. Implications of fiber network," *Nordic Pulp Paper Res. J.* 11(1), 36-42.

Swerin, A., and Ödberg, L. (1993). "Flocculation and floc strength in suspensions flocculated by retention aids," *Nordic Pulp Paper Res. J.* 8(1), 141-147.

Swerin, A., and Ödberg, L. (1996). "Flocculation and floc strength – From the laboratory to the FEX paper machine," *Papier* 50(10A), V45-V47.

Swerin, A., and Ödberg, L. (1997). "Some aspects of retention aids," in *The Fundamentals of Papermaking Materials*, C. F. Baker (ed.), Pira Intl., Leatherhead, UK, 265-350.

Swerin, A., Ödberg, L., and Wågberg, L. (1996b). "An extended model for the estimation of flocculation efficiency factors in multicomponent flocculation systems," *Colloids Surf.* 113(1-2), 25-38.

Swerin, A., Powell, R. L., and Ödberg, L. (1992). "Linear and nonlinear dynamic visco-elasticity of pulp suspensions," *Nordic Pulp Paper Res. J.* 7(3), 126-132,143.

Swerin, A., Risinger, G., and Ödberg, L. (1996a). "Shear strength in papermaking suspensions flocculated by retention aid systems," *Nordic Pulp Paper Res. J.* 11(1), 30-35.

Swerin, A., Risinger, G., and Ödberg, L. (1997). "Flocculation in suspensions of microcrystalline cellulose by microparticle retention aid systems," *J. Pulp Paper Sci.* 23(8), J374-J381.

Swerin, A., Sjödin, U., and Ödberg, L. (1993). "Flocculation of cellulosic fiber suspension by model microparticulate retention aid systems: Effect of polymer charge density and type of microparticle," *Nordic Pulp Paper Res. J.* 8(4), 389-398.

Takamura, K., Adler, P. M., Goldsmith, H. L., and Mason, S. G. (1981). "Particle motions in sheared suspensions. 31. Rotations of rigid and flexible dumbbells (experimental)," *J. Colloid Interface Sci.* 83(2), 516-530.

Tam Doo, P. A., and Kerekes, R. J. (1982). "The flexibility of wet pulp fibers," *Pulp Paper Can.* 83(2), T37-T41.

Tam Doo, P. A., Kerekes, R. J., and Pelton, R. H. (1984). "Estimates of maximum hydrodynamic shear stresses on fiber surfaces in papermaking," *J. Pulp Paper Sci.* 10(7), J80-J88.

Tanaka, H., Swerin, A., and Ödberg, L. (1993). "Transfer of cationic retention aid from fibers to fine particles and cleavage of polymer chains under wet-end papermaking conditions," *Tappi J.* 76(5), 157-163.

Tripattharanan, T., Hubbe, M.A., Venditti, R.A., and Heitmann, J.A. (2004a). "Effect of idealized flow conditions on retention aid performance. 1. Cationic acrylamide copolymer," *Appita J.* 57(5), 404-410.

Tripattharanan, T., Hubbe, M. A., Heitmann, J. A., and Venditti, R. A. (2004b). "Effect of idealized flow conditions on retention aid performance. Part 2: Polymer bridging, charged patches, and charge neutralization," *Appita J.* 57(6), 448-454.

Ulmar, M., and Norman, B. (1997). "Observations of fiber orientation in a headbox nozzle at low consistency," *Proc. TAPPI 1997 Engineering and Paper Conf.*, TAPPI Press, Atlanta, 865-873.

Unbehend, J. E. (1976). "Mechanisms of 'soft' and 'hard' floc formation in dynamic retention measurement," *Tappi* 59(10), 74-77.

Van de Ven, T. G. M. (1984). "Theoretical aspects of drainage and retention of small particles on the Fourdrinier," *Pulp Paper Can.* 85(3), T58-T63.

Van de Ven, T. G. M., and Mason, S. G. (1981). "Comparison of hydrodynamic and colloidal forces in paper machine headboxes," *Tappi* 64(9), 171-175.

Wågberg, L. (2000). "Polyelectrolyte adsorption onto cellulose fibers – A review," *Nordic Pulp Paper Res. J.* 15(5), 586-597.

Wågberg, L., Björklund, M., Åsell, I., and Swerin, A. (1996). "On the mechanism of flocculation by microparticle retention-aid system," *Tappi J.* 79(6), 157-164.

Wågberg, L., and Lindström, T. (1987a). "Some fundamental aspects of dual-component retention aid systems," *Nordic Pulp Paper Res. J.* 2(2), 49-55.

Wågberg, L., and Lindström, T. (1987b). "Flocculation of cellulosic fibers by cationic poly-acrylamides with different charge densities," *Nordic Pulp Paper Res. J.* 2(4), 152-160.

Wågberg, L., and Ödberg, L. (1991). "The action of cationic polyelectrolytes used for the fixation of dissolved and colloidal substances," *Nordic Pulp Paper Res. J.* 6(3), 127-135.

Wagle, D. G., Lee, C. W., and Brodkey, R. S. (1988). "Further comments on a visual study of pulp floc dispersion mechanisms," *Tappi J.* 71(8), 137-141.

Walkush, J. C., and Williams, D. G. (1974). "The coagulation of cellulose pulp fibers and fines as a mechanism of retention," *Tappi* 57(1), 112-116.

Walser, R., Eames, J. D., and Clark, W. M. (1970). "Performance analysis of hydrofoils with blades of various widths," *Pulp Paper Mag. Can.* 71(8), T183-T187.

Wasser, R. B. (1978). "Formation aids for paper: An evaluation of chemical additives for dispersing long-fibered pulps," *Tappi* 61(11), 115-118.

Waterhouse, J. F. (1993). "Effect of papermaking variables on formation," *Tappi J.* 76(9), 129-134.

Wikström, T., and Rasmuson, A. (1998). "Yield stress of pulp suspensions. The influence of fiber properties and processing conditions," *Nordic Pulp Paper Res. J.* 13(3), 243-250.

Yeung, A., Gibbs, A., and Pelton, R. (1997). "Effect of shear on the strength of polymer-induced flocs," *J. Colloid Interface Sci.* 196(1), 113-115.

Zauscher, S., and Klingenberg, D. J. (2000). "Surface and friction forces between cellulose surfaces measured with colloidal probe microscopy," *Nordic Pulp Paper Res. J.* 15(5), 459-468.

Zauscher, S., and Klingenberg, D. J. (2001). "Friction between cellulose surfaces measured with colloidal probe microscopy," *Colloids Surf. A* 178(1-3), 213-229.